# Transformation of iron oxides in presence of mixed iron-reducing bacterial communities and dynamics of the associated trace elements As, Cr, and Cd

Fengfeng Zhang

# UNIVERSITÉ D'ORLÉANS

***ÉCOLE DOCTORALE***

***ENERGIE, MATERIAUX, SCIENCES DE LA TERRE ET DE L'UNIVERS***

**Institut des Sciences de la Terre d'Orléans**

**THÈSE** présentée par : **Fengfeng ZHANG**

soutenue le **17 novembre 2020**

pour obtenir le grade de : **Docteur de l'Université d'Orléans**

Discipline/ Spécialité : Science de la Terre et de l'Univers

# Transformation of iron oxides in presence of mixed iron-reducing bacterial communities and dynamics of the associated trace elements As, Cr, and Cd

**THÈSE dirigée par :**

| | |
|---|---|
| **MOTELICA-HEINO Mikael** | Professeur, Université d'Orléans |
| **BATTAGLIA-BRUNET Fabienne** | Chercheur, BRGM Orléans |

**RAPPORTEURS :**

| | |
|---|---|
| **DAVRANCHE Mélanie** | Professeur, Université de Rennes 1 |
| **JORAND Frédéric** | Professeur, Université de Lorraine |

---

**JURY :**

| | |
|---|---|
| **GROSBOIS Cécile** | Président, Professeur, Université de Tours |
| **BYRNE James** | Maître de conférences, Université de Bristol |
| **MORIN Guillaume** | Professeur, Sorbonne Université |
| **GAUTRET Pascale** | CR CNRS, ISTO Orléans |
| **HELLAL Jennifer** | Chercheur, BRGM Orléans |
| **MOTELICA-HEINO Mikael** | Professeur, Université d'Orléans |
| **BATTAGLIA-BRUNET Fabienne** | Chercheur, BRGM Orléans |

# UNIVERSITÉ D'ORLÉANS

*ÉCOLE DOCTORALE*

*ENERGIE, MATERIAUX, SCIENCES DE LA TERRE ET DE L'UNIVERS*

**Institut des Sciences de la Terre d'Orléans**

**THÈSE** présentée par : **Fengfeng ZHANG**

soutenue le : **17 novembre 2020**

pour obtenir le grade de : **Docteur de l'Université d'Orléans**

Discipline/ Spécialité : Science de la Terre et de l'Univers

# Transformation of iron oxides in presence of mixed iron-reducing bacterial communities and dynamics of the associated trace elements As, Cr, and Cd

**THÈSE dirigée par :**

| | |
|---|---|
| **MOTELICA-HEINO Mikael** | Pr, Université d'Orléans |
| **BATTAGLIA-BRUNET Fabienne** | Chercheur, BRGM Orléans |

**Co-encadrée par :**

| | |
|---|---|
| **GAUTRET Pascale** | CR CNRS, ISTO Orléans |
| **HELLAL Jennifer** | Chercheur, BRGM Orléans |

**Acknowledgements**

First of all, I really appreciate the attendance of the reviewers Pr. Frédéric Jorand, Pr. Mélanie Davranche and external jury members Pr. Cécile Grosbois, Dr. James Byrne, Dr. Guillaume Morin to my PhD defense. Thanks so much of their time and efforts, their suggestions and comments are really helpful to improve this PhD work!

I would like to sincerely thank 4 of my supervisors, Fabienne who is a wonderful supervisor and has directed this thesis very professionally with her knowledge and patience, Mikael who is also a great supervisor and provided me full supports with his specialty and kindness, Jenny who helps me a lot with her high scientific quality and strict efficiency, and Pascale who helped me a lot in her field which was very good time. I'm really grateful that they provided me this chance for a PhD journey and were with me all the time, to share the happiness and get me through difficulties. I can't imagine how lucky I am to have them to be with me for this long study period. During the past years, they provided me all the supports to everything in work and in daily life, I appreciate their help more than they know.

I would like to thank BRGM and Center-Val de Loire Region for having co-funded this thesis and I would like to thank all the colleagues from BRGM, e.g., Cathy who gave me a lot and very specific help in molecular work and Mickael, Hafida, Cindy who were always with me in the labs in BRGM. It's my honor to work with them and all the other researchers, they might be not involved into my PhD project but I cherish all the past time that staying with them.

I would also like to thank all the colleagues and friends from ISTO, it's a great pleasure to know other PhD students, postdocs and staff there. Many thanks to all the happiness and funny moments they brought me.

I would like to give special thanks to my family and friends from China, they never been to France yet but I know that they are always stand by me.

Finally, I won't forget to thank to my great partner, Clément. It's not easy to have two people finishing their PhDs in the same moment, but we did it.

Life is a long journey and I believe that PhD experiences make us more critical, more open-minded and stronger.

# Contents

# Résumé étendu de la thèse en Français

## Introduction

La mobilité des contaminants dans l'environnement, et en particulier celle des éléments traces potentiellement toxiques (ETPT), tels que l'arsenic, le chrome et le cadmium, induisent des risques de contamination des hydrosystèmes et de la chaîne alimentaire. Comprendre et prévoir la mobilité et la biogéochimie de ces ETPT dans l'environnement permettra de développer et d'appliquer des stratégies adaptées aux sites pollués. En général, le devenir et la mobilité de ces ETPT dans le sol ou les aquifères sont étroitement liés aux conditions physico-chimiques, telles que les conditions d'oxydo-réduction et le pH, mais aussi aux activités microbiennes, en particulier de réduction ou d'oxydation du fer, par des voies directes ou indirectes. En effet, les ETPT sont souvent associés à divers minéraux de fer dans les sols et les sédiments. Les bactéries ferri-réductrices (BFR) sont fortement impliquées dans le cycle du fer dans les environnements de surface qui attirent de plus en plus l'attention des communautés scientifiques et industrielles.

Les minéraux riches en fer peuvent changer en fonction de la disponibilité et du niveau d'oxygène dans l'environnement. Ils sont généralement stables dans les zones bien oxygénées, comme les sols aérés, mais peuvent être dissous lorsque l'oxygène n'est plus disponible, dans des environnements saturés en eau: zones touchées par les crues en bord de rivière, zones inondées ou sites présentant un aquifère peu profond à table variable, fond de vallées et de zones humides. La dissolution de minéraux riches en fer, en l'absence d'oxygène, peut être liée à des activités bactériennes dans les sols ou les sédiments. La réduction microbienne directe du fer par voie enzymatique couplée à l'oxydation du carbone organique est le principal mécanisme de réduction du Fe(III) en milieu anoxique non sulfuré. La réduction bactérienne du Fe(III) joue un rôle important dans les fronts / interfaces redox. Les réactions redox contrôlent les principaux cycles biogéochimiques (carbone, respiration et photosynthèse; fer, azote, etc.). En particulier, ils influencent la mobilité et la biodisponibilité de nombreux oligo-éléments dans les sols et les sédiments soumis à des conditions redox variables.

Jusqu'à présent, ces phénomènes ont été décrits dans des conditions de laboratoire contrôlées, et la plupart d'entre eux ont été expliqués par interaction entre des souches pures et des systèmes à un seul minéral ou à un polluant simple. Cependant, l'évaluation des flux de polluants associés dans des systèmes complexes, avec des communautés bactériennes et plusieurs polluants associés aux minéraux, nécessite le développement d'expériences multi-échelles.

Dans ce contexte, la présente thèse de doctorat était axée sur les questions scientifiques suivantes: (1) quelle est l'influence du type de minerai Fe sur l'efficacité de la libération de Fe en présence de communautés bactériennes mixtes? (2) Comment le type de minéral influence la structure de ces communautés mixtes et la proportion dans ces communautés de deux espèces bactériennes réductrices de fer spécifiques bien connues, à savoir Shewanella et Geobacter? (3) Quelle est l'influence du mode de croissance, c'est-à-dire planctonique du biofilm, sur la proportion de ces espèces réductrices de fer? (4) Quelle est l'influence du développement de communautés bactériennes complexes réductrices de fer sur le comportement des oligo-éléments ciblés, As, Cr et Cd, associés aux oxy-hydroxydes de fer?

Afin de répondre à ces questions, les objectifs de la présente étude étaient les suivants :

(1) déterminer l'influence du type d'oxydes de Fe(III) sur l'efficacité de la libération de Fe et la formation de minéraux secondaires en présence de communautés bactériennes mixtes réductrices de fer (BFR),

(2) observer comment le type d'oxyde de Fe influence la structure de ces communautés mixtes, et la proportion dans ces communautés de deux espèces BFR spécifiques bien connues : *Shewanella* et *Geobacter*,

(3) développer des stratégies expérimentales et évaluer l'effet des transformations du fer sur la spéciation et la mobilité de trois éléments traces potentiellement toxiques (ETPT) fréquemment associés au fer : As, Cr, Cd.

Un environnement naturel soumis à des oscillations redox a été sélectionné comme source de bactéries réductrices de fer. Le site d'échantillonnage est situé à Decize (Bourgogne, France) près d'un chenal de la Loire inondé une partie de l'année. Trois échantillons au total ont été prélevés au niveau : du sol de la rive du fleuve, du sol inondé et des sédiments sous l'eau. Les cultures BFR ont été obtenues en inoculant les échantillons de site dans un milieu contenant du Fe(III) -NTA 10 mM comme accepteur d'électrons et plusieurs substrats (acétate, lactate, formiate, glucose et petone) comme donneurs d'électrons. Trois enrichissements de bactéries réductrices de fer ont été obtenus qui ont totalement réduit le Fe(III) -NTA en 1-2 jours.

Le programme de recherche de thèse de doctorat a ensuite été réalisé en trois étapes :

(1) Des expériences en batch avec des solides en suspension,

(2) Des expérience en batch avec des (oxyhydr)oxydes de fer immobilisés sur des lames de verre,

(3) Des expériences en continu avec des (oxyhydr)oxydes de fer immobilisés avec du sable en colonnes.

## 1. Expériences en suspension avec quatre oxydes de fer différents

Dans des expériences en batch avec des solides en suspension dans le milieu de culture, des minéraux de ferrihydrite et de lépidocrocite synthétiques (abrégé FoL), de goethite et d'hématite ont été fournis comme accepteurs d'électrons pour les enrichissements en BFR, et les espèces minérales dissoutes de Fe(II) et Fe(III) ont été analysées. Les taux de mise en solution du fer à partor des oxydes solides ont varié de façon décroissante d'un (oxyhydr)oxydes à l'autre selon l'ordre suivant : FoL > ferrihydrite> goethite> hématite. Deux espèces bactériennes réductrices de fer bien connues, *Shewanella* et *Geobacter*, ont été quantifiées à l'aide de techniques qPCR. Ces deux espèces ont été détectées dans toutes les conditions, et la proportion de *Shewanella* a toujours été prépondérante. De plus, *Shewanella* était plus abondante en présence de FoL, l'oxydes le plus facilement réduit.

Ces résultats, obtenus avec une communauté de BFR complexe, est en accord avec ceux des études précédentes réalisées avec des souches bactériennes pures. La FoL mal cristallisée et la ferrihydrite amorphe ont des surfaces spécifiques plus élevées, qui pourraient favoriser des taux élevés de solubilisation du fer. Par ailleurs, les proportions les plus élevées de *Shewanella* dans les communautés bactériennes ont été obtenues avec une FoL mal cristallisée avec laquelle les niveaux les plus élevés de solubilisation du fer ont été obtenus. De nouveaux minéraux de fer secondaires néo-formés ont été observés en présence de ferrihydrite synthétique, en fin de batch en suspension et en fin d'expérience sur colonne, par des observations en MEB-EDS. Des analyses par spectroscopie Mössbauer ont indiqué la présence de phases de Fe(II) après incubation en fin d'expérience en batch avec la goethite, et en fin d'expérience en colonne avec la ferrihydrite. L'existence de ces phases de Fe(II) générées par des interactions entre des microbes et des oxydes de fer a confirmé que la réduction du Fe(III) n'entraîne pas seulement la production de Fe(II) en phase liquide mais aussi des «minéraux secondaires» contenant du Fe(II).

L'expérience batch en suspension a montré que : (1) la procédure d'enrichissement avec le milieu de culture riche en donneurs d'électrons, ainsi que l'apport de Fe(II)-NTA ou d'oxydes

de fer a modifié de manière significative la composition des communautés bactériennes par rapport aux communautés naturelles du site; (2) dans nos conditions expérimentales, la diversité bactérienne n'était pas significativement différente d'un type d'oxyde de fer pur à un autre; (3) le type d'oxyde de Fe peut influencer la proportion de *Geobacter* et *Shewanella*. Parallèlement, la nature des oxydes de fer semble avoir exercé une sélection sur le rapport de *Geobacter* et *Shewanella*, alors qu'elle n'a pas eu d'impact significatif sur la structure de la communauté bactérienne dans son ensemble. La concentration en Fe(III) biodisponible et le mélange de donneurs d'électrons dans le milieu d'enrichissement ont favorisé le développement de *Shewanella* par rapport au genre *Geobacter*. En présence d'oxydes de fer, les proportions les plus élevées de *Shewanella* dans les communautés bactériennes ont été obtenues avec les oxydes de fer formés avec le protocole de synthèse de lépidocrocite, et correspondaient aux niveaux les plus élevés de solubilisation du fer. Ce résultat est cohérent avec l'hypothèse que le développement de *Shewanella* pourrait être favorisé par une biodisponibilité élevée de Fe(III). En revanche, *Geobacter* a été détecté dans des proportions plus élevées avec de la goethite qui se dissout moins facilement. Globalement, tous les résultats suggèrent que la composition du milieu de culture, en termes de substrats organiques, favorisait fortement *Shewanella* par rapport à *Geobacter*, cependant le type de Fe(III) utilisé comme accepteur d'électrons a également influencé les proportions finales et les abondances de *Geobacter* et *Shewanella*. *Geobacter* semble être plus présent avec un minerai de fer présentant une solubilité plus faible, peut-être parce que cette bactérie présente une affinité plus élevée pour Fe(III), qui favoriserait cet organisme à de faibles niveaux de disponibilité en Fe(III).

## 2. Ferrihydrite fixée sur des lames pour étudier les bactéries réductrices de fer dans les biofilms

Les expériences en batch avec des oxy(hydroxydes) de fer immobilisés sur des lames de verre ont été focalisées uniquement sur la ferrihydrite. Des lames de verre contenant de la ferrihydrite immobilisée ont été inoculées et incubées dans des bocaux étanches contenantdu milieu de culture liquide. Pendant 85 jours, l'évolution de la concentration totale en fer dissous, du potentiel redox, du pH et du nombre de cellules en suspension a été suivie et la morphologie de la ferrihydrite a également été observée avant et après expérience. La ferrihydrite sur des lames de verre a été prélevée à la fin de l'expérience pour étudier les deux genres de BFR: *Shewanella* et *Geobacter* ont été quantifiées en fin d'expérimentation, à l'aide de techniques qPCR, en milieu liquide et dans le biofilm attaché aux oxydes de fer solides. La proportion de *Shewanella* était encore prépondérante à la fois, en milieu liquide et dans le biofilm, mais en proportion

équivalente, dans les communautés bactériennes globales, sous forme de cellules libres ou attachées aux oxydes de fer. A l'inverse, *Geobacter* était moins abondant que *Shewanella* (de 102* à 203* moins), mais la proportion de *Geobacter* associée à la phase solide était 25 fois plus élevée que sa proportion dans la communauté bactérienne non attachée (cellules planctoniques). Nous avons donc trouvé des abondances différentes des deux IRB bien caractérisés, à savoir, *Shewanella* et *Geobacter* dans le biofilm et le milieu liquide environnant en fonction de leur métabolisme. *Geobacter*, un genre qui nécessite un contact direct avec des solides pour utiliser Fe(III) comme accepteur d'électrons était significativement plus abondant dans le biofilm que dans le milieu liquide, tandis que *Shewanella*, un genre qui peut utiliser la respiration Fe(III) ou la fermentation pour se développer a été trouvé aussi. Les observations au MEB-EDS ont montré que de minéraux secondaires contenant Fe, P et/ou C se sont formés en présence de bactéries mais pas dans les témoins stériles. Cette expérience a donc permis de visualiser le développement du biofilm sur les oxydes de fer et d'identifier la formation de nouveaux minéraux. Dans de futurs projets, la méthode de préparation de lames de verre pourrait être appliquée afin d'étudier l'influence du type de minéral Fe(III) sur la composition des biofilms naturels, avec la possibilité d'immobiliser une gamme d'oxydes différents. Afin d'être plus proche du système naturel, des concentrations en donneurs d'électrons moins élevées devront être testées. Au-delà des études en laboratoire, des lames pourraient être placées sur le terrain, insérées dans des sols ou des sédiments aquatiques, afin d'acquérir une meilleure connaissance de l'apport et de la répartition des communautés BFR fixées sur les surfaces d'oxy(hydroxydes) de fer. Cette approche pourrait aider à élucider la dynamique du Fe dans les environnements de surface.

### 3. Mobilité d'As, Cr et Cd adsorbés sur des oxy(hydroxydes) de fer en présence de bactéries ferri-réductrices

Deux expériences sur colonne ont été réalisées avec respectivement de la ferrihydrite et de la goethite, enrichies en As, Cr et Cd par une étape d'adsorption préliminaire. Des colonnes inoculées et non inoculées ont été mise en place en parallèle Le programme expérimental comprenait trois phases successives : stabilisation avec de l'eau synthétique, inoculation avec l'enrichissement en BFR, puis alimentation avec des mélanges d'eau synthétique et de substrats organiques (glucose, acétate, formiate, lactate et peptone). L'évolution des concentrations totales dissoutes en Fe, As, Cd et Cr, ainsi que les valeurs du potentiel redox et du pH ont été suivies en sorties de colonnes. La concentration en fer était toujours plus élevée à la sortie des colonnes ensemencées que dans les conditions abiotiques. A la fin de l'expérience, 96 mg de Fe

avaient été extraits de la colonne de goethite inoculée (0,8 mg de la condition abiotique), tandis que 141 mg de Fe avaient été lessivés de la colonne de ferrihydrite (13 mg pour la condition abiotique).

Concernant le comportement des ETPT, les résultats diffèrent selon les polluants considérés. Avec la ferrihydrite, la libération d'arsenic liée à des réactions biologiques n'a été observée qu'après 40 jours d'expérience, et semble augmenter du jour 40 au jour 99 (fin de l'expérience). En revanche, l'effet de l'inoculation de la libération d'As de la colonne de goethite n'a été observé que pendant les 10 premiers jours d'alimentation avec des substrats organiques et était équivalent en sortie de colonnes biotiques et abiotiques. Le chrome était moins mobile en conditions biotiques qu'en conditions abiotiques, pour les deux oxydes de fer, et moins mobile avec la ferrihydrite qu'avec la goethite. Ainsi, l'activité biologique de réduction du fer n'a pas induit la libération de Cr dans notre expérience. Le Cd était plus mobile dans la première période (du jour 0 au jour 50) dans les conditions abiotiques que dans les conditions biotiques avec la ferrihydrite. Cette tendance a été inversée de manière transitoire (du jour 57 au jour 86), avec des concentrations plus élevées de Cd à la sortie de la colonne biotique, puis les deux colonnes se sont comportées de manière similaire à la fin de l'expérience. Avec la goethite, le Cd était toujours plus mobile en conditions abiotiques qu'en présence de bactéries. À la fin de l'expérience, des échantillons ont été prélevés à trois niveaux différents dans chaque colonne pour des analyses moléculaires, des analyses de spectrométrie Mössbauer et des observations MEB-EDS. Les gènes 16S étaient plus abondants avec la ferrihydrite que dans la colonne de goethite. Comme observé précédemment dans des expériences en suspension et sur lames, la proportion de *Shewanella* dans les communautés bactériennes était toujours plus élevée que celle de *Geobacter*. L'abondance de *Geobacter*, dans les colonnes de ferrihydrite et de goethite, a diminué du bas (près de l'alimentation) vers le haut. En revanche, l'abondance de *Shewanella* dans la colonne de ferrihydrite variait de façon décroissante suivant l'ordre milieu > bas > haut et avec la goethite, elle était plus élevée dans les conditions du bas et du haut qu'au milieu de la colonne. Les observations MEB-EDS suggèrent la formation de minéraux contenant Fe, P et/ou C dans la colonne inoculée de ferrihydrite, mais pas en présence de goethite. Les analyses en spectroscopie Mössbauer ont confirmé la présence de minéraux contenant du Fe(II) dans la colonne de ferrihydrite inoculée, en quantités plus élevées en bas qu'en haut de colonne. En revanche, les minéraux de Fe(II) n'ont pas été détectés dans la colonne de goethite.

Selon la littérature, les interactions entre les BFR, les bactéries sulfato-réductrices (BSR) et les oxydes de Fe (oxihydr) pourraient influencer différemment les motilités des ETPT associées

aux oxydes de fer. En particulier, l'As est plus susceptible d'être mobilisé dans des conditions réductrices qu'un métal divalent tel que le Cd, ou d'autres types de métaux tels que Cr, et ce phénomène semble être lié à des processus biologiques, tels que la réduction d'As(V) en As(III), ou la biosorption des métaux par le biofilm. En effet, l'immobilisation par des bio-mécanismes semble contrecarrer l'effet de la dissolution de l'oxyde de fer qui représente le piège initial des métaux Cd et Cr, alors que pour l'As, les mécanismes de mobilisation sont prépondérants. L'expérience en colonne a également montré que le type d'oxyde de fer utilisé comme accepteur d'électrons influençait la distribution spatiale finale et l'abondance de *Geobacter* et *Shewanella*.

## 4. Conclusion et perspectives

Dans leur ensemble, les résultats des différentes phases expérimentales de cette thèse de doctorat ont montré que la minéralogie de l'oxyde de fer influençait la diversité des communautés bactériennes réductrices du fer. Compte-tenu des deux espèces de BFR suivies au cours de cette thèse, *Shewanella* a toujours été prépondérante par rapport à *Geobacter* dans les communautés bactériennes, et ces deux espèces étaient différentiellement réparties entre les populations attachées et planctoniques. De plus, dans les systèmes à colonnes, leur distribution spatiale diffère. Les taux de réduction du fer dépendaient de la minéralogie des oxydes de fer, selon des études antérieures. L'originalité du présent travail repose sur l'étude simultanée du comportement de trois ETPT différents adsorbés sur deux oxy(hydroxydes) de fer différents et soumis à des activités de communautés BFR complexes. La mobilité respective de ces éléments différait d'un oxy(hydroxydes) de fer à l'autre, temporellement et en termes d'effets des activités biologiques.

Ces résultats permettent de mieux comprendre la dynamique bactérienne du fer et du ETPT associé dans l'environnement, dans des conditions expérimentales originales avec des systèmes multi-polluants et des communautés bactériennes mixtes réductrices de fer.

Les observations originales et les résultats présentés dans ce manuscrit sont liés aux transformations des oxy(hydroxydes) de fer et à la mobilité globale de trois ETPT pendant la réduction microbienne de Fe(III) dans des conditions de laboratoire, avec des enrichissements microbiens mixtes complexes en BFR. Cependant, des études complémentaires pourraient apporter des réponses plus spécifiques sur le rôle de la réduction microbienne du Fe(III) dans les systèmes naturels, étudier de nouvelles technologies sur site pour la surveillance des processus mobilisant des polluants et des technologies moléculaires pour cibler les communautés de BFR.

Par exemple, les nombreuses données acquises au cours des travaux de ce doctorat pourraient être utilisées pour modéliser les processus associés à la réduction du Fe(III). Par conséquent, ces résultats seront potentiellement utiles pour acquérir des connaissances supplémentaires sur les interactions entre les cycles des ETPT et le cycle du fer en fonction de l'activité bactérienne, grâce par exemple à la simulation du transport réactif de soluté / précipitation par modélisation à l'aide de PhreeqC. Cela pourrait aider à comprendre les cycles biogéochimiques des ETPT associés à la réduction microbienne du fer dans les sites pollués, à travers les mécanismes identifiés et le développement méthodologique de lames recouvertes d'oxydes de Fe(III) immobilisés qui pourraient être transportés sur site et insérés dans les sols et / ou sédiments. Une meilleure connaissance de l'activité microbienne sur les sites pollués permettrait également d'évaluer l'évolution de la qualité de l'environnement à moyen et long terme, à partir des données acquises à partir des travaux de laboratoire et des simulations de modélisation.

Le travail effectué avec des techniques de biologie moléculaire utilisant des amorces spécifiques pour cibler deux genres de BFR s'est avéré approprié et efficace pour étudier et surveiller les proportions de *Shewanella* et *Geobacter* dans les systèmes de réduction de Fe(III). D'autres technologies moléculaires pourraient être développées ciblé par ces amorces, comme la détection/quantification des deux genres ciblés à partir des ARN ribosomiques produits par les bactéries actives, et non seulement des ADNs présents dans toutes les cellules, comme réalisé au cours de la présente thèse. Ainsi, une meilleure compréhension de la structure et de la fonctionnalité des communautés microbiennes actives pourrait aider à évaluer et à surveiller les processus biogéochimiques dans l'environnement.

Globalement, la présente thèse a généré des résultats liés aux interactions entre les activités microbiennes et les oxy(hydroxydes) de fer purs ou mélangés à des sables, au lieu d'échantillons de sites réels, et représentent une base pour des recherches ultérieures sur les environnements pollués par des ETPT, afin de comprendre le fonctionnement des systèmes réels et élaborer des stratégies efficaces de surveillance ou d’assainissement.

# Chapter 0: General introduction and objectives

Contaminants' mobility in surface environment, and particularly for potentially toxic trace elements (PTTE), metals and metalloids, such as As, Cr and Cd, induces risks of contamination of ecosystems and food chain. These elements can be naturally present in soils and sediments through the local geology, or contaminated by diverse human activities (mines, industries, agriculture…). They are often associated with Fe in soils and sediments. Yet, Fe-rich minerals can change according to oxygen availability and concentration. These minerals are generally stable in well oxygenated zones, such as aerated soils, but can be dissolved when oxygen is no longer available, in water saturated environments, such as zones impacted by flooding in river sides, flooded zones or sites presenting a shallow aquifer with a variable water table, bottom of valleys and wetlands. The dissolution of Fe-rich minerals, in absence of oxygen, can be linked to bacterial activities in soils or sediments. The direct microbial, enzymatic, iron reduction pathway, coupled with the oxidation of organic carbon is the main mechanism for Fe(III) reduction in non-sulfidic anoxic media. Bacterial reduction of Fe(III) plays an important role in redox fronts / interfaces. Redox reactions control the major biogeochemical cycles (carbon, respiration and photosynthesis; iron, nitrogen, etc.). In particular, they influence the mobility and bioavailability of many trace elements in soils and sediments submitted to variable redox conditions.

Up to now, these phenomena have mainly been described in controlled laboratory conditions, studying interactions between pure bacterial strains and single minerals or simple pollutant systems. However the evaluation of associated PTTE remobilisation in complex systems, with bacterial communities and several PTTEs associated with Fe-minerals, requires the development of multi-scale experiments with more realistic conditions.

In this context, this PhD thesis' general objective was to evaluate the respective roles of biological activity of complex bacterial communities and abiotic reactions in the control of mineralogical transformation of different types of Fe(III) (oxyhydr)oxides, and the effects of these transformations on the mobility of three PTTEs often associated with iron: As, Cr and Cd.

This research program aims to improve our understanding of the dynamics of trace contaminants linked to biological iron cycling through focusing on specific phenomena that have not already been well documented, at the interface between simplified fundamental

laboratory knowledge and complex natural environments, through multi-disciplinary approaches.

More specifically, the PhD thesis was focused on the following scientific questions: (1) what is the influence of the type of Fe mineral on the efficiency of Fe release in presence of mixed bacterial communities? (2) How does the type of mineral influence the structure of these mixed communities, and how are the abunances of two well known specific iron reducing bacterial genera, i.e. *Shewanella* and *Geobacter affected*? (3) What is the influence of the growth mode, i.e. planktonic or biofilm, on the proportion of these iron-reducing genera? (4) What is the influence of the development of complex iron-reducing bacterial communities on the behavior of the targeted PTTEs, As, Cr and Cd, associated to Fe (oxyhydr)oxides?

In order to assess the impact of reductive dissolution of Fe by microorganisms on the chemical and mineralogical transformations of Fe oxides in comparison to abiotic processes, specific experiments were set up. Laboratory scale experiments of complementary design were carried out during this PhD thesis: batch tests in slurries, studies in batches with minerals immobilized on slides, and finally continuous fed systems in columns, in presence of trace contaminants. These different types of experiments should allow us not only to appreciate the structural and mineralogical evolution of solid phases over time, but also to study the evolution of the bacterial diversity and the proportion of known iron-reducing genera.

The scientific methods and the associated results are described and discussed in the present manuscript, of which the organization presents the following structure:

- Chapter I gives an overview of the background knowledge in the subjects related with iron cycling, iron oxides and their reduction in environment and laboratory systems, iron reducing bacteria, mechanisms of iron bio-reduction, and mobility of trace elements associated with these processes.

- Chapter II details the materials and methods that were used in all the following experiments.

- Chapter III reports experiments performed with iron oxides without trace elements: (1) the selection of iron-reducing bacterial enrichments, (2) batch experiments in slurry with these enrichments and four different iron oxide minerals, and (3) development of

an experimental system to study the development of biofilms onto iron oxides immobilized on glass slides.

- Chapter IV relates the study of the dynamics of three trace elements presenting contrasting chemical behaviors, immobilized on iron oxides, in continuously fed column systems.

- Finally, chapter V presents a general discussion, the conclusions and perspectives of the whole research program.

# Chapter I: Background knowledge

Fe is the fourth most-abundant element on Earth representing about 5% of the Earth's crust and is an essential redox buffer on Earth (Bekker et al., 2010; Huston and Logan, 2004). In sediments and soils, Fe exists mainly in two states: +II and +III and the ability of its species to become oxidized or reduced plays a central role in redox chemistry and biogeochemistry (Bonneville, 2005). As a redox-sensitive transition element, it is widely accepted that iron can be used as an electron acceptor through chemical and biological reduction processes under anaerobic conditions (atmosphere, oceans, soils, sediments) (Frenzel et al., 1999; Fuller et al., 2014; Stumm and Sulzberger, 1992). Dissimilatory iron reducing bacteria (DIRB) transform Fe(III) to Fe(II) at the surface of Fe(III) (oxyhydr)oxides particles in natural systems through microbial processes (Bonneville et al., 2004; Esther et al., 2015; Zachara et al., 2001). During these processes, not only the mineral's surface reactivity is changed but also associated PTTEs on (oxyhydr)oxides in soils and sediments. In doing so, the mineral's ability to adsorb or release metals, nutrients, and organic molecules is altered, which can thereby have a dramatic impact on environmental quality (Bose et al., 2009).

## I-1 Biogeochemical cycle of Fe

### I-1.1 Global Fe cycle

The Fe cycle involves the atmosphere, hydrosphere, biosphere and lithosphere. The main Fe fluxes in the global cycle of this element (Figure I-1) are linked to human activities: mining and waste production. The main natural fluxes are atmospheric dust deposition, oceanic fluids release and the melting of iceberg sediments. The remaining fluxes are linked to living organisms (Figure I-2).

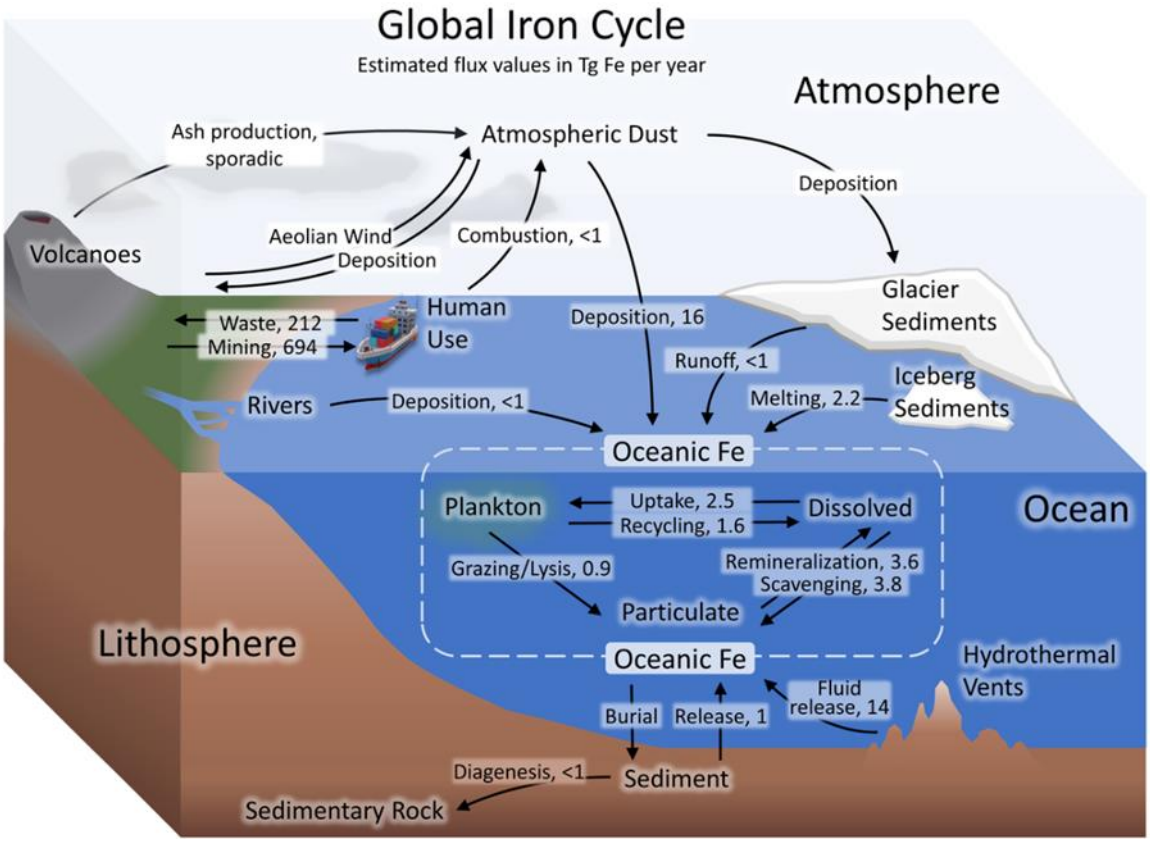


***Figure I-1.*** *Global iron cycle (https://commons.wikimedia.org/wiki/File:Iron_cycle7.png).*

In general, Fe circulates through the atmosphere, lithosphere, and oceans. Figure I-1 shows the present global Fe cycle in the ocean, atmosphere and lithosphere, including bioavailable and non-bioavailable Fe (Archer and Johnson, 2000; Wang et al., 2007). Labeled arrows show flux in Tg of Fe per year (Jickells et al., 2005; Nickelsen et al., 2015; Raiswell and Canfield, 2012; Wang et al., 2007). Atmospheric iron, including Fe coming from anthropogenic combustion cycles, that is deposited in the ocean and then it could affect cycles of other elements e.g., carbon (Matsui et al., 2018).

Fe is the main essential metal for living organisms, present in many enzymes, and involved in oxygen transport in blood. Fe is abundant on earth but is biologically scarce. Fe in all the main redox states, Fe(0), Fe(II) and Fe(III), is able to persist as solid phases almost indefinitely in oxygenated environments although only the Fe(III) state is thermodynamically stable (Raiswell and Canfield, 2012). As a consequence, Fe is not very available in oxygenated neutral conditions. Apart from microbial reactions (which are described in the following sections), assimilation of Fe by plankton and plants is essential. In terrestrial ecosystems, Fe uptake by plants can be facilitated by chelating molecules (siderophores) produced by microbes and certain groups of plants (Dimkpa, 2016).

Figure I-2 presents the main bioprocesses involved in iron cycle, including oxidation of rocks and Fe(II), biodegradation of Fe-containing organic matter, assimilation by living organisms, and bio-reduction of diverse Fe(III) minerals.

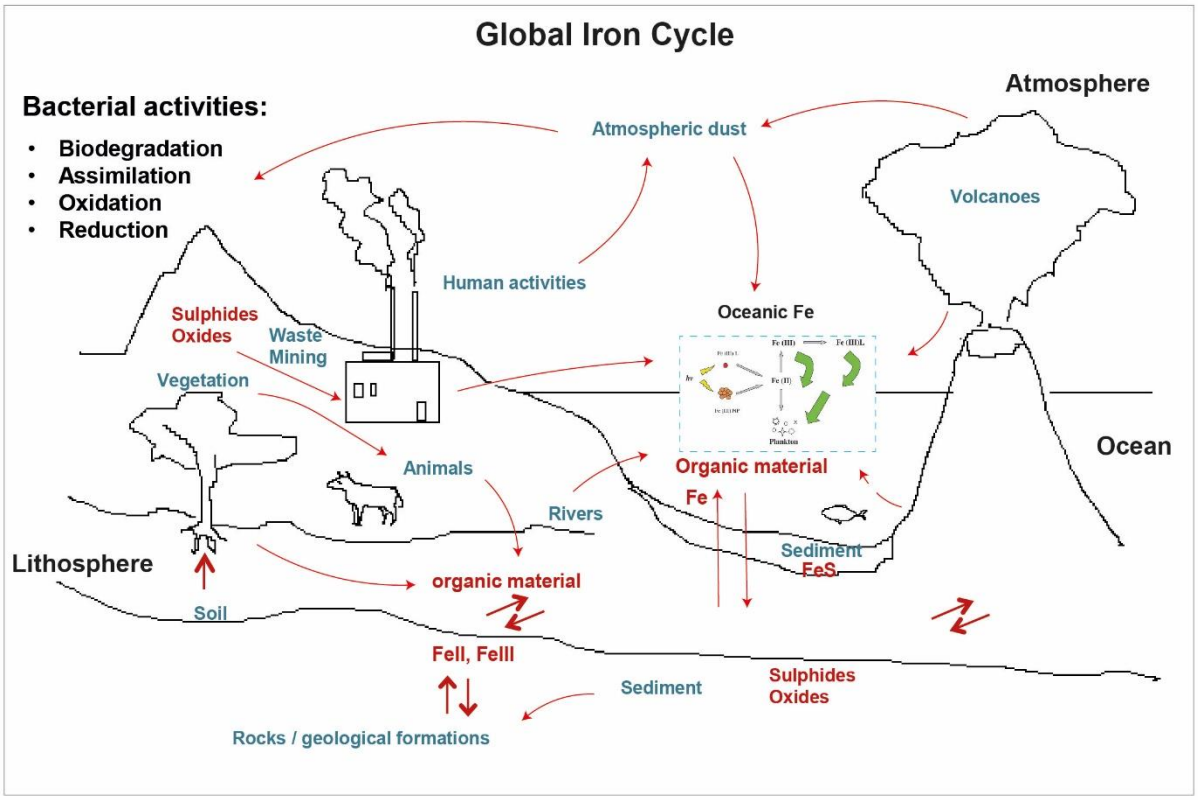


***Figure I-2.*** *Biogeochemical processes involved in the iron cycle*

The ferrous-ferric system is reversible, the reversibility is independent of pH, Eh, and the reduction of Fe(III) (oxyhydr)oxides to dissolved Fe(II) is an important biogeochemical process in all anaerobic sedimentary systems. Microbial reduction of Fe(III) also plays an important role in the fate and transport of trace metals and nutrients in soils, sediments and aquatic environments (Konhauser et al., 2011). Microbial reduction of Fe(III) (oxyhydr)oxides has been extensively studied in relation to its essential roles on iron cycling.

### I-1.2 Microbial transformations of Fe in the biogeosphere

Different groups of bacteria are responsible for direct Fe(II) oxidation in presence of oxygen ($O_2$) or of Fe(III) reduction in anaerobic conditions, in a large range of pH (Figure I-3).

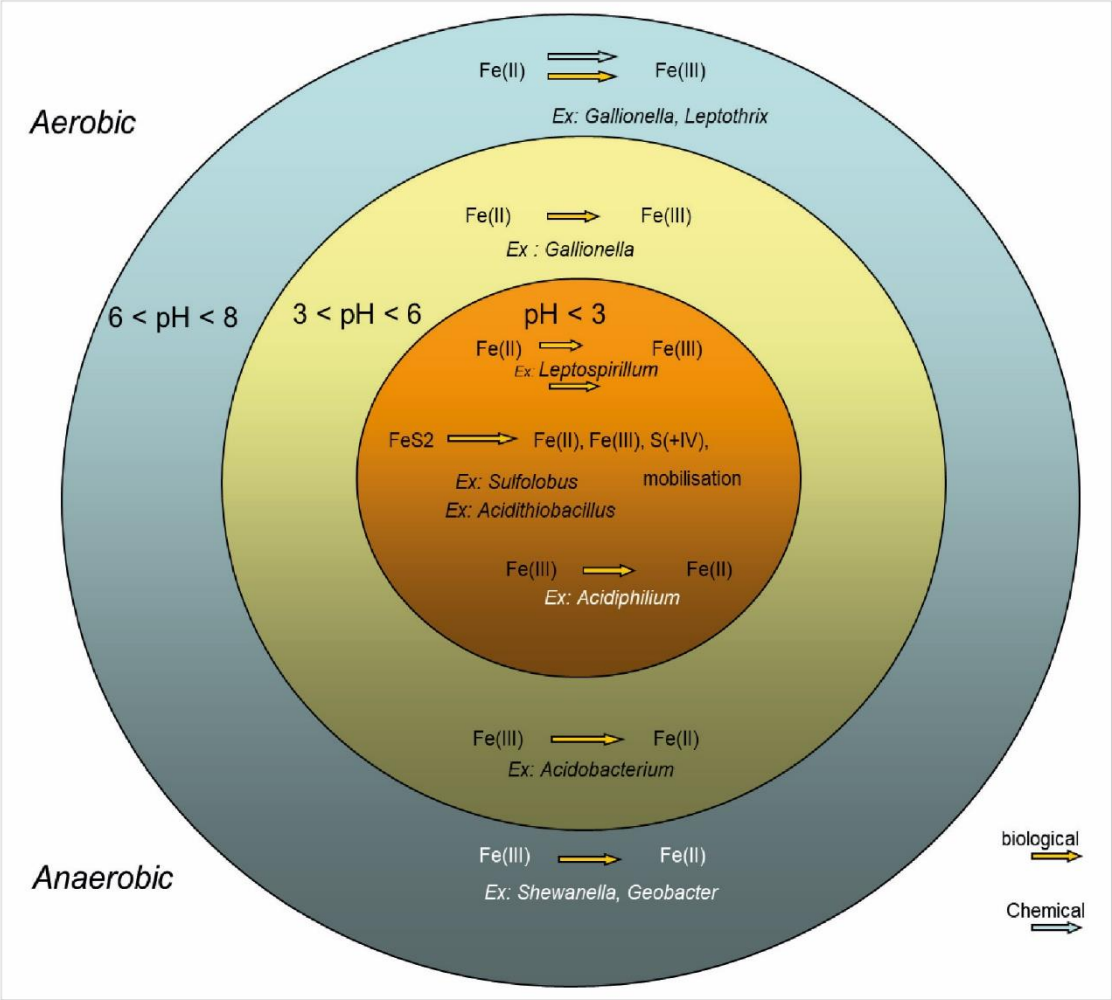


***Figure I-3.*** *Bacterial group Fe(II) oxidation in oxic condition and Fe(III) reduction in anoxic conditions with a large range of pH*

The biological catalysis of Fe oxidation/reduction is thought to be responsible for the formation of most naturally occurring insoluble Fe(II, III) oxides and consequently plays a key role in the biogeochemical cycling of Fe (Kappler and Straub, 2005; Li et al., 2015). Fe(II) can function as an electron source for iron-oxidizing bacteria under both oxic and anoxic conditions and Fe(III) can function as a terminal electron acceptor under anoxic conditions for iron-reducing bacteria (Weber et al., 2006). Variable pH values also select iron-oxidizing/reducing bacteria, and below pH 3, acidophilic groups of bacteria e.g., *Acidithiobacillus* and *Sulfolobus* (sulfur oxidation) thrive in acidic pH and help in dissolving the iron minerals e.g., pyrite ($FeS_2$) from the solid phase into the aqueous phase (Brock et al., 1972; Kelly and Wood, 2000; Rodríguez et al., 2003). Moreover, iron-reducing bacteria *Acidiphilium* was isolated from acidic coal mine drainage and was able to reduce ferric iron under anoxic acidic environments even possibly in oxygen-containing condition (Johnson and

Bridge, 2002; Wichlacz et al., 1986). Microbial ferrous Fe oxidation provides energy to acidophiles such as *Leptospirillum* which is well known to achieve Fe(II) oxidation at pH below 3 (Ojumu and Petersen, 2011; Van Scherpenzeel et al., 1998). In the pH range 3-6, *Acidobacterium* is an acidophilic, chemoorganotrophic bacterial genus isolated from acidic mineral environments and capable of dissimilatory iron reduction under anaerobic conditions (Coupland and Johnson, 2008; Kishimoto et al., 1991). The bacterial species of the genus *Gallionella* are typical iron-oxidizing bacteria that grow under neutral (pH 6.5-8) or moderately acidic (pH 4) conditions (De Vet et al., 2011; Fabisch et al., 2013). The genus *Leptothrix* contains "iron-oxidizing" or "model Mn(II)-oxidizing" species and is ubiquitously distributed in the aquatic environment (El Gheriany et al., 2009; Ghiorse, 1984). *Leptothrix* can be readily found in sites with a circumneutral pH, an oxygen gradient and a source of reduced Fe and manganese minerals (Emerson and Moyer, 1997; Sawayama et al., 2011). Finally, *Geobacter* and *Shewanella* are the two most studied dissimilatory Fe reducing genera under anaerobic and near-neutral pH conditions up to now (Engel et al., 2019; Han et al., 2018; Jiang et al., 2020; Li et al., 2012).

### I-1.3 Influence of redox conditions and organic matter on iron reduction

Iron redox reactions have the potential to support substantial microbial populations in soil and sedimentary environments, as Fe is the fourth most abundant element in the Earth's crust (Weber et al., 2006). Motomuraand and Yokoi (1969) have suggested that the different forms of ferrous Fe in flooded soils have a physical and chemical influence on the development and stabilization of soil structure, which in turn exerts an influence on soil productivity (Gotoh and Patrick Jr, 1974; Motomura and Yokoi, 1969). It is also well established now that flooded soils in anaerobic conditions are subjected to a succession of Fe transformations from the ferric to ferrous state under reducing conditions caused by a wide variety of facultative anaerobic soil bacteria. Fe reduction can be the result of bacterial metabolism, Fe functioning as an electron acceptor in dissimilatory iron reduction (DIR). Redox potential (oxidation-reduction) has a marked effect on microbial Fe behavior because a change in redox status in soils implies changing the availability of electron acceptors. As shown on the electron donors/acceptors tower in Figure I-4, Fe(III) may be used as an electron acceptor after depletion of oxygen, nitrate and manganese oxides. Pett-Ridge and Silver (2006) have indicated that some flexible microorganisms were able to respire/ferment or use multiple electron acceptors under fluctuating redox conditions, thus microbial populations can be periodically activated and

inactivated, which in turn quickly alters the nature and rate of key biogeochemical transformations (DeAngelis et al., 2010; Husson, 2013; Pett-Ridge et al., 2006).

Ginn et al. (2017) studied the influence of oxygen variations on Fe speciation in soils from the Luquillo Critical Zone Observatory (Puerto Rico) through batch experiments in flasks inoculated with *Shewanell*a. *Shewanella* cultures reduced Fe(III) much faster under redox fluctuations (cycles of oxic-anoxic conditions) than the oxic controls from soils (Ginn et al., 2017).

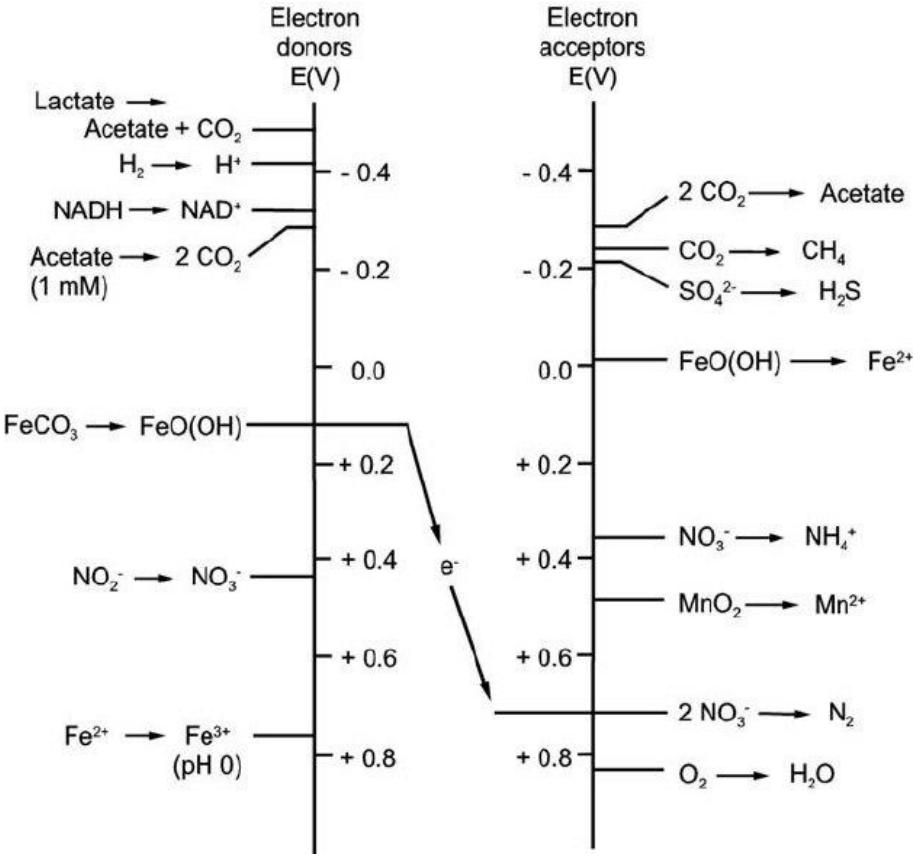


***Figure I-4.*** *The "electron towers" of redox processes in biogeochemistry (Jørgensen, 2000). The redox potentials are calculated for standard conditions at pH 7 and 1 mM concentrations of substances.*

Moreover, several mechanisms are involved in the dynamics of metals and metalloids connected with the iron cycle: (1) dissolution of Fe(III) oxides can release the adsorbed/co-precipitated elements; (2) DIRB may directly change the speciation of the associated elements, because they can use both Fe(III) and other metals/metalloids as electron acceptors (Lovley, 2008), and (3) the natural microbial communities include both DIRB and other bacteria that use

metals / metalloids as electron acceptors. The bio-reduction of the different metals/metalloids can depend on the redox potential (Figure I-5).

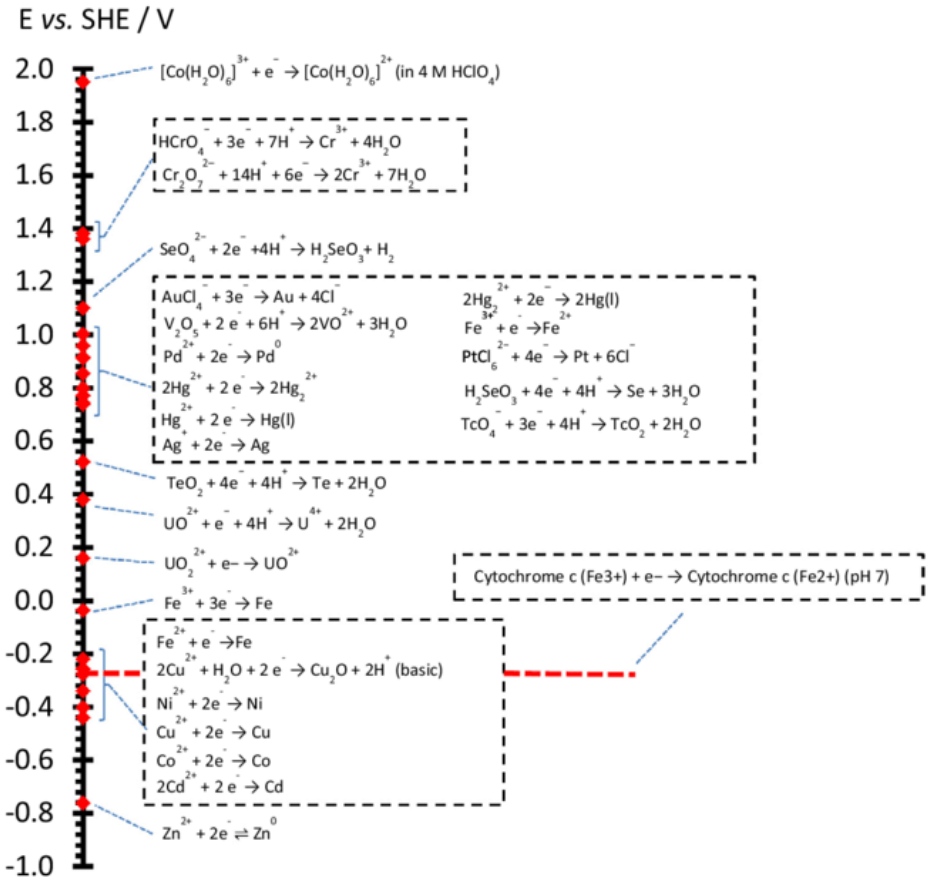


***Figure I-5.*** *Redox tower of metal ion standard reduction potentials in acidic solutions, and cytochrome-c reported vs. standard hydrogen electrode (SHE) (Bard, 2017; Dominguez-Benetton et al., 2018).*

Figure I-5 shows some standard reduction potentials of microbial electron transfer in metal reduction (Dominguez-Benetton et al., 2018). Cytochrome-c oxidase was found to be implicated in electron transfer during microbial metal reduction as an exemplar bacterial outer membrane protein enzyme, with a standard potential of 0.26 vs. SHE/V (pH 7) (Lovley et al., 1993b; Mathews, 1985). Cytochrome-c or other cell wall-associated enzymes are involved in microbial metal reduction within specific ranges of redox potentials. Therefore this potential provides an approximate thermodynamic limit for metal reduction. I.e., only metals with redox potentials above 0.26 vs. SHE/V can be reduced by bacterial cells with these characteristics.

In soils, oxidation of FeII(aq) can induce the formation of colloidal complexes of Fe and organic matter (Peiffer et al., 1999; Pullin and Cabaniss, 2003). Dissolved organic matter appears to be

a key factor in the control of the Fe(III)-oxyhydroxide dissolution rate. More specifically, organic matter, by strongly binding Fe(II), prevents Fe(II) readsorption and subsequent Fe secondary mineral formation, both of which are known to strongly decrease Fe(III)-oxyhydroxide dissolution rates (Davranche et al, 2013). In presence of humic substances, Fe particles of nanometric size (colloids) are formed in the humic matrix (Pédrot et al., 2011). Bioreduction experiments demonstrated that bacteria *(Shewanella putrefaciens* CIP 80.40 T) were able to reduce these Fe nanoparticles associated with humic organic matter about eight times faster than pure nano-lepidocrocite. These results suggest that in natural environments organic matter influence the type of iron phases formed in presence of oxygen, and the rate of Fe(II) production in anaerobic conditions. Alternance of redox conditions can lead to the formation of colloids in soils, composed of natural organic matter, complexed iron and other soil elements such as Al, Ti or Si (Thompson et al., 2006a). Moreover, under reducing conditions, the pH rise can be a key factor controlling organic matter solubilization during Mn- and Fe-oxyhydroxides reductive dissolution, as observed by Grybos et al., 2009 with a wetland soil. Pédrot et al. (2008) performed soil column experiments and showed that some trace elements, in particular Pb, Ti and U, were mobilized by humic acids containing iron nanoparticles. Humic substances directly or indirectly promoted the colloidal transport of insoluble trace elements either by binding trace elements or by stabilizing a ferric carrier phase (Pédrot et al., 2008).

## I-2 Classification of Fe-minerals

Fe and Fe-minerals are common components in several compartments of the critical zone (e.g. soils, sediments and aquifers) and are present in many different mineralogical forms. Many different scientific disciplines are interested in Fe oxides (Figure I-6). There are sixteen known Fe oxides, oxy-hydroxides and hydroxides with different mineral structures which are listed in Table I-1 (Bonneville, 2005; Cornell and Schwertmann, 2003b; Fernández-Remolar, 2015).

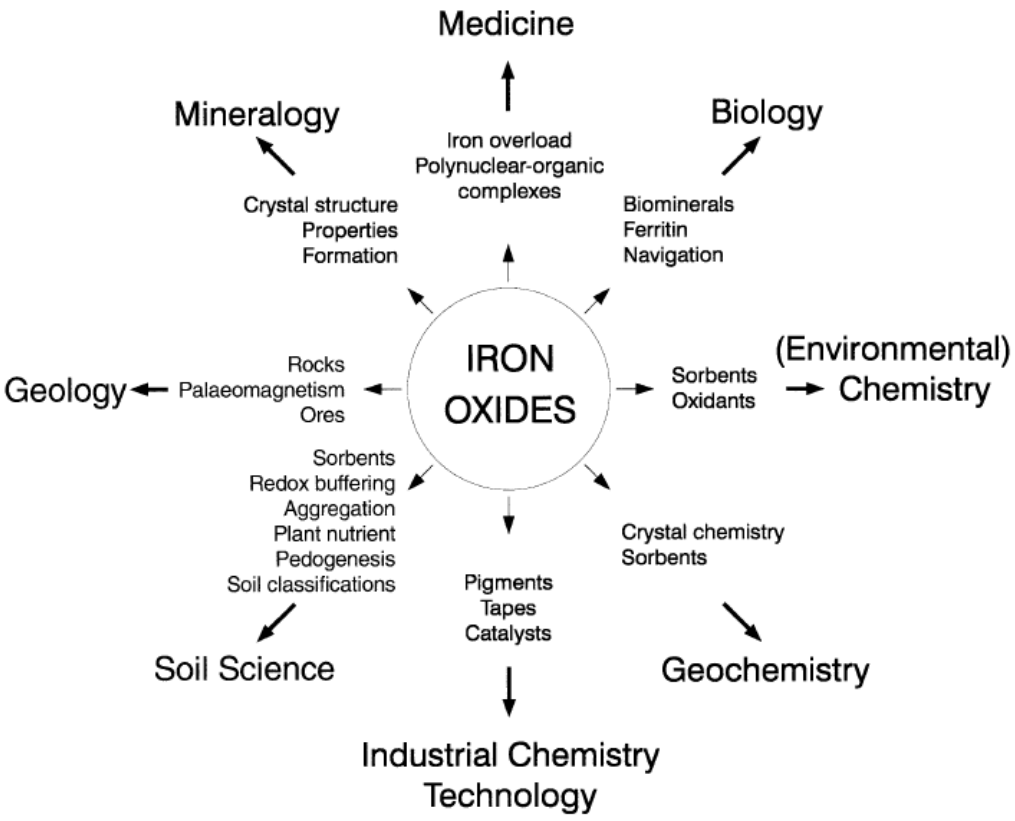


***Figure I-6.*** *The multidisciplinarity of iron oxides research (Cornell and Schwertmann, 2003b).*

***Table I-1.*** *Formula of the main Fe(III) oxides (Bonneville, 2005; Cornell and Schwertmann, 2003b; Fernández-Remolar, 2015).*

| Hydroxides/(Oxyhydr)oxides | | Oxides | |
|---|---|---|---|
| Mineral name | Formula | Mineral name | Formula |
| Goethite | α-FeOOH | Hematite | $\alpha$-$Fe_2O_3$ |
| Lepidocrocite | γ-FeOOH | Magnetite | $Fe_3O_4(Fe^{II}Fe_2^{III}O_4)$ |
| Akaganéite | β-FeOOH | Maghemite | γ-$Fe_2O_3$ |
| Schwertmannite | $Fe_{16}O_{16}(OH)_y(SO_4)_z{\cdot}nH_2O$ | β-$Fe_2O_3$ | - |
| δ-FeOOH | - | ε-$Fe_2O_3$ | - |
| Feroxyhyte | δ'-FeOOH | Wüstite | FeO |
| Ferrihydrite | $Fe_5HO_8{\cdot}4H_2O$ | Unamed high-pressure phase | $Fe_4O_5$ |
| Bernalite | $Fe(OH)_3$ | | |
| $Fe(OH)_2$ | - | | |
| Green Rust | $Fe_x^{III}Fe_y^{II}(OH)_{3x+2y-z}(A^-)_z$ | | |

Fe(III) (oxyhydr)oxides differ by their crystallinity, initially amorphous (the first formed after oxidation of Fe(II), maturation under different conditions then leads to other forms. Iron oxides polymorphs differ in the organization of the Fe(OH)n building blocks as shown in Figure I-7.

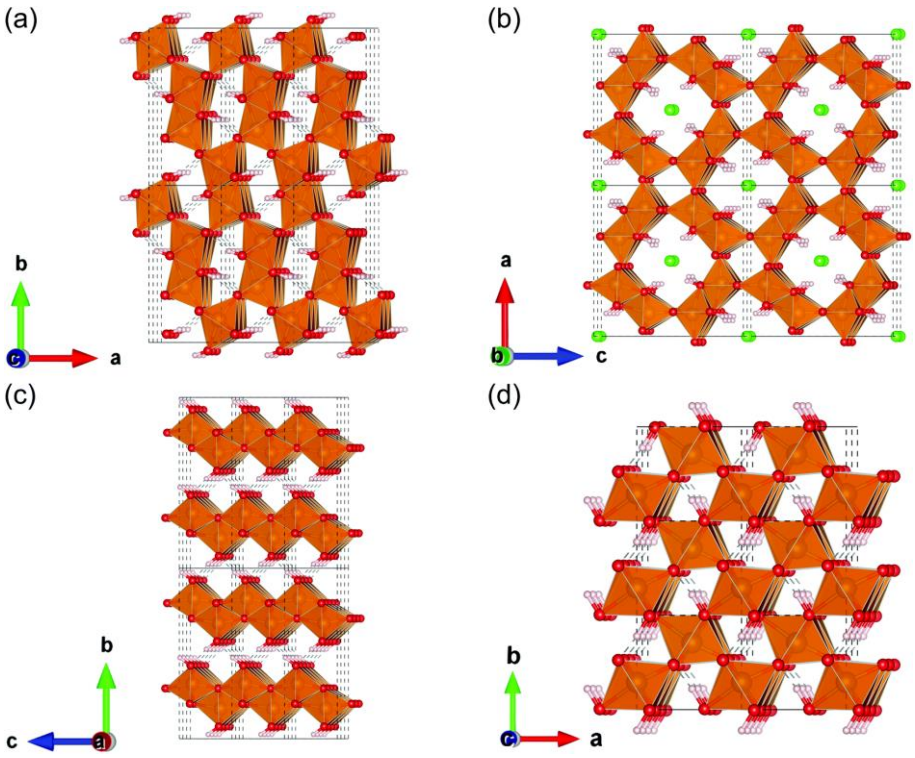


***Figure I-7.*** *FeOOH polymorphs (a) α-FeOOH; (b) β-Fe-OOH; (c) γ-FeOOH; (d) ε-FeOOH. Centered atom is iron. Red atom is oxygen, white atom is hydrogen (green atom is chloride for b = akageneite) (Sakamoto et al., 2019).*

In flooded soils, the presence of Fe(III) will induce precipitation of Fe(II) from carbonate. Baas Becking et al. (1960) reported the formation of the Fe(II)/Fe(III) hydroxy-carbonates siderite and maghemite under natural aqueous environments and Halama et al. (2016) suggested that diagenetic magnetite in banded iron formations was possibly formed by microbial Fe(III) reduction during early diagenesis (Becking et al., 1960; Helama et al., 2016). Moreover, various concentrations of Fe(II) and forms/amounts of total Fe(III) might cause other phases such as magnetite/siderite/green rust to be formed in microbial (biotic) iron reduction systems (Mortimer et al., 2011; Ona-Nguema et al., 2002; Taylor, 1980). In addition, oxidation leads to the formation of either goethite, lepidocrocite, ferrihydrite or mixtures of these phases, depending on the mode of oxidation, and the presence of impurities also may result in the release of initially co-precipitated ions (Senn et al., 2017; Taylor, 1980).

Apart from Fe (oxyhydr)oxides, iron sulfide, carbonate, phosphate and silicate minerals also play a crucial role in a variety of biogeochemical processes (Raiswell and Canfield, 2012). The principal features of the known Fe minerals are presented in the following sections. The main characteristics of the minerals studied in previous researches are given in Tables I-2 and I-3.

***Table I-2.*** *The physicochemical parameters, crystal size, morphology and range of specific surface area of the main studied Fe-oxides (Bonneville, 2005; Raiswell and Canfield, 2012; Lagroix et al., 2016; Etique et al., 2016).*

| Fe mineral class | Fe mineral name | Formula | Crystal size | Specific surface area ($m^2$ /g) | Morphology and crystal symmetry |
|---|---|---|---|---|---|
| (Oxyhydr) oxides | ferrihydrite | $Fe_2O_3$/HFO/ $Fe_4HO_8 \cdot 4H_2O$ | a few nm | 150 - 700 | more or less spherical, hexagonal |
| | goethite | α-FeOOH | tens of nm to several microns | 8 - 200 | acicular or needle shaped, orthorhombic |
| | hematite | α-$Fe_2O_3$ | - | 10 - 90 | plates, discs, rods, spindles, cubes, ellipsoids and spheres, rhombohedral |
| | lepidocrocite | γ-FeOOH | - | 15 - 260 | lath-like, tabular, diamond-shaped or rectangular, orthorhombic |
| | Magnetite | $Fe_3O_4$ | | 29-83 | cubo-octahedron and octahedron, cubic spinel |

***Table I-3.*** *Formula of Fe minerals.*

| (Oxy)hydroxyl-sulphate | Schwertmannite | $Fe_3O_8(OH)_{1\text{-}1.8}\cdot 8H_2O$ | Morphology | References |
|---|---|---|---|---|
| Sulphides | Pyrite | $FeS_2$ | grains, spherical grains, spherulites, euhedral grains | (Bonneville, 2005; Wang & Morse, 1996) |
| | Mackinawite | FeS | thin, tabular crystals | (Devey et al., 2008) |
| | Greigite | $Fe_3S_4$ | octahedral | (Hunger & Benning, 2007) |
| Carbonates | Siderite | $FeCO_3$ | globule, rhombohedral, disk-like, | ( Bonneville, 2005; Roh et al., 2003) |
| Phosphates | Vivianite | $Fe^{2+}{}_3(PO_4)_2\cdot 8H_2O$ | spherical, monoclinic-prismatic | (Roldán et al., 2002) |
| | Metavivianite | $Fe^{2+}{}_{3-x}Fe^{3+}{}_x(PO_4)_2(OH)_x\cdot(8-x)H_2O$ | flat, prismatic crystals | (Ritz et al., 1974) |
| | Chukanovite | $Fe_2(CO_3)(OH)_2$ | acicular, fibrous individuals combined in spherulites | (Pekov et al., 2007) |
| Silicates : 7 Å Minerals | Kaolinite | $Al_2Si_2O_5(OH)_4$ | high-crystallinity, blocky | (Raiswell and Canfield, 2012; Kameda et al., 2005) |
| Silicates: 10 Å Minerals | Illite | $(K, H_3O)(Al, Mg, Fe)_2(Si, Al)_4O_{10}(OH)_2(H_2O)$ | parallelepiped | (Raiswell and Canfield, 2012; Derrendinger & Sposito, 2000) |
| Silicates: 14 Å Minerals | Smectite | $(Ca, Na)(Al, Mg, Fe)_2(Si, Al)_4O_{10}(OH)_2\cdot x\,H_2O$ | dioctahedral | (Raiswell and Canfield, 2012; Delavernhe et al., 2015) |
| | Ripidolite (Mg, Fe-Chlorite) | $(Mg, Fe, Mg)_6(Si, Al)_4O_{10}(OH)_8$ | ripidolite grain | (Hamer et al., 2003) |
| | Fougerite | $*[Fe_1{}^{2+}\text{-}xFe_x{}^{3+}Mg_y(OH)_{2+2y}]^{+x}[x/nA^{-n}.mH_2O]^{-x}$ | hexagonal crystals | (Raiswell and Canfield, 2012; Trolard et al., 2007) |

* A is the interlayer anion and n its valency, with 1/4 <= x/(1+y) <= 1/3 and m <= (1-x+y)

Ferrihydrite is an amorphous or weakly crystalline Fe mineral (Bonneville, 2005). Structural studies carried out by (Feitknecht et al., 1973) indicated that 2-line ferrihydrite consists of local coherently scattered regions formed by four planar $Fe(O,OH)_6$ octahedrons and Michel et al. indicated that ferrihydrite is nano-crystalline with a delta-Keggin local structure (Michel et al., 2007; Michel et al., 2011). Whereas, in goethite each Fe(III) ion is surrounded by three $O^{2-}$ and three $OH^-$ resulting in $FeO_3(OH_3)$ octahedrons (Bonneville, 2005). Moreover, (Hiemstra, 2013) elucidated the surface structure of ferrihydrite particles whose faces have a much higher site density of singly-coordinated FeOH(H) groups in comparison to the main faces of goethite. Therefore, the related adsorption capacity per unit surface area of ferrihydrite is much higher than that of goethite. Lepidocrocite is metastable with respect to goethite which consists of double chains of $Fe(O, OH)_6$ octahedrons running parallel to the c-axis. Hematite consists of layers of $Fe(O)_6$ octahedrons and it has a similar thermodynamic stability to goethite, thus it is very often found in association with goethite (Tardy and Nahon, 1985).

## I-3 Dissolution of Fe(III) (oxyhydr)oxides and iron cycling in surface environments

Fe (oxyhydr)oxides are common components in several compartments of the critical zone (e.g. soils, sediments and aquifers) and are present in many different mineralogical forms. Understanding biogeochemical behavior and iron cycling is fundamental for many scientific communities (Bonneville et al., 2004; Roden et al., 2004). Indeed, the mobility of trace elements (TE) is partly controlled by iron speciation, mineralogy and reactivity (Cornell and Schwertmann, 2003b).

### I-3.1 Abiotic dissolution

Fe(III) (oxyhydr)oxides can be dissolved by surface protonation, a dissolution mechanism depending on pH conditions that can be enhanced by organic acids and anions ($Cl^-$) (Zinder et al., 1986). Besides, two other dissolution mechanisms have also been reported, ligand promoted dissolution and bulk reductive dissolution (Afonso et al., 1990; Holmén and Casey, 1996; Kraemer, 2004). (Siffert and Sulzberger, 1991) indicated that reductive dissolution of hematite in the presence of oxalate occurs as a photocatalytic process, and Holmén & Casey studied the rate of goethite dissolution in the presence of acetohydroxamic acid in different pH conditions. The rate of reductive dissolution of several synthetic Fe(III) (oxyhydr)oxides in 10 mM

ascorbate at pH 3 has been shown to occur according to the order ferrihydrite> lepidocrocite > goethite> hematite (Bonneville et al., 2004; Larsen and Postma, 2001).

In natural environments, reduction of Fe(III) (oxyhydr)oxides may also be linked to the presence of hydrogen sulfide ($H_2S/HS^-$) produced by sulfate-reducing bacteria (Dos Santos Afonso and Stumm, 1992; Neal et al., 2001).

### I-3.2 Biotic dissolution

The natural solubility of crystalline Fe (oxyhydr)oxides is low. However, interactions with microbes and organic substances can improve the formation of soluble Fe(III) and increase the availability of Fe and associated TEs (Colombo et al., 2014). Biogeochemical aspects of Fe cycling in the major microbially mediated and abiotic reactions have been extensively covered (Melton et al., 2014), together with Fe redox transformations and availability of TEs (Zhang et al., 2012), as well as Fe redox cycling in bacteriogenic Fe oxide-rich sediments (Gault et al., 2011). In aerobic environments at circumneutral pH conditions, Fe is generally relatively stable and highly insoluble in the form of (oxyhydr)oxides (e.g., $Fe(OH)_3$, FeOOH, $Fe_2O_3$). However, in anaerobic conditions these minerals can be reductively dissolved (Roden et al., 2004; Roden and Wetzel, 2002) by microbial and abiotic pathways (Bonneville et al., 2004; Hansel et al., 2004; Shi et al., 2016; Thompson et al., 2006b). Microbial Fe(III) reduction is an important mechanism for iron cycling: heterotrophic Fe(III)-reducing bacteria could convert solid-phase Fe(III) minerals into dissolved and solid Fe(II) phases during their metabolic processes (Lovley, 1997). In particular, dissolutive reduction of iron (oxyhydr)oxides can be driven by dissimilatory iron reducing bacteria (DIRB), significantly contributing to the biogeochemical cycle of Fe and subsequent TE cycling (Cooper et al., 2006; Ghorbanzadeh et al., 2017; Levar et al., 2017). Microbial dissimilatory iron reduction (DIR) is an ubiquitous biogeochemical process in suboxic environments (Crosby et al., 2005; Lovley, 2000; Schilling et al., 2019; Wilkins et al., 2006). DIRB use Fe (oxyhydr)oxides as electron acceptors instead of oxygen for oxidizing organic matter. In general, for ferrihydrite and other short-range ordered (SRO) poorly crystallized iron minerals, the microbial Fe(III) reduction rates are more rapid (typically within hours), than the microbial reduction of the well-ordered minerals hematite ($\alpha$-$Fe_2O_3$), goethite ($\alpha$-FeOOH) (e.g., several months), and lepidocrocite ($\gamma$-FeOOH) (Ginn et al., 2017; Roden, 2006a). The rate of Fe(III) reduction will influence mobility of TEs initially immobilized on or in Fe (oxyhydr)oxides through adsorption or co-precipitation. Crystallinity, specific surface area and size among other factors may influence the reactivity of Fe

(oxyhydr)oxides in relation to the metabolic activity and diversity of DIRB (Aino et al., 2018; Cutting et al., 2009), as detailed in the next section.

### I-3.3 Secondary minerals formed during the bio-reduction of Fe oxides

The first product of the bioreduction of iron oxides is soluble Fe(II). This chemical species can sorb to residual Fe(III)-oxides, or be involved in (bio)geochemical reactions generating secondary minerals (Table I-4) such as green rust (Génin et al., 1998; Ona-Nguema, et al., 2002), vivianite, siderite, magnetite (Fredrickson et al., 1998; Maitte et al., 2015; Urrutia et al., 1998; Zachara et al., 1998), chukanovite (O'Loughlin et al., 2010). The type of secondary product depends on the composition of the liquid phase, the presence of complexants, and on bacterial activity.

***Table I-4.*** *Formula of the main minerals potentially formed during bio-reduction of Fe(III)-oxides.*

| Mineral | Formula | References |
|---|---|---|
| Siderite | $Fe^{2+}CO_3$ | (Roh et al., 2003; Zachara et al., 1998) |
| Chukanovite | $Fe^{2+}_2(CO_3)(OH)_2$ | (O'Loughlin et al., 2010) |
| Vivianite | $Fe^{2+}_3(PO_4)_2{\cdot}8H_2O$ | (Roldán et al., 2002; Urrutia et al., 1998) |
| Green rust | $[Fe^{2+}_4Fe^{3+}_2(HO^-)_{12}]^{2+}\cdot[CO^{2-}_3\cdot 2H_2O]^{2-}$ / $[Fe^{2+}_4Fe^{3+}_2(HO^-)_{12}]^{2+}\cdot[SO^{2-}_4\cdot 2H_2O]^{2-}$ | (Ona-Nguema et al., 2002; Ona-Nguema et al., 2009; Zegeye et al., 2005) |
| Magnetite | $Fe^{2+}Fe^{3+}_2O_3$ | (Maitte et al., 2015) |

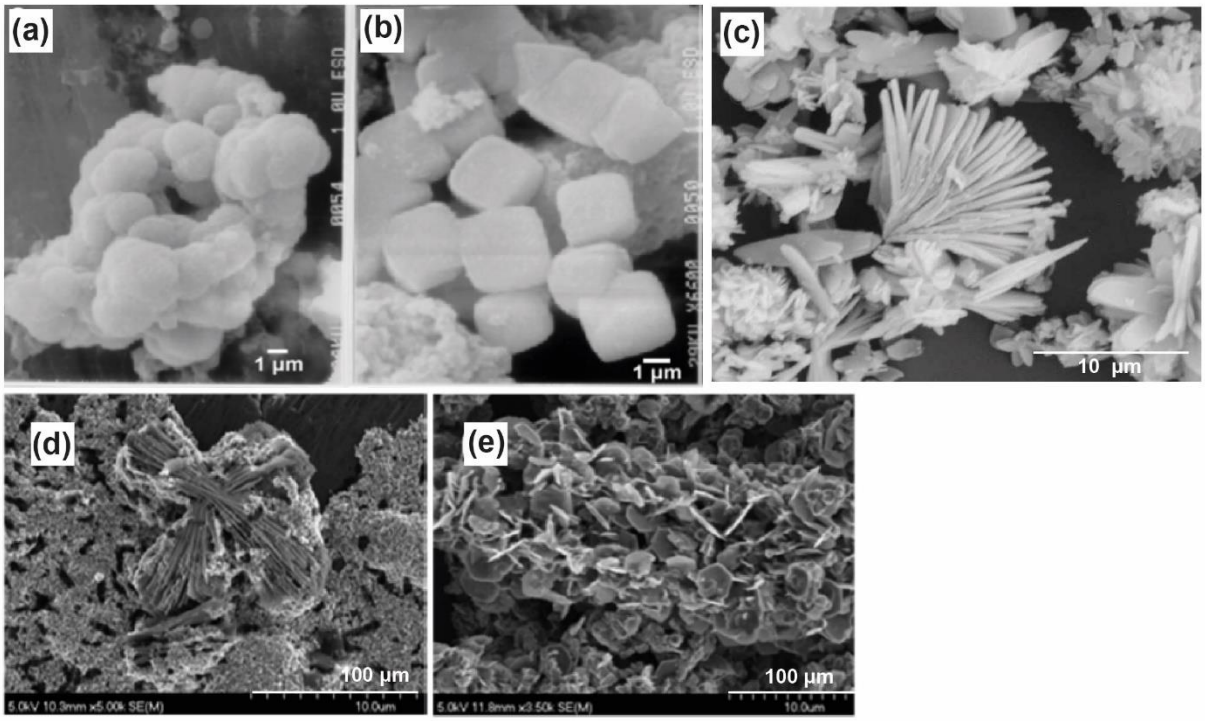


***Figure I-8.*** *SEM images of (**a**) siderite globule formed by Shewanella (W3-7-1) under a H2/CO2 atmosphere and (**b**) rhombohedral siderite formed by Shewanella (NV-1) under a H2/CO2 atmosphere (Roh et al., 2003), (**c**) SEM images of the starting vivianite (Roldán et al., 2002); SEM images of (**d**) magnetite/FHC formed in the unamended system and of (**e**) green rust formed in the systems containing 500 µM phosphate (O'Loughlin et al., 2010).*

As an example, using a continuously fed column experiment, Hansel et al. (2003) observed the transformation of ferrihydrite by *Shewanella* into goethite (via dissolution/reprecipitation) and/or magnetite (via solid-state conversion) (Hansel et al., 2003b), whereas Ona-Nguema et al. (2002) observed the formation of carbonate green rust by *Shewanella putrefaciens* (Ona-Nguema et al., 2002) and Kukkadapu et al. (2004) observed the formation of magnetite in the absence of phosphate whereas carbonate green rust and vivianite were formed in presence of phosphate during the bio-reduction of 2-line Si-ferrihydrite by the same iron-reducing bacterial genus (Kukkadapu et al., 2004).

## I-4 Iron-reducing bacteria (IRB)

### I-4.1 Dissimilatory Iron-Reducing Bacteria (DIRB)

Dissimilatory Fe(III) reducing microorganisms are a group of microorganisms (both bacteria and archaea) that can perform anaerobic respiration using Fe(III) as a terminal electron acceptor before using molecular oxygen ($O_2$), which is the terminal electron acceptor reduced to water ($H_2O$) in aerobic respiration (Lloyd, 2003). The role of DIRB in Fe redox transformations has

been evidenced for more than three decades (Lovley, 1991; Lovley et al., 1987; Meile and Scheibe, 2019; Stern et al., 2018; Su et al., 2020), during which more than 100 distinct IRB species have been found. *Geobacter* and *Shewanella* are the two most studied IRB genera up to now (Engel et al., 2019; Han et al., 2018; Jiang et al., 2020; Li et al., 2012), however DIRB are widely distributed phylogenetically DIRB and iron-reducing archaea have been isolated from a range of environments, including freshwater (Laverman et al., 1995) or sea water (Rosselló-Mora et al., 1995), marsh sediments, groundwater (MacRae et al., 2007), soils (Ottow and Glathe, 1971), geothermal systems (Lee et al., 2017), deep sea hydrothermal fields (Lin et al., 2016; Zeng et al., 2015), and sediments (Tebo and Obraztsova, 1998).

Table I-5 gives a non-exhaustive overview of the diversity of Fe(III)-reducing bacteria.

***Table I-5.*** *Iron-reducing archaea and other iron-reducing bacteria strains.*

| Iron reducing microorganism | Context | References |
|---|---|---|
| *Geoglobus acetivorans sp. nov.* | A Fe(III)-reducing archaeon | (Slobodkina et al., 2009) |
| *Deferribacter thermophilus gen. nov., sp. nov.* | A Novel Thermophilic Manganese- and Iron-Reducing Bacterium | (Greene et al., 1997) |
| *Geothrix fermentans gen. nov., sp. nov.* | A novel Fe(III)-reducing bacterium | (Coates et al., 1999) |
| *Acidiphilium cryptum JF-5* | Microbial Reduction of Fe(III) in Acidic Sediments (Glucose) | (Küsel et al., 1999) |
| *Bacillus subterraneus sp. nov.* | An iron and manganese reducing bacterium | (Kanso et al., 2002) |
| *Pelosinus fermentans gen. nov.* | An iron(III)-reducing bacteria | (Shelobolina et al., 2007) |
| *Geoalkalibacter subterraneus sp. nov.* | An anaerobic Fe(III)- and Mn(IV)-reducing bacterium | (Greene et al., 2009) |
| *Bacillus pseudofirmus MC02* | Extracellular reduction: AQDS (anthraquinone-2, 6-disulfonae), humic | (Ma et al., 2012) |

| | | |
|---|---|---|
| | acids (HA) and Fe(III) oxides were electron acceptors. | |
| *Pelobacter carbinolicus* | Fe(III) and S(0) reduction | (Lovley et al., 1995) |
| *Clostridium butyricum* | Isolated from a microbial fuel cell | (Park et al., 2001) |
| *Pyrobaculum igneiluti* | Thermophile isolated from geothermal system | (Lee et al., 2017) |
| *Pyrodictium delaneyi* | Thermophile isolated from active deep-sea hydrothermal vent chimney | (Lin et al., 2016) |
| *Caloranaerobacter ferrireducens* | Thermophile isolated from ocean hydrothermal field | (Zeng et al., 2015) |
| *Wolinella succinogenes* | Isolated from freshwater marsh | (Laverman et al., 1995) |
| *Desulfotomaculum reducens* | Isolated from metal-contaminated sediments, capable reducing Fe(III) in presence of electron donors | (Dalla Vecchia et al., 2014; Tebo and Obraztsova, 1998) |

Thus, iron-reducing bacteria form a very diverse group, with microbes belonging to a large range of phyla. Up to now, no functional gene specific to dissimilatory Fe(III) reduction and common to all these organisms has been identified, so it is very difficult to monitor all Fe(III)-reducing micro-organisms in a natural complex communities. Enrichment and isolation methods can still be applied, however they don't give access to the whole Fe(III)-reducing community. An alternative approach is to target specific well-known Fe(III)-reducing micro-organisms.

The two most studied DIRB belong to the genera *Shewanella* and *Geobacter*. These model strains have been used in many research studies, in particular those focused on the elucidation of the mechanisms of bacterial Fe(III) reduction.

### I-4.2 Iron reduction by fermentative bacteria

A wide variety of fermentative micro-organisms are able to reduce Fe(III) into Fe(II) during anaerobic growth with fermetable sugars or amino-acids. As soon as 1926, Runov described the reduction of Fe(III) by pure strains of *Escherichia coli*, *Clostridium pasteurianum* and

*Lactobacillus lactis*. During fermentation in presence of Fe(III), a part of the electron flow contributes to Fe(III) reduction. The benefit of this reaction for the growth of bacteria was debated, less than 5% of the reducing equivalents were reported to be transferred to Fe(III) (Lovley, 1987) however this reaction can significantly contribute to Fe(III) reduction in presence of fermentable substrates.

Robert (1947) found with strains of *Bacillus polymyxa* that even if, in principle, 24 mol Fe(III) should be reduced per mol of glucose, most of the electron equivalent were recovered as ethanol, 2,3 ethylene glycol, lactic acid, formic acid and hydrogen. Even if only a small part of electron equivalents are transferred to Fe(III), this mechanism improves the fermentation balance inducing more favorable thermodynamic conditions for the organism able to perform this reduction. This could confer competitive advantage to these fermentative microbes in carbon-limited environment like deep biosphere, according to Vandieken et al. (2018).

The composition of iron oxides can influence their bioreduction by fermentative micro-organisms. In particular, the substitution of Fe by Al, Mn, Cr, or Co in synthetic goethites induced a decrease of their reduction during fermentation of glucose (Bousserrhine et al., 1999; Dominik et al., 2002).

The fermentation of glucose can be enhanced in presence of iron oxides (such as hematite, Dong et al., 2017), not only by consuming electron equivalents, but also because of a buffering effect preventing acidification of the medium. This phenomenon is linked to $H_2$ production during fermentation and a reaction of $H_2$ with iron oxide that consumes $H^+$:

$Fe_2O_3 + 4H^+ + H_2 = 2\ Fe^{2+} + 3\ H_2O$ (Dong et al., 2017)

Recently, a metagenomics analyse was performed on a glucose-fermenting microbial consortium capable of reducing goethite in presence of glucose (Gagen et al., 2019). A metagenome assembled genome (MAG) of an iron reducer belonging to the alphaproteobacterial genus *Telmatospirillum* was obtained, encoding putative metal transfer reductases and a novel outer membrane cytochrome potentially contributing to extracellular electron transfer. Metabolic products suggested that goethite was a hydrogen sink in the culture. Therefore, recent results from Dong et al. (2017) and Gagen et al., (2019) suggest that fermentative bacteria could induce iron reduction via hydrogen production.

Beside the Fe(III) reduction directly linked to the metabolism of fermentative bacteria, fermentation products, such as organic acids and $H_2$, can be important electron donors for dissimilatory iron-reducing bacteria, either in laboratory culture media with mixed cultures, or, possibly in natural environments (Lovley, 1987).

### I-4.3 The genus *Shewanella*

*Shewanella* spp. are Gram negative (Gamma proteobacteria), non spore forming motile rods with positive oxidase and catalase reactions (Satomi, 2014). *Shewanella* spp. are widely distributed in natural environments and their natural habitats are all forms of water and soil compartments, they have been found in marine environments, proteinaceous foods, and occasionally clinical samples (Fredrickson et al., 2008; Vignier et al., 2013). The organism belonging to the genus *Shewanella* was first isolated in 1931 from putrefied butter and was successively called *Achromobacter putrefaciens*, *Pseudomonas putrefaciens*, *Alteromonas putrefaciens* (Derby and Hammer, 1931; Vignier et al., 2013). Finally MacDonnell and Colwell suggested that *Alteromonas putrefaciens*, along with two other marine species should be transferred to a completely new genus, *Shewanella*, which was named in honor of Dr J. Shewan for his work on the microbiology of fish (MacDonell and Colwell, 1985). Up to date, more than 50 species have been classified in this genus, showing various activities, such as metal reduction (e.g., Fe reduction) or trimethylamine production (Satomi, 2014).

In fact, microbial Fe reduction was described by researchers at the beginning of 20$^{th}$ century (Starkey and Halvorson, 1927), however the first strain of *Shewanella* with dissimilation Fe reduction activity was isolated in 1987 from petroleum reservoirs (Semple and Westlake, 1987). Currently known and studied *Shewanella* species are tolerant to oxygen and thus reasonably robust for applications such as remediation of polluted environments with various oxygen concentrations (Satomi, 2014; Serres and Riley, 2006).

#### Metabolic characteristics of *Shewanella*

*Shewanella* genus gather facultative anaerobe species displaying a wide diversity of metabolic features. Frequent characteristics of species are the reduction of $H_2S$ from thiosulfate, reduction of nitrate and iron oxides. A large diversity of organic molecules can be used in aerobic conditions, including sugars, organic acids, amino-acids, polymers such as dextrin. In the absence of oxygen, members of this genus have been proved to be capable of using a variety of other electron acceptors e.g., iron, thiosulfate, sulfite, or elemental sulfur (Burns and DiChristina, 2009), as well as fumarate (Pinchuk et al., 2011) while using a smaller range of

organic electron donors such as lactate, formate and $H_2$ for respiration (Meshulam-Simon et al., 2007). Moreover, some *Shewanella* species can also grow by fermentation of glucose (Bowman et al., 1997; Ivanova et al., 2001), tryptone, peptone, yeast extract and pyruvate when Fe(III) is limited (Toffin et al., 2004). Apart from iron, some members of this genus have the ability to use a wide range of metals and metalloids as electron acceptors, including manganese, chromium, uranium and arsenic, due to the broad specificity of the anaerobic reductase enzyme system in *Shewanella* (Tiedje, 2002). Moreover, *S. oneidensis* MR-1 strains have been shown to be able to reduce and mobilize toxic and radioactive metallic pollutants, including arsenic, cobalt, chromium, mercury, plutonium, selenium, technetium, and uranium (Satomi, 2014). Morphologic observations on two species of *Shewanella* are given in Figure I-9.

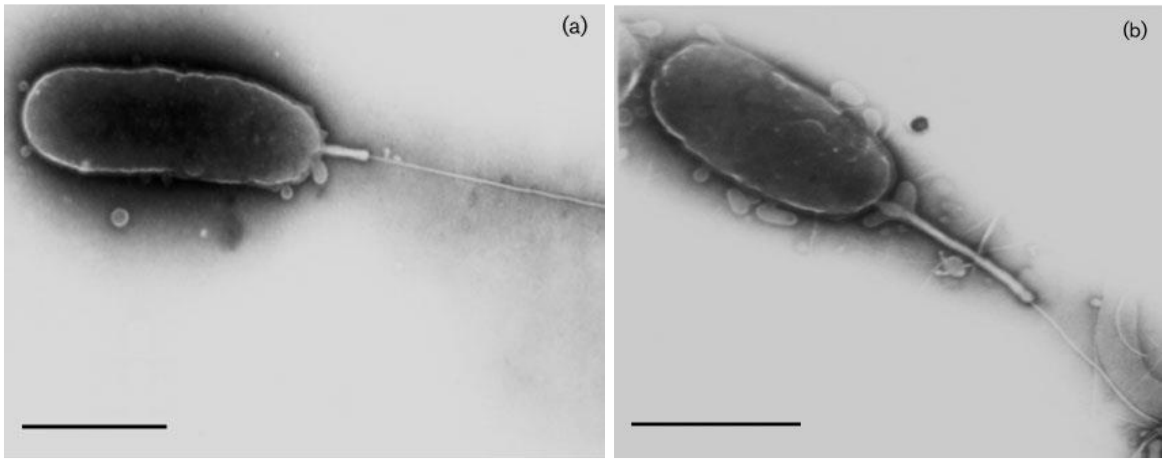


***Figure I-9.*** *Transmission electron micrographs of cells of strains Shewanella psychrophila (a) and Shewanella piezotolerans (b). Cells were grown on 2216E agar plates at 15 ˚C for 16 h. One colony was picked and dispersed in 100 µL PBS buffer, and 5 µL liquid was placed on a copper grid for negative staining using 1% uranyl acetate. Bars, 0.5 µm (Xiao et al., 2007).*

The main studies performed with *Shewanella* species are summarized in Table I-6.

***Table I-6.*** *Selected studies about some Shewanella strains and Fe(III) reduction.*

| DIRB | Context | References |
|---|---|---|
| *Shewanella amazonensis* sp. nov. | A novel metal-reducing facultative anaerobe from Amazonian shelf muds | (Venkateswaran et al., 1998) |
| *Shewanella algae* strain *BrY* | Microbial and surface chemistry controls on reduction of synthetic Fe(III) oxide minerals by DIRB | (Urrutia et al., 1998) |

| | | |
|---|---|---|
| *Shewanella putrefaciens* IR-1 | Isolation, identification, electrochemical activity and direct electrode reaction of an anaerobic dissimilatory Fe(III)-Reducing bacterium | (Hyun et al., 1999; Kim et al., 1999a; Kim et al., 1999b) |
| *Shewanella* sp. HN-41 | Organic acid-dependent iron mineral formation by IRB | (Lee et al., 2007) |
| *Shewanella* sp. strain PV-4 | Metal reduction and iron biomineralization by a psychrotolerant Fe(III)-reducing bacterium. | (Roh et al., 2006) |
| *Shewanella baltica* W3-6-1(close to *oneidensis* MR-1) | Metal reduction at cold temperatures by *Shewanella* | (Stapleton Jr et al., 2005) |
| *Shewanella piezotolerans* WP3 | Iron reduction of magnetite biomineralization mediated by IRB | (Wu et al., 2011) |
| *Shewanella putrefaciens* strain CN32 | Iron reduction of structural Fe(III) in illite and goethite and Influence of electron donor/acceptor concentrations on hydrous ferric oxide (HFO) bioreduction | (Dong et al., 2003; Fredrickson et al., 2003) |
| *Shewanella putrefaciens* strain CN32 | Biomineralization of Poorly Crystalline Fe(III) Oxides by DMRB; Influence of electron donor/acceptor on HFO bioreduction It is shown that crystalline ferric (goethite, hematite, lepidocrocite), ferrous(siderite, vivianite), and mixed valence(magnetite, green rust) iron solids are formed in anoxic, circumneutral DMRB incubations. | (Fredrickson et al., 2003; Zachara et al., 2002) |
| *Shewanella putrefaciens* strain CN32 | Biotransformation of two-line silica-ferrihydrite by a DIRB: formation of carbonate green rust in the presence of phosphate | (Hansel et al., 2003b; Kukkadapu et al., 2004) |

| | | |
|---|---|---|
| *Shewanella putrefaciens* strain CN32 | Structural constraints of ferric (hydr)oxides on dissimilatory iron reduction and the fate of Fe(II): | (Hansel et al., 2004) |
| *Shewanella putrefaciens* 200 | Effect of redox cycling on transition metal speciation in iron bearing sediments | (Cooper et al., 2006) |
| *Shewanella putrefaciens* 200R | Transformation of hematite into magnetite during DIRB process | (Behrends and Van Cappellen, 2007) |
| *Shewanella oneidensis* MR-1 | Ferrihydrite-associated organic matter (OM) stimulates reduction by *Shewanella oneidensis MR-1* and a complex microbial consortia | (Cooper et al., 2017b) |
| *S. oneidensis MR-1* | It can live in both oxic and anoxic conditions | (Ginn et al., 2017) |

### I-4.3 The genus *Geobacter*

*Geobacter* spp. are Gram-negative, which are distributed in a diverse range of soils and aquatic sediments (Lovley et al., 2004). *Geobacter* is a genus belonging to *Proteobacteria*, which is located within the *Deltaproteobacteria*, comprising the family *Geobacteraceae* and including also the genera *Desulfuromonas*, *Desulfuromusa*, *Geoalkalibacter*, *Geopsychrobacter*, *Geothermobacter*, *Malonomonas*, and *Pelobacter*, and several species of Fe(III)-reducing bacteria (Lovley et al., 1993a; Straub, 2011). *Geobacter* spp. strains were the first organisms to be isolated that could carry out the reduction of insoluble metal oxides coupled with the oxidation of acetate (Lovley et al., 1987). The first strain of *Geobacter metallireducens* was isolated from the Potomac River in 1987 and identified as GS-15 (Lovley and Phillips, 1988). *Geobacter* spp. are abundant in anaerobic soils and sediments, thus they have been supposed to play an important role in the cycling of carbon, iron and manganese, phosphorous and trace metals which are associated with Fe(III) and Mn(II) oxides in anaerobic soils, sediments and subsurface environments (Lovley, 1993; Lovley et al., 2004).

#### Metabolic characteristics of *Geobacter*

This strict anaerobe chemoorganotroph oxidizes several short-chain fatty acids (acetate, propionate, butyrate, isobutyrate, valerate, isovalerate, pyruvate, formate, lactate), alcohols (ethanol, propanol, butanol), and monoaromatic compounds, and sometimes $H_2$, with Fe(III) as the sole electron acceptor (Lovley et al., 1993; Coates et al., 1996).

Following the successful isolation of *Geobacter metallireducens*, several other *Geobacte*r spp. have been found and studied to explore their metabolic functions, including the potential for biodegradation of environmental toxic pollutants. *Geobacter* spp. are capable of oxidizing organic compounds to carbon dioxide through the reduction of various extracellular electron acceptors, which makes them remarkable on those applications (Mahadevan et al., 2011). These acceptors include insoluble Fe(III) and Mn(IV) oxides (Lovley and Phillips, 1988; Lovley et al., 1987), other metal species such as uranium(VI) (Lovley et al., 1991) and vanadium(V) (Ortiz-Bernad et al., 2004), and also humic substances (Lovley et al., 1996a).

Morphologic observations of *Geobacter sulfurreducens* are given in Figure I-10.

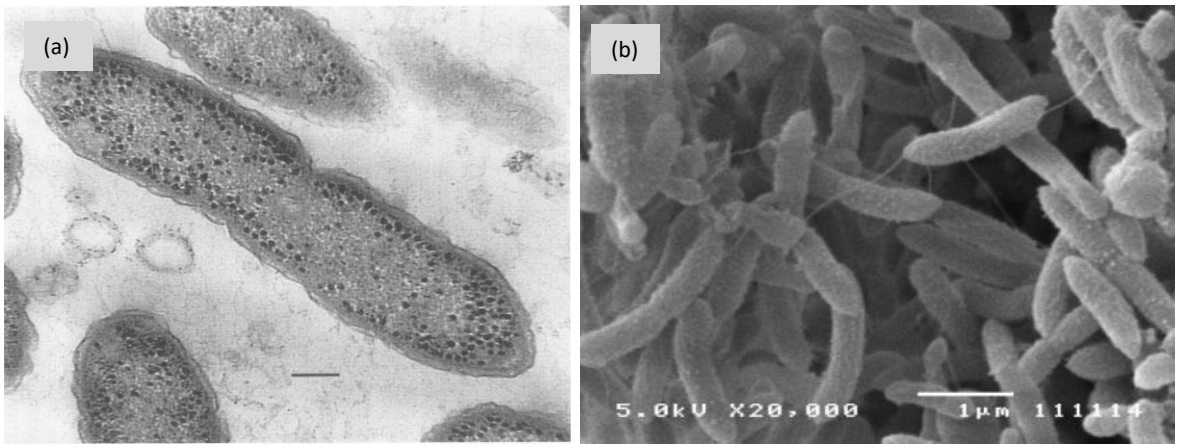


***Figure I-10.*** *(a) Transmission electron micrograph of a thin section of strain Geobacter sulfurreducens PCA, bar 0.2 µm (Caccavo et al., 1994); (b) SEM images of Geobacter sulfurreducens growing on a gold electrode (Richter et al., 2008).*

Selected studies performed with some *Geobacter* species are summarized in Table I-7.

***Table I-7.*** *Selected studies about some Shewanella strains and Fe(III) reduction.*

| DIRB | Researches | References |
|---|---|---|

| | | |
|---|---|---|
| *Geobacter bremensis* sp. nov. and *pelophilus* sp. nov. | iron(III)-reducing bacteria | (Straub and Buchholz-Cleven, 2001) |
| *Geobacter bemidjiensis* sp. nov. and *psychrophilus* sp. nov. | iron(III) citrate, iron(III) oxides, AQDS as electron acceptors and adaptation to disruption of the electron transfer pathway | (Leang et al., 2005; Nevin et al., 2005) |
| *Geobacter lovleyi sp. nov. Strain SZ* | Fe(III), Mn(IV), fumarate and malate as electron acceptors | (Sung et al., 2006) |
| *Geobacter pickeringii sp. nov.* and *Geobacter argillaceus sp. nov.* | Fe(III), AQDS, humic acids as electron acceptors | (Shelobolina et al., 2007) |
| *Geobacter sulfurreducens* | Microbial Reduction of Fe(III) in Hematite Nanoparticles: under two $H_2$ partial pressures (0.01 and 1 atm) and three pH (7.0, 7.5, and 8.0) conditions | (Yan et al., 2008) |
| *Geobacter uraniireducens sp. nov.* | Fe(III), Mn(IV), AQDS and ferruginous smectite as electron acceptors | (Kashefi et al., 2008; Shelobolina et al., 2008) |
| *Geobacter daltonii sp. nov* | Fe(III)-oxhydroxide, Fe(III) citrate, elemental sulfur as electron acceptors | (Prakash et al., 2010) |
| *Geobater metallireducens* | Dissolved fulvic acids to enhance microbial iron reduction | (Kulkarni et al., 2018) |

### I-4.4 Comparison of the genera *Shewanella* and *Geobacter*

When we consider only the characteristics common to all species of the genera, the main phenotypic differences between *Shewanella* and *Geobacter* are the behaviour according to redox conditions, *Shewanella* genus is facultative anaerobic whereas *Geobacter* genus is strictly anaerobic (Table I-8). The motility of *Shewanella* genus also contrast with the non-motile character of *Geobacter*.

If we look upon the two genera as groups of classified species, *Shewanella* is characterized by a larger versatility of characteristics, in particular in the field of physiology and respiration, than *Geobacter*.

***Table I-8.*** *Detailed description of the genera Shewanella and Geobacter.*

| Genus | *Shewanella* (Holt et al., 2005; Lemaire et al., 2020; MacDonell & Colwell, 1985) | *Geobacter* (Childers et al., 2002; Coppi et al., 2007; Lovley et al., 1993; Lovley et al., 2011; Prakash et al., 2010) |
|---|---|---|
| Morphology and motility | Straight or curved rods, non-pigmented, motile by polar flagella. | Rod-shaped cells 2-4 by 0.5 µm, non motile, no spore formation. |
| Gram | negative | negative |
| Metabolism | facultative anaerobic chemoorganotroph physiological and respiratory versatility. | strict anaerobic chemoorganotroph completely oxidizes acetate, ethanol, propionate, butyrate, isobutyrate, propanol, butanol, toluene, benzoate, benzaldehyde, benzylalcool, polyhydroxybutirate, p-hydroxybenzaldehyde, p-hydroxybenzylalcool, phenol, p-cresol into $CO_2$ with Fe(III) as electron acceptor. also degrade acetate with Mn(IV), nitrate and U(VI). Nitrate is reduced into ammonium. The organic electron donor is completely oxidized to carbon dioxide. |
| Other characters | produces hydrogen sulphide | cells contain menaquinone and c-type cytochromes, but lack ubiquinone. Vitamins are not required for growth, but growth is enhanced by their presence. |
| Number of described species | 70 (in 2020) | 19 (in 2019) |

| Type species | *Shewanella putrefaciens* | *Geobacter metallireducens* |
|---|---|---|
| GC% | 44-47 | 50–61 |

### I-4.5 Primers for the detection and quantification of *Shewanella* and *Geobacter*

Both *Shewanella* and *Geobacter* are genera with many species that have diverse respiratory abilities. They are also considered to play an important role in bioremediation and in biogeochemical cycles of several elements. The use of primers to detect specific species or genera of bacteria or to quantify their abundance are well developed methods based on molecular microbiology (Li et al., 2018). Thus, for the development of research programs related to Fe(III) bioreduction it would be useful to find primers allowing to target and quantify *Shewanella* and *Geobacter* by qPCR with accuracy and broad coverage, considering the increasing number of isolated species belonging to these two genera.

According to several studies, different primers developed for the detection and/or quantification of *Shewanella* and *Geobacter* in environmental samples are listed in Table I-9.

***Table I-9.*** *Primers for detection and/or quantification of Shewanella and Geobacter 16S rRNA genes.*

| Gene target | Primer | Primer sequence alignment (5' - 3') | References |
|---|---|---|---|
| *Shewanella* 16S rRNA | 211F<br>1259R | CGCGATTGGATGAACCTAG<br>GGCTTTGCAACCCTCTGTA | (Todorova and Costello, 2006) |
| *Shewanella* 16S rDNA | 783F<br>l245R | AAAGACTGACGCTCAKGCA<br>TTYGCAACCCTCTGTACT | (Snoeyenbos-West et al., 2000; Zhou, 2008) |
| *Shewanella* 16S rRNA | 640F<br>815R | RACTAGAGTCTTGTAGAGG<br>AAGDYACCAAAYTCCGAGTA | (Li et al., 2018) |
| *Shewanella* 16S rRNA | 120F<br>220R | GCCTAGGGATCTGCCCAGTCG<br>CTAGGTTCATCCAATCGCG | (Himmelheber et al., 2009) |

| | | | |
|---|---|---|---|
| *Shewanella* 16S rRNA | 211F<br>815cR | CGCGATTGGATGAACCTAG<br>AAGDCACCAAAYTCCGAGTA | (Li et al., 2018) |
| *Geobacter* 16S rDNA | 561F<br>825R | GCGTGTAGGCGGTTTCTTAA<br>TACCCGCRACACCTAGTTCT | (Cummings et al., 2003) |
| *Geobacter* 16S rRNA | 564F<br>840R | AAGCGTTGTTCG GAWTTAT<br>GGCACTGCAGGGGTCAAT | (Cummings et al., 2003; Kim et al., 2012) |
| *Geobacter* 16S rDNA | Gx.182F<br>Gx.472R | AGA CCT TCG GCT GGG ATG CT<br>AGG TAC CGT CAA GTA ACA SS | (Snoeyenbos-West et al., 2000) |
| *Geobacter* 16S rRNA | 196F<br>535R | GAATATGCTCCTGATTC<br>TAAATCCGAACAACGCTT | (Amos et al., 2007) |

For the listed primers in Table I-9, target species, gene fragment length, PCR/qPCR condition, coverage and specificity described in literature are given in Table I-10.

***Table I-10.*** *Summary of the primers coverage and specificity for Shewanella and Geobacter species.*

| Primer paris | Length /bp | Target species | *PCR/**qPCR condition | Coverage (%) | Specificity (%) |
|---|---|---|---|---|---|
| 211F/1259R | 1048 | *Shewanella sp.* | *3 min at 94 °C, 33 cycles of 30 s at 94 °C, 30 s at 53 °C and 60 s at 72 °C | 70 | 95 |
| 783F/1245R | 518 | *Shewanella sp.* | **15 min at 95 °C; 40 cycles of 10 s at 95 °C, 20 s at 55 °C, and 20 s at 72 °C | 90 | 71 |
| 640F/815R | 195 | *Shewanellaceae* | **1 min at 95 °C, 40 cycles of 5 s at 95 °C, 30 s at 55 °C and 30 s at 72 °C | 92.4 | 100 |
| 120F/220R | 116 | *Shewanellaceae* | **1 min at 95 °C, 40cycles of 5 s at 95 °C and 30 s at 61 °C | 70.8 | 100 |

| | | | | | |
|---|---|---|---|---|---|
| 211F/815cR | 625 | *Shewanellaceae* | *3 min at 94 °C, followed by 8 cycles of 30 s at 94 °C, 30 s at 60 °C and 40 s at 72 °C, then annealing temperature decreases one degree per cycle, followed by 27 cycles of 30 s at 94 °C, 30 s at 53 °C and 40 s at 72 °C | 71.6 | 100 |
| 561F/825R | 264 | *Geobacteraceae* | *4 min at 94 °C, 35 cycles of 30 s at 94°C, 30 s at 60 to 55 °C, 30 s at 72 °C | | |
| 564F/840R | 312 | *Geobacteraceae* | **15 min at 95 °C, 40 cycles of 10 s at 95°C, 20 s at 60 °C, 20 s at 72 °C | | |
| Gx.182F/ Gx.472R | 323 | *Geothrix spp.* | - | | |
| 196F/535R | 357 | *Geobacter lovleyi* | **2 min at 50 °C, 15 min at 95 °C, 40 cycles of 30 s at 94 °C, 30 s at 50 °C, and 30 s at 72 °C | | |

Thus, primers have already been designed for the quantification of the two genera, but it is necessary to check their efficiency in the specific environments/experimental conditions of the applications of the present thesis, and PCR conditions should be optimized in order to obtain accurate determination of abundances of the bacteria.

### I-4.6 Biofilms of iron reducing bacteria

Both *Geobacter* and *Shewanella* are able to form biofilms. *Shewanella oneidensis* biofilm presents a stratification of growth activity and metabolism (Teal et al., 2006). This study showed that most of the cells in mature *S. oneidensis* biofilms present metabolic activities adapted to their local microenvironment and developmental stage. The two model strains *Shewanella* and *Geobacter* were studied in biofilms formed on electrodes in the research domain of microbial fuel cells (Biffinger et al., 2007; Bond et al., 2012; Liu et al., 2015; Liu et

al., 2019b). With *Geobacter*, flagella are widely expressed in anode biofilms and increases the electron diffusion rate within the electroactive biofilm (Liu et al., 2019b). Reguera et al. (2007) showed that *Geobacter sulfurreducens* needed the expression of electrically conductive pili to grow as biofilms on Fe(III)-oxide surfaces, but pili were also necessary for the development of the biofilm on a glass surface in presence of fumarate as an electron acceptor (Reguera et al., 2007). These authors used a method developed by van Schie and Fletcher (1999) to develop biofilms of pure *Geobacter* strains onto glass coverslips: glass slides surfaces with attached amorphous Fe(III) oxide were obtained by dipping clean coverslips into a siliconizing agent then coating coverslips by incubating them in a solution of $FeCl_3$ for 12 h under gentle agitation, then washed several times in distilled water followed by 0.1 mM NaCl, and air dried (van Schie and Fletcher, 1999). The resulting preparations were sufficiently optically transparent to allow light microscopy. Most studies of biofilms of iron-reducing bacteria were performed with pure individual strains.

### I-4.7 Studies involving complex iron reducing microbial communities

A few research studies reported results obtained with complex microbial communities reducing iron oxides. Lentini et al. (2012) performed experiments to determine which proc

esses and microbial groups were responsible for the reduction of crystalline Fe(III) oxides within sedimentary environments and how the type of Fe mineral could influence microbial populations (Lentini et al., 2012). These authors performed cultures with several Fe(III) oxides (ferrihydrite, goethite, hematite) and organic substrates (glucose, lactate, acetate) along a dilution gradient to enrich microbial populations able to reduce Fe oxides displaying a wide range of crystallinities. The type of electron donor was the most important factor influencing community structure, that also varied with the nature of the Fe(III)-mineral. The availability of carbon sources distinct from acetate induced the development of sulfate-reducing bacteria, that could be able to indirectly dissolve Fe(III)-minerals through the production of $H_2S$, whereas acetate alone induced the dissolution of ferrihydrite and the development of *Geobacter*. When glucose and lactate were provided, all Fe oxides were reduced and this reduction occurred with the development of fermentative (e.g., *Enterobacter* spp.) and sulfate-reducing bacteria (e.g., *Desulfovibrio* spp.).

Hori et al. (2015) obtained IRB enrichments from diverse environments with only acetate as an electron donor (Hori et al., 2015). A two-stage cultivation method was applied to selectively enrich and isolate crystalline Fe(III) oxide reducing microorganisms from soils and sediments

by 2-years successive culture on the crystalline ferric iron oxides goethite, lepidocrocite, hematite, or magnetite as electron acceptors. High-throughput Illumina sequencing and clone library analysis based on 16S rRNA genes showed that the enrichment cultures contained bacteria belonging to the Deltaproteobacteria (mainly *Geobacteraceae*), followed by *Firmicutes* and *Chloroflexi*. At the end of this research program, the chosen electron donor (acetate) had favored the selection and isolation of organisms mainly belonging to the *Geobacter* genus (five strains) and one strain belonging to the *Pelobacter* genus.

## I-5 Mechanisms of microbial Fe(III) reduction

Fe microbial reduction, also known as Fe respiration, refers to the microbial extracellular insoluble Fe oxide used as the terminal electron acceptor by bacteria. In this mechanism, oxidation of an electron donor is coupled with Fe(III) reduction, and this process is required for energy storage in microbial metabolisms (Tor and Lovley, 2001). The reduction product, Fe(II), of the dissimilatory Fe(III) reduction process, accumulates outside the cell and does not enter the cell as a cellular component. Moreover, in zones of oxic to anoxic transitions, Fe(III) (oxyhydr)oxides reductively dissolve via a number of direct and indirect microbial pathways. It can serve as a terminal electron acceptor for oxidation of organic matter by heterotrophic bacteria respiring Fe(III) as described before. Fe(III) reduction is also a minor pathway for electron flows in fermentative microorganisms (Lovley, 1987). In many soils, sediments and groundwaters, ferric iron is a major potential electron acceptor for the oxidation of organic matter. The concentration of ferric Fe (aq), is however limited by low solubility of Fe(III) oxyhydroxides under circumneutral pH conditions compared with other terminal electron acceptors, such as nitrate and sulfate. Consequently, strategies for transferring electrons to the structural Fe(III) centers of the solid phases by some Fe reducing microorganisms have been researched according to previous studies (Bonneville, 2005).

In order to know the details of the metabolic pathways and microbial Fe reduction strategies, it is important to understand the microbe-mineral interactions. Iron and manganese redox-active minerals are abundant in soils, aquatic and subsurface sediments, in which they support microbial growth through at least four different pathways which are shown in Figure I-10 according to Shi et al., 2016. For solid Fe(III) reduction, biofilm formation is the major point to connect iron reducers and solid Fe surfaces, which is the basis for current theories on electron transfer, e.g., extracellular electron transport (EET) (Ding et al., 2016; Okamoto et al., 2014) including the roles of extracellular polymeric substances (EPS) (Rollefson et al., 2011; Yang et

al., 2019) and direct electron transfer between microbial cells through conductive nanowires produced by organisms in response to electron acceptor limitation (Cologgi et al., 2011; Gorby et al., 2006; Reguera et al., 2005).

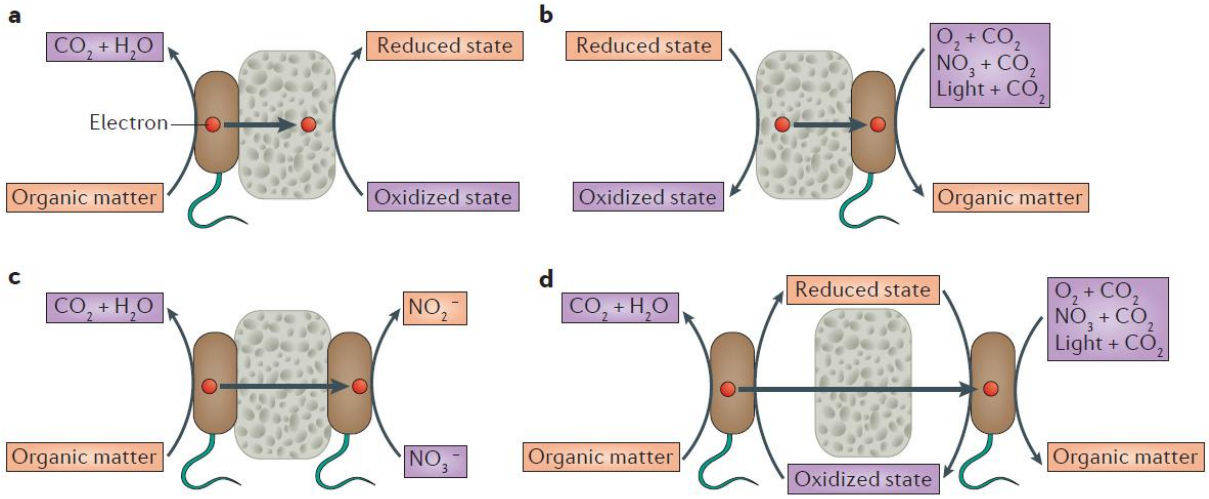


***Figure I-11.*** *Electrical interactive processes between microorganisms and minerals. Microorganisms use minerals that contain metal ions as terminal electron acceptors for respiration (part a), electron and/or energy sources for growth (part b), electrical conductors that facilitate electron transfer between microbial cells of the same and different species (part c) and electron-storage materials, or batteries, to support microbial metabolism (part d).*

In the absence of $O_2$, *Geobacter metallireducens GS-15* and *Shewanella oneidensis MR-1* have been reported to use Fe-minerals as electron sinks for heterotrophy-based respiration. In this process, either organic matter or hydrogen ($H_2$) are oxidized, then the released electrons are transferred to Fe or Mn minerals (Lovley and Phillips, 1988; Lovley et al., 1987). Moreover, the bacterium *Geobacter sulfurreducens* PCA was reported to be able to transfer electrons from minerals to nitrate reducing bacteria to reduce nitrate, which was also called interspecies electron transfer (IET) (Kato et al., 2012). Finally, some minerals function as electron storage during the procedure of electron transferring between Fe(II)-oxidizing bacteria and Fe(III)-reducing bacteria (Byrne et al., 2015).

In these four different cell-mineral interactions, Figure I-11 (a) and (d) present microbial Fe reduction. Detailing these two pathways, Jacintha Esther et al. (2015) summarized four mechanisms given in Figure I-12 that have been conceptualized for the electron transfer between bacterial cells and mineral surface (Childers et al., 2002; Esther et al., 2015).

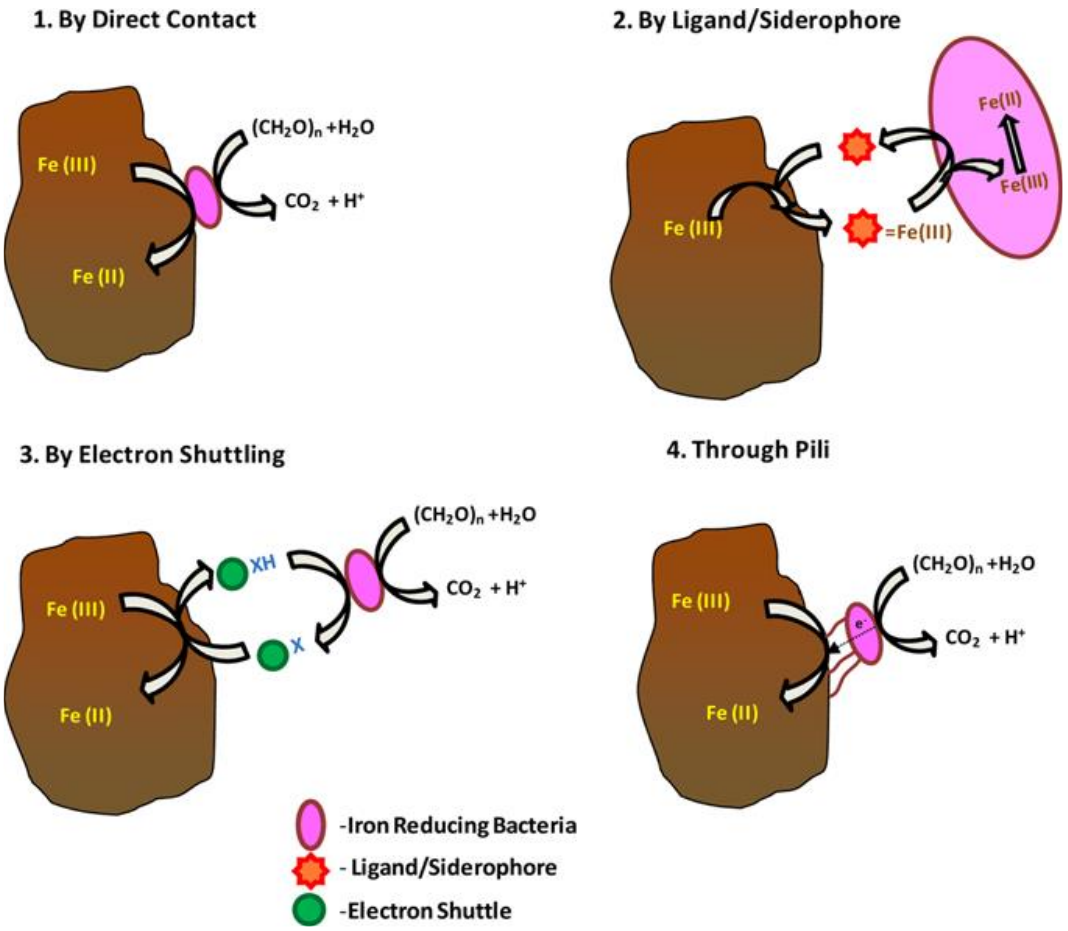


***Figure I-12.*** *Schematic illustrating solid phase Fe (III)-DIRB electron transfer mechanisms (Esther et al., 2015).*

Cell-mineral electron transfer can occur through: (1) direct contact between the cell and Fe (III) oxyhydroxides mineral, (2) production of Fe chelators by organism, (3) transfer of electrons from the microorganisms to reduced soluble compounds (the electron shuttle), (4) cell appendages. When there are no soluble Fe(III) compounds in the environment, the bacteria produce flagella and fluff these appendages to adhere to Fe(III) to achieve Fe(III) reduction (Childers et al., 2002; Esther et al., 2015).

Electron shuttles transfer electrons from the microorganism to insoluble compounds such as ferric oxides. For instance, excreted quinones can play a role in extracellular electron transfer (Newman and Kolter, 2000). Humic substances were used as electron shuttles for microbial respiration (Lovley et al., 1996b) of Fe(III) by *Geobacter metallireducens*. Fulvic acids (FAs) and humic acids were shown to enhance Fe(III) reduction by *Geobacter metallireducens* (Kulkarni et al., 2018).

Normally, the electron shuttles promoting the electron transfer during microbial Fe(III) reduction come from natural organic compounds such as humic acids and fulvic acids (FAs) (as electron acceptors), or analog quinones produced by bacteria. They are measured indirectly through the release of Fe(II) (Newman and Kolter, 2000) or by other indirect ways such as analyze of the electron accepting capacity.

## I-6 Cycling of Fe and mobility of associated As, Cr, Cd and other trace elements

Mobility of contaminants in the environment, and particularly that of toxic metals and metalloids, such as As, Cr and Cd, induces risks of contamination of hydrosystems and food chain (Beesley et al., 2010; Kumpiene et al., 2008). These elements can be present in soils and sediments naturally enriched in metal trace elements (MTE) through the local geology, or contaminated by diverse human activities (mines, industries, agriculture) (Flues et al., 2013; Prokop et al., 2003). And MTEs are often associated with Fe in soils and sediments. As described in previous section, Fe-rich minerals can change according to oxygen availability and level in the environment. They are generally stable and highly insoluble in the form of (oxyhydr)oxides (e.g., $Fe(OH)_3$, FeOOH, $Fe_2O_3$) in well oxygenated zones at circumneutral pH conditions. However, in anaerobic conditions, these minerals can be reductively dissolved (Roden et al., 2004; Roden and Wetzel, 2002) by microbial and abiotic pathways (Bonneville et al., 2004; Hansel et al., 2004; Shi et al., 2016; Thompson et al., 2006b). The dissolution of Fe-rich minerals, in absence of oxygen, could be linked to bacterial activities in soils or sediments. These phenomena were well described in controlled laboratory in liquid medium conditions between iron (oxyhydr)oxides and IRB, however the evaluation of associated pollutants fluxes, in real sediment conditions, need the development of multi-scale experiments.

### I-6.1 Association of As, Cr and Cd with Fe-Oxides

The mobility of As associated with iron oxides depends on its speciation and pH (Dixit and Hering, 2003). According to these authors, below pH 5-6, As(V) sorbs more readily to amorphous iron oxides (HFO) than does As(III). Wang et al. (2003) state that the residual concentration of As(V), after co-precipitation with iron hydroxide, is minimized in the pH 4-6 interval (Wang et al., 2003). Above pH 7-8, As(III) has a higher affinity for the solids (Dixit and Hering, 2003). Wang et al. (2003) found that the residual concentration of As(III), after co-precipitation with iron hydroxide, was minimized in the pH 6-9 interval. The toxicity of

different forms of arsenic is quite different. The oxidation or methylation of arsenic generally reduces its toxicity.

Cr(III) is poorly soluble and relatively nontoxic, while Cr(VI) is soluble and a known carcinogen. Solid Fe(II) in iron-bearing minerals, such as pyrite, magnetite, and green rusts, reduce the oxidation state of chromium, reducing its toxicity and mobility. Under oxic conditions, solid Fe(II) associated with goethite resulting from rapid redox cycling is reactive and available for electron transfer to Cr(VI), suggesting Fe(III) (hydr)oxides may act as reservoirs of reactive electron density, even in oxygen saturated environments (Tomaszewski et al., 2017).

Cd can be adsorbed by Fe(III) (oxyhydr)oxides and its adsorption on goethite and ferrihydrite is enhanced by the presence of sulfate with metal-ligand bonding (Swedlund et al., 2003; Swedlund et al., 2009). Zhang et al. (2016) studied whether crystalline structures influence the adsorption of heavy metals on magnetic iron oxides metals and suggested adsorption of Cd by amorphous iron oxide was superior to that of oxides with higher degrees of crystallization (Zhang et al., 2016).

### I.6.2 Transformations of As, Cr and Cd by bacteria

Bacteria are abundant in many environments and interact with iron oxides and As through different mechanisms, e.g., sorption, mobilization, precipitation and redox and methylation transformation (Huang, 2014). Some bacteria can use either Fe(III) or As(V) as electron acceptors. Laverman et al. (1995) have found that some iron-reducing bacteria such as SES-3 reduce As(V) to As(III) (Laverman et al., 1995).

When dissimilatory metal reducing bacteria *Shewanella alga* strain BrY, *Shewanella putrefaciens* strain CN32, *Shewanella oneidensis* strain MR-1, and *Geobacter metallireducens* strain GS-15 were used to study metal reduction in presence of $H_2$ used as an electron donor, reduction rates were metal specific with the following decreasing rate order: Fe(III)citrate ≥ Fe(III)NTA > Co(III)EDTA$^-$ > $UO_2^{2+}$ > $CrO_4^{2-}$ > $TcO_4^-$, except for $CrO_4^{2-}$ (Liu et al., 2002).

Independently from Fe transformations, diverse bacterial isolates from soil and sediment have been shown to oxidize As(III) and/or reduce As(V) (Bachate et al., 2012; Inskeep et al., 2007; Macur et al., 2004), or to methylate this toxic metalloid (Huang et al., 2011). These widespread bio-reactions can be either linked to resistance mechanisms or coupled to growth though energetic metabolisms, lithotrophic growth on As(III) or dissimilatory reduction of As(V).

During the transformation of lepidocrocite to magnetite and green rust, As(III) could be adsorbed on both lepidocrocite and green rust, whereas As(V) was associated only with green rust. Morever, As(III) formed surface complexes on magnetite nanoparticles and As(V) was thought to have been incorporated into the magnetite structure when magnetite precipitated (Ona-Nguema wt al., 2009; Wang et al., 2010; Wang et al., 2014).

Among oxidized forms of chromium, the anionic hexavalent chromium Cr(VI) is, highly soluble and toxic (Petrilli and De Flora, 1977), whereas the cationic trivalent form Cr(III), much less toxic, plays a physiological role in mammals by participating in glycaemia regulation (Schroeder, 1968) and tends to form insoluble hydroxides. Cr(III) is dominant in most environmental compartments. Diverse microorganisms reduce Cr(VI) directly into Cr(III) under either anaerobic (Turick and Apel, 1997) or aerobic (Wang and Chirwa, 1996) conditions. When growth is anaerobic, the reduction might result in respiration (Tebo and Obraztsova, 1998), Cr(VI) resistance, or may be a non-specific enzymatic reaction.

Cadmium is not directly transformed by bacteria, however micro-organisms can indirectly change the forms of Cd through binding to microbial biomass, or to microbial metabolism products (Czaban and Wróblewska, 2005; Zhou et al., 2020). When sulfate-reduction activity occurs, Cd can be precipitated as sulfide CdS, however sorption by bio-polymers produced by sulfate-reducing bacteria also contributes to Cd immobilization (Pérez et al., 2015).

### I-6.3 Mobility of trace elements during Fe-oxides microbial dissolution

A range of research studies provide information on the behavior of trace elements during the reductive dissolution of iron oxides. Some were performed with model minerals and bacteria, and others with real soils or sediments containing trace elements and complex bacterial communities.

- Experiments with defined Fe-oxides

Solubilisation of synthetic goethite-bound Co or Ni by *Shewanella* was observed in batch systems (Zachara et al., 2001). This study showed that the two metals can be mobilized in the aqueous phase during bacterial reduction.

Impact of bio-reduction on remobilization of adsorbed cadmium on Fe minerals including hematite, goethite, and two iron(III)-rich clay minerals in anoxic condition was studied by Ghorbanzadeh et al. (2017) in batch experiments. The desorption of Cd(II) was related to

production of Fe(II) as a result of bio-reduction of the minerals by *Shewanella* (Ghorbanzadeh et al., 2017).

Recently, Zhou et al. (2020) studied the influence of the concentration of natural organic matter on the mobility of Cd during bioreduction of ferrihydrite by *Geobacter*. They showed that Cd was immobilized by bonding with organic matter during the reductive dissolution of ferrihydrite (Zhou et al., 2020).

Indirect dissolution of Fe-oxides by the $H_2S$ produced by SRB can also lead to the mobilization of traces elements. The two mechanisms, direct Fe-oxide reduction by IRB and indirect Fe-oxide reduction by biogenic $H_2S$ were studied in continuously fed columns filled with synthetic Fe oxides spiked with Hg(II) (Hellal et al., 2015) and inoculated with microbial enrichments. In the column where IRB were dominant, Hg mobilization was directly correlated to bacterial Fe reduction. Conversely, when SRB were dominant, the biologically produced sulfide induced indirect iron oxide reduction and rapid adsorption of the mobilized Hg on neo-formed iron sulfides or its precipitation as HgS. Moreover, secondary minerals formed during iron reduction can interact with the trace elements: reduction of HgII to Hg° by biogenic green rust produced by microbial reduction of lepidocrocite was observed (Remy et al. 2015).

These studies provide useful information on the behavior of individual trace elements during the dissolution of defined Fe(III)-oxides. However, data are lacking about the behavior of systems simultaneously contaminated with several trace elements. Moreover, most of these results were obtained with single pure IRB strains.

- Experiments with naturally complex materials

Fe oxides and mercury solubilization in tropical oxisols was studied in presence of autochthonous ferri-reducing bacteria (Harris-Hellal et al., 2011. During bacterial growth in batch conditions, no mercury was detected in the culture medium, however, chemical analysis showed a decrease of the amounts of Hg associated to amorphous and well crystallized Fe-oxides after 14 days of incubation, underlining the potential for iron-reducing bacteria to modify mercury distribution in soil.

Muehe et al. (2013) provided evidence that secondary Fe(II) and Fe(II)/Fe(III) mixed minerals could be a sink for Cd in soils under reducing conditions, thus decreasing the mobility of Cd in the soil. By testing the mobility of Cd changes when a Cd-bearing soil was faced with organic carbon input and reducing conditions (Muehe et al., 2013).

While imposing a decrease of redox potential in a stirred bioreactor filled with a slurry of multi-metals contaminated soil, Hindersmann and Mansfeldt (2014) observed the behavior of Fe and a range of trace elements including As, Cd and Cr (Hindersmann and Mansfeldt, 2014). A moderate release of Fe(II) (from undetectable to 1 mg $L^{-1}$) was accompanied by the mobilization of 2 µg $L^{-1}$ Cd, 10 µg $L^{-1}$ As and 10 µg $L^{-1}$ Cr (Zachara et al., 2001).

Other experiments in batch bioreactors submitted clay soils contaminated with trace elements to successive steps of oxic and anoxic conditions. Mn, Fe, and As were mobilized under anoxic conditions, whereas Sb, Se, and U were mobilized under oxic conditions (Couture et al., 2015). Fan et al. (2018) demonstrated with batch laboratory incubation experiments that SRB were able to reductive dissolve high levels of arsenical ferric (oxyhydr)oxides in mine tailing sediments at the soil/water interface. Their results showed that reactions with aqueous As(III) and As(V) presented different trends, with As(III) being the dominant arsenic species. Aqueous As behavior showed two distinct stages, first As(V) was released and then immediately reduced to As(III) by biogenic sulfide (Fan et al., 2018a).

All these experiments demonstrate correlations between the mobility of trace elements and reducing conditions that allow iron oxide bio-dissolution. There is a lot of data on these mechanisms, however it's difficult to access to a clear distinction between several mechanisms. These subjects such as biological Fe(III) or sulfate reduction, and between the roles of the different mineral and organic phases in the final distribution of metals and metalloids are still needed to be verified.

## I-7 Positioning of the PhD thesis in regards to the state of the art

This overview of the available literature on the subject of Fe(III)-oxides bio-reduction and the fate of associated trace elements showed that detailed and abundant information is available on (1) simplified model laboratory processes combining pure minerals and single bacterial strains or (2) microcosms implemented with real complex soils or sediments, with their natural complete microbial communities. However, a gap exists in the knowledge acquired in these two radically different conditions. More specifically, the following research needs were identified:

- Only a few studies looked at mixed IRB communities, most research was performed with model strains of *Shewanella* or *Geobacter*, not grown together but separately as pure strains.

- When previous studies were performed with natural mixed bacterial communities in laboratory Fe-reducing experiments, the occurrence/dynamics of *Shewanella* and *Geobacter* were not monitored.

All the knowledge acquired on these two organisms would be beneficially exploited if we could understand how they are present and function in competition with other microbes in complex communities.

- From the point of view of mineralogy, data is scarce about the formation of secondary minerals during Fe(III)-oxides reduction in presence of complex bacterial communities, starting with different types of oxides, most of the information was acquired with model strains.

- The trace elements associated to Fe(III)-oxides are studied separately in studies with model strains and minerals. When several elements are present, the studies were performed with natural soils or sediments, thus the trace-elements-oxides proportion and association is not controlled. Data about the relative behavior of several TE simultaneously present in controlled conditions are lacking.

- Biofilms play a major role in natural environments, therefore biofilms of IRB attached on iron oxides still need to be further studied, in particular biofilms of mixed IRB populations were not described, and no data is available on the influence of biofilm development on the proportion of different IRB.

Globally, the analysis of the state of the art reveals a need for tools to study the transformation of different Fe(III)-oxides in natural environments, with complex natural bacterial communities.

In this context, the present PhD thesis was focused on the following objectives:

(1) To determine what is the influence of the type of Fe(III)-oxide on the efficiency of Fe release and formation of secondary minerals in presence of mixed iron-reducing bacterial communities in conditions favoring a high diversity of Fe(III)-reducing bioprocesses (reduction and fermentation),

(2) To observe how the type of iron oxide influences the structure of these mixed communities, and the proportion in these communities of the two well-known specific iron reducing bacterial genera *Shewanella* and *Geobacter*, applied as indicator parameters,

(3) To develop experimental strategies in order to evaluate the proportion of these two iron-reducing genera in the planktonic bacterial community and in biofilms formed on Fe(III)-oxides, for laboratory and on-site studies,

(4) To describe the influence of the development of complex Fe(III)-reducing bacterial communities on the dynamics of targeted trace elements As, Cr and Cd, co-adsorbed on different Fe (oxyhydr)oxides, and the distribution of *Shewanella* and *Geobacter* in these systems whose complexity is intermediary between fully controlled conditions (pure strains and defined oxided) and natural complex environments.

# Chapter II: General materials and methods

The present chapter describes materials and methods that are common to all the experiments performed during the PhD thesis. Information specific to each experiment is then detailed in the corresponding chapters.

## II-1 Site information and soil / sediment sampling

The place of study is located near the Loire, bordered by the town of Decize and by an alluvial island formed by the river (Figure II-1). The Loire River basin (117,800 km$^2$-1013 km long) is among the ten largest W-European basins and is the largest in France (Dhivert et al., 2015). The site chosen for the present work, a non-active Loire river tributary, is located in an environment naturally subjected to oscillations of redox conditions according to the level of the river.

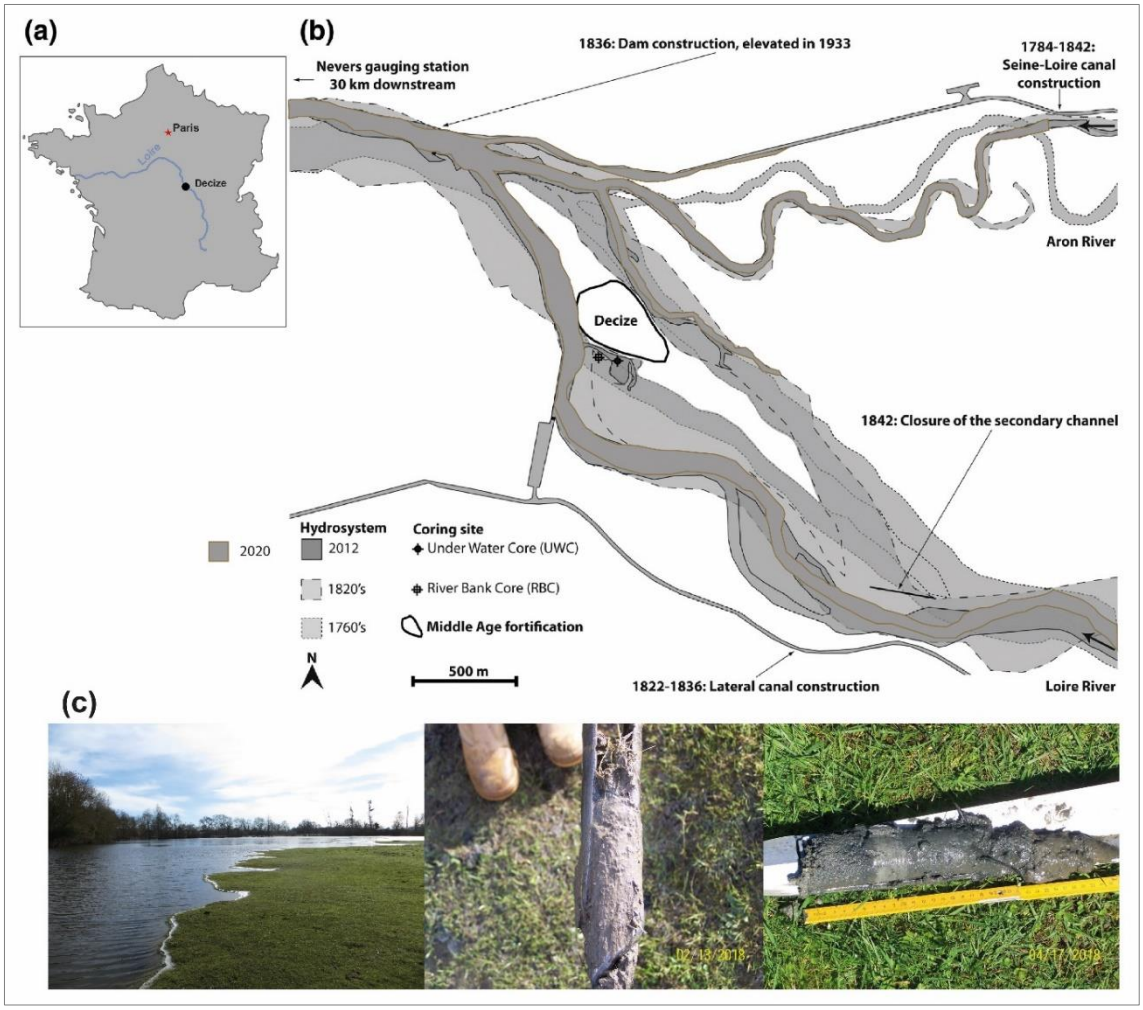

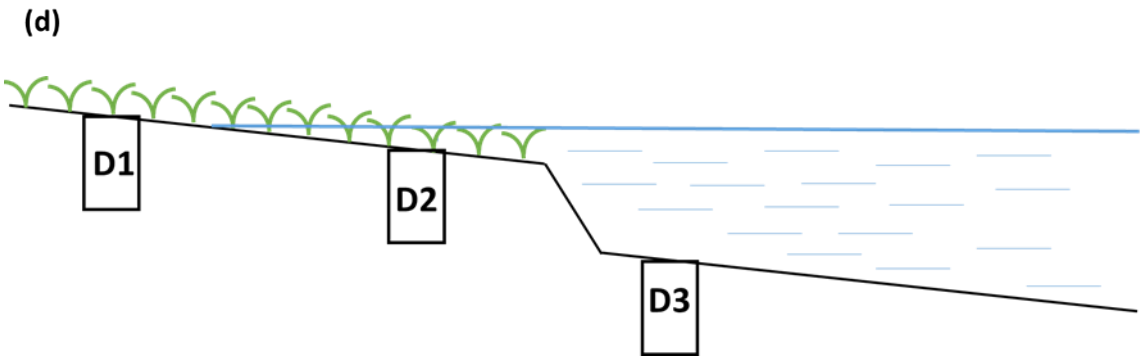


***Figure II-1.*** *(a) Location of the study area in Decize, France; (b) Morphodynamic history, hydrosystem anthropization and local industrial histories of the study area (data from data from www.geoportail.fr, 2020; Decize Municipal Archive, 2014; Dhivert et al., 2015a), and (c) Site view and sampling pictures (d) Sampling points in the non flooded soil (D1), flooded soil (D2) and aquatic sediment (D3).*

Two sampling campaigns were organized on February 13$^{th}$, 2018 and on the 17$^{th}$ April 2018 for bacterial enrichments and core characterizations respectively (Figure II-1). For the bacterial enrichments, three samples were collected using an auger and stored into glass bottles full of $N_2$ atmosphere: soil from the riverbank (10-15 cm depth), soil from flooded ground in an area transiently flooded (0-7 cm depth) and the aquatic sediment (7-17 cm depth). These three samples were flushed with $N_2$ before storing them at 4 $^{\circ}$C and named D1, D2 and D3, respectively. During the second sampling campaign, three core samples were taken by auger, i.e., 2 cores of aquatic sediment (0-28 cm and 0-36 cm depth) and 1 core of river bank (0-33 cm depth).

## II-2. Enrichment of iron-reducing bacteria (IRB) and subculture

The enrichment medium was designed based on litterature (Cummings et al., 1999; Gould et al., 2003; Park et al., 2001; Straub et al., 1998; Valencia-Cantero et al., 2007), in order to favor the development of a large diversity of IRB, including DIRB and fermentative bacteria contribution to Fe(III) reduction. Is was inspired from the composition of media used to enumerate Fe(III)-reducing bacteria in environmental samples by the most probable number method (MPN), designed to maximize the growth of diverse IRB. However, in terms of composition, this study only focused on the presence and abundance of the two genera *Shewanella* and *Geobacter*, and more information about other features of the obtained complex communities will be provided in further studies.

In order to obtain Fe-reducing enrichments, 10 g of each soil and sediment sample (D1, D2 and D3, see chapter II-1) were inoculated (1 week after sampling on site) into 200 mL basic medium (composition detailed in the Table II-1) autoclaved (121°C, 20 min) then flushed with sterile $N_2$ just after autoclaving. Sodium molybdate was added in the medium as a SRB inhibitor, because the present study was focused on Fe cycling so it was preferred to inhibit sulfate respiration metabolism. The headspace of vials (small volume because 200 mL bottles were used) was $N_2$. The following components were added to this medium: 10 mM of Fe(III) Nitrilotriacetic Acid (NTA) as electron acceptor (Huguet, 2009; Lovley, 2006), 1.5 $g \cdot L^{-1}$ peptone, 10 mM of acetate, lactate, and formate, 2 mM glucose as electron donors (Coates et al., 1996; Lovely et al., 1989; Kwon et al., 2016; Shelobolina et al., 2007) in anaerobic conditions, and 0.4 mM of sodium molybdate (these concentrations are very high and very different from the natural conditions). Fe(III)-NTA (100 mM stock solution) was prepared by dissolving 1.64 g of $NaHCO_3$ in 80 ml water, adding 2.56 g $C_6H_6NO_6Na_3$ and 2.7 g $FeCl_3 \cdot 6H_2O$, bringing the solution up to 100 ml, flushing with $N_2$ and filter sterilizing (0.22 µm, Millex -GP Syringe Filter, 33 mm diameter) into a sterile, anaerobic serum bottle. Sterilization of the electron donors was performed by autoclaving for acetate, lactate and formate, and filtration at 0.22 µm for peptone and glucose. Sodium molybdate was autoclaved. All stock solutions were kept anaerobic under $N_2$ after sterilization. Cultures were incubated at 20°C under agitation (100 rpm) for 10 days. Then, they were sub-cultured by inoculating at 10% (v/v) 50 mL of the same medium, under $N_2$. Samples (1.5-2 mL) were collected every day, in anaerobic conditions, filtered at 0.22 µm (Millex -GP Syringe Filter, 33 mm diameter) and analyzed for Fe(II) content in order to evaluate Fe(III) reduction. After 3-5 steps of sub-culturing (inoculation at 10% in fresh medium, every two weeks), the three Fe-reducing cultures were able to reduce 10 mM Fe(III)-NTA in 1-2 days, and were used as inocula for the following batch incubation experiments in slurry (chapter III), slide experiments (chapter III) and column experiments (chapter IV). In order to maintain the cultures activity, the enrichments were sub-cultured once in 1-2 weeks.

***Table II-1**. Composition of the enrichment medium (Cummings et al., 1999; Gould et al., 2003; Park et al., 2001; Straub et al., 1998; Valencia-Cantero et al., 2007).*

| **Basic solution** | **Electron donors** (added as 10X concentrated | **Fe-NTA solution** | ***SRB inhibitor** (Added in the concentrated |
|---|---|---|---|

| | | | |
|---|---|---|---|
| | solution, filtered 0.22 µm) | (added as 10X concentrated solution, filtered 0.22 µm) | electron donor solution, filtered 0.22 µm) |
| $NaHCO_3$: 2.5 g $L^{-1}$;<br>$NH_4Cl$: 0.25 g $L^{-1}$;<br>KCl: 0.1 g $L^{-1}$;<br>$NaH_2PO_4 \cdot H_2O$: 0.6 g $L^{-1}$;<br>10 mL $L^{-1}$ of vitamins solution* and trace elements solution* | Final concentrations:<br>Acetate, lactate and formate: 10 mM of each;<br>Glucose: 2 mM;<br>Peptone: 1.5 g $L^{-1}$ | Final concentration, 10 mM:<br>$NaHCO_3$: 1.64 g $L^{-1}$,<br>$C_6H_6NO_6Na_3$ (sodium nitrilotriacetic acid): 2.56 g $L^{-1}$, and<br>$FeCl_3 \cdot 6H_2O$: 2.7 g $L^{-1}$ | Sodium molybdate: 0.04 mM |

**SRB : sulfate-reducing bacteria; *Vitamins solution (1L): 2 mg biotin, 2 mg folic acid, 10 mg pyridoxine HCL, 5 mg Riboflavin,5 mg Thiamine, 5 mg Nicotinic acid, 5 mg Pantothenic acid, 0.1g B12 vitamin, 5 mg p-aminobenzoic acid, 5 mg thioctic acid ; * Trace elements solution (1L): 1.5 g Trisodium nitrilotriacetic, 0.5 g $MgSO_4$, 0.5 g $MgSO_4 \cdot H_2O$, 1 g NaCl, 0.1 g $FeSO_4 \cdot 7\ H_2O$, 0.1 g $CaCl_2 \cdot 2H_2O$, 0.1 g $CoCl_2 \cdot 6H_2O$, 0.13 g $ZnCl_2$, 0.1 g $CuSO_4\ 5H_2O$, 0.1 g $AlK(SO_4) \cdot 12H_2O$, 0.1 g $H_3BO_3$, 0.25 g $NaMoO_4$, 0.24 g $NiCl_2 \cdot 6H_2O$, 0.25 g $Na_2WO_4 \cdot 2H_2O$. Note: (Fe-NTA solution needs to be purged with $N_2$ gas and filter-sterilized into a sterile, then stored in anaerobic serum bottle)*

## II-3 Iron (oxyhydr)oxides and laboratory synthesis

### II-3.1 Ferrihydrite

Ferrihydrite and lepidocrocite were synthesized in the laboratory using the modified protocol of Schwertmann and Cornell, (2008). Ferrihydrite was obtained by dissolving 40 g $Fe(NO_3)_3 \cdot 9H_2O$ (M = 404.00 g $mol^{-1}$) in 500 mL distilled water and adding 330 mL of 1 M KOH (M = 56.11 g $mol^{-1}$) to adjust the pH to 7-8. The mixture was centrifuged at 5,000 rpm for 10 min and the supernatant was subsequently removed. The solid fraction was then washed 5 times with ultrapure water according to MilliQ quality. Then the ferrihydrite was freeze dried at -90 °C (Lyophilizer Christ Beta 2-8).

### II-3.2 Lepidocrocite

Lepidocrocite was prepared with 11.93 g of unoxidized $FeCl_2 \cdot 4H_2O$ (60 mmol Fe) salts dissolved into 300 mL distilled water by stirring. The solution was adjusted to pH 6.7-6.9 with 1M NaOH using a pH-stat under aeration (100 mL $min^{-1}$ air). The experimental arrangement consisted of a 1-2 L glass beaker equipped with a stirrer, a pH electrode, a gas inlet and a burette (containing 1 M NaOH) with the outlet just above the solution. If the crystals had an ochreous tinge, the solution was filtered to remove any akaganeite precipitations. pH of the acidic solution was adjusted to pH 6.7-6.9 with NaOH. During oxidation, the color of the suspension changed from dark greenish blue to grey and finally to orange. Protons produced during the oxidation/ hydrolysis reaction were constantly neutralized by NaOH added with the burette. After consumption of 120 mL NaOH, oxidation was completed and the pH remained constant without further addition of an alkaline solution. The entire reaction took 2-3 hr. Washing and drying were performed as described for ferrihydrite.

### II-3.3 Goethite and hematite

Goethite and hematite were ordered on line. Goethite was from Sigma-Aldrich (CAS No. 20344-49-4) and hematite was from VWR Chemicals (CAS No. 1309-37-1).

## II-4 Physico-chemical analysis: pH, Eh, Fe(II)/FeT, As, Cr and Cd

pH and redox potential (Eh, ref. Ag/AgCl) were measured immediately after sampling using standard hand-held portable meters (WTW Multi340i set) in the glove box for the slide and column experiments.

During all the experiments described in the following chapters, 1.5 -10 mL aliquots were collected with a syringe and filtered through a 0.2 μm filter (Millex -GP Syringe Filter, 33 mm diameter) into sterile plastic tubes and acidified with concentrated HCl immediately in the glove box before further analysis.

$[FeII]_D$ (the dissolved Fe(II) concentration) was measured using the ortho-phenanthroline colorimetric method (Mamindy-Pajany et al., 2013; Murti et al., 1966). Analyses were performed in Spectrophotometer cuvettes, 10 mm, into which were added 0.5 mL acetate buffer (pH 4.5), 0.1 mL ortho-phenantroline 0.5%, and 0 to 0.9 mL of filtered sample. The mixture was left at ambient temperature for 15 min in the dark, then 1 mL of buffer was added and the total volume was adjusted to 2.5 mL with demineralized water. After mixing, the absorbance at

510 nm was read with the UV-Visible spectrophotometer (Agilent G9821A CARY 100 UV-Vis Spectrophotometer). A standard curve ranging between 0.1 and 5 mg $L^{-1}$ $[FeII]_D$ and prepared in the same conditions was used to convert absorbance measures.

$[FeT]_D$ (total dissolved iron concentration) was determined using the same method but with the addition of 0.1 mL of 1% hydroquinone prepared in acetate buffer to reduce dissolved $[FeIII]_D$ into $[FeII]_D$, which was added in Spectrophotometer cuvettes before analyze.

In filtered samples, $[As]_D$ was determined with Atomic Absorption Spectroscopy (AAS, Varian SpectrAA 220-Z) and $[Cr]_D$ and $[Cd]_D$ were determined by Microwave Plasma-Atomic Emission Spectrometry (Agilent 4210 MP-AES).

## II-5 BET surface areas

BET surface areas were determined by multipoint BET $N_2$ adsorption (Brunauer et al., 1938) in ISTO laboratory (University of Orléans). Specific surface areas were determined from $N_2$ adsorption isotherms in the best linear range (with a minimum of 15 points) between the relative pressure P/Po 0.03 and 0.33 (Cavelan et al., 2019).

## II-6 SEM-EDS and SEM observations

### II-6.1 Observation of iron (oxyhydr)oxides

Scanning electron microscopy (SEM) and energy dispersive X-ray spectroscopy (EDS) were used for a general description of the sample (morphological view), and provided an identification of elements (EDS microanalysis). SEM-EDS was performed to explore the composition and distribution of Fe, TEs (As, Cr, Cd), and other elements in Fe (oxyhydr)oxides and experimental samples. SEM was performed on a TM 3000 accompanied by a SwiftED3000 X-Stream module (Hitachi), and operated at 15 kV accelerating voltage, without any coating needed (Thouin et al., 2016). SwiftED3000 provides standardless quantitative analyses, normalized to 100%. The AZtecEnergy Analyser Software displays and interprets X-ray data to provide accurate and reliable analysis without standard (Burgess et al., 2007). The acquisition time of EDS point analyses was 300 s. All post-incubation samples were freeze dried and observed by the same method described before from the following IRB incubation experiments (chapter III), slide experiments (chapter III) and column experiments (chapter IV).

### II-6.2 Bacteria Observations

Frozen samples were observed under cryo-SEM conditions using the backscattered detector imaging (BSE) mode and Secondary electrons imaging (SE) mode. The SEM was equipped with a Peltier cryo-stage at a temperature of -50 °C, under low vacuum conditions (nitrogen pressure 80 Pa). Morphologies of bacteria and bacterial biofilms are presented for slide (chapter III) and column experiments (chapter IV).

## II-7 $^{57}$Fe Mössbauer spectrometry

Two series of Fe oxides samples from the following incubation experiments (chapter III) and column experiments (chapter IV) were freeze dried and sent to the University of Tübingen to perform Mössbauer spectrometry.

Samples were loaded into Plexiglas holders (1 cm²). Samples were then transferred to the instrument and loaded inside a closed-cycle exchange gas cryostat (Janis cryogenics). Measurements were collected at 140 K with a constant acceleration drive system (WissEL) in transmission mode with a $^{57}$Co/Rh source and calibrated against a 7 µm thick α-$^{57}$Fe foil measured at room temperature. All spectra were analyzed using Recoil (University of Ottawa) by applying a Voight Based Fitting (VBF) routine (Rancourt and Ping, 1991). The half width at half maximum (HWHM) was fixed to a value of 0.124 mm $s^{-1}$ for all samples.

## II-8 Diversity and physiology of bacteria

### II-8.1 Observation and counting of bacteria by Thoma cell

Images of bacteria were obtained with an optical microscope (X400 magnification). Cells were estimated using a Thoma cell counting chamber (N* $10^4$ *f cell $mL^{-1}$, N= counted cell number, f = medium concentration/dilution factor).

### II-8.2 DNA extraction and PCR amplifications

DNA extractions were performed on solid and liquid samples either from the site or the end of three laboratory experiments (chapter III and V). For liquid samples, biomass was harvested by centrifugation at 10,000 rpm for 10 min of 2 mL of culture. Extractions were performed with the Fast DNA™ SPIN Kit for Soil (MP Biomedicals, USA) according to the manufacturer's instructions. The integrity of the DNA products was checked using agarose gel electrophoresis. DNA concentrations were determined with a Quantus™ Fluorometer (Promega, USA).

Primers Sw.783-F/1245-R Sw 640-F/815-R specific to the *Shewanella* 16S rRNA gene (Li et al., 2018; Snoeyenbos-West et al., 2000), and primers Geo 564-F/840-R specific to the *Geobacter* 16S rRNA gene (Kim et al., 2012) were used for PCR amplification (Table II-2). The 20 µL reaction solution contained 4 µL of buffer 5X, 0.2 µL of dNTP mixture (10 mM), 0.2 µL of Go Taq DNA polymerase (Promega), 0.2 µL of forward primer (50 µM), 0.2 µL of reverse primer (50 µM), 1 µL of template DNA (1-10 ng $\mu L^{-1}$), and 12.2 µL nuclease- and nucleic acid-free water. PCR reaction program for *Shewanella* and *Geobacter* with different primers were given in Table II-2.

***Table II-2.*** *Primers for detection and/or quantification of Shewanella and Geobacter 16S rRNA genes.*

| DNA Target | Primer paris | Length/ bp | Primer sequence alignment (5' - 3') | *PCR/**qPCR condition |
|---|---|---|---|---|
| *Shewanella* 16S rDNA | 783F/1245R | 518 | AAAGACTGACGCTCAKGCATTYGCAACCCTCTGTACT | *2 min at 95 °C; 40 cycles of 10 s at 95 °C, 20 s at 55 °C, and 20 s at 72 °C |
| *Shewanella* 16S rRNA | 640F/815R | 195 | RACTAGAGTCTTGTAGAGGAAGDYACCAAAYTCCGAGTA | */**1 min at 95 °C, 40 cycles of 5 s at 95 °C, 30 s at 55 °C and 30 s at 72 °C |
| *Geobacter* 16S rRNA | 564F/840R | 312 | AAGCGTTGTTCG GAWTTATGGCACTGCAGGGGTCAAT | **2 min at 95 °C, 45 cycles of 10 s at 95°C, 20 s at 60 °C, 20 s at 72 °C |

### II-8.3 CE-SSCP fingerprints

CE-SSCP (Capillary Electrophoresis-Single Strand Conformational Polymorphism) profiles were performed in order to characterize bacterial diversity structure in cultures. Amplicons of about 200 bp of the V3 region of bacterial 16S rRNA genes were obtained from DNA extracts with the forward primer w49 (5′-ACGGTCCAGACTCCTACGGG-3′; *E. coli* position, 331) and the reverse primer w34 (5′-TTACCGCGGCTGCTGGCAC-3′; *E. coli* position, 533). The 5′end of w34 was labelled with the fluorescent dye FAM. Twenty-five cycles, with

hybridization at 61°C, and 30 s elongation at 72°C were used. 1 µL of diluted (20 or 50 fold in nuclease-free water) PCR product was added to a mixture of 18.6 µL of deionized formamide and 0.4 µL of Genescan-600 LIZ internal standard (Applied Biosystems). To obtain single-strand DNA, samples were heat-denaturized for 5 min at 95 °C, and immediately cooled on ice. CE-SSCP analyses were performed on an ABI Prism 310 genetic analyzer using a 47-cm length capillary, a non-denaturating 5.6% CAP polymer (Applied Biosystems) and the following electrophoresis conditions: run temperature 32°C, sample injection for 5 s at 15 kV, data collection for 35 min at 12 kV.

### II-8.4 Bacterial 16S rRNA gene quantification

Quantification of the bacterial 16S rRNA gene copies (abbreviated bacterial 16S), was performed with primers 341-F (5'-CCT ACG GGA GGC AGC AG-3') and 515-R (5'-TGC CAG CAG CCG CGG TAA T-3'), as described from *Shewanella* and *Geobacter* except 0.2 µL T4GP32 at 500 ng·µL$^{-1}$ were added into the reaction mixture. qPCR reaction program was as follows: 3 min at 95°C, followed by 35 cycles: 30s at 95°C/30s at 60°C/30s at 72°C/30s at 80°C. Plasmid DNA containing the 16S rRNA gene of *Pseudomonas putida* KT 2440 was 10-fold serially diluted to obtain a calibration curve of known copy numbers of *Pseudomonas putida* KT 2440 16S rRNA.

### II-8.5 Detection of *Shewanella* and *Geobacter*

PCR conditions has been optimized in order to obtain accurate determination of abundances of *Shewanella* and *Geobacter*.

*Shewanella* 16S and *Geobacter* 16S were performed by PCR using a CFX96 Touch™ Real-Time PCR Detection System (Bio Rad, USA). Primers listed in Table II-2 specific to *Shewanella* and *Geobacter* 16S rRNA genes were used for that. PCR reactions were performed in a total volume of 20 µL containing solution containing 4 µL of buffer 5X, 0.2 µl of dNTP mixture (10 mM), 0.2 µL of Go Taq DNA polymerase (GoTaq® Flexi DNA polymerase, Promega), 0.2 µL of forward primer (50 µM), 0.2 µL of reverse primer (50 µM), 1 µL of template DNA (1-5 ng/µL), and 12.2 µL $H_2O$. PCR reaction programs are given in Table II-2.

### II-8.6 Quantification of *Shewanella* and *Geobacter* by qPCR

Quantification of the *Shewanella* and *Geobacter* 16S rRNA gene copies (abbreviated *Shewanella* 16S and *Geobacter* 16S) were performed by quantitative PCR (qPCR) using a CFX96 Touch™ Real-Time PCR Detection System (Bio Rad, USA). The same primers as

described in section II.8.2 were used. Reactions were performed in a total volume of 20 µL containing: 7.68 µL of sterile nuclease- and nucleic acids-free water, 10 µL of SSO Advanced Universal SYBR Green Supermix (Bio-Rad), 0.16 µL of each primer at 50 µM, and 2 µL of culture DNA (1-5 $ng \cdot \mu L^{-1}$). qPCR reaction programs were given in Table II-2. Plasmid DNA containing the target genes were constructed from *Shewanella putrefaciens* and *Geobacter metallireducens* 16S rRNA gene PCR amplified with primers 640F/815R and 564F/840R primers, respectively, and cloned using the TOPO™ TA Cloning™ Kit for Sequencing (Invitrogen, USA) according to the instructions (more primer information was given in Index). A calibration curve was obtained from serial dilutions of a known quantity of linearized plasmids containing known copy numbers of *Shewanella putrefaciens* or *Geobacter metallireducens* 16S rRNA genes. All samples, controls and standards were analyzed in duplicates. Results were reported as gene copies per gram soil or microliter of culture. Generation of a specific PCR product was confirmed by DNA melting curve analysis and agarose gel electrophoresis.

# Chapter III: Experiments in slurry with four different iron oxides

This section has been published in jounal “Frontiers in Microbiology”, the corresponding manuscript is given in Annex 1.

## III-1 Introduction

Fe (oxyhydr)oxides are common components in several compartments of the critical zone (e.g. soils, sediments and aquifers) and are present in many different mineralogical forms. Understanding biogeochemical behavior and iron cycling is fundamental for many scientific communities (Bonneville et al., 2004; Roden et al., 2004). Indeed, the mobility of trace elements (TE) is partly controlled by iron speciation, mineralogy and reactivity (Cornell and Schwertmann, 2003b). The natural solubility of crystalline Fe (oxyhydr)oxides is low. However, the interaction with microbes and organic substances can improve the formation of soluble Fe(III) and increase the availability of Fe and associated TE (Colombo et al., 2014). Biogeochemical aspects of Fe cycling in the major microbially mediated and abiotic reactions have been extensively covered (Melton et al., 2014), together with Fe redox transformations and availability of TE (Zhang et al., 2012), as well as Fe redox cycling in bacteriogenic Fe oxide-rich sediments (Gault et al., 2011). In aerobic environments at circumneutral pH conditions, Fe is generally relatively stable and highly insoluble in the form of (oxyhydr)oxides (e.g., $Fe(OH)_3$, FeOOH, $Fe_2O_3$). However, in anaerobic conditions these minerals can be reductively dissolved (Roden et al., 2004; Roden and Wetzel, 2002) by microbial and abiotic pathways (Bonneville et al., 2004; Hansel et al., 2004; Shi et al., 2016; Thompson et al., 2006b). In particular, reductive dissolution of iron (oxyhydr)oxides can be driven by dissimilatory iron reducing bacteria (DIRB), significantly contributing to the biogeochemical cycle of Fe and subsequent TE cycling (Cooper et al., 2006; Ghorbanzadeh et al., 2017; Levar et al., 2017). Microbial dissimilatory iron reduction (DIR) is an ubiquitous biogeochemical process in suboxic environments (Crosby et al., 2005; Lovley, 2000; Schilling et al., 2019; Wilkins et al., 2006). DIRB use Fe (oxyhydr)oxides as electron accepters for oxidizing organic matter. Moreover, the rate of Fe(III) reduction will influence mobility of TE initially immobilized on or in Fe (oxyhydr)oxides through adsorption or co-precipitation. Crystallinity, specific surface area and size among other factors may influence reactivity of Fe (oxyhydr)oxides in relation to the metabolic activity and diversity of DIRB (Aino et al., 2018; Cutting et al., 2009).

The role of DIRB in Fe redox transformations has been evidenced for more than three decades (Lovley, 1991; Lovley et al., 1987; Meile and Scheibe, 2019; Stern et al., 2018; Su et al., 2020),

during which more than 100 distinct DIRB species were found. However, *Geobacter* and *Shewanella* are the two most studied DIRB genera up to now (Engel et al., 2019; Han et al., 2018; Jiang et al., 2020; Li et al., 2012). Some studies have focused on the observation of secondary mineral formation in presence of *Geobacter* or *Shewanella* strains during the bio-transformation of amorphous, poorly crystalline and highly crystalline iron (oxyhydr)oxides i.e. ferric (ferrihydrite, goethite, hematite, lepidocrocite), ferrous (siderite, vivianite), and mixed valence (magnetite, green rust) (Fredrickson et al., 1998; Han et al., 2018; Ona-Nguema et al., 2002; Zachara et al., 2002; Zegeye et al., 2005). Moreover, molecular mechanisms that occur during Fe(III) reduction have been characterized by electromicrobiology for *Geobacter* and *Shewanella* (Nealson, 2017; Shi et al., 2019). Additionally, IRB communities may be influenced by initial Fe mineralogy and the nature of available electron donors. Lentini et al., (2012) compared IRB cultures obtained with different organic substrates, i.e., glucose, lactate and acetate, and different Fe(III)-minerals, i.e., ferrihydrite, goethite and hematite. Type of electron donor was the most important factor influencing community structure, that also varied with the nature of the Fe(III)-mineral. The availability of carbon sources, other than acetate, induced the development of sulfate-reducing bacteria, that could indirectly dissolve Fe(III)-minerals through the production of $H_2S$, whereas acetate alone induced the dissolution of ferrihydrite and the development of *Geobacter*. Hori et al., (2015) obtained IRB enrichments from diverse environments with only acetate that favored the selection and isolation of organisms belonging to the *Geobacter* genus (Hori et al., 2015). Acetate is a common small organic acid that cannot support fermentation, thus its consumption is generally linked to respiratory mechanisms. However, mixtures of organic substrates can be found in soils and sediments. In order to obtain complementary information on complex IRB communities that could be helpful to make the link with previous experiments involving pure strains only, the present study was performed with a mixture of simple (acetate, formate, lactate, glucose) and complex (peptone) electron donors and focused on the abundance of the two model genera, *Geobacter* and *Shewanella*, in bacterial communities originating from natural environments. Bio-reduction of four different Fe (oxyhydr)oxides presenting contrasting specific surfaces, crystallinity and solubility features, i.e., two freshly synthetized Fe (oxyhydr)oxides, and the two defined Fe-oxides goethite and hematite, was investigated with the obtained IRB enrichments. The objective of this experiment was to assess (1) the dissolution rate of these minerals in presence of mixed IRB communities while inhibiting sulfate reduction, and (2) the

influence of the type of Fe(III)-mineral on the relative abundances of *Shewanella* and *Geobacter*, when a complex mixture of organic substrates is provided.

## III-2 Specific Materials and Methods

### III-2.1 Characterization of the environmental source of bacteria

**Iron extraction in soils/sediments samples**

All Fe sequential extractions were performed under oxic conditions in constantly agitated centrifuge tubes, with the exception of the boiling HCl and total Fe techniques which were performed in glass test tubes (Poulton and Canfield, 2005). Reagent concentrations and sediment to extractant ratios were 1:100 (0.4 g to 40 mL) for each step (Keon et al., 2001). Sediment extractions were performed with 0.1-0.2 g wet sample with 10 mL extractant volume. More details were given in Table III-1.

***Table III-1.*** *Extraction procedure for Fe in soil/sediments, successive steps applied on the same initial sediment sample.*

| Step | Extractant | Target phase | Possible mechanism | References |
|---|---|---|---|---|
| 1 | 1 M $MgCl_2$ extraction at pH 7 for 2 h<br>one repetition | ionically bound iron | anion exchange | (Heron et al., 1994; Poulton and Canfield, 2005; Tessier et al., 1979) |
| 2 | 1 M $NaH_2PO_4$, pH 5, 16h, 25 °C<br>one repetition | strongly adsorbed iron | anion exchange | (Keon et al., 2001; Poulton and Canfield, 2005; Tessier et al., 1979) |
| 3 | 1 N HCl, 1 h, 25 °C<br>one repetition | “easily reducible” oxides (ferrihydrite and lepidicrocite) | proton dissolution | (Chester and Hughes, 1967; Keon et al., 2001; Poulton and Canfield, 2005) |

| | | | | |
|---|---|---|---|---|
| 4 | 0.2 M ammonium oxalate/oxalic acid, pH 3, 2 h, 25 °C in dark (wrapped in Al foil) one repetition | "reducible" oxides (goethite, hematite, ferrihydrite, lepidocrocite and akaganéite) | ligand-promoted dissolution | (Keon et al., 2001; Poulton and Canfield, 2005; Ryan and Gschwend, 1991) |
| 5 | DCB: Dithionite citrate-bicarbonate, pH 7, 2 h, 25 °C one repetition + one water wash | Magnetite, goethite, hematite | reduction | (McKeague and Day, 1966; Phillips and Lovley, 1987; Poulton and Canfield, 2005) |
| 6 | 6 N HCl 24 h 125 rpm two repetitions + one water wash | Fe (oxyhydr) oxides, FeS | Oxidation and dissolution | (Hellal et al., 2015; Mikac et al., 2002) |

### III-2.2 Synthetic Fe(III) (oxyhydr)oxides and bacterial inocula

Two fresh Fe (oxyhydr)oxides were synthesized in the laboratory under the modified protocol of (Schwertmann and Cornell, 2008). The Fe (oxyhydr)oxide named FoF was prepared according to the protocol for ferrihydrite, by dissolving 40 g $Fe(NO_3)_3 \cdot 9H_2O$ in 500 mL distilled water and adding 330 mL of 1 M KOH to adjust the pH to 7-8. The mixture was centrifuged at 5,000 rpm for 10 min and the supernatant was subsequently removed. The solid fraction was then washed 5 times with ultrapure water according to MilliQ quality. The Fe (oxyhydr)oxide named FoL was prepared according to the protocol for lepidocrocite with 11.93 g of unoxidized $FeCl_2 \cdot 4H_2O$ salts dissolved into 300 mL distilled water by stirring. The solution was adjusted to pH 6.7-6.9 with NaOH using a pH-stat under aeration (100 mL/min air). Washing was performed as described for FoF. Both synthesized minerals were freeze-dried. Goethite from Sigma-Aldrich (CAS No. 20344-49-4) and hematite from VWR Chemicals (CAS No. 1309-37-1) were also used. Mineralogical morphologies of all Fe (oxyhydr)oxides were characterized using a scanning electron microscope (SEM) and BET surface area measurement (determined by multipoint (Brunauer, Emmett and Teller) BET $N_2$ adsorption) (Brunauer et al., 1938). Specific surface areas were determined from $N_2$ adsorption isotherms in the best linear range (with a minimum of 15 points) between the relative pressure P/Po 0.03 and 0.33 (Cavelan et al., 2019).

Specific surface areas of Fe (oxyhydr)oxides varied from 11.7 to 337 $m^2.g^{-1}$ (Table 1), and compared well to some other synthetic (oxyhydr)oxides (Bonneville et al., 2004; Das et al., 2013; Larsen and Postma, 2001; Pedersen et al., 2005). SEM was performed on a TM 3000 coupled to a SwiftED3000 X-Stream module (Hitachi), and operated at 15 kV accelerating voltage (Thouin et al., 2016). The corresponding observed morphologies are given in Table III-2.

***Table III-2.*** *Characteristics of Fe(III) oxides submitted to Fe-reducing bacteria.*

| Iron oxide | Assumed morphology[a] | Specific surface area[b] ($m^2g^{-1}$) |
|---|---|---|
| goethite | acicular | 11.7 |
| hematite | cylinder/rod | 31.4 |
| FoF | blocky | 232 |
| FoL | blocky | 337 |

*[a]For use in estimating mean particle size from morphology by SEM-EDS (TM3000 accompanied by a SwiftED3000 X-Stream module (Hitachi)); [b]Determined by multipoint BET $N_2$ adsorption.*

The 5th subcultures of inocula, D1, D2 and D3 described in chapter II-2 were used for the following IRB incubation experiments.

### III-2.3 IRB incubation experiments

Incubation experiments were performed in 50 mL glass bottles equipped with chlorobutyl rubber stoppers, using 10 % (v/v) of inocula from D1, D2 and D3 enriched from the site samples of Decize and the four Fe (oxyhydr)oxides presenting contrasting specific surfaces (FoF, FoL, goethite and hematite), under anaerobic conditions. The compositions of the different solutions used to prepare the culture medium were the same as for the enrichment cultures and are also listed in **Supplementary Figure III-S1**. The total Fe(III) concentration added as Fe (oxyhydr)oxides was adjusted to be close to that of dissolved Fe(III)-NTA in the enrichment medium, i.e., 20 mM, based on the theoretical formula of each iron oxide (**Supplementary Table III-S1**). The inoculation of Fe-reducing cultures was performed in an anaerobic glove box. The gas phase of the bottles was $N_2$ and the bottles were flushed with $N_2$ before and after sampling. The flasks were incubated at 20°C, under agitation (100 rpm). Not inoculated controls were prepared in the same conditions. Samples (1.5-2 mL) were collected as described in 2.1

and analyzed for $[FeT]_D$. The Fe solubilisation rates were calculated using the data of $[FeT]_D$ collected during the first phase of the incubation, when this parameter increased linearly. After 27 days incubation, the remaining cultures were centrifuged at 5,000 rpm for 10 min. Supernatants were removed and solids freeze-dried for observation under SEM-EDS (chapter II-6.1).

### III-2.4 Fe analyses and pH/Eh monitoring

For Fe analyses, 1.5 mL aliquot was sampled with a syringe and filtered through a 0.2 μm filter into 5 mL tubes and immediately acidified with concentrated HCl in the glove box. $[FeII]_D$ (dissolved Fe(II) concentration) and $[FeT]_D$ (total dissolved iron concentration) were determined using the methods described in chapter II-4. pH and redox potential (Eh, ref. Ag/AgCl) were measured using standard hand-held portable meters (WTW Multi340i set) in glove box as described in chapter II-4 before and after the incubation.

### III-2.5 Determination of iron oxides solubilisation parameters

The total dissolved Fe (Fe solubilisation) was calculated as the addition of the quantities of FeT solubilized during all the discrete FeT solubilization events (from one sampling event to the next one) during all the incubation period for the batch experiments. The decrease in FeT were not taken into account in the calculation. The initial Fe reduction rate (mg $L^{-1} \cdot h^{-1}$) was calculated for the period of rapid increase of $[FeT]_D$ during the first stage (3-8 days) of the batch experiments. The total dissolved Fe and initial Fe (oxyhydr)oxide dissolution rates are indicated as “Fe solubilisation” and “solubilisation rate” in the following statistics.

### III-2.6 SEM-EDS observation and Mössbauer spectrometry

Initial and post-incubation Fe (oxyhydr)oxides were observed by SEM-EDS using the method described in chapter II-6.1 after freeze-drying (-90 ˚C Martin Christ Beta 2-8 LSCplus). Mössbauer spectrometry was used to determine Fe species by the method described in chapter II-7.

### III-2.7 Biological analyses

DNA extractions were performed on samples using the method described in chapter II-8.2. Bacterial 16S rRNA genes and *Shewanella* / *Goebacter* 16S rRNA genes quantification were performed by the methods described in chapter II-8.4 and 8.6. CE-SSCP fingerprints were performed by the method described in chapter II-8.3.

### III-2.8 Statistics

DNA quantification and qPCR data were analyzed using a Kruskal-Wallis test with XLSTAT software (version 2019 21.1.3) to determine the significant differences between each culture or between iron oxides. Variations in bacterial community structure were further analyzed by Non-Metric multiDimensional Scaling –nMDS) and ANOSIM analysis and ANOSIM analysis applied to a Bray-Curtis dissimilarity matrix of CE-SSCP data (generated in BioNumerics V7.5), using R-Studio software (Vegan Package) (Team R, 2015).

Principal component analysis (PCA) was used to summarize the relationships between chemical (Fe-reducing speed for the first few days and Fe reduction proportion) and microbial (molecular biomass, i.e., DNA concentration, and *Geobacter* and *Shewanella* gene abundances) data with XLSTAT software (version 2019 21.1.3).

## III-3 Results

### III-3.1 Characterization of the environmental sources of bacteria

Figure III-1 illustrates the visual aspect of the site materials (Figures III-1 a and b), and gives the results of the sequential extractions of iron forms (Figure III-1 c). The sediment core can be described by a horizon with anmoor (An), 3 reductic horizons (Gr) and the parent material (alluvium from the Loire). Two Fe forms were detected in all samples, strongly adsorbed Fe and the crystallized Fe forms (including magnetite, goethite, hematite and lepidocrocite). This last category of Fe was more abundant in the riverbank soil than in the aquatic sediments. The amorphous easily reducible oxides such as ferrihydrite was detected only in the riverbank soil and in one sample of aquatic sediment (7-17 cm). Thus, the characterization of site samples showed the probable presence of different types of Fe(III)-oxides in the environmental samples used as source of IRB during the PhD thesis.

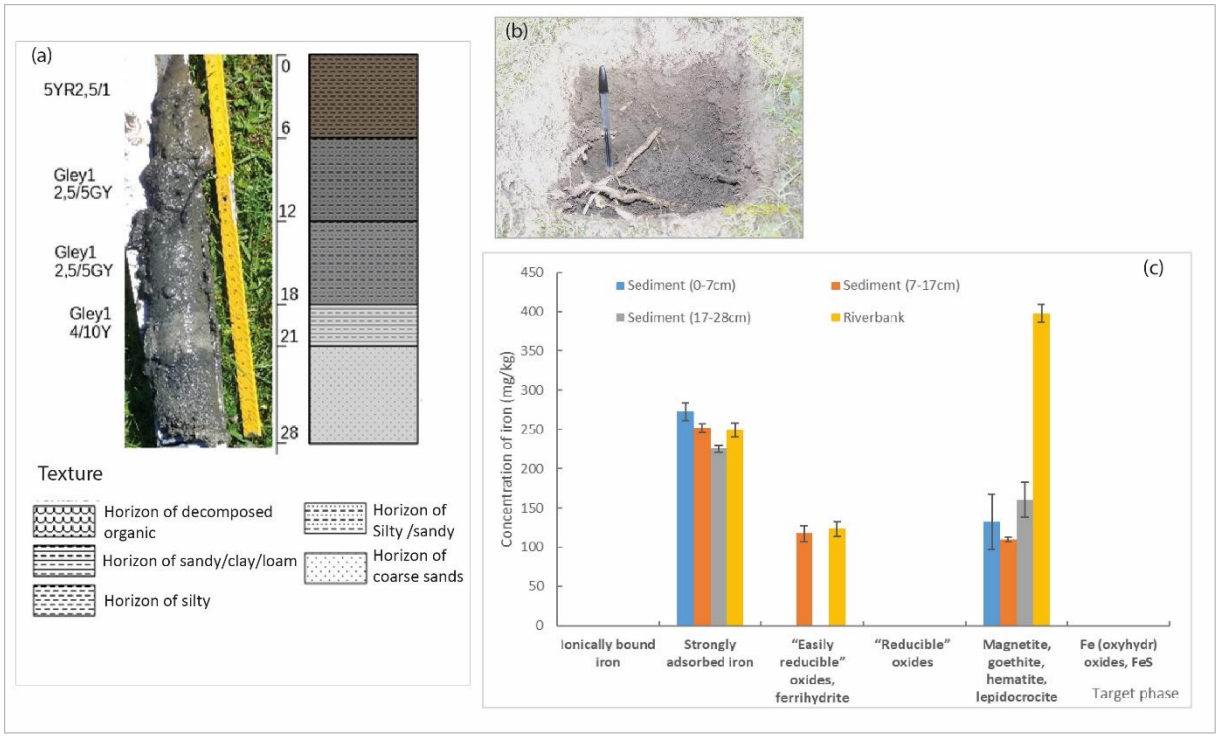


***Figure III-1.*** *(a) Description of the "sediment" core with the corresponding photo taken on the day of sampling; (b) Picture of sampling area in riverbank; (a) Concentrations of different iron species (potential) in sediment samples and in riverbank samples.*

### III-3.2 Dissolution of Fe (oxyhydr)oxides

Fe (oxyhydr)oxide solubilisation in the incubations was mainly influenced by the type of Fe (oxyhydr)oxide. For all cultures, D1, D2 and D3, the highest iron solubilisation rates were observed in presence of FoL (Figure III-2). The iron solubilisation rates during the first week of the experiment, regardless of mineral structure, roughly matched the order of specific surface area except for goethite/hematite with D1 and D2 (**Supplementary Table III-S2**). When this solubilisation rate is divided by the specific surface of each mineral **(Supplementary Table III-S3)**, the highest (rate / specific surface ratio) values are observed with goethite, followed by hematite, FoL and finally FoF. In abiotic control flasks, iron dissolution remained lower than 0.4 %.

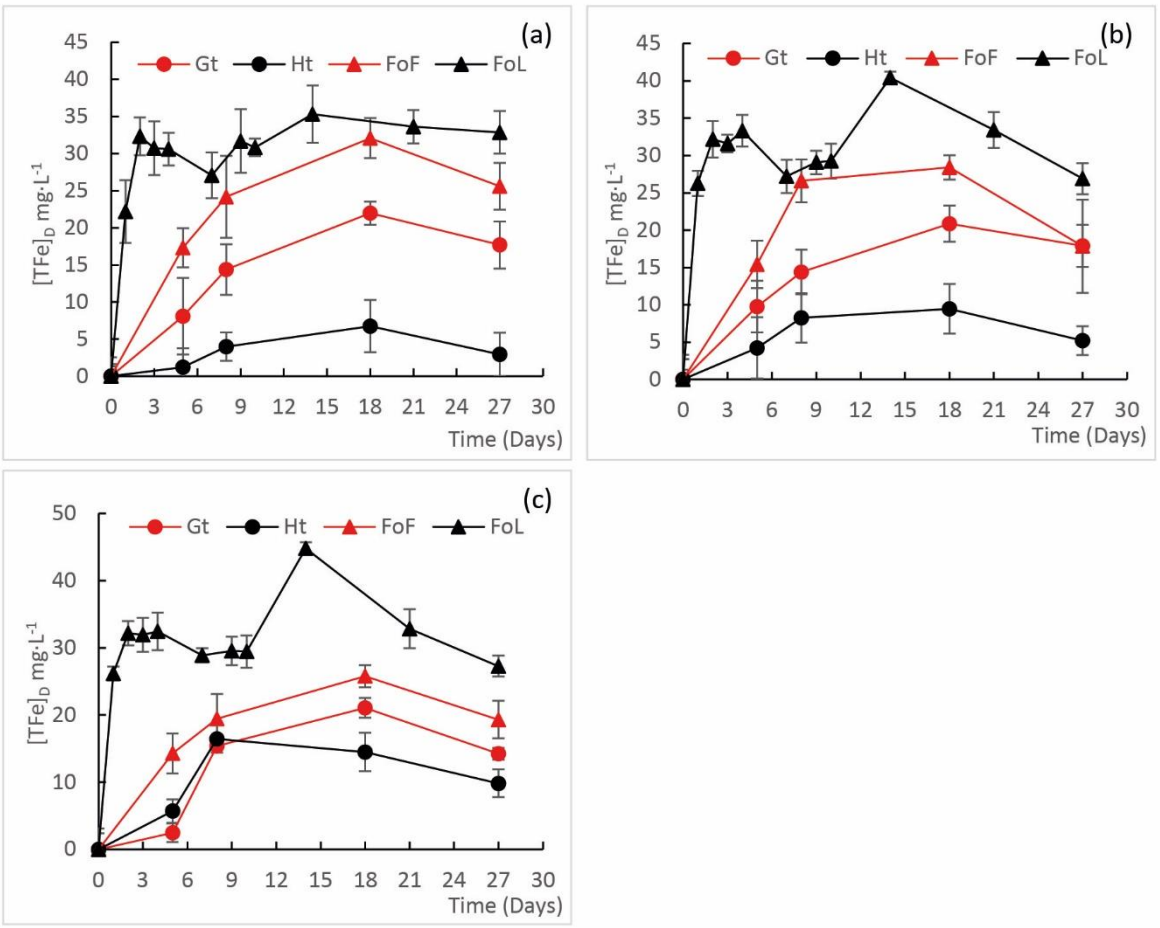


***Figure III-2.*** *Evolution of the concentration of total Fe during incubation experiments with four Fe(III) (oxyhydr)oxides in presence of D1(a), D2(b) and D3(c) iron-reducing cultures, Fe(III)-NTA is given in* ***Supplementary Figure III-S2****. Error bars represent the standard deviation of triplicate measurements.*

Initial pH of the medium was close to 7.5. This parameter did not significantly change during the incubation in presence of FoL and goethite. The final pH increased slightly to 7.6 in presence of FoF and decreased to 7.4 in presence of hematite. The initial Eh was -30 mV (ref. Ag/AgCl). This parameter decreased to -230 ±10 mV after incubation in presence of bacteria. In abiotic control flasks, the Eh value decreased down to -130 mV.

According to the $[FeT]_D$ during the incubation period, total dissolved Fe from Fe (oxyhydr)oxides was calculated (Figure III-3). Considering that total Fe provided as Fe minerals was close to 20 mM, the percentage of Fe solubilisation was in the range from 1 to 15 % of total solid iron oxides.

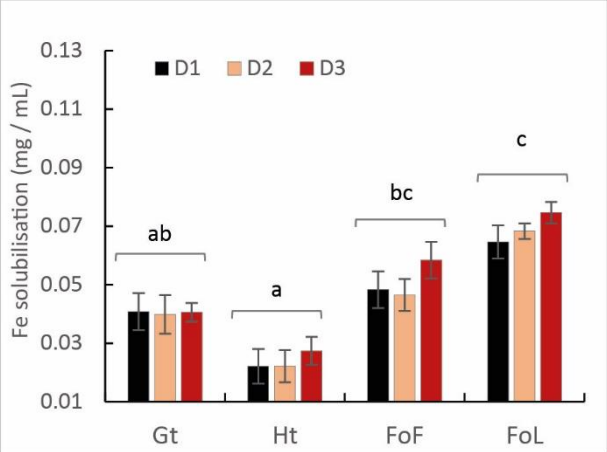


***Figure III-3.*** *Total amount of solubilized Fe from Fe (oxyhydr)oxides: goethite, hematite, FoF and FoL in presence of D1, D2 and D3 inocula. The letters "a" and "b" represent the significance of differences (Kruskal-Wallis test at p<0.05) between cultures. Values in the same Fe (oxyhydr)oxides group are not significantly different from one another. Error bars represent the standard deviation of triplicate measurements.*

The highest quantities of dissolved Fe were obtained for FoL, with 0.074 mg iron per mL with D3 inoculum. The extent of FoL solubilisation was more than 3 times higher than that of hematite with the same inoculum. For goethite, low solubilisation, around 0.022 mg iron per mL, were obtained, with no significant difference between the three inocula. Moreover, when Fe (oxyhydr)oxides are grouped without distinguishing the origin of the inocula, the solubilisation of FoL was significantly different from that of goethite and hematite (Figure III-3), and that of FoF was significantly higher than that of hematite. For the same data set, the significance of differences calculated for different inocula (**Supplementary Figure III-S3**) shows that for both D1 and D2, FoL solubilisation was significantly different from that of hematite. However, there was no significant difference in iron solubilisation between iron oxides with D3. This suggests that D3 could be less influenced by Fe mineralogy than the other two inocula.

## III-3.3 Biological parameters

### *III-3.3.1 Soil samples*

The ratio of gene copies of *Shewanella* and *Geobacter* (Figure III-4 b) 16S genes over total bacterial 16S genes abundance increased from D1 to D2 and D3. Globally, *Geobacter* was

clearly present in higher proportions than *Shewanella* in the bacterial communities present in the environmental samples used to enrich D1, D2 and D3.

*III-3.3.2 Effect of Fe (oxyhydr)oxides on bacterial community structure*

The bacterial community structure profiles of the initial soil and sediment samples, the Fe-NTA enrichments and the cultures in presence of the four different (oxyhydr)oxides were compared using an nMDS ordination approach (Figure III-5). Full CE-SSCP profiles are available in **Supplementary Figure III-S4**. These profiles show a high diversity with many peaks, with thus the presence of different bacterial strains.

The structures of the initial communities were modified after inoculation on Fe (oxyhydr)oxides samples (Figure III-5): the enrichments on Fe(III)-NTA are grouped on the right side of the representation, whereas communities obtained by cultures with iron oxides are gathered on the left side. The three initial communities from environmental samples are located between these two poles. No clear separation is observed between the communities obtained with the four pure iron oxides. Although, according to ANOSIM analysis, no significant difference in community composition was found between initial inocula (significance >0.05), a significant dissimilarity was found between community origins (i.e. initial soils and form of Fe(III) provided to the consortia) (R = 0.345 and significance = 0.0249).

### *III-3.3.3 Bacterial abundance and abundances of Shewanella and Geobacter 16S genes*

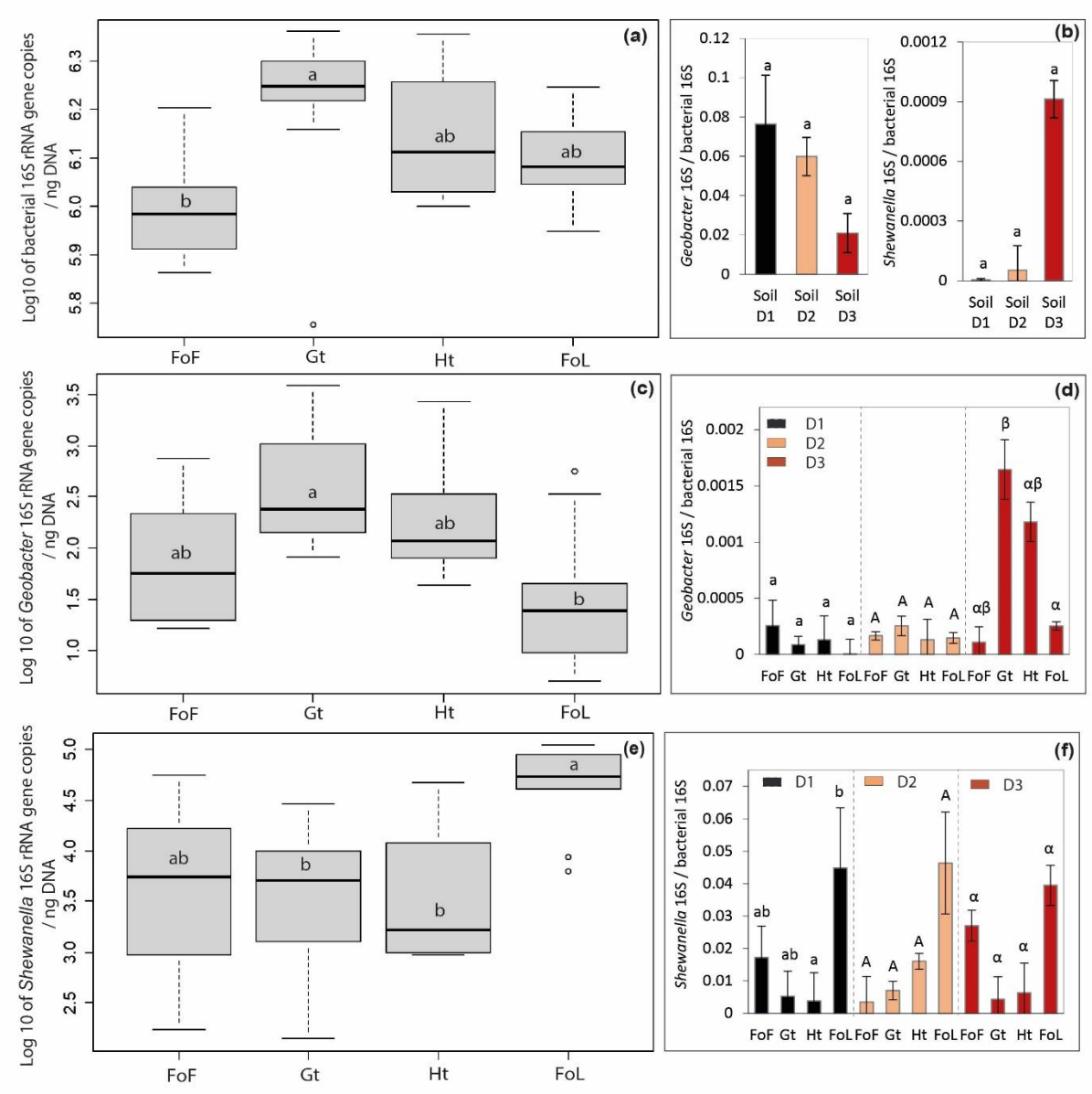


***Figure III-4.*** *Parameters linked to bacterial abundance: (a) Log10 of bacterial 16S rRNA (rrs gene) copies, (b) Ratio of Shewanella and Geobacter over bacterial 16S rRNA (rrs gene) copies for all three site samples D1, D2 and D3, (c) Log 10 of Geobacter 16S gene copies, (d) Ratio Geobacter 16S over bacterial 16S rRNA (rrs gene) copies, (e) Log 10 of Shewanella 16S gene copies, and (f) Ratio Shewanella 16S over bacterial 16S rRNA (rrs gene) copies. Details of bacterial, Shewanella and Geobacter 16S rRNA (rrs gene) copies for all three site samples D1, D2 and D3 are given in Supplementary Figure III-S6. The letters "a" and "b" differed significantly (Kruskal-Wallis test at $p<0.05$) between group of iron oxide for graph "(a), (b), (c), and (e)"; the small letter, capital letter and Greek letter were used for differing significantly by group of inocula D1, D2 and D3 for graphs "(d) and (f)". Data represent average values of three experimental replicates and their standard deviation (σ) for graph "(b), (d) and (f)", 3 inocula * 3 replicates for graphs "(a), (c), and (e)". Ht: hematite; Fh: FoF; Lp: FoL; Gt: goethite. Error bars represent the standard deviation of triplicate measurements.*

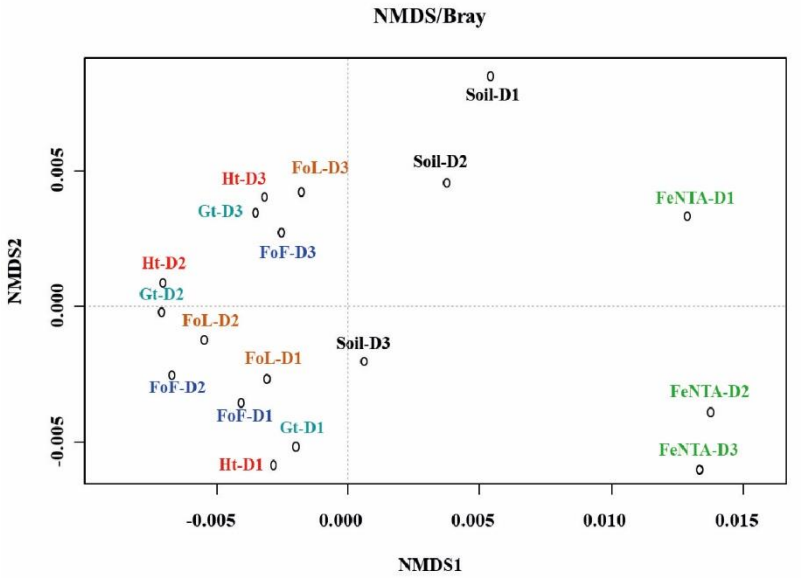


***Figure III-5.*** *nMDS ordination of D1, D2 and D3 community fingerprints applied to a Bray-Curtis dissimilarity matrix. Plot stress = 0.15. Ht: hematite; Fh: FoF; Lp: FoL; Gt: goethite.*

The *rrs* gene abundances and *Shewanella* 16S/bacterial 16S ratio did not highlight any significant differences between the three initial enrichments D1, D2 and D3 (Supplementary Figure III-S4). As shown in Figure III-4 (a), globally, *rrs* gene abundance in goethite samples was significantly different to FoF samples. It decreased in iron oxide cultures compared with Fe(III)-NTA cultures (**Supplementary Figure III-S5**). Conversely, the abundance of the two quantified IRB genera, i.e., *Geobacter* and *Shewanella*, differ between the types of Fe oxides provided as Fe(III) source (Figure III-4 e and f). Globally, compared with *Geobacter*, *Shewanella* was present in a larger proportion in all bacterial communities with the four iron oxides. Moreover, the number of gene copies of *Shewanella* for FoL is significantly different from that observed in presence of other iron oxides, but there are no significant differences between the cultures for FoF, goethite and hematite samples. When the type of inocula is not taken into account, the proportion of *Shewanella* 16S genes for FoL samples is significantly different for goethite samples.

Considering specifically each quantified genus-specific 16S gene, the cultures in presence of goethite inoculated with D3 bacteria contained a significantly different proportion of *Geobacter* 16S genes than the same culture (D3) with FoL (Figure III-4 d). In the other conditions (D1, D2 with all oxides), no significant differences between the proportion of *Geobacter* 16S genes in the global bacterial population was observed.

### III-3.4 Mineral SEM-EDS observation

SEM observations showed that initial FoF and hematite samples were characterized by amorphous or poorly crystallized morphologies whereas crystalline minerals with an acicular and a prismatic texture were observed in goethite and FoL (lepidocrocite) samples (Figure III-6 (a, b, c, d-1)). No significant morphological changes were observed in abiotic samples after incubation (Figure III-6 (a, b, c, d-2)). However, new crystalline forms with a prismatic texture were observed in biotic samples of FoF and FoL after incubation (Figure III-6 (a-3, d-3)).

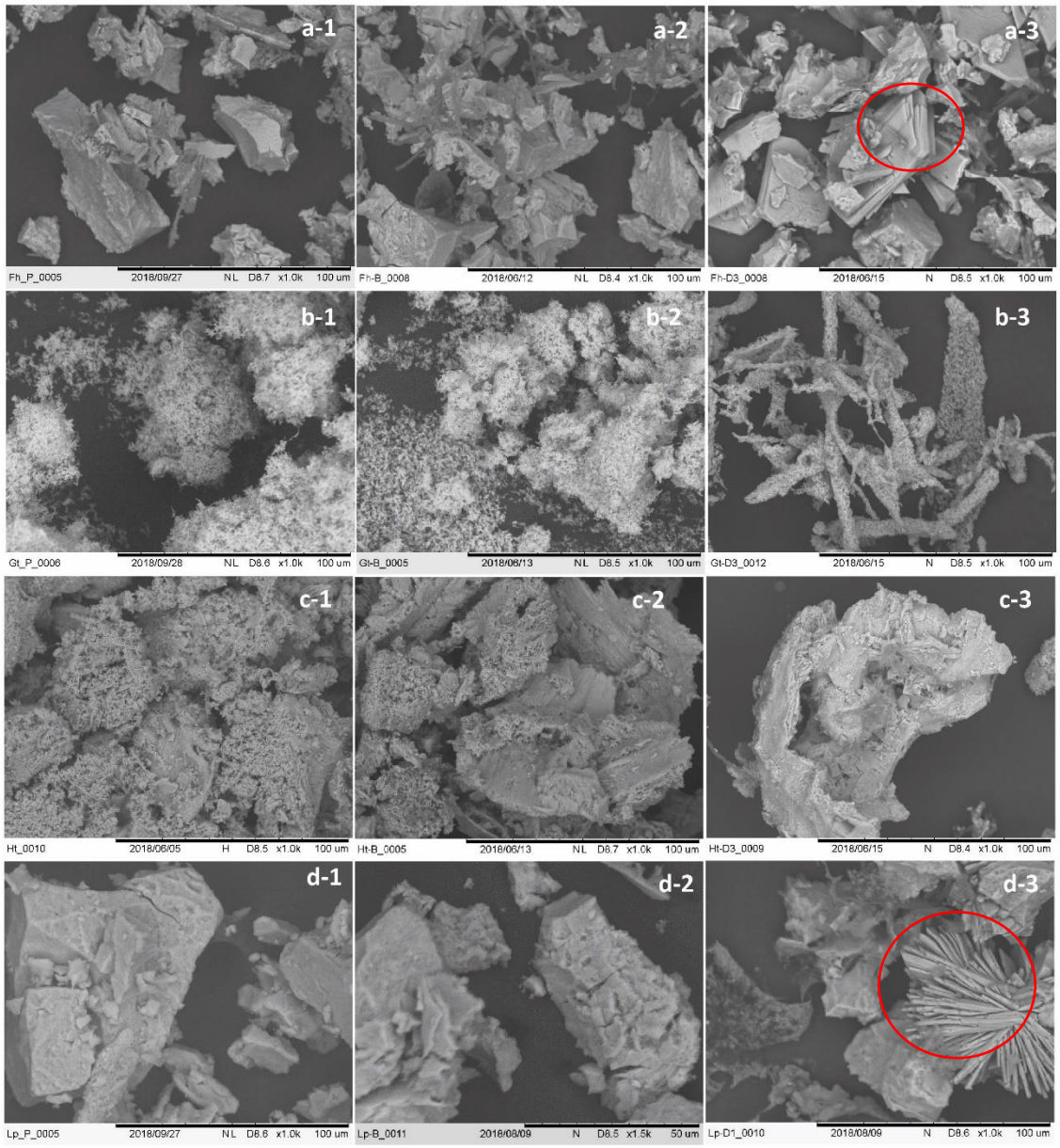


***Figure III-6.*** *Microscopic pictures of Fe(III) (oxhydr)oxides samples, FOF (ferrihydrite) (a), goethite (b), hematite (c) and FOL (lepidocrocite) (d). Number "1" represented initial samples,*

*"2" represented abiotic samples after incubation and "3" represented biotic samples after incubation. Red circles show the morphology of secondary minerals.*

### III-3.5 Mössbauer spectroscopy

The spectra collected at 140 K for samples of initial and post-incubation goethite are shown in Figure III-7, with the result of fitting shown in Table III-3.

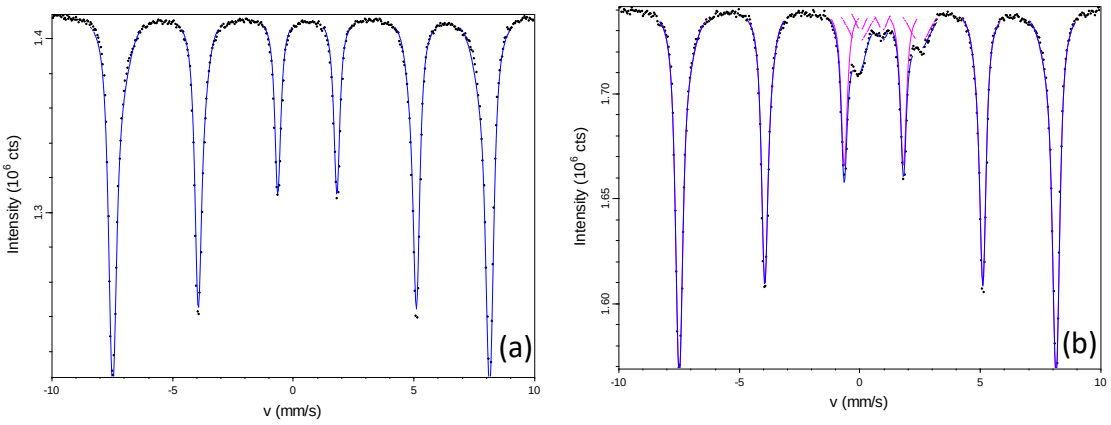


***Figure III-7.*** *Mössbauer spectra collected at 140 K for samples initial goethite (a) and post-incubation goethite (b).*

***Table III-3.*** *Fitting results of Mössbauer spectroscopy. CS – center shift, QS – quadrupole splitting, e – quadrupole shift, H – hyperfine field, stdev(H) – standard deviation of hyperfine field, Pop. – Relative abundance, χ2 – goodness of fit.*

| Sample | Mineral phase | CS mm/s | QS mm/s | stdev(QS) mm/s | e mm/s | H T | stdev(H) T | Pop % | Error | *χ2* |
|---|---|---|---|---|---|---|---|---|---|---|
| Initial Gt | Goethite | 0.45 | | | -0.13 | 48.0 | 1.4 | 100.0 | 0.0 | 8.9 |
| Post-Gt | Fe(II) | 1.20 | 2.57 | 0.73 | | | | 8.4 | 0.4 | 2.4 |
| | Fe(III) | 0.47 | 0.92 | 0.28 | | | | 2.9 | 0.3 | |
| | Goethite | 0.45 | | | -0.13 | 48.2 | 1.2 | 88.7 | 0.4 | |

The initial goethite had a spectrum which is characteristic of a pure goethite mineral (Cornell and Schwertmann, 2003a). No other mineral phases were visible in this spectrum. The spectrum for sample post-incubation Gt was dominated by goethite, however there was also clear

indications for Fe(II) (8.4 %), and a short range Fe(III) phase (2.9 %) which was not magnetically ordered at 140 K.

The FoF was also characterized by Mössbauer spectroscopy (Supplementary Figure III-S7) that confirmed it was ferrihydrite. Operational problems prevented us from analyzing the other samples.

## III-4 Discussion

### III-4.1 Influence of the type of iron oxide on bacterial iron solubilisation

FoL and FoF were synthetized in the laboratory and were more amorphous, thus more reactive, than goethite and hematite (Usman et al., 2012). According to the literature, abiotic rates of reductive iron dissolution are correlated with the solubility of Fe (oxyhydr)oxides (Larsen and Postma, 2001). The rates of this abiotic reductive bulk dissolution decrease according to ferrihydrite >lepidocrocite> goethite> hematite, emphasizing the importance of the crystal structure on the dissolution rate (Larsen and Postma, 2001). Moreover, the rate of iron oxides solubilisation is usually a function of surface area, rates increasing with surface area for a given mineral (Schwertmann, 1991). However, Roden, (2006) found that in presence of IRB, oxides' mineralogical and thermodynamical properties exert a minor influence on reduction rates compared with the abundance of available oxide surface sites controlled by oxide surface area and the accumulation of surface-bound biogenic Fe(II). This last process, of the precipitation of new Fe(II) minerals (Urrutia et al., 1998; Zachara et al., 2002), might explain the late decrease of soluble Fe and the fact that the iron solubilization rate by specific surface unit was the highest with goethite, followed by hematite, FoL and finally FoF, thus it did not follow the expected abiotic dissolution rate rank (Table III-S3). However, Fe solubilisation effectiveness increased with the specific surface, in particular for the two freshly synthesized oxides. Here, the fresh mineral prepared with the protocol of lepidocrocite (FoL) synthesis presented a higher specific surface than the mineral produced using the protocol for ferrihydrite (FoF). Synthetic lepidocrocites can present a very large range of specific surface areas, depending on their level of crystallinity (Schwertmann, 1973). In the present case, the specific area of synthetic FoL (337 $m^2.g^{-1}$) is much higher than for other Fe (oxyhydr)oxides, possibly due to a rapid oxidation of Fe(II) during synthesis that produced poor crystallization and formation of lepidocrocite impurities (Schwertmann and Taylor, 1979). Schwertmann (1973) showed that the specific surface of lepidocrocite increases with its solubility in presence of oxalate, and this specific

surface area is anti-correlated with the crystallinity. In the present experiment, at the end of the incubation, we detected 8 $mg.L^{-1}$ total Fe in the FoL abiotic control, but almost no Fe in FoF abiotic control. This supports the idea that FoL was more soluble than FoF. The high specific surface area and probable poor crystallinity of FoL could have favored solubilisation by IRB.

Fe solubilisation rates were limited after a few days, probably due to evolution of the composition of the liquid medium, or the accumulation of surface-bound biogenic Fe(II) (Roden, 2006), as Fe(III) was not the limiting factor. Parameters such as humic substances, quinones and organic carbon can strongly influence microbial Fe(III) reduction rates for *Shewanella* (Adhikari et al., 2017) or *Geobacter* (Wolf et al., 2009) in natural environments. Generally, in these studies, the highest reducing rates were observed during the first few days of microbial Fe(III) reduction. In our study, the influence of the type of Fe (oxyhydr)oxides on initial iron oxide-reducing rates were consistent with those of previous studies performed with pure strains.

### III-4.2 Bacterial communities

The structures of the initial bacterial communities present in the environmental samples were modified by the enrichment in Fe(III)-NTA medium, and again showed an evolution when the enrichments were grown in presence of solid Fe (oxyhydr)oxides (Figure III-5). This last result could be due to the difference of bio-availability of Fe with minerals compared to Fe(III)-NTA. Cai et al., (2019) also showed an influence of bio-available Fe(III) on microbial community structure (Cai et al., 2019). Here, the accessibility of Fe(III) in the Fe(III)-NTA incubations favored the iron reducing community that may have rapidly consumed available organic substrates and probably lowered the development of other bacteria. With minerals, however, Fe(III) is less accessible and competition for Fe(III) may induce changes in community structure. For example, Zhuang et al., (2011) indicated that *Rhodoferax* and *Geobacter* genera were acetate-oxidizing Fe(III)-reducers that compete in anoxic subsurface environments and this competition could influence the *in situ* bioremediation of uranium-contaminated groundwater by changing diversity structure (Zhuang et al., 2011). On the other hand, no clear effect of the type of Fe mineral on the global community profile was observed. This may be linked to the culture medium composition. Indeed, the addition of diverse C sources could enable fermentative bacteria to develop without using Fe(III) for their growth. In contrast, (Lentini et al., 2012) observed an effect of the type of Fe (oxyhydr)oxide, i.e. ferrihydrite, goethite or hematite, on the global structure of bacterial communities in enrichment cultures

using T-RFLP fingerprints. However, these authors did not use an initial Fe(III)-NTA enrichment step and did not use a sulfate-reducing bacteria inhibitor, as in our study.

### III-4.3 *Geobacter* and *Shewanella* 16S genes abundances

The relative abundance of *Geobacter* and *Shewanella* in the initial soils and sediment used as sources of IRB in our experiment could be linked to the redox conditions of the environment. Indeed, *Shewanella* 16S genes was present in higher proportions in the river sediment D3, than in the flooded soil D2, itself richer than the non-saturated soil D1 whereas *Geobacter* presented the opposite behavior. This indicates that the reducing conditions in the aquatic sediment was more favorable for some IRB, such as *Shewanella*, but not for *Geobacter*.

*Shewanella* and *Geobacter* represented in our incubation experiments a small proportion of the total community, however we made a focus on these two genera because they are the most studied iron reducing bacteria. However, the other members of the community could contribute either directly or indirectly to the iron solubilisation process. Considering the evolution of the two targeted IRB genera, namely *Geobacter* and *Shewanella*, after the enrichment with Fe(III)-NTA, the *Shewanella* / *Geobacter* 16S abundance ratio increased significantly compared to the site samples (Figure III-4  compared with Supplementary Figure III-S5), suggesting that the presence of a large amount of bio-available Fe(III) in the enrichment culture medium was in favor of *Shewanella*.

*Shewanella* could have from 8 to 11 copies of the gene encoding 16S rRNA, whereas *Geobacter* has 1 or 2 copies (Dikow, 2011; Holmes et al., 2004). Thus, the quantification of specific 16S genes does not reflect the cell abundances of the respective strains. All the same, this factor alone does not explain the differences between the abundances of *Shewanella* and *Geobacter* in our cultures, even if it could attenuate the difference in terms of specific cells numbers.

Another explanation for the sharp increase of *Shewanella* 16S gene abundance compared to *Geobacter* 16S gene abundance could be the composition of the culture medium in terms of organic substrates. *Geobacter* can use acetate as electron donors while performing the dissimilatory Fe reduction (Caccavo et al., 1994; Coates et al., 1996), but does not use lactate nor glucose. Conversely, some *Shewanella* species were shown to be able to use glucose and can present either respiratory or fermentative types of metabolisms (Ivanova et al., 2004; Nogi et al., 1998; Ziemke et al., 1998). Lentini et al., (2012) showed that the presence of *Geobacter* was favored by acetate whereas the growth of *Shewanella* was rather stimulated by lactate.

Moreover, these authors suggested that production of acetate through incomplete degradation of lactate by *Shewanella* could benefit *Geobacter* (Hori et al., 2015). Our medium contained both acetate, formate, lactate and glucose, thus it should potentially support growth of both *Shewanella* and *Geobacter*. However, a fermentative metabolism could explain the medium is favored by *Shewanella* over *Geobacter* in our enrichments and in all incubation conditions, because some species of this genus can grow either using fermentation or Fe(III) reduction (Bowman, 1997). As our medium contained 1.5 $g.L^{-1}$ peptone, this substrate could also favor the growth of bacteria belonging to the *Shewanella* genus by fermentation (Toffin et al., 2004).

When these communities were grown in presence of solid iron oxides, the abundance of *Shewanella* 16S gene (average of D1, D2 and D3) was 112, 30, 52 and 3058 times higher than the abundance of *Geobacter* 16S gene, for FoF, goethite, hematite and FoL, respectively. Moreover, we found that the cultures in presence of goethite inoculated with D3 bacteria contained higher proportions of *Geobacter* 16S gene than the same culture (D3) with FoL. These results might suggest that *Geobacter* could be more favored, in the competition with other IRB such as *Shewanella*, for growth in presence of goethite and hematite than for growth in presence of the more easily dissolved oxides, i.e., FoF and FoL. The type of Fe mineral can exert a selection pressure on the communities of IRB, as previously shown by Lentini et al., (2012). This result could be linked to a higher affinity of *Geobacter* for Fe(III), that would favor this organism at low Fe(III) availability levels. Reported Ks values for Fe(III) are 1.0 mM with *G. sulfurreducens* (Esteve-Nunez et al., 2005) compared to 29 mM with *S. putrefaciens* (Liu et al., 2001).

Yet, the solubility of ferrihydrite and lepidocrocite are higher than that of goethite and hematite (Cornell and Schwertmann, 2003b; Liu et al., 2007), thus the availability of Fe(III) could be higher with the first two oxides. *Shewanella* might be favored by high bio-available Fe(III), but could be less efficient for growth in presence of less soluble Fe-oxides such as goethite and hematite. The anaerobic respiration of *Shewanella* was highly dependent on electron shuttles. Nevin and Lovley (2002) suggested that *Shewanella alga* strain BrY released compounds that could solubilize Fe(III) from Fe(III) oxides, however, *Geobacter metallireducens* did not produce electron shuttles or Fe(III) chelators to solubilize Fe(III) oxides (Nevin and Lovley, 2002). Kotloski and Gralnick (2013) determined the contribution of flavin electron shuttles in extracellular electron transfer by *Shewanella oneidensis* (Kotloski and Gralnick, 2013) and Wu et al., (2020) showed that exogenous electron mediators (EMs) favored high density current production and increased the synthesis of extracellular polymeric substances which promoted

biofilm formation during electron shuttling process (Wu et al., 2020). The conduction of electrons along pili or other filamentous structures is one of the mechanisms proposed for electron transfer to solid iron oxides. (Leang et al., 2010) showed that OmcS, a cytochrome that is required for Fe(III) reduction by *Geobacter sulfurreducens*, was localized along the pili (Leang et al., 2010). The electrically conductive pili play a major role in the adaptation of *Geobacter* to perform dissimilatory iron reduction in natural environments (Liu et al., 2019a). These differences in the Fe(III)-reducing mechanisms between the two genera might explain their difference of affinity for Fe(III) (Esteve-Núñez et al., 2005; Liu et al., 2001) and the relative increase of *Geobacter* 16S gene abundance, observed here in presence of goethite and hematite, with the enrichment culture that was the most efficient for Fe-oxide solubilisation, i.e., culture D3.

### III-4.4 Relation between iron solubilisation effectiveness and *Geobacter* and *Shewanella* 16S gene abundances

In batch experiments, the three inocula D1, D2 and D3, enriched from soil from the river bank, flooded soil and an aquatic sediment of the Decize site gave similar results in terms of Fe solubilisation effectiveness of iron (oxyhydr)oxides. However, there were differences between different Fe (oxyhydr)oxides: the type of Fe (oxyhydr)oxides had more influence on Fe solubilisation effectiveness than the origin of the inocula. Fe solubilisation rates were slower with goethite and hematite compared to FoF and FoL. The same tendency was observed by Bonneville et al., (2004), who found that, with the pure strain *S. putrefaciens* in presence of 20 mM Fe(III), reduction of 6-line ferrihydrite was faster than that obtained with lepidocrocite, and faster than that obtained with low surface area hematite. (Li et al., 2012) reported similar results for the microbial reduction of Fe(III) oxides by *S. decolorationis* strain S12, the reducing speed decreasing according to the following order: lepidocrocite > goethite > hematite.

Principal Component Analysis (PCA) integrating chemical (**Supplementary Table III-S2**) and molecular data was performed to identify the relationships and contributions between iron solubilisation effectiveness and *Geobacter* / *Shewanella* 16S genes abundances in batch experiment samples (Hong et al., 2015; Mercier et al., 2014; Zhu et al., 2014). In this study, a biplot (**Supplementary Figure III-S6**) summarizes PCA results. The first principal component is strongly influenced by the iron solubilisation effectiveness (higher on the right than on the left side of the representation), with higher values associated with FoL, and the lowest associated with goethite and hematite (not separated), FoF being in an intermediary position.

Meanwhile proportion of *Shewanella* 16S gene, but not to the proportion of *Geobacter* 16S gene, seems to be correlated to FoL. The second principal component reflects high values of the proportion of *Geobacter* 16S gene in the bacterial communities. Thus, the proportion of *Shewanella* 16S gene seems to be more correlated to iron solubilisation parameters than the proportion of *Geobacter* 16S gene. PCA allows clear discrimination with different groups of iron oxides, however not for the different types of inoculum (D1, D2 and D3).

According to Bonneville et al., (2004), the dissolution and solubility of goethite and hematite are lower than that of ferrihydrite and lepidocrocite in the presence of *Shewanella.* (Cutting et al., 2009) indicated that hematite and goethite are susceptible to limited Fe(III) reduction in presence of *G. sulfurreducens.* Moreover, Poggenburg et al., (2016) mentioned that Fe(III)-organic compounds (coprecipitates from solutions of $FeCl_3$ and natural organic matter) reduction by *Shewanella putrefaciens* was influenced by the amount of available electron shuttling molecules induced by sorbed natural organic matter. Fe(III)-organic compounds' reduction by *Geobacter metallireducens* was more influenced by particle size, physicochemical properties and iron (oxyhydr)oxides (composition of sorbed natural organic matter and aggregation state) (Poggenburg et al., 2016). In our study, FoL samples with a higher proportion of *Shewanella* 16S gene in their total bacterial 16S genes were correlated with high initial iron solubilisation rates and electron shuttling molecules might have a role in this phenomenon. In contrast, *Geobacter* 16S gene abundance was not specifically associated to FoL but was found in higher proportions with goethite in one condition. This tendency is in accordance with findings of previous research performed with the less soluble iron oxides (Crosby et al., 2007), showing that *Geobacter sulfurreducens* reduced 0.7 % hematite and 4.0 % goethite while *Shewanella putrefaciens* reduced only 0.5 % of hematite 3.1 % goethite after 280 days of incubation. Thus, our results suggest that *Geobacter* might suffer less from the competition with *Shewanella* in low bio-available Fe(III) conditions, whereas the contribution of this genus, present in lower quantities than *Shewanella*, to the iron solubilisation effectiveness is not demonstrated. Moreover, other members in the community of IRB probably contributed to Fe solubilisation. Our culture medium contained substrates such as glucose and peptone that could support the growth of fermentative organisms. Lentini (2012) and Gagen (2019) indicated that fermentation likely plays a key role in reduction of crystalline iron oxides by diverse bacteria, such as *Telmatospirillum,* both through direct reduction and by the production of $H_2$, potentially used by dissimilatory iron reducers, during fermentation.

### III-4.5 SEM observations of Fe (oxyhydr)oxides and Mössbauer spectroscopy

In our study, the morphologies of four Fe (oxyhydr)oxides were observed by SEM before and after incubation with a mixed IRB enrichment. As previously observed in the literature for ferrihydrite, FoF presented an aggregated form with conchoidal fractures indicating its amorphous nature (Das et al., 2013; Schwertmann and Cornell, 2008) and as previously observed for lepidocrocite (Schwertmann, 1973; Schwertmann and Taylor, 1979) FoL presented a poor crystallization in accordance with the high specific surface of this synthetic material. Hematite samples presented submicron grains (Kim et al., 2008; Tadic et al., 2012) and goethite showed acicular or needle-shaped crystallized forms (Das et al., 2013; Schwertmann and Cornell, 2008). After incubation in presence of bacteria, secondary crystallized minerals were observed with FoF and FoL. The secondary minerals formed in FoL samples submitted to bioreduction showed a strong morphological similarity with the Fe(II)-phosphate vivianite observed by (Roldán et al., 2002; Muehe et al., 2016). Our goethite mineral before incubation presented a Mössbauer spectrum which was characteristic of goethite (Cornell and Schwertmann, 2003a). At the end of incubation, Fe(II) phases were observed in biotic goethite samples. We were not able to acquire Mössbauer spectra from the incubations of other minerals, however this result confirms the reduction of Fe(III)-oxides in biotic conditions, and suggests that the extent of reduction was higher than that evaluated only with the soluble Fe concentration, because some Fe(II) was partially immobilized in secondary minerals (Urrutia et al., 1998; Zachara et al., 2002). These observations and analyses proved to be informative, thus SEM observation and Mössbauer analyses were applied to samples generated by the further experiments, presented and discussed in the following sections.

## III-5 Conclusions and perspective

Microbial enrichments containing IRB, obtained from a site submitted to regular variations of redox conditions, were able to grow and reduce Fe(III) in a short time. Experiments performed with synthetic fresh oxides, goethite, and hematite confirmed the type of Fe mineral could influence reducing rates and the abundances of two DIRB genera, *Geobacter* and *Shewanella*.

The present study's results showed that: (1) the sub-culturing of IRB enrichments from Fe(III)-NTA to pure iron oxides media markedly modified the bacterial communities; (2) the global bacterial diversity was not significantly different from one type of pure (oxyhydr)oxide to another; (3) the type of Fe oxide in terms of mineralogy can influence the proportion of specific IRB genera, such as *Geobacter* and *Shewanella*. Meanwhile, the nature of Fe (oxyhydr)oxides

seems to have exerted a selection on the ratio of *Geobacter* and *Shewanella* 16S genes, whereas it did not impact the global bacterial community fingerprints. The concentration of bio-available Fe(III) in the enrichment medium may have favored the development of *Shewanella* genus that was clearly dominant compared with *Geobacter* genus. In presence of solid iron oxides, the highest proportions of *Shewanella* in bacterial communities were obtained with FoL and corresponded to the highest levels of iron reduction, possibly linked to the fact that FoL was the most soluble (oxyhydr)oxide in our experiments. This result is consistent with a hypothesis that *Shewanella* development could be favored by a high bioavailability of Fe(III). In contrast, *Geobacter* was detected in higher proportions with goethite that is less easily dissolved, when D3 culture was used.

Globally, all results suggest that both initial community composition of the sample used to prepare the enrichments, as well as the type of Fe(III) oxide used as electron acceptor influenced the relative abundance of *Geobacter* and *Shewanella* 16S genes. A better knowledge of the influence of biological parameters, such as biomass, diversity and activity, associated with iron reduction involving complex bacterial communities can help to elucidate Fe dynamics in surface environments. As biofilms in natural soils and sediments contain a large part of the bacterial biomass, future research could be focused on the contribution and distribution of IRB communities attached on iron oxides surfaces.

*Supplementary material*

## Supplementary Figures

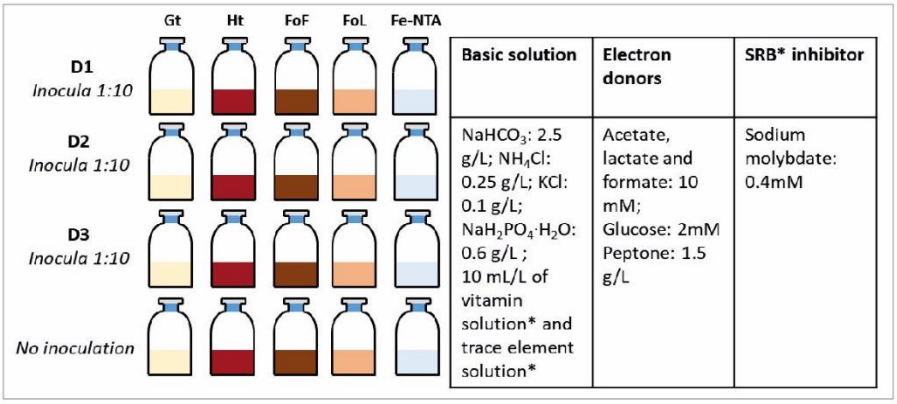


***Supplementary Figure III-S1**. Design and initial compositions of the batch experiments.*

***SRB**[1] : sulfate-reducing bacteria ; 2. **Vitamin solution** (1L): 2 mg biotin, 2 mg folic acid, 10 mg pyridoxine HCL, 5 mg Riboflavin,5 mg Thiamine, 5 mg Nicotinic acid, 5 mg Pantothenic acid, 0.1g B12 vitamin, 5 mg p-aminobenzoic acid, 5 mg thioctic acid ; 3. **Trace element solution** (1L): 1.5 g Trisodium nitrilotriacetic, 0.5 g $MgSO_4$, 0.5 g $MgSO_4 \cdot H_2O$, 1 g NaCl, 0.1 g $FeSO_4 \cdot 7\ H_2O$, 0.1 g $CaCl_2 \cdot 2H_2O$, 0.1 g $CoCl_2 \cdot 6H_2O$, 0.13 g ZnCl, 0.1 g $CuSO_4\ 5H_2O$, 0.1 g $AlK(SO_4) \cdot 12H_2O$, 0.1 g $H_3BO_3$, 0.25 g $NaMoO_4$, 0.24 g $NiCl \cdot 6H_2O$, 0.25 g $Na_2WO_4 \cdot 2H_2O$.*

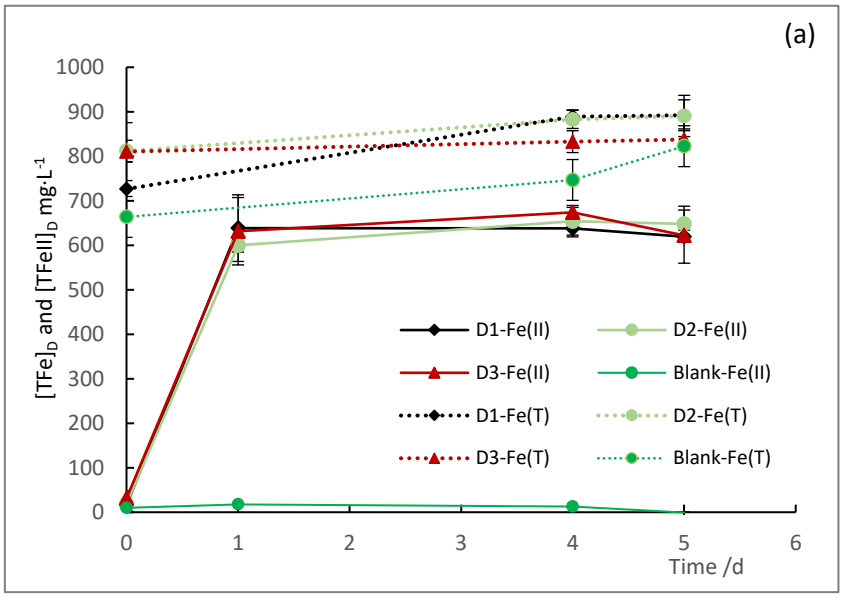

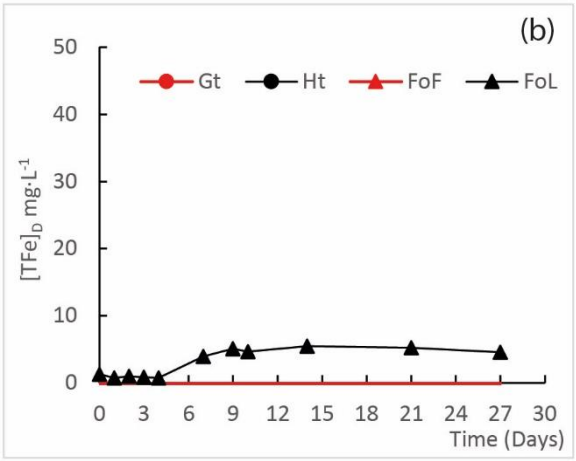


***Supplementary Figure III-S2.*** *Concentration of Fe(II) and total Fe (FeT) of D1, D2 and D3 incubated on Fe(III)-NTA medium (a), and evolution of the concentration of total Fe during incubation experiments with four abiotic Fe(III) (oxyhydr)oxides (b). Error bars represent the standard deviation of triplicate measurements.*

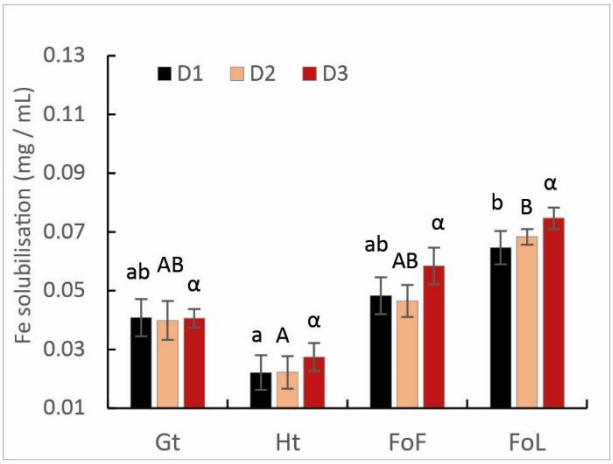


***Supplementary Figure III-S3.*** *Fe(III) dissolution of Fe oxides: goethite, hematite, FoF and FoL in presence of D1, D2 and D3 inocula. The small letter, capital letter and Greek letter were used for differing significantly (Kruskal-Wallis test at $p<0.05$) by group of inocula D1, D2 and D3 for different iron oxides. Error bars represent the standard deviation of triplicate measurements.*

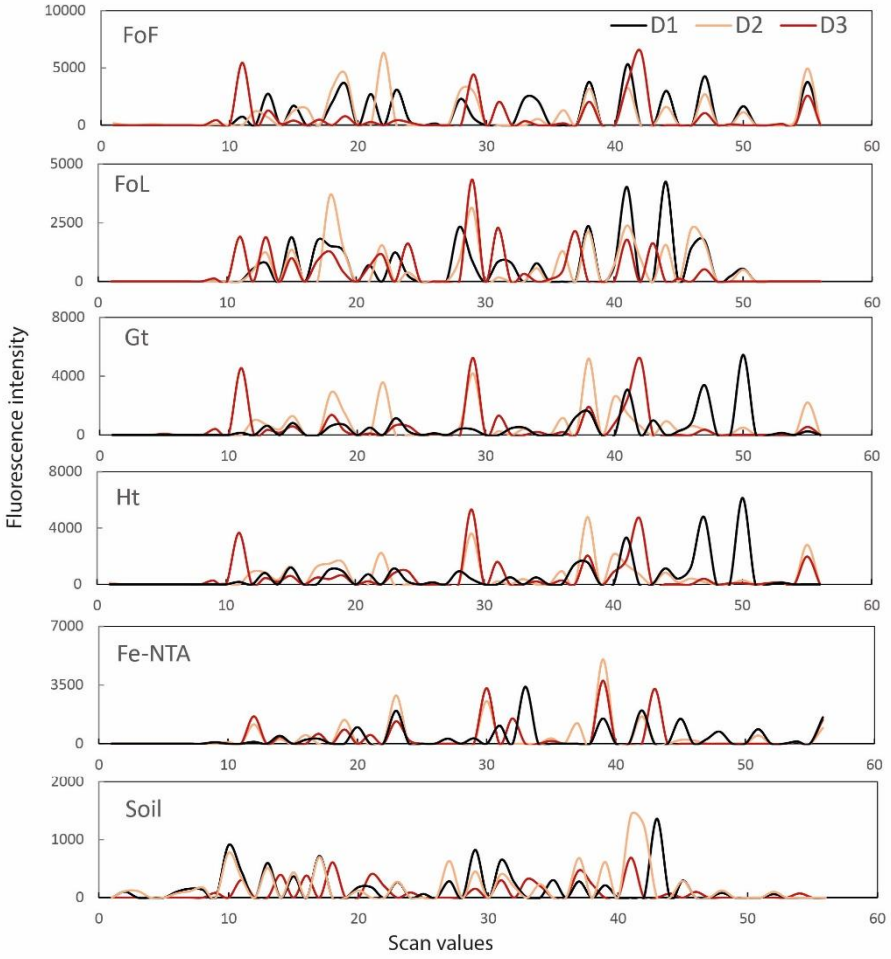


***Supplementary Figure III-S4.*** *CE-SSCP diversity profiles of the site samples (Soil), the Fe(III)-NTA enrichments (Fe-NTA) and cultures in presence of the four Fe oxides: FoF, FoL, goethite (Gt) and hematite (Ht). D1: soil from river bank; D2: sediment interface, flooded soil; D3: sediment under water. SSCP is a fingerprinting approach, fluorescently labeled blunt-ended PCR products are obtained from the highly variable V3 region of the 16S rRNA (rrs gene), denatured at high temperature, and then rapidly cooled to form unique single-strand conformations, which are separated based on their electrophoretic mobility in a polymer-filled capillary (Delbes et al., 2000). The scales are relative to standards. These profiles present high diversity with many peaks, with thus the presence of different bacterial strains.*

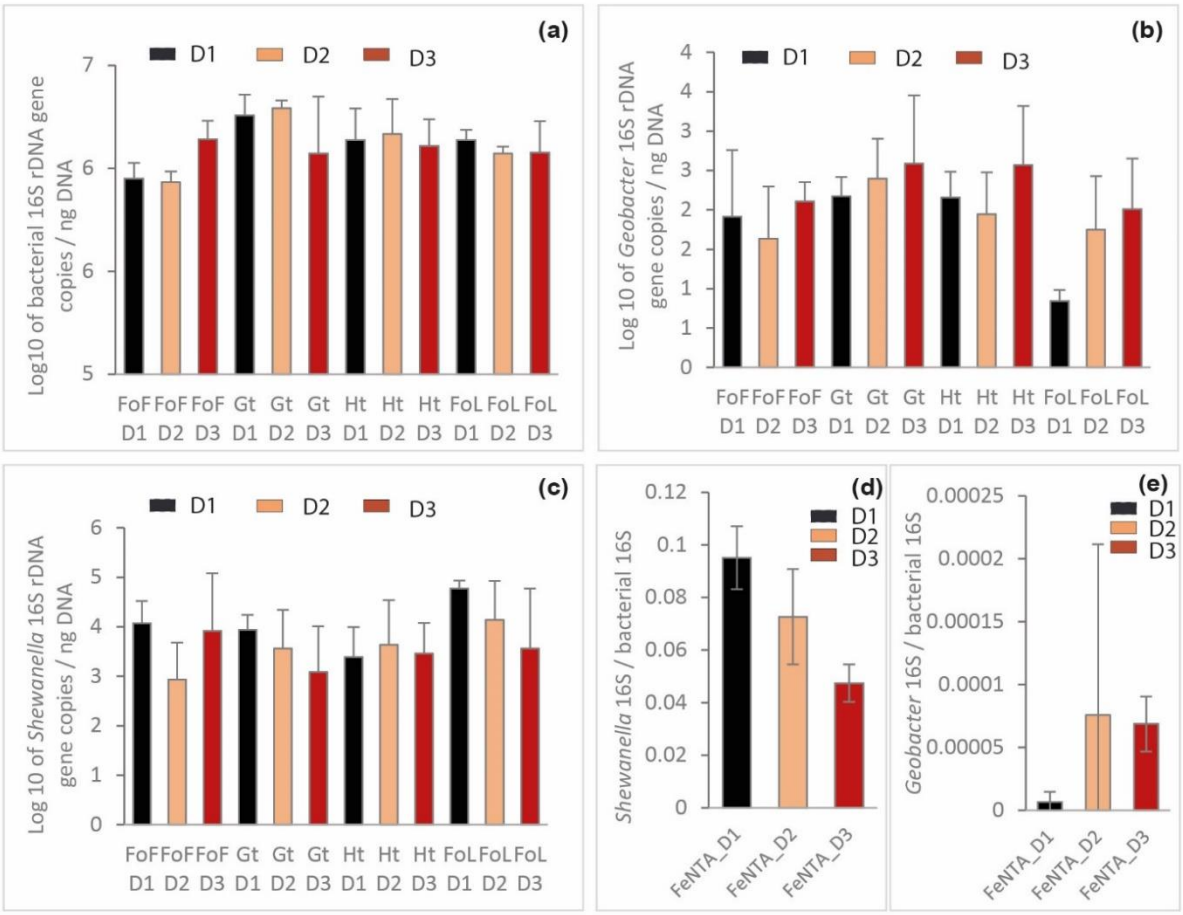


***Supplementary Figure III-S5.*** *Parameters linked to bacterial abundance: (a) Log10 of bacterial 16S rRNA (rrs gene) copies, (b) Log 10 of Geobacter 16S gene copies, (c) Log 10 of Shewanella 16S gene copies, for the three site samples D1, D2 and D3; Ratios of Shewanella 16S (d) and Geobacter 16S (e) over bacterial 16S rRNA genes copies in Fe(III)-NTA enrichments. Error bars represent the standard deviation of triplicate measurements.*

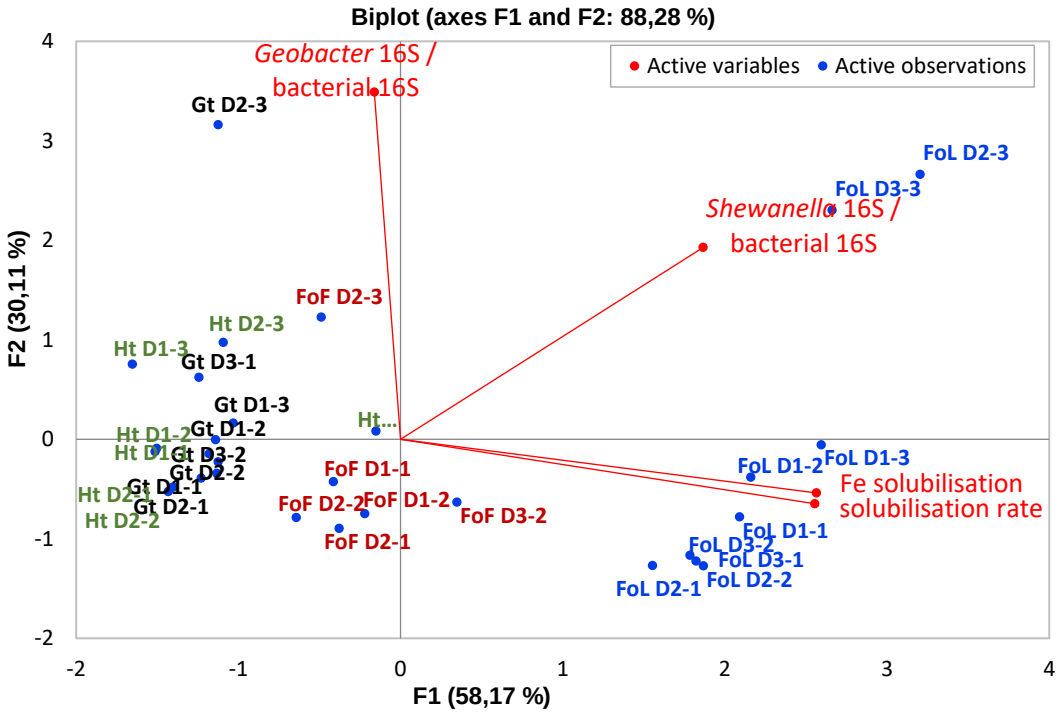


***Supplementary Figure III-S6.*** *Principal component analysis (F1 × F2) biplot map generated from iron solubilisation (percentage and rate of iron solubilisation) and ratios of Shewanella (Shewanella 16S / bacterial 16S) and Geobacter (Geobacter 16S / bacterial 16S) in the bacterial community, obtained for the FoF, goethite hematite and FoL incubations with D1, D2 and D3.*

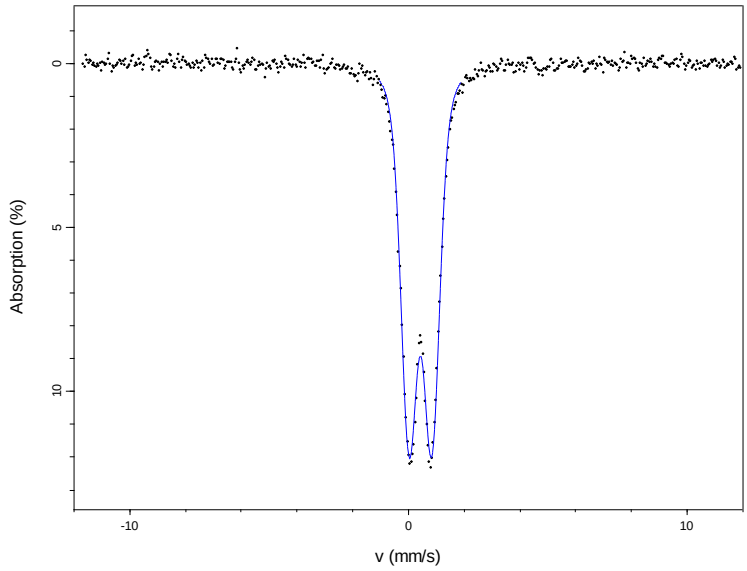


***Supplementary Figure III-S7*** *Mössbauer spectra collected at 140 K for synthetic ferrihydrite samples.*

## Supplementary Tables

***Supplementary Table III-S1.*** *Calculation of the iron oxides concentrations to obtain 20 mM Fe in the incubation experiments.*

| Minerals | Formula | Fe | Products of Fe(III) oxide |
|---|---|---|---|
| "Ferrihydrite" FoF | $Fe_2O_3 \cdot 0.5H_2O$ | 20 mM | 1.68 g/L |
| Goethite | FeOOH (30-63%: 46%) | | 3.86 g/L |
| Hematite | $Fe_2O_3$ (97%) | | 1.65 g/L |
| "Lepidocrocite" FoL | FeOOH | | 1.78 g/L |

***Supplementary Table III-S2.*** *Initial iron reduction*/solubilisation** rates (mg $L^{-1} \cdot h^{-1}$) of incubation experiment with dissolved Fe(III) and solid minerals. NA: not available data or abnormal data.*

| Inocula/ Minerals | Fe-NTA* | Goethite** | Hematite** | FoF** | FoL** |
|---|---|---|---|---|---|
| D1-1 | 26.17 | 0.07 | 0.03 | 0.09 | 0.47 |
| D1-2 | 29.42 | 0.09 | 0.03 | 0.16 | 0.42 |
| D1-3 | 22.26 | 0.07 | 0.00 | 0.13 | 0.38 |
| D2-1 | 23.51 | 0.07 | 0.04 | 0.16 | 0.42 |
| D2-2 | 24.29 | 0.09 | 0.05 | 0.11 | 0.48 |
| D2-3 | 24.87 | 0.06 | 0.04 | 0.14 | 0.42 |
| D3-1 | 29.21 | 0.08 | NA | NA | 0.46 |
| D3-2 | 23.82 | 0.09 | 0.27 | 0.33 | 0.45 |
| D3-3 | 21.98 | 0.08 | NA | NA | 0.42 |

***Supplementary Table III-S3.*** *Ratio of Initial iron solubilisation rates (mg $L^{-1}\cdot h^{-1}$) to the specific surface of minerals ($m^2/g$), incubation experiment with solid minerals. NA: not available data or abnormal data.*

| | Goethite | Hematite | FoF | FoL |
|---|---|---|---|---|
| D1-1 | $6.0\cdot10^{-03}$ | $9.6\cdot10^{-04}$ | $3.9\cdot10^{-04}$ | $1.4\cdot10^{-03}$ |
| D1-2 | $7.7\cdot10^{-03}$ | $9.6\cdot10^{-04}$ | $6.9\cdot10^{-04}$ | $1.0\cdot10^{-03}$ |
| D1-3 | $6.0\cdot10^{-03}$ | 0.0 | $5.6\cdot10^{-04}$ | $1.1\cdot10^{-03}$ |
| D2-1 | $6.0\cdot10^{-03}$ | $1.3\cdot10^{-03}$ | $6.9\cdot10^{-04}$ | $1.3\cdot10^{-03}$ |
| D2-2 | $7.7\cdot10^{-03}$ | $1.6\cdot10^{-03}$ | $4.7\cdot10^{-04}$ | $1.4\cdot10^{-03}$ |
| D2-3 | $5.1\cdot10^{-03}$ | $1.3\cdot10^{-03}$ | $6.0\cdot10^{-04}$ | $1.3\cdot10^{-03}$ |
| D3-1 | $6.8\cdot10^{-03}$ | NA | NA | $1.4\cdot10^{-03}$ |
| D3-2 | $7.7\cdot10^{-03}$ | $8.6\cdot10^{-03}$ | $1.4\ 10^{-03}$ | $1.3\cdot10^{-03}$ |
| D3-3 | $6.8\cdot10^{-03}$ | NA | NA | $1.3\cdot10^{-03}$ |

***Supplementary Table III-S4****. Characteristics of Fe(III) oxides submitted to Fe-reducing bacteria.*

| Iron oxide | Assumed morphology[a] | Surface area[b] ($m^2g^{-1}$) | Estimated mean particle size[c] (µm) |
|---|---|---|---|
| goethite | acicular | 11.7 | 1-2 |
| hematite | cylinder/rod | 31.4 | 30-120 |
| ferrihydrite | blocky | 232 | 20-60 |
| lepidocrocite | blocky | 337 | 10-80 |

[a]For use in estimating mean particle size from morphology by SEM-EDS (TM3000 accompanied by a SwiftED3000 X-Stream module (Hitachi)); [b]Determined by multipoint BET $N_2$ adsorption; [c]Estimated using the oxide densities quoted by (Roden, 2003), it assumed the following proportions for plate and cylindrical and particle morphologies: plate diameter: thickness = 10:1; cylinder length: diameter =10:1. Note that particle aggregation was ignored in these calculations.

# IV: Experiments with ferrihydrite fixed on slides

## IV-1 Introduction

Microbial attachment to mineral surfaces is a fundamental process relevant to geomicrobiology, the interdisciplinary field of geology and microbiology. Biofilm formation could be responsible for geochemical cycling of multiple elements and local environmental pollution and is also relevant to a broad variety of disciplines and applications (Dong, 2010; Elzinga et al., 2012; Roberts et al., 2006; Torrentó et al., 2012; Yan et al., 2016). In aqueous environments, microbial attachment behavior can significantly increase rates of mineral weathering (Ahmed and Holmström, 2015; Sampson et al., 2000), controlling the mobility of metals via cell wall sorption and metabolic utilization (Fein et al., 2001; Fein et al., 2002; Fowle and Fein, 1999; Melton et al., 2014).

In general, it is essential for bacterial cells to gain access to surface adherent nutrients or other substances e.g., electron donors/acceptors for cell metabolism by attachment on minerals (Harneit et al., 2006; Li et al., 2019; Mueller, 1996). Dissimilatory iron reduction may require microorganisms attachment onto the minerals in order to couple the oxidation of organic matter to the reduction of mineral sources of Fe(III) (Lovley, 1987; Roberts et al., 2006). Therefore, the solubility and bioavailability of Fe(III) might be the factor limiting interactions between DIRB and Fe minerals in subsurface environments (Sulzberger et al., 1989). According to previous research, DIRB have some proved strategies to overcome the inherent insoluble nature of iron oxides in the environment, including the hypothesis of use of chelators and electron shuttles to mobilize Fe(III) (Nevin and Lovley, 2002). Moreover, Esther et al. (2015) summarized four mechanisms for the electron transfer between IRB cells and Fe mineral surface, for two of which attachment is important: (1) direct contact between the cell and Fe (III) (oxyhydr)oxides mineral, and (2) cell appendages. When there is no soluble Fe(III) in the environment, bacteria produce flagella and fluff these appendages to adhere to Fe(III) to achieve Fe(III) reduction (Childers et al., 2002; Esther et al., 2015). Direct attachment is widely accepted as the predominant mechanism for accessing Fe(III) minerals in the environment (Lovley et al., 2004).

In the absence of $O_2$, *Geobacter metallireducens GS-15* and *Shewanella oneidensis MR-1* have been reported to use minerals as electron sinks for heterotrophy-based respiration, by oxidizing

organic matter or hydrogen ($H_2$) then transferring the released electrons to Fe or Mn minerals (Lovley and Phillips, 1988; Lovley et al., 1987). This dissimilatory mineral reduction could be linked to outer membrane (OM) expression of terminal reductases, joined to transmembrane and intracellular electron transport components. Hartshorne et al. (2009) indicated that in some species of *Shewanella*, deca-heme electron transfer proteins lie at the extracellular face of the OM, where they can interact with insoluble substrates (Hartshorne et al., 2009), a process referred to as extracellular electron transport (EET). To reduce extracellular substrates, these redox proteins must be charged by the inner membrane/periplasmic electron transfer system. Yang et al. (2019) used electrochemical measurements to demonstrate the correlation between redox protein concentration and the extracellular electron transfer function linked to extracellular polymeric substance (EPS) components by *Geobacter* biofilm (Yang et al., 2019). These results are consistent with studies showing that *Shewanella* and *Geobacter* exhibit heme-containing proteins located in the OM, suggesting a role of attachment in the reduction of Fe(III). Furthermore, some IRB could also have direct electron transfer between microbial cells through conductive nanowires (Cologgi et al., 2011; Gorby et al., 2006; Reguera et al., 2005). When taken together, these results support the concept that direct cell-mineral contact is necessary for certain IRB to access insoluble Fe(III) oxide and hydroxide phases. Both *Shewanella* and *Geobacter* were reported to use specialized pili to attach onto Fe minerals used as terminal electron acceptors (Childers et al., 2002; Elzinga et al., 2012; Jr and Das, 2002; Roberts et al., 2006). However, some *Shewanella* species could continue to grow by fermentation when Fe(III) became limiting (Ivanova et al., 2004; Nogi et al., 1998). *Shewanella putrefaciens* strain CN-32 was attached to the surface of hematite at variable pH values (4.5 -7.7) which indicated that phosphate-based functional groups on the cell wall play an important role in mediating adhesion through formation of inner-sphere coordinative bonds to hematite surface sites (Elzinga et al., 2012). While specific adhesion mechanisms for IRB pure stains have been studied in details at the molecular scale, comparatively less attention has been given to the quantification of their attachment behavior, in particular in mixed bacterial communities. Moreover, because of the multiple metabolic respiration pathways of IRB genera, quantitative measurements of IRB attachment to Fe(III) (oxyhydro)xides are still important to evaluate microbial iron reduction and microbial contribution in environment. In this study, we examined the attachment behavior of a mixed IRB community enriched from a natural site, as a function of microbial ferrihydrite reduction, and quantified two genera of IRB i.e, *Geobater* and *Shewanella*, present in this bacterial community together with many other potential bacteria contributing directly or

indirectly to Fe(III)-reduction. As biofilms play a major role in the porosity of natural soils (Christiani et al., 2008) and sediments (Griebler et al., 2002), it seems relevant to explore the link between biofilm formation and iron reduction, and the distribution of different IRB between biofilm and free cells. On the way to develop experimental device to observe natural biofilms formed at the surface of iron oxides, the objective of this experiment was to assess (1) the distribution of *Geobacter* and *Shewanella* in mixed communities containing diverse IRB in presence of ferrihydrite fixed on glass slides, and (2) the morphological evolution of the mineral particles on the slides, linked to ferrihydrite reduction, when a complex mixture of organic substrates is provided.

## IV-2 Specific materials and methods

### IV-2.1 Slide preparation with Fe(III) (oxyhydr)oxides

Glass slides (4.5*3 cm) were scratched by grinding and polishing machine to favor resin attachment. The previously used synthetized iron (oxyhyd)oxide that was confirmed to be ferrihydrite by Mössbauer spectra (Supplementary Figure III-S7), was attached to the slides using resin Loctite glue-3. Resin was spread on the glass slide and then 20-30 mg ferryhidrite powder was dispersed on the surface of glass uniformly using a 200 µm sieve. Then the glass slides were let at ambient temperature (20-25 ˚C) at least 30 min in order to harden the resin.

The prepared glass slides with fixed ferrihydrite were observed under SEM (SwiftED3000 X-Stream module, Hitachi) at 15 kV accelerating voltage (Thouin et al., 2016) before and after incubation. SEM-EDS were performed to explore the composition and distribution of Fe, and other elements, the acquisition time of EDS point analyses was 300 s.

10 slides with fixed ferrihydrite (Figure IV-1) were prepared and 2 of them were observed with whole views. Based on initial views, several specific positions were marked to make a focus to compare mineralogy change before and after incubation.

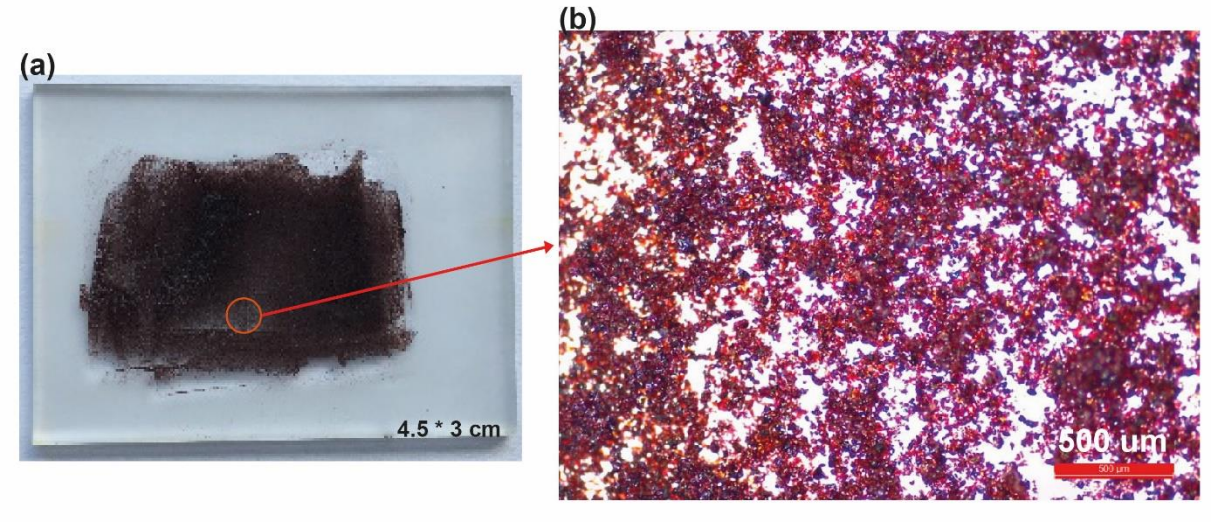


***Figure IV-1.*** *Photo of slide with fixed ferrihydrite (a) images ferrihydrite observed with an optical microscope (X40) (b).*

### IV-2.2 Slides incubation experiments

The culture medium used for slide-batch experiments was the same as the medium for IRB, without iron, detailed in chapter II-3.

Experiments were performed in 9 glass sealed jars, each containing 100 mL of sterile culture medium, prepared for 9 slides with fixed ferrihydrite. Sealed jars were sterilized at 121°C for 20 min and slides with fixed ferrihydrite were exposed to UV light for 10-20 min to decrease the number of potential contaminants. All the jars were prepared identically, but 3 of them were used for mineral observation, 3 for molecular analysis, 1 for SEM-EDS observation, and 2 were not inoculated in order to represent control condition.

Bacteria inoculum was prepared with the 11$^{th}$ subculture of D3 bacterial enrichment. The bacteria were collected on 0.22 µm filters to avoid the addition of dissolved iron from the inoculum media into the fresh medium. In order to inoculate the jars, 10 mL bacterial culture for each jar were filtered onto 0.22 µm filter, then the filter with bacteria was introduced into the jar. All these operations were performed into the glove box under anaerobic conditions. The jars sealed after inoculation are shown in Figure IV-2. They were incubated at 20°C in static conditions.


***Figure IV-2.*** *The slides with fixed ferrihydrite in jars.*

### IV-2.3 Monitoring

$[FeII]_D$ (dissolved Fe(II) concentration) was measured using the ortho-phenanthroline colorimetric method (Murti et al., 1966; Mamindy-Pajany et al., 2013) and $[FeT]_D$ (total dissolved iron concentration) was determined using the same method but with the addition of 0.1 mL of 1% hydroquinone prepared in acetate buffer to reduce dissolved $[FeIII]_D$ into $[FeII]_D$ (chapter II-4). During the incubation, 0.5 mL aliquot was collected with a syringe and placed into a 2 mL eppendorf tube for bacteria counting (chapter II-8.1), and 1.5 mL aliquot was collected and filtered through a 0.2 μm filter into 5 mL tubes and acidified with concentrated HCl immediately in the glove box, once a day for the first week, and once a week in the following weeks. At the same time, pH and Eh (ref. Ag/AgCl) were measured using standard hand-held portable meters (WTW Multi340i set) in the glove box.

After 85 days incubation, the slides for biofilm collection were taken out of the jars and rinsed with sterilized water, the other slides were rinsed with alcohol (75% v/v). Supernatants were removed and freeze-dried for observation of bacteria and minerals under SEM-EDS, as described in chapter II-6.

### IV-2.4 DNA extraction and molecular analysis

Liquid cultures were collected for DNA extraction by centrifuging 10 mL at 10,000 rpm for 10 min. Solid cultures were collected for DNA extraction by harvesting the remaining solids on slides surfaces by scraping the glass with a sterile blade (Figure IV-3).

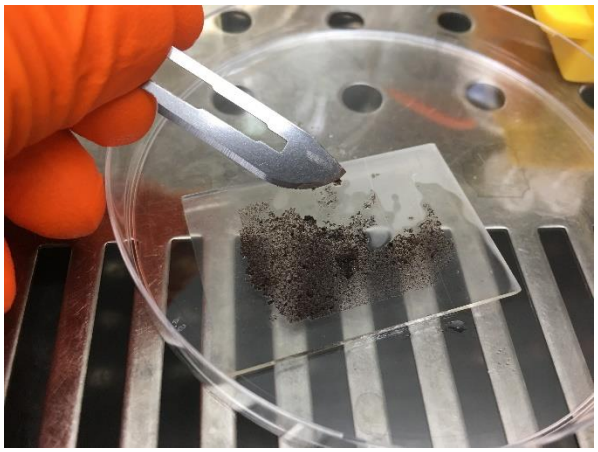

***Figure IV-3.*** *Solid culture collection for DNA extraction after incubation*

## IV-3 Experimental results

### IV-3.1 Bacterial growth

Evolution of bacterial concentration (cells $mL^{-1}$) during 85 days incubation with ferrihydrite fixed on slides is shown in Figure IV-4. The enumeration method (Thoma cell) can be reliable in the conditions of the present experiment because bacterial concentration was in the $10^9 – 10^{10}$ cells·$mL^{-1}$ range, far more concentrated than the suspended mineral particles resulting from precipitation reactions.

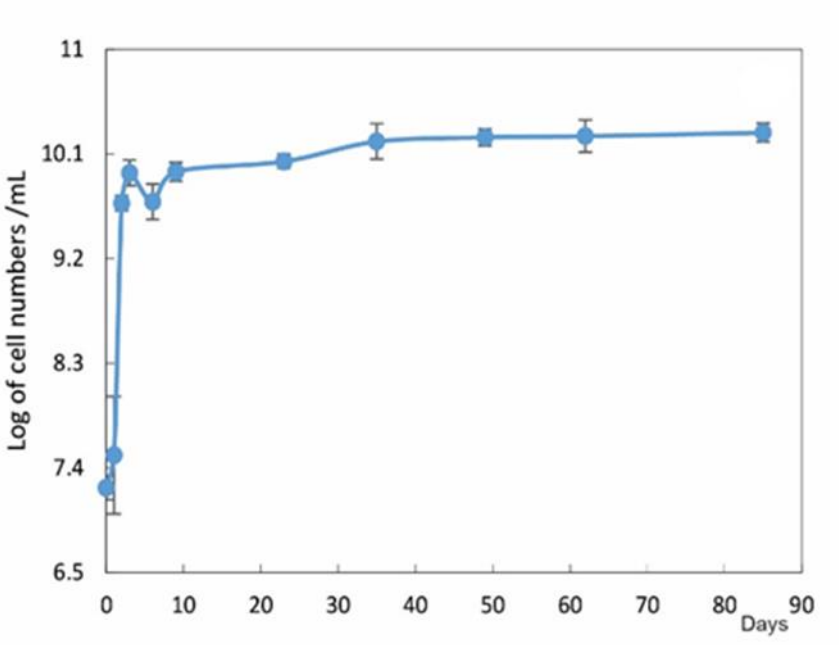


***Figure IV-4.*** *Evolution of bacteria numbers (Log cells $mL^{-1}$) in the liquid medium of 7 biotic jars during incubation. Cell numbers in the two abiotic jars were always below 1.84E+3 $mL^{-1}$ (not shown).*

Cell density increased very rapidly during the first 5 days and kept increasing until day 35, then remained almost constant in the following phase. Conversely, there were always only very few visible bacteria in abiotic jars.

### IV-3.2 Physico-chemical monitoring

Slide incubation experiments lasted 85 days. Evolution of $[FeT]_D$ and the correlation between bacterial concentration and $[FeT]_D$ are given in Figure IV-5 a and b respectively.

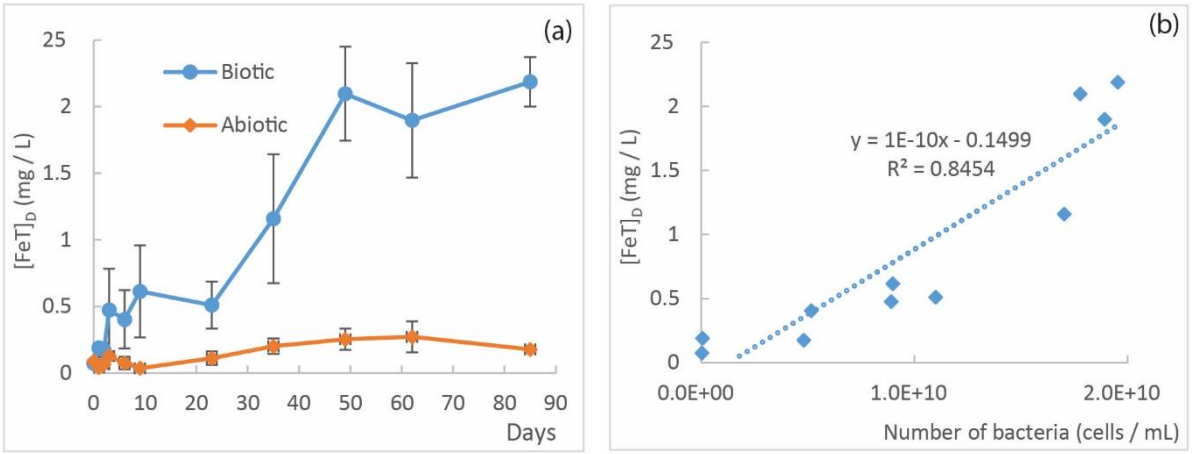


***Figure IV-5.*** *Temporal evolution of $[TFe]_D$ (mg $L^{-1}$) in biotic and abiotic jars (a), the correlation between the dissolved $[TFe]_D$ and the number of bacteria (cells $mL^{-1}$) in solutions of biotic jars(b).*

Ferrihydrite dissolution during the incubation was detected by the increase of $[FeT]_D$ in the biotic experimental system. The IRB reduced Fe(III) of ferrihydrite during the first 50 days of experiment (Figure IV-5 a). $[FeT]_D$ stabilized after day 50, corresponding to the end of bacterial growth, possibly related with the depletion of the nutrients (electron donors). No ferrihydrite dissolution was detected according to the evolution of $[FeT]_D$ in the abiotic experimental system. A good correlation between $[FeT]_D$ and the concentration of bacteria in the liquid medium was obtained (Figure IV-5 b).

Evolution of pH and Eh (ref. Ag/AgCl) monitored in jars are given in Figure IV-6.

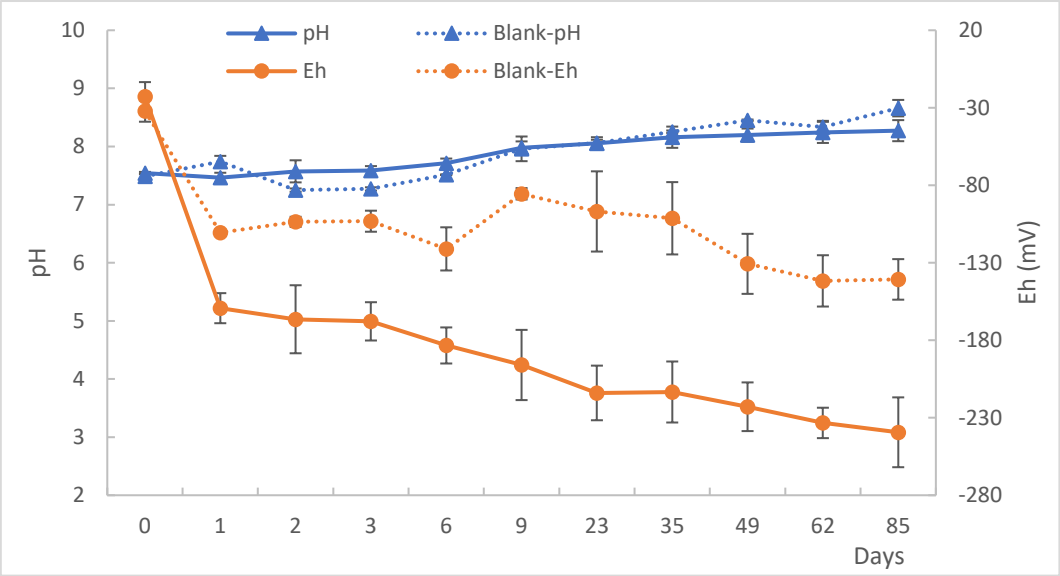


***Figure IV-6. 8****Evolution of pH and Eh (ref. Ag/AgCl) monitored in jars. Error bars represent the standard deviation of measurements in 7 the biotic jars / 2 abiotic jars.*

During the experimental period, pH was globally identical in the biotic and abiotic jars. Globally, the pH of the biotic jars slowly increased from 7.5 to 8.3 and the pH from abiotic jars between 7.2 and 8.7 (Figure IV-6). Concerning Eh, it was identical in biotic and abiotic jars at the beginning, then it gradually decreased in the biotic jars more intensely than in the abiotic jars, reaching values as low as -240 mV at the end of the experiment in biotic conditions, compared with -130 mV in abiotic conditions.

## IV-3.3 Bacterial observations and molecular analysis

### *IV-3.3.1 Bacteria observations under SEM*

After incubation, bacterial cells were observed on frozen samples by cryo-SEM using the backscattered detector imaging (BSE) mode and Secondary electrons imaging (SE) mode (Figure IV-S1).

### *IV-3.3.2 Bacterial abundance and abundances of Shewanella and Geobacter*

Microbial biomass was quantified at the end of incubation by measuring the concentration of total microbial DNA extracted from liquid and solid samples (Figure IV-7).

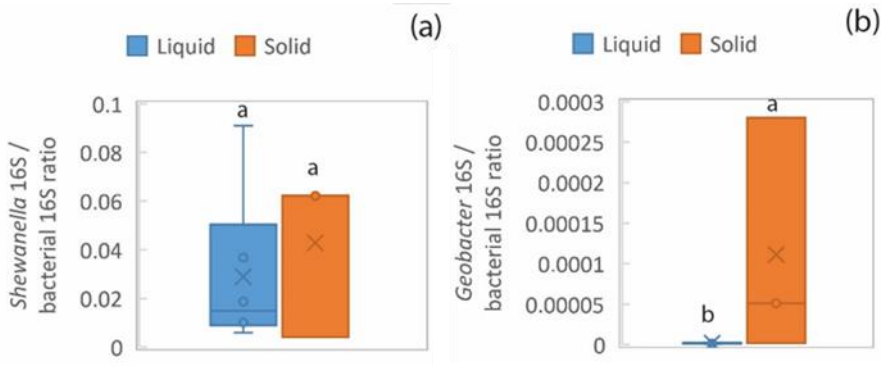


***Figure IV-7.*** *Parameters linked to bacterial abundance (**a**) ratio of Shewanella over bacterial 16S rRNA genes copies, (**b**) ratio of Geobacter over bacterial 16S rRNA genes copies, for liquid and solid cultures. The letters "a" and "b" differed significantly (Kruskal-Wallis test at $p<0.05$) between liquid and solid cultures. Data represent average values of experimental replicates and their standard deviation (σ). Solid cultures included three replicates, liquid cultures included 6 replicates.*

No significant differences were observed between liquid and solid compartments for the *Shewanella* 16S / bacterial 16S ratio (Figure IV-7). Conversely, a significantly higher proportion of *Geobacter* / 16S gene in solids than in liquid medium was observed (Figure IV-7). Thus, the proportion of the two quantified IRB i.e. *Geobacter* and *Shewanella*, differs in the two bacterial communities, free suspended in the liquid medium and attached to the solids. As already observed in previous experiments with our IRB enrichments, the proportion of *Shewanella* in both liquid and solid cultures were significantly higher than for *Geobacter*.

### IV-3.4 Mineral SEM-EDS observations

The global view of a glass slide fixed with ferrihydrite is shown in Figure IV-8 under 30X. The marked area "23" was used to compare the mineral morphology change before and after incubation with IRB.

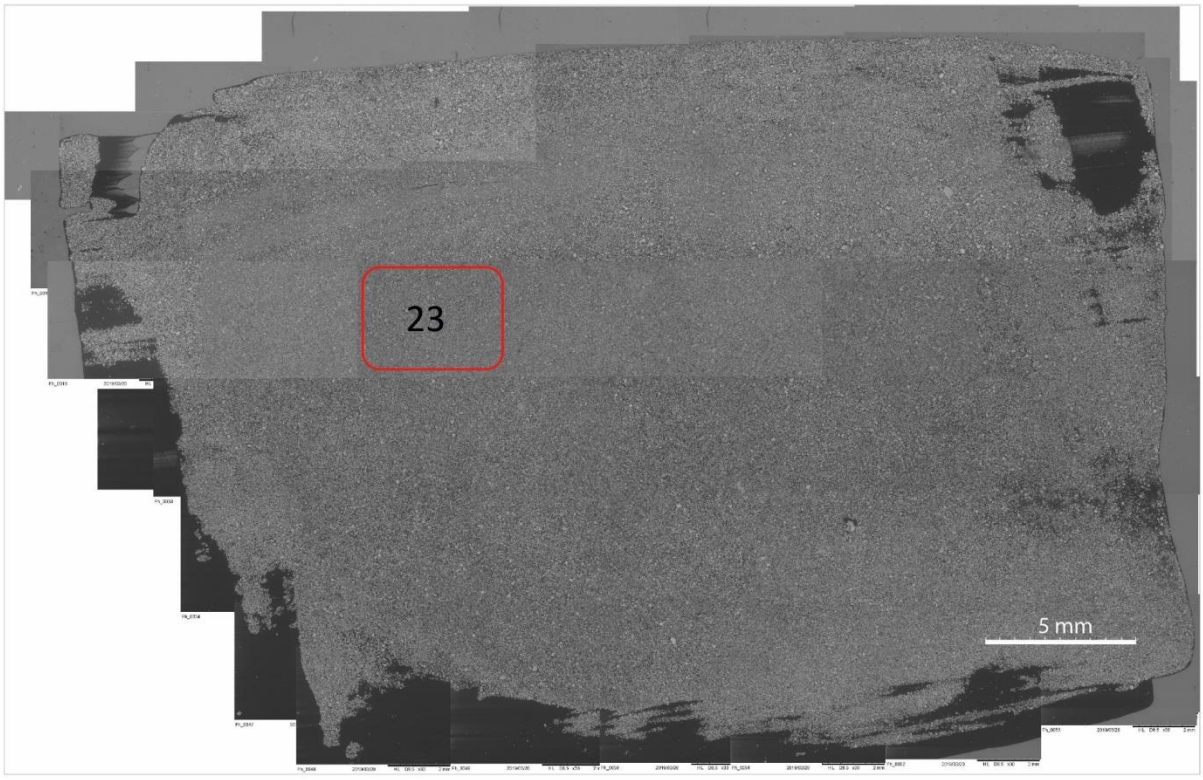


***Figure IV-8.*** *The global morphology view of a glass slide with fixed ferrihydrite under SEM, the marked number "23" was the main area used to focus on changes of mineral morphology before and after incubation with IRB.*

The comparison of SEM-EDS observations on area "23" before and after incubation are given in Figure IV-9.

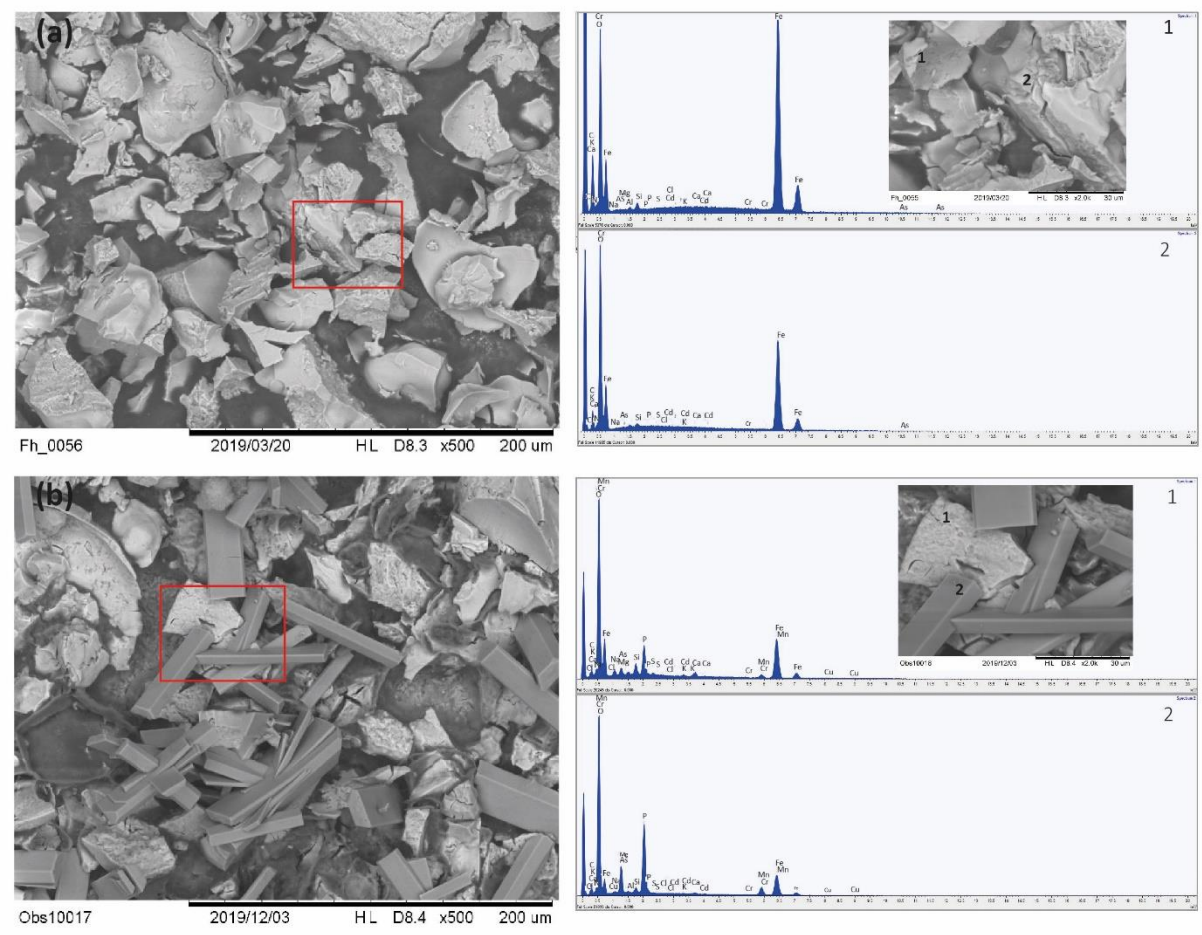


***Figure IV-99.*** *SEM-EDS analysis of ferrihydrite samples in the specific area "23" on the glass slide, before incubation (a) and after incubation (b).*

***Table IV-11.*** *Semi-quantitative EDS analysis (relative concentrations in weight %) of main elements in point analyses located on SEM pictures and corresponding spectra shown Figure IV-9 and P/Fe, O/Fe, C/Fe rations.*

| Sample | Point | C | O | Si | P | S | Fe | P/Fe | O/Fe | C/Fe |
|---|---|---|---|---|---|---|---|---|---|---|
| Before | 1 | 7.41 | 24.64 | 0.46 | 0.01 | 0.00 | 66.93 | 0.00 | 0.37 | 0.11 |
| | 2 | 6.93 | 40.34 | 0.32 | 0.00 | 0.00 | 52.07 | 0.00 | 0.77 | 0.13 |
| After | 1 | 7.25 | 52.86 | 1.35 | 4.33 | 0.26 | 28.18 | **0.15** | 1.88 | **0.26** |
| | 2 | 7.61 | 57.38 | 0.58 | 10.04 | 0.07 | 14.85 | **0.68** | 3.86 | **0.51** |

The microscopic picture on the whole glass slide with fixed ferrihydrite was taken before the experiment. The specific area was marked with number "23" to follow the morphology change (Figure IV-9). Ferrihydrite was characterized, before incubation, by diverse particles of 10-50 µm presenting irregular shapes (Figure IV-9) that mainly contained the elements O (20-40%) and Fe (50-70%) (Table IV-1). After incubation, new forms of particles with crystalline aspects and a prismatic morphology, 100 µm long and 10 µm large, were observed in the same area on

the glass slide (Figure IV-9). As revealed by SEM/EDS analysis, these prismatic crystals still contained O (50-60%) and Fe (10-20%), but also P (10-15%) that was not detected in the initial particles (Table IV-1).

More information on post-incubation slides (biotic and abiotic) were given by additional SEM-EDS observations of fixed minerals and precipitates collected from the liquid medium of biotic jars (Figure IV-10).

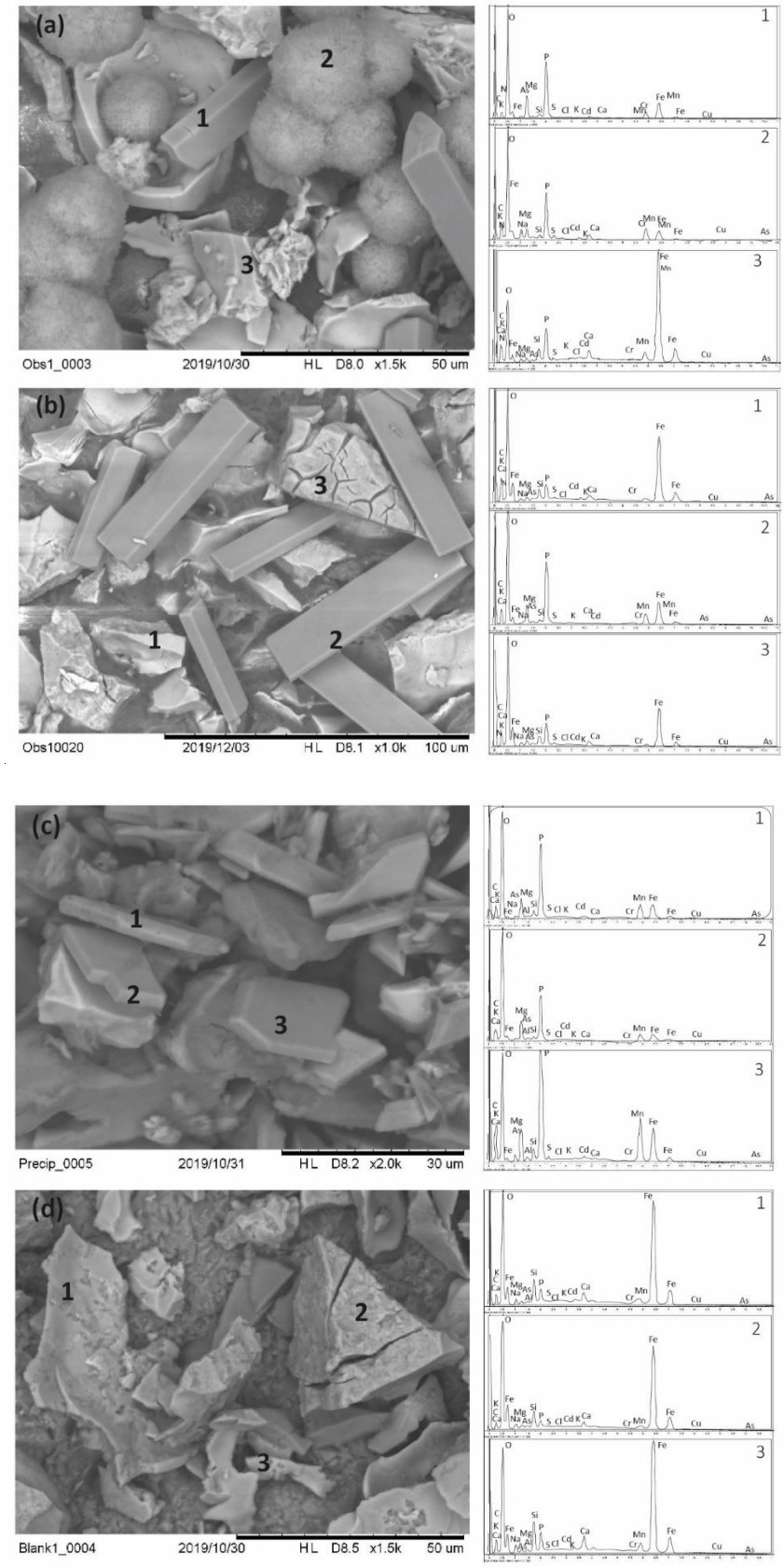


***Figure IV-101.*** *SEM-EDS analysis of ferrihydrite samples after incubation, biotic glass slides with fixed ferrihydrite ("a" and "b"), precipitates collected in the liquid medium (c), and abiotic glass slides with fixed ferrihydrite (d).*

Samples of biotic glass slides, abiotic glass slides and precipitates harvested from the biotic medium were observed and analyzed by SEM/EDS. The crystalline minerals with a prismatic texture described in the previous section were observed in all the biotic samples, glass slides and precipitations (Figure IV-10). SEM/EDS analysis indicated that these crystals mainly contained O (30-60%), Fe (10-20%), and P (10-15%) (Table IV-2). These secondary minerals all presented a higher P/Fe ratio than the typical ferrihydrite particles observed in Figure IV-10 d. Moreover, a spherical mineral presenting high P/Fe and C/Fe ratios was also observed on the glass slides (Figure IV-10). No morphology changes during incubation were observed on abiotic glass slides and the main elements e.g., O (20-40%) and Fe (50-70%) analyzed by SEM/EDS presented similar results as the initial sample, with no mineral enriched in P or in C.

***Table IV-12.*** *Semi-quantitative EDS analysis (relative concentrations in weight %) of main elements in point analyses located on SEM pictures and corresponding spectra shown Figure IV-10 and P/Fe, O/Fe, C/Fe rations.*

| Samples | Point | C | O | Si | P | S | Fe | P/Fe | O/Fe | C/Fe |
|---|---|---|---|---|---|---|---|---|---|---|
| a : biotic | 1 | 7.72 | 51.09 | 0.54 | 11.75 | 0.09 | 17.35 | **0.68** | 2.95 | 0.45 |
| fixed 1 | 2 | 10.01 | 53.37 | 0.48 | 9.16 | 0.54 | 9.47 | **0.97** | 5.63 | **1.06** |
| | 3 | 5.87 | 16.58 | 1.31 | 3.97 | 0.32 | 64.38 | 0.06 | 0.26 | 0.09 |
| b: biotic | 1 | 7.98 | 35.27 | 1.26 | 2.37 | 0.14 | 49.53 | 0.05 | 0.71 | 0.16 |
| fixed 2 | 2 | 8.29 | 48.11 | 0.30 | 11.71 | 0.03 | 20.41 | **0.57** | 2.36 | 0.41 |
| | 3 | 7.99 | 45.27 | 1.38 | 4.24 | 0.25 | 36.17 | 0.12 | 1.25 | 0.22 |
| c: | 1 | 9.21 | 48.78 | 0.61 | 13.36 | 0.09 | 12.56 | **1.06** | 3.89 | **0.73** |
| biotic | 2 | 9.35 | 58.62 | 0.41 | 10.62 | 0.08 | 8.17 | **1.30** | 7.18 | **1.14** |
| precipitates | 3 | 11.01 | 32.39 | 0.92 | 12.38 | 0.24 | 17.43 | **0.71** | 1.86 | **0.63** |
| not fixed | | | | | | | | | | |
| d: abiotic | 1 | 5.63 | 26.77 | 2.45 | 1.45 | 0.06 | 58.23 | 0.02 | 0.46 | 0.10 |
| fixed | 2 | 5.22 | 30.59 | 1.95 | 0.85 | 0.02 | 57.78 | 0.01 | 0.53 | 0.09 |
| | 3 | 5.30 | 23.21 | 2.98 | 2.00 | 0.02 | 58.74 | 0.03 | 0.40 | 0.09 |

# IV-4 Discussion

## IV-4.1 Fe dissolution

$[FeT]_D$ increased over time in the biotic systems, but not in the abiotic control experiments. Futhermore, the increase in $[FeT]_D$ was correlated to the increase of the bacterial cell numbers, which suggested that ferrihydrite dissolution was due to bacterial activity in the biotic conditions. Microbial ferrihydrite dissolution rate and efficiency in presence of inoculum D3 have been discussed in chapter III, where we showed the dissolution of 4-6 % of the initial 20 mM iron supplied as ferrihydrite in slurry experiments. In the present experiment, according to $[FeT]_D$ reached in the liquid medium, 1-2 % (approximately) of the initial ferrihydrite was dissolved. Although ferrihydrite reduction was less efficient in the present study compared with the previous slurry system, bacteria were metabolically active. They might have contributed less to iron dissolution for two reasons: (1) the ferrihydrite fixed on the glass slides was less available for IRB because a part of its surface was inserted into the resin; (2) the static experimental setup reduced the transfer of substances between the surface of ferrihydrite and IRB present in the liquid medium. A study from (Bose et al., 2009) suggested that hematite morphology, particle size, and/or degree of aggregation seemed to influence the mechanism that *Shewanella* uses to access Fe(III) sites on hematite surfaces.

## IV-4.2 Distribution of *Shewanella* and *Geobacter* 16S gene copies in the liquid medium and in the biofilm

Evolution of bacterial numbers in suspension in the liquid phase indicated that the bacterial population increased during the first 50 days. The proportion of *Shewanella* and *Geobacter* 16S gene copies were quantified as free-living cells or attached to the solid phase at the end of the experiment. Ratio of *Shewanella*/total bacteria (qPCR 16S approach, Figure IV-7) in the liquid compartment was comparable to the ratio in the previous slurry experiment, and around 0.01 - 0.03 (chapter III). A similar ratio of *Shewanella/*total bacteria was in the biofilm. Conversely, the ratio of *Geobacter/*total bacteria (qPCR 16S approach, Figure IV-7) was significantly higher in the biofilm attached to the solid phase than in suspension in the liquid phase. However, as observed in slurry (chapter III), *Geobacter* 16S gene abundance was still around 100 times lower than *Shewanella* 16S gene in the bacterial community that developed during the slide experiment. This could be attributed to the composition of the culture medium.

Previously, it has been shown that cell-ferrihydrite contact is necessary for IRB e.g., *Shewanella* and *Geobacter* genera to use the electrons from Fe(III) (oxyhydro)oxides to reduce Fe(III) (Gorby et al., 2006; Reguera et al., 2005). *Geobacter* genus requires iron reduction for its metabolism, whereas, for *Shewanella* genus, some species can either use iron reduction or switch to fermentation (Nogi et al., 1998). On the other hand, according to research on the mechanisms of Fe(III) use as the electron acceptor by IRB cells, four IRB-mineral interactions were evidenced, e.g., by direct contact, by ligands/siderophore, by electron shuttles, and by pili (Esther et al., 2015). *Shewanella* has been reported to use electron shuttles for indirect iron reduction, these electron shuttles can be exogenous like humic substances and sulfur compounds (Liu et al., 2011a; Stams et al., 2006) or endogenous as those secreted by the organism itself (Marsili et al., 2008; Newman and Kolter, 2000; Von Canstein et al., 2008). Conversely, *Geobacter* genus has been found and reported to need physical contact during Fe(III) reduction rather than use indirect reduction pathways. *Geobacter* genus is well known to interact with solid Fe(III) (oxyhydr)oxides using pili filaments, also named as 'bacterial nanowires' (Esther et al., 2015; Reguera et al., 2005; Roberts et al., 2006).

Moreover, Reguera et al., 2007 showed that *Geobacter* genus required the expression of electrically conductive pili to form biofilms on Fe(III) oxide surfaces, and pili are also essential for biofilm development on plain glass when fumarate was the sole electron acceptor. These authors suggested that the pili of *Geobacter* genus had a structural role in biofilm formation (Reguera et al., 2007). So, according to literature, ferrihydrite reduction by IRB could occur by direct and indirect contact with IRB belonging to *Shewanella genus* and mainly by direct contact with IRB belonging to *Geobacter* genus. This could explain why, in the present experiment, *Geobacter* proportion was more important in the biofilm than in the in the bacterial community suspended in the liquid medium.

### IV-4.3 SEM observation of the solid particles

SEM observation showed the formation of new types of particles in biotic conditions. These secondary minerals were enriched in phosphorous and/or in carbon. Precipitation of iron phosphate minerals could have occurred (Zachara et al., 1998). Heiberg et al., 2012 observed the precipitation of the Fe(II)-phosphate vivianite during the anoxic incubation of a natural soil. In our systems, the phosphate present in the culture medium could precipitate with the Fe(II) produced by the IRB. Muehe et al. indicated that Fe(II) inputs generally lead to vivianite precipitation in phosphate-bearing environmentsfound that As(V) partly replaced phosphate in

vivianite, thus forming a vivianite-symplesite solid solution identified as $Fe_3(PO_4)_{1.7}(AsO_4)_{0.3}\cdot 8H_2O$ (Muehe et al., 2016).

In addition, particles with high C/Fe proportion could represent forms of iron carbonates (siderite). The siderite could be formed by reducing akaganeite in the presence of *Shewanella* under a $H_2$-$CO_2$ atmosphere (Roh et al., 2003). Such globular morphology of Fe carbonate were already observed (Wiesli et al., 2004). The formation of Fe carbonate during the incubation of *Shewanella putrefasciens* in presence of natural Fe(III) oxides was reported (Maitte et al., 2015). In this study, the liquid phase was composed of synthetic mine water amended with formate only, as an electron donor, contrary to our conditions corresponding to a culture medium with high concentrations of phosphate and several electron donors. In our biotic conditions, the degradation of organic electron donors resulted in the production of inorganic C that could react with Fe(II) and other substances present in the liquid medium, to form secondary minerals.

SEM observations also showed the presence of bacteira on the attached solid particles. (Thormann et al., 2004) reported the very rapid biofilm formation of *Shewanella*, in 48 to 120 h, in presence of a rich culture medium. However, bacteria were observed not only on the ferrihydrite particles, but also on the secondary minerals. This observation suggests that the particles were not colonized exclusively to facilitate Fe(III) dissolution, but also as a solid support for the development of other bacteria, that could grow by fermentation of organic molecules.

## IV-5 Conclusion and perspective

This original experiment using ferrihydrite fixed with resin onto glass slides enabled biofilm development on iron oxides and secondary minerals formation. In particular, we found different abundances of two well characterized IRB genera in the biofilm and surrounding liquid medium, and these differences might be related with their metabolism. Indeed, *Geobacter*, a genus that requires direct contact with solids to use Fe(III) as an electron acceptor was significantly more abundant in the biofilm than in the liquid medium, whereas *Shewanella*, a genus includes species that can either use Fe(III) respiration or fermentation to thrive was found equally distributed between the two phases. Up to now, studies have mainly been performed with pure strains of IRB, and our results obtained with a complex enrichment of IRB, including many potential DIRB and fermentative IRB, and focusing on quantification of *Shewanella* and

*Geobacter* in these communities, opens the perspective to study Fe(III) reduction processes in conditions closer to those of natural sites.

Globally, all results suggest that our IRB inoculum contains a certain percentage of bacteria affiliated to *Geobacter* and *Shewanella* genera which include species known to use Fe(III) (oxyhydr)oxides as an electron acceptor during dissimilatory iron reduction. The method to prepare glass slides could be applied in order to study the influence of the type of Fe(III) mineral on the composition of natural biofilms, with the possibility to immobilize a range of different oxides. Beyond laboratory studies, slides could be placed on site, inserted in soils or aquatic sediments, in order to acquire a better knowledge of the contribution and distribution of IRB communities attached on iron oxides surfaces can help to elucidate Fe dynamics in surface environments.

# *Supplementary material*

## Supplementary Figures

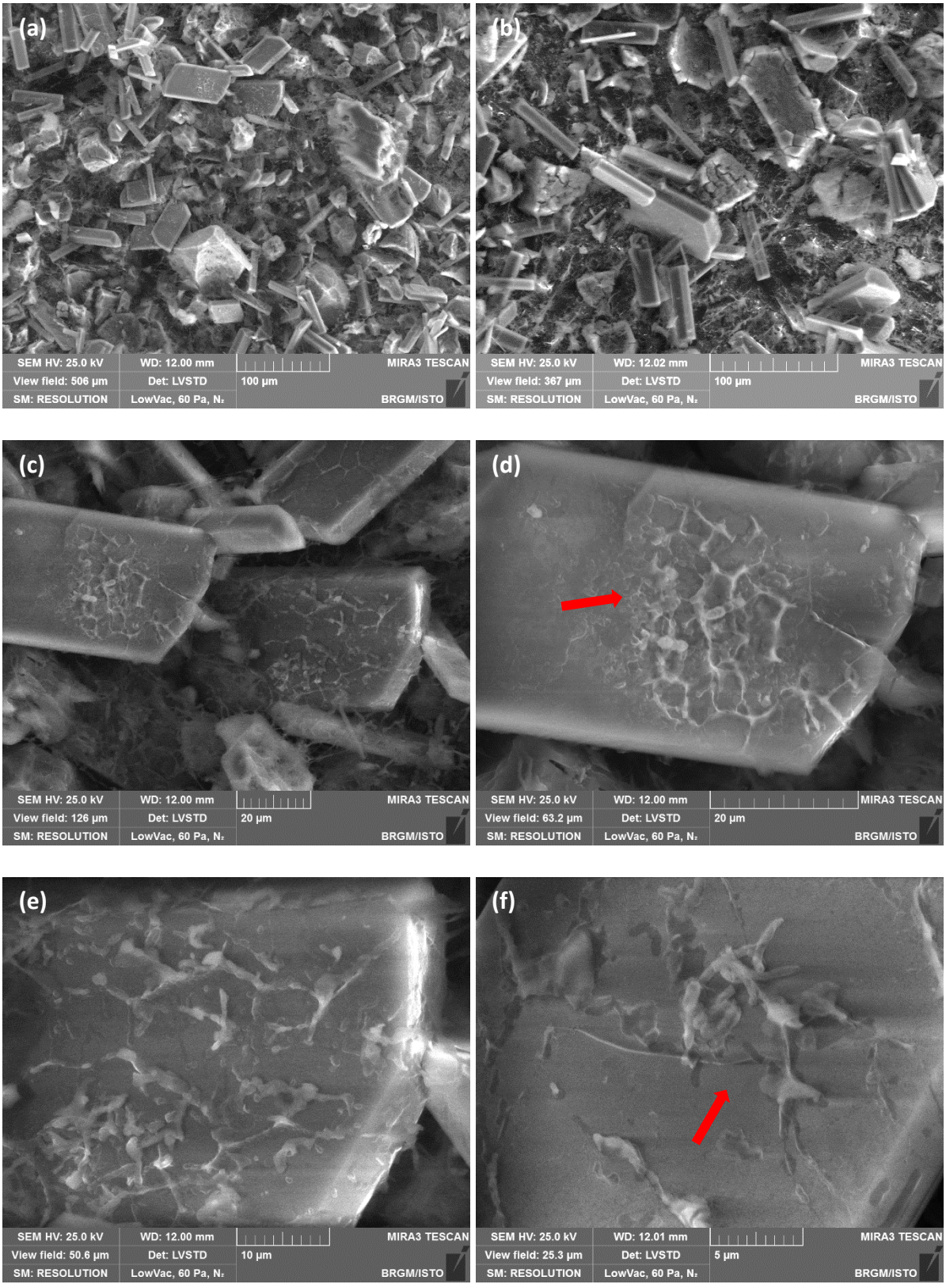

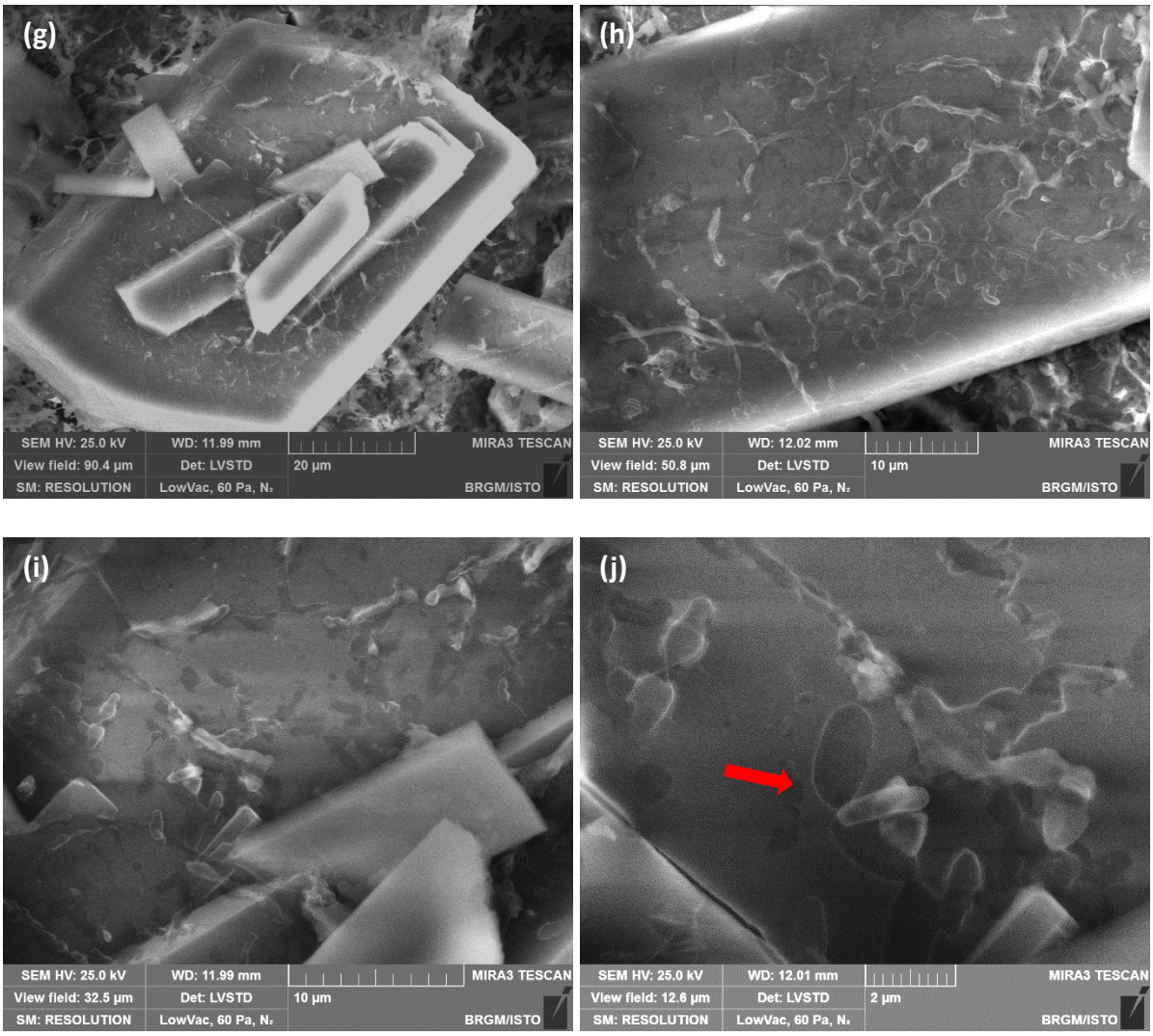


***Figure IV-S1.*** *Cryo-SEM photomicrographs of bacteria on the surface of glass slides with fixed ferrihydrite at the end of the experiment. Red arrows indicate the minerals observed in (a) and (b), and cells attached to minerals in (d), (f) and (j).*

Some bacterial cells appeared spherical shaped and rod shaped, separated from each other, turgid, and complete with smooth surface, on secondary mineral grains. Bacterial morphology was very clear under the microscope field of Figure IV-S1 (i) and (j), cell size was between 1-4 µm. Other bacteria seemed to be embedded in an exopolymeric matrix typical of biofilms (Figure IV-S1 c to f). Moreover, ferrihydrite (Figure IV-S1 (a) and "secondary minerals" (Figure IV-S1 (b) were both observed on the surface of glass slides, but bacterial cells and biofilms were mainly present on surface of "secondary minerals" (Figure IV-S1 (c, d, e, f)) and some "traces" (might be networks of corrosion-like channels that accommodate bacterial cells and exopolymer filaments) were observed on the position of bacteria (Figure IV-S1 (j)).

# Chapter V: Mobility of As, Cr and Cd adsorbed on Fe (oxyhydr)oxides submitted to IRB

## V-1. Abstract

A continuous column experiment was carried out to investigate the mobility of trace elements (TEs, i.e. As, Cr, Cd) and transformation of ferrihydrite and goethite under iron-reducing conditions. Two column experiments were performed with ferrihydrite and goethite respectively, spiked with As, Cr and Cd through a preliminary adsorption step. The experimental program included three successive phases: stabilization with synthetic water, inoculation with IRB and feeding with mixtures of synthetic water and organic substrates (glucose, acetate, formate, lactate and peptone). Evolution of total dissolved concentrations of Fe, As, Cd and Cr, and the values of redox potential and pH were monitored in the column's outlets. Iron concentration was always higher in the outlet of inoculated columns than in un-inoculated conditions. At the end of the experiment, 96 mg of Fe had been leached from the inoculated goethite column (0.8 mg from the un-inoculated condition), whereas 141 mg of Fe had been leached from the ferrihydrite column (13 mg for the un-inoculated condition). The evolution of iron and TEs in inoculated and un-inoculated columns confirmed microbial Fe reduction and that the type of Fe (oxyhydr)oxides could influence the mobility of As, Cr, and Cd. Relation between type of Fe oxide and the relative abundances of two IRB genera (*Geobacter* and *Shewanella*) was observed.

## V-2. Introduction

In the previous chapters, we studied Fe reducing rates of three bacterial consortia enriched from the site of Decize, in presence of four different synthetic Fe (oxyhydr)oxides (ferrihydrite, goethite, hematite and lepidocrocite) in batch conditions. Results highlighted the influence of the type of iron (oxyhydr)oxide in terms of iron reduction rates and abundances of two well-known DIRB genera, *Shewanella* and *Geobacter*, in the complex iron-reducing community potentially including both DIRB and fermentative bacteria. The highest reducing rates were measured for ferrihydrite and lepidocrocite in the presence of a consortia enriched from D3, an aquatic sediment (Decize), followed by hematite and goethite with the same inoculum. *Geobacter* sp. was more abundant in presence of goethite than with the other (oxyhydr)oxides and *Shewanella* was more abundant in presence of ferrihydrite and lepidocrocite.

Based on the interactions between Fe (oxyhydr)oxides and bacteria, microbial activities can play either a direct role or an indirect role on speciation and mobility of trace elements (TEs). The understanding and prediction of TEs' mobility and biogeochemical cycling is essential to develop remediation and management strategies for polluted sites. Although metal(oid)s bound to iron oxides can be mobilized by changing physical and chemical conditions, which could explain the solubilisation patterns of TEs within some fractions of sediment (Calmano et al., 1993; Chuan et al., 1996), bacterial activities and their functions are attracting more and more attention in relation to the fate of TEs in aquatic systems and soils (Gounou et al., 2010; Hansel et al., 2003a; Kurek, 2002; Kurek and Bollag, 2004; Li et al., 2016).

Some iron-reducing bacteria (IRB), such as *Shewanella*, have the ability to reduce polyferric sulfate, resulting in the release of Fe(II) and Cd(II) into solution, the released $Cd(II)_{aq}$ could then be re-adsorbed by secondary iron minerals (Li et al., 2016). Cd (II) was also stabilized in bacterial reactors using iron-reducing bacteria and magnetite iron oxide powder ($Fe_3O_4$) during the process of wastewater treatment (Su et al., 2019). The impact of reducing conditions and bacterial activities on the mobility of As adsorbed to iron oxyhydr(oxides), leading to lower adsorption and higher mobility of As has previously been demonstrated (Bowell, 1994; Cummings et al., 1999; Hellal et al., 2017). However Tufanoa and Fendorf, (2008), found that reductive transformation of ferrihydrite promoted As retention, rather than releasing it, during an experiment under Fe-reducing conditions with *Shewanella*. They also suggested As(III) retention during Fe reduction to be temporally dependent on new formed secondary Fe minerals. Cr(IV) could be reduced to Cr(III) by the direct role of IRB to mitigate its hazard (Gandhi et al., 2002; Liu et al., 2011b; Peng et al., 2015; Wielinga et al., 2001). However, there are very few studies on the bacterial mobility of Cr(III) in iron-reducing condition. Furthermore, few studies are available regarding microbial impact on multiple TEs' mobility in anaerobic sediments. Much of the research carried out on TE mobility in various environments under iron-reducing conditions has been performed with pure bacterial strains or one specific TE. In the environment, however, we are faced with complex TE pollutions and highly diverse bacterial communities. Thus it is necessary to carry out further research to understand the impact of mixed IRB groups on the reduction of different Fe (oxyhydr)oxides, and indirectly on the speciation and mobility of several TEs in combination. Continuously fed columns are systems that enable long-term experiments mimicking a water flow in controlled conditions. They have been previously used for monitoring the mobility and fate of some TEs e.g. As, Zn, Cd, Cu, Pb,

Hg, (Crampon et al., 2018; De Matos et al., 2001; Hartley et al., 2004; Hellal et al., 2015; Hu et al., 2015), for studying interactions with bacteria.

To illustrate the influence of geo-microbial phenomena and the speciation and mobility of iron-associated TEs, e.g., As, Cr and Cd, we developed a laboratory continuously-fed column experiment representing a simplified model aquifer under anaerobic conditions (Hellal et al., 2017). One amorphous and one crystallized Fe (oxyhydr)oxides: synthetic ferrihydrite and goethite were used for this column study. Column systems were implemented with the previously obtained IRB enrichment to assess the role of mixed bacterial communities in the transformations of ferrihydrite and goethite in reducing conditions.

## V-3 Specific materials and methods

## V-3.1 Adsorption of As, Cr and Cd on synthetic iron (oxyhydr)oxides

### V-3.1.1 Preparation of TEs stock solution

As, Cr and Cd solutions were prepared as following:

(1) As(V) stock solution: 1000 mg $L^{-1}$, ($Na_2HAsO_4$), dilution of a 10 g $L^{-1}$ stock solution.
(2) Cr(III) stock solution: $CrCl_3$ $6H_2O$, 100 mg $L^{-1}$, dissolve 0.512 g $CrCl_3$ $6H_2O$ into 1L ultrapure water.
(3) Cd(II) stock solution: $CdCl_2$, 100 mg $L^{-1}$, dissolve 0.163 g $CdCl_2$ into 1L ultrapure water

### V-3.1.2 Adsorption of TEs to iron oxyhydr(oxides)

Before initiating the column experiments, we determined the adsorption capacity of 4 types of iron (oxyhydr)oxides: ferrihydrite, lepidocrocite, goethite and hematite for mixtures of As, Cr and Cd. Experiments were performed in 250 mL erlenmeyer flasks, under agitation (100 RPM) and at 20°C for 24 h. Each batch experiment had 3 replicates for each condition.

Iron (oxyhydr)oxides (8 g $L^{-1}$) were added as powders into 150 mL As(V), Cr(III), Cd(II) mixed stock solutions, details can be found in Table V-1. Initial samples were collected from the mixtures at the beginning of the adsorption reaction and filtered at 0.45 µm (Millex -GP Syringe Filter, 33 mm diameter) to determine the total concentrations of As, Cr and Cd (abbreviated $[As]_D$, $[Cr]_D$ and $[Cd]_D$). After 24h, the mixture was centrifuged at 15,000 rpm for 10 min and the recovered solid Fe (oxyhydr)oxides were rinsed 11 times with ultrapure water. All rinsed samples were collected and filtered to analyze $[As]_D$, $[Cr]_D$ and $[Cd]_D$ in order to determine the

rinsing efficiency. In the end, the solid Fe (oxyhydr)oxide were recovered after freeze-drying (-90 ˚C Martin Christ Beta 2-8 LSCplus). An amount of 0.1 g of each Fe (oxyhydr)oxide was then dissolved into 10-20 mL HCl (1M) to measure the capacity of Fe (oxyhydr)oxides to adsorb As(V), Cr(III), Cd(II). Final TEs' adsorption capacities on Fe (oxyhydr)oxides were determined and calculated by analysis of $[As]_D$, $[Cr]_D$ and $[Cd]_D$ ($[]_D$ for dissolved elements) in these solutions. $[As]_D$, $[Cr]_D$ and $[Cd]_D$ were determined with Atomic Absorption Spectroscopy (AAS, Varian SpectrAA 220-Z) and Microwave Plasma-Atomic Emission Spectrometry (Agilent 4210 MP-AES). The pH was measured using standard hand-held portable meters (WTW Multi340i set) before and after the adsorption reaction to avoid an effect of pH on adsorption capacity (Figure V-2 (d)).

***Table V-1.*** *Initial TEs (As, Cr, and Cr) concentrations and Fe (oxyhydr)oxides solid/liquid concentration during adsorption batch experiment.*

| TE adsorption | ferrihydrite | goethite | hematite | lepidocrocite |
|---|---|---|---|---|
| $[As]_D$ mg $L^{-1}$ | 167 | 333 | 333 | 333 |
| $[Cr]_D$ mg $L^{-1}$ | 67 | 67 | 67 | 67 |
| $[Cd]_D$ mg $L^{-1}$ | 100 | 67 | 67 | 67 |
| Fe (oxyhydr)oxides | 1.2 g | 1.2 g | 1.2 g | 1.2 g |
| Concentration of solid / liquid phase | 8 g $L^{-1}$ | 8 g $L^{-1}$ | 8 g $L^{-1}$ | 8 g $L^{-1}$ |

## V-3.2 Columns experimental setup

### V-3.2.1 Preparation of Fe (oxyhydr)oxides

Based on the previous discussion in chapter III, synthetic ferrihydrite with its amorphous nature and goethite with its acicular or needle-shaped crystallized forms were used for the column study. According to the results from the adsorption assays, 20 g of ferrihydrite and 20 g of goethite were prepared using the same method for adsorping TEs (As, Cr and Cd) with 6 rinsing steps. The final adsorption results, determined as metal contents on the solid oxides, are presented in Table V-2.

***Table V-2.*** *Concentrations of TEs adsorbed by ferrihydrite and goethite.*

| mg $g^{-1}$ | ferrihydrite | goethite |
|---|---|---|

| | | |
|---|---|---|
| As | 14.5 | 5.28 |
| Cr | 1.4 | 2.53 |
| Cd | 2.01 | 3.03 |

### V-3.2.2 Preparation of silica gel and sand matrix

Silica gel (6 %) was used to stop the fine iron (oxyhydr)oxides migrating from the sand/iron oxide mixture under the water flow as described in Hellal et al., (2017). A 10% silica gel mixture was prepared by heating 20 g of silica gel in 200 mL of a solution of 7% KOH on a hot plate, stirring with a magnetic stir bar until dissolution; then 300 mL of ultra-pure water was added and the solution was cooled to ~20 °C as stock solution. This solution was quickly titrated with diluted phosphoric acid (20 %) to pH 7.

For each column, we quickly mixed 50 mL liquid silica gel with 153 g of sterile sand and previously added 8.7 g of As, Cd and Cr-absorbed Fe (oxyhydr)oxides (previously exposed to UV light for 5-10 min) before it solidifies. We broke up the "jellified" mixture by mixing with a spatula and kept it sterile before filling the columns.

### V-3.2.3 Column setup and experimental conditions

In total, 4 columns were set up for this experiment: two for ferrihydrite which included one inoculated column and one un-inoculated control column, and the same for goethite. All columns used for mobility experiments were 25 cm long glass columns, with an internal diameter of 2.5 cm, provided by Omnifit® (Diba industries, USA). Columns, pipes and conenctions were sterilized by autoclaving. The columns were sealed in aseptic conditions and set up vertically with an ascendant inflow of different solutions in 3 steps (more details are given in Figure V-1 and Table V-3). All silicone tubes and caps used in the experiment were made of PTFE to avoid interactions with TE. Columns were first filled with the mixture of sand, Fe oxide (ferrihydrite/goethite with absorbed As, Cr and Cd) and 6% silica gel. The columns were flushed with $N_2$ (filtered through a 0.2 µm filter, flow speed between 1-5 mL $min^{-1}$) to evacuate $O_2$ and avoid the formation of bubbles in the column, and thus obtain realistic anaerobic conditions. For stabilization, columns were then filled with synthetic water, made to mimic the composition of groundwater, sterilized by autoclaving (121 °C for 20 min), and described as FIm (moderately hard) water by US EPA Report EPA-821-R-02-012, Section 7.2.3.1 (US EPA, 2002). This water was composed of 96 mg $L^{-1}$ $NaHCO_3$, 60 mg $L^{-1}$ $CaSO_4$ ($2H_2O$) (separate autoclave), 60 mg $L^{-1}$ $MgSO_4$ and 4 mg $L^{-1}$ KCl (Crampon et al., 2018). pH

ranged from 7.4 to 7.8, and the synthetic water was purged with $N_2$ to remove any oxygen prior to injection into the column. A mixture of organic substrates was used to stimulate Fe reducing bacterial activities, providing electron donors and carbon sources. It was composed of 100 mM acetate, 100 mM lactate, 100 mM formate, 20 mM glucose, 15 g $L^{-1}$ peptone, 4 mM sodium molybdate (to inhibit sulfate-reduction), 10 mL $L^{-1}$ vitamin solution and trace element solution (composition can be found in Chapter II-2 ).

*Preparation of substrate and inoculum*

The substrate concontrations used for column feeding was the same as in the medium for IRB cultures described in chapter II-2.

The initial column inoculum was prepared with the 23$^{rd}$ subculture of D3 bacterial enrichments. 2*200 mL of medium were prepared with Fe(III)-NTA solution (10 mM) and were inoculated at 10% with D3 then incubated 1-2 days. After 10 min centrifugation at 10,000 RPM of the cultures, supernatants were discarded and the recovered cells were transferred into the same volume of subculture medium (without Fe) as inoculum culture. In order to inoculate the columns (2$^{nd}$ step in Table V-3), 200 mL of inoculum were set up with the second pump and split into two silicone tubes to feed the 2 inoculated columns. Substrate was supplied by the same pump system but split into four silicone tubes to feed the 4 columns.

***Table V- 3.*** *Experimental conditions of continuous feeding.*

| Step | Dates | Conditions | Medium and flow-rate | Other solution and flow-rate |
|---|---|---|---|---|
| 1 | Days 0-14 | Stabilization step | Synthetic water, 2 mL $h^{-1}$ | No |
| 2 | Days 15-22 | Inoculation | Substrate (10X), 2 mL $h^{-1}$ | Inoculum, 0.2 mL $h^{-1}$ |
| 3 | Days 22-99 | Experimental incubation | Synthetic water + Substrate, 2 mL $h^{-1}$ | No |

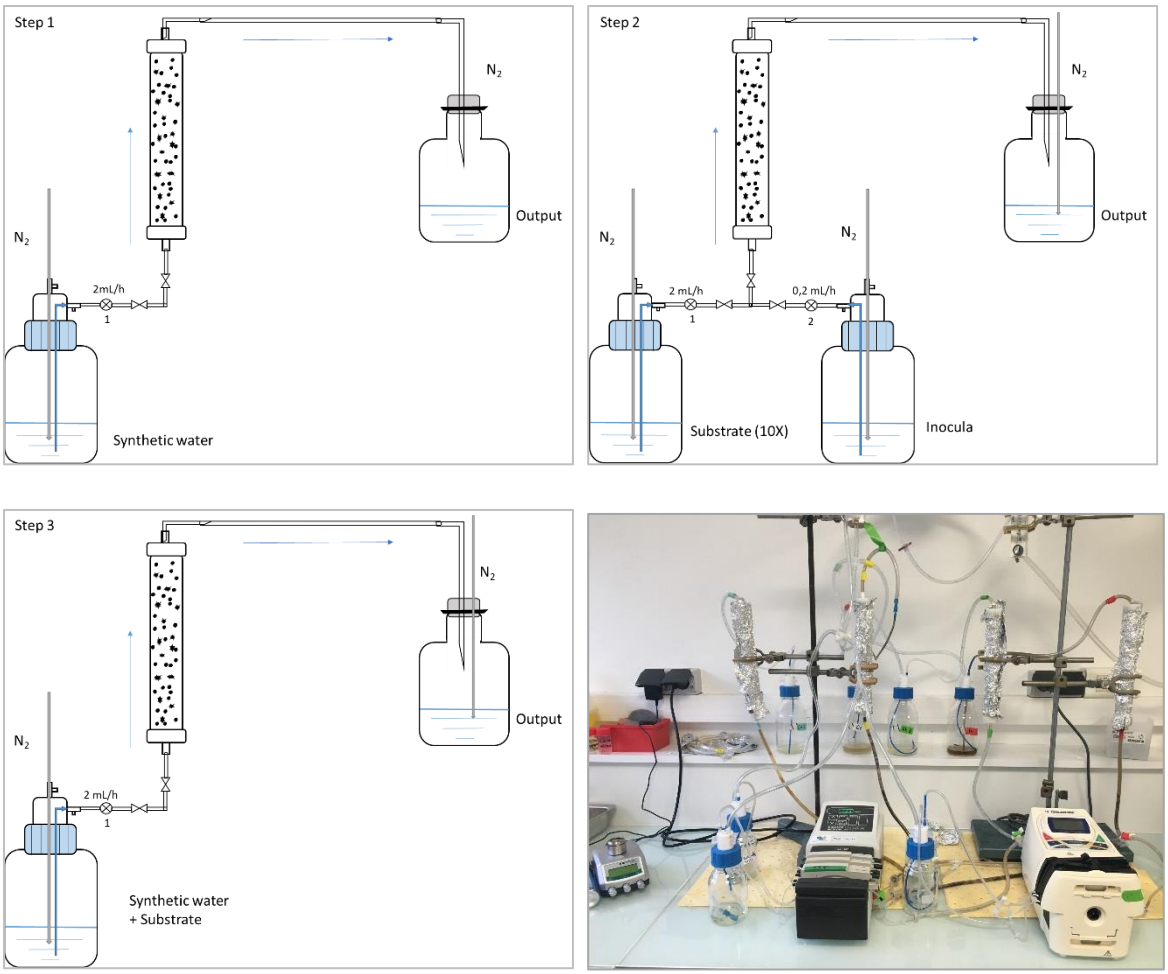


***Figure V-2.*** *Photo and sketch (protocol in 3 steps) of the columns experiment.*

### V-3.2.4 Monitoring

Columns experiments lasted 99 days and were divided into 3 steps as described in Table V-3. Outlet bottles were emptied everyday (except weekends) and the liquid samples were collected in a glove box to analyse pH, redox potential (Eh, ref. Ag/AgCl), $[FeT]_D$ (total dissolved Fe concentration), $[As]_D$, $[Cr]_D$ and $[Cd]_D$, and to observe the bacteria. $[FeT]_D$, $[As]_D$, $[Cr]_D$ and $[Cd]_D$ were determined using the same method as described in chapter II-4 and samples for those chemical analyses were filtered through a 0.2 µm filter into plastic tubes and acidified with concentrated HCl in anaerobic condition. [AsIII] and [AsV] were separated using resins (AG® 1-X8 Resin, Cat. # 140-1431, Biorad) (Battaglia-Brunet et al., 2006) and determined by the same method as described in chapter II-4. pH and redox potential (Eh, ref. Ag/AgCl) were measured after sampling immediately using standard hand-held portable meters (WTW Multi340i set) in the glove box.

At the end of the experiment, the column system was stopped and the remaining liquid from the columns was collected to analyze the biological parameters when columns were disconnected. Then columns were weighed and the depths of visible reactions were measured by observing the color change. The solid samples from the top, middle and bottom of the columns were collected in a glove box to determine biological and chemical parameters.

### V-3.2.5 SEM-EDS observation and Mössbauer spectrometry

Initial column samples and post-incubation samples were observed by SEM-EDS using the same method as described in chapter II-6.1 after freeze-drying (-90 °C Martin Christ Beta 2-8 LSCplus). An amount of 0.1 g of each dried sample was dissolved in 10-20 mL HCl (1M) to measure the remaining Fe, As, Cr and Cd in columns.

After incubation, the column samples for Mössbauer spectrometry analysis were collected in a glove box and kept under anaerobic conditions. Mössbauer spectrometry was used to determine Fe species in different depths of the column by the method described in chapter II-7.

### V-3.2.6 Biological analyses

Bacterial biofilm was observed by SEM using the method described in chapter II-6.2 and images of bacteria in outlet samples were observed with an optical microscope (X400) described in chapter II-8.1.

DNA extractions were performed on samples solid and liquid samples using the method described in chapter II-8.2. Bacterial 16S rRNA and *Shewanella* / *Geobacter* 16S rRNA gene quantifications were performed by qPCR following the methods described in chapter II-8.4 and 8.6.

## V-4 Experimental results

### V-4.1 Adsorption experimental results

Concentrations of As, Cr and Cd in rinsing solutions after adsorption reactions are presented in Figure V-2. This step aimed to eliminate as much as possible the remaining un-adsorbed metals from the Fe (oxyhydr)oxides.

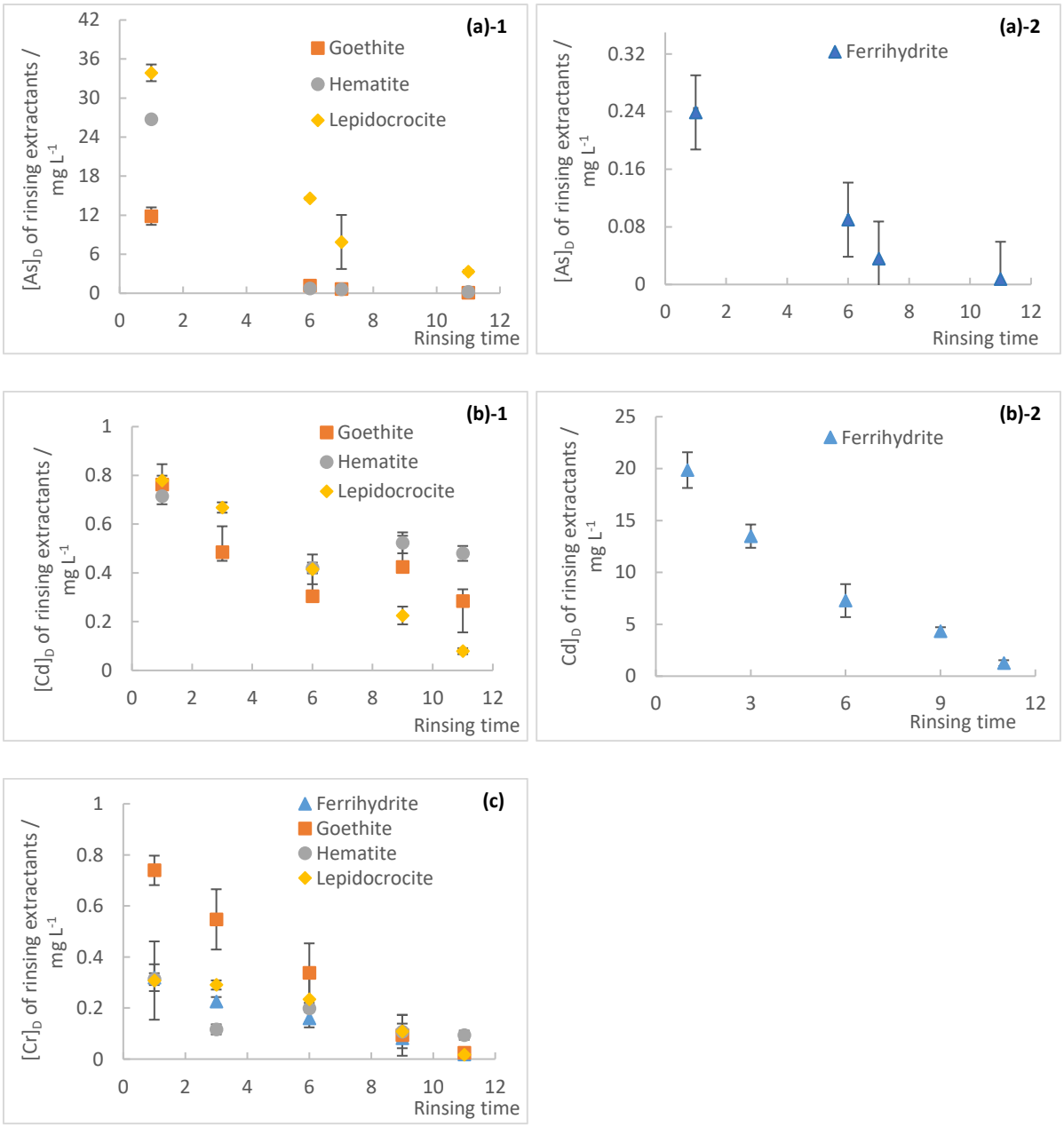


***Figure V- 3.*** *Concentrations of As(a), Cd(b) and Cr(c) in the according pellet-rinsing solutions for the four studied iron (oxyhydr)oxides (ferrihydrite, goethite, hematite and lepidocrocite).*

Results (Figure V-2) showed that after 6 rinsing steps most of the remaining un-adsorbed metals were removed.

Adsorption capacities of As, Cr and Cd on iron (oxyhydr)oxides are presented in Figure V-3. Globally, all the iron (oxyhydr)oxides had higher adsorption capacities for As than for Cr and Cd (Figure V-3). As shown in Figure V-3 (a), lepidocrocite had the biggest adsorption capacity on As, 31.7 mg $g^{-1}$ at room temperature, pH 5-6. Adsorption capacity then decreased from ferrihydrite to goethite and finally hematite. While the adsorption capacity for Cr was the

highest with ferrihydrite, it was equivalent for the three other oxides. For Cd, the adsorption capacities of the different iron oxides were not significantly different (Figure V-3 (b) and (c)). pH values for all the experiments did not change before and after the adsorption reaction.

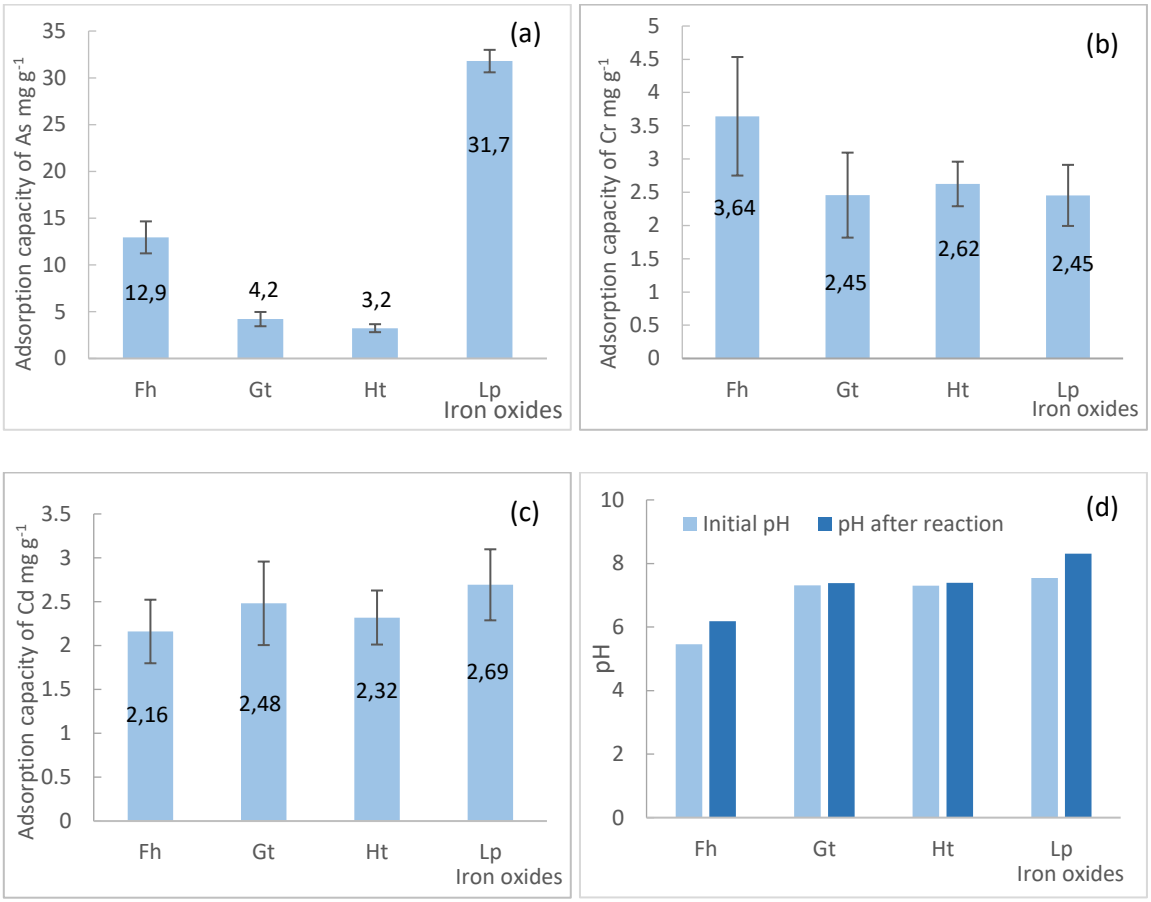


***Figure V-4.*** *Adsorption capacity of and As (a), Cd (b) and Cr (c) on 4 Fe (oxyhydr)oxides (ferrihydrite, goethite, hematite and lepidocrocite, pH values before and after adsorption reaction (d).*

## V-4.2 Column experiments

### V-4.2.1 Visual evolution of the columns

During the experiment, a black color appeared in both the columns inoculated with a bacterial consortium. The feeding medium contained molybdate to inhibit the sulfate-reducing activity, however this was possibly not sufficient to completely inhibit sulfate reduction in the column system. As a fact, in the previous batch condition,

As shown in Figure V-4, inoculated columns presented color changes: in the ferrihydrite column a dark precipitation fromed at the bottom from 0cm to12 cm, replacing the original reddish brown color. In the goethite goethite column a dark precipitation formed from 0 -16 cm, replacing the original yellow color. Un-inoculated columns did not present any color changes.

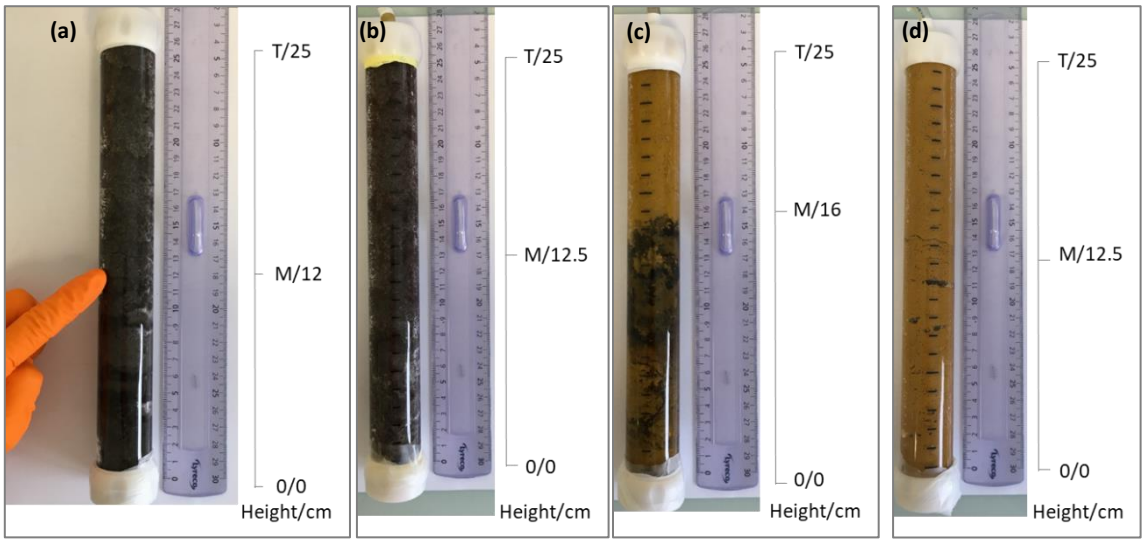


***Figure V-5.*** *Photos of the columns at the end of the experiments. Inoculated column: ferrihydrite (a) and goethite (c), un-inoculated columns: ferrihydrite (b) and goethite (d).*

The sampling positions were determined according to the color changes and are provided in Table V-4. Three samples were taken in each column, from bottom (0), middle (M) and top (T). The middle samples were taken for inoculated columns at the boundary of the black color, i.e., at 12 cm for ferrihydrite and at 16 cm for goethite. Un-inoculated columns were sampled at 12.5 cm for middle positions.

***Table V-4.*** *Weight parameters and sampling position in columns.*

| Column | Weight/g | | | Bottom/cm ( “0”) | Height/cm ( “M”) | Top/cm ( “T”) |
|---|---|---|---|---|---|---|
| | Empty column | Pre-incubation | Post-incubation | | | |
| Gt | 170.6 | 394.4 | 403.2 | 0 | 16 | 25 |
| Gt-B | 170.3 | 388.4 | 377.3 | 0 | 12.5 | 25 |
| Fh | 173.3 | 384.7 | 387.3 | 0 | 12 | 25 |
| Fh-B | 174.9 | 382.7 | 381.3 | 0 | 12.5 | 25 |

### V-4.2.2 Spatial and temporal evolution of iron and absorbed elements in columns

*V-4.2.2.1 Ferrihydrite columns*

*Step 1: stabilization*

During the first 14 days columns were flushed with sterile synthetic water in order to finalize the removal of non-adsorbed metals.

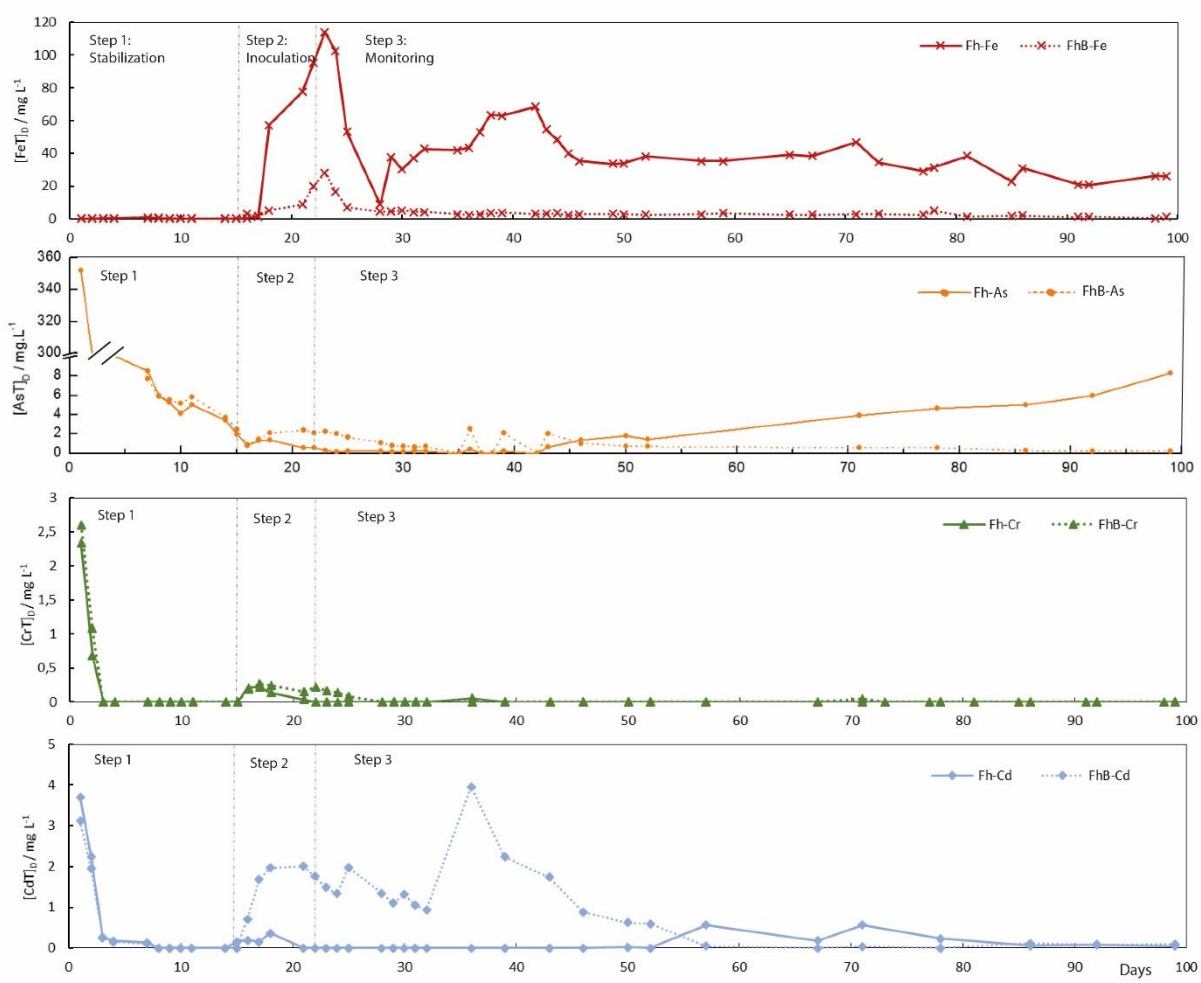


***Figure V-6.*** *Temporal evolution of dissolved $[FeT]_D$ (upper panel), $[AsT]_D$, $[CrT]_D$ and $[CdT]_D$ (lower panel) monitored at the outlet of the ferrihydrite columns: Fh (inoculated column) and FhB (un-inoculated blank column).*

For ferrihydrite columns, the released elements detected at the column outlet during this step are shown in Figure V-5 (lower panel). Cr was not detected at the column outlet except for the first two days. Cadmium was leached on the first day and was no longer detected before bacterial inoculation. The quantities of leached Cr and Cd during this first step were less than 1% of the total Cr and Cd contents of the columns. The released As represented more than 100

mg $L^{-1}$ during the first 2 days, but leaching resulted in a total loss of 11.6 and 14.1 mg (being ~ 10% and ~13% of the total As contents of the columns) in the inoculated and un-inoculated columns, respectively. During this equilibration phase, pH oscillated between 8 and 9, and Eh oscillated between -200 mV and -100 mV (ref. Ag/AgCl).

*Steps 2 (inoculation days 15-22) and 3 (monitoring days 23-99)*

Following inoculation of the inoculated columns with the DIRB communities, Fe leaching increased sharply in this column while remaining low in the un-inoculated one (Figure V-5, upper panel). In both columns $[FeT]_D$ reached a maximum concentration on day 23 (the end of the inoculation period) in both columns, with 114 mg $L^{-1}$ in the outlet of the inoculated column and 28.2 mg $L^{-1}$ in the un-inoculated one. Leaching from the un-inoculated column could be due to the change in composition of the inflowing water which was mixed with carbon substrates and minerals. Indeed, after the inoculation period, $[FeT]_D$ in the un-inoculated column decreased rapidly to reach concentrations around 3 mg $L^{-1}$ from day 36 until the end of the experiment. In the inoculated column, $[FeT]_D$ decreased after day 22 and then increased gradually to reach 68.4 mg $L^{-1}$ at day 42, before oscillating in the range of 20-40 mg $L^{-1}$. At the end of the experiment, the total dissolved and reduced iron that was collected at the column outlet amounted to 141 mg and 13.7 mg, representing ~ 2.8% and ~ 0.02% of the total iron content of the columns, leached from the inoculated and un-inoculated columns, respectively.

During the experiment, from day 15 to day 99, $[AsT]_D$ showed a different trend to $[FeT]_D$. Indeed, $[AsT]_D$ oscillated between 0.1 and 0.3 mg $L^{-1}$ during the period corresponding to days 23-39, but after day 39, where $[FeT]_D$ reached the value of 62.3 mg $L^{-1}$ and became stable, As concentration in the outlet increased from 0.1 to 8.3 mg $L^{-1}$ until the end of the experiment. On the contrary, $[AsT]_D$ in the un-inoculated column exhibited a similar trend to $[FeT]_{D,}$ with an increase from 0.78 to 2.2 mg $L^{-1}$ on day 23 and then a decrease to 0.67 mg $L^{-1}$ at day 32. After day 32, the release of $[AsT]_D$ peaked to a maximum of 2.5 mg $L^{-1}$ at day 36 and then decreased again until end of the experiment.

During the post-inoculation period of the experiment, pH of the inoculated column oscillated steadily between 7.8 and 9 (Figure V-6). The pH of the un-inoculated column was identical to that of the inoculated column during the inoculation period, then it decreased between days 15 and 29. After day 29, it showed similar values to the inoculated column. Eh was globally identical in the inoculated and un-inoculated columns during inoculation, then Eh was lower in the inoculated column than in the un-inoculated column, reaching values as low as -350 mV on

days 21-23. After this period, the redox values in the inoculated column increased slowly up to -200 / -150 mV, joining the values of the un-inoculated column at the end of experiment.

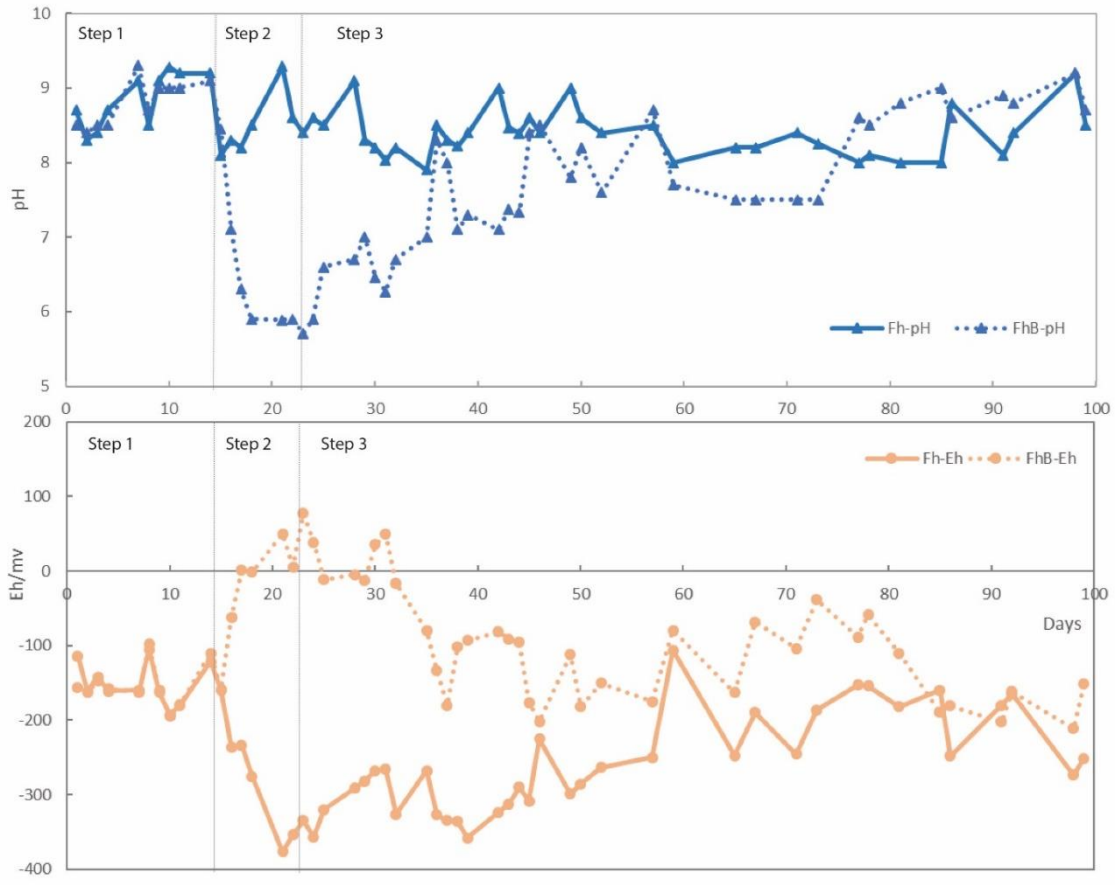


***Figure V-7.*** *Temporal pH and Eh (ref. Ag/AgCl) profiles monitored at the outlet of ferrihydrite columns.*

As described in the previous section, the release of [As] from the inoculated column was higher than from the un-inoculated column for the ferrihydrite experiment. In Figure V-7, the distribution of $[AsT]_D$ between [AsIII] and [AsV] are given for samples of outlets at days 86, 92 and 99. In the inoculated column $[AsT]_D$ was more than 1 mg $L^{-1}$ at these sampling dates, reaching up to 1.6 mg $L^{-1}$ on day 99. At all three sampling dates [AsIII] was present in concentrations higher than [AsV] except for day 92 where it was identical. As it was initially AsV that was adsorbed to the Fe (oxyhydr)oxides, this suggests that AsV was reduced by the presence of bacteria. Conversely, very little $[AsT]_D$ was detected in the outlet of the un-inoculated column and it was essentially [AsV].

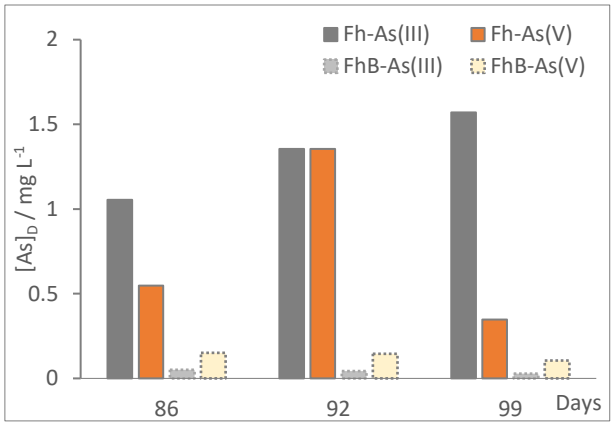


***Figure V-8.*** *Distribution of $[AsIII]_D$ and $[AsV]_D$ in ferrihydrite columns (Fh: inoculated column and FhB: un-inoculated blank column) outlets on days 86, 92 and 99.*

After the column monitoring, solid phase samples were collected and analyzed for the concentration of remaining Fe, As, Cr and Cd. Vertical distribution of remaining [FeT], [AsT], [CrT] and [CdT] in the profiles of solid phases in the ferrihydrite columns are shown in Figure V-8. Globally, the remaining [FeT] decreased from top to bottom of the inoculated ferrihydrite column, the same tendency was observed for remaining [AsT]. Both [CrT] and [CdT] did not show any obvious trend from bottom to top in the inoculated column. However, the concentration of remaining of [CrT] and [CdT] were higher in the inoculated column than in the un-inoculated column suggesting Cr and Cd were less mobile in the presence of bacteria. In un-inoculated column, the remaining [FeT] did not present higher concentrations in either the top or the bottom and remaining [AsT] showed the same tendency as in the inoculated column.

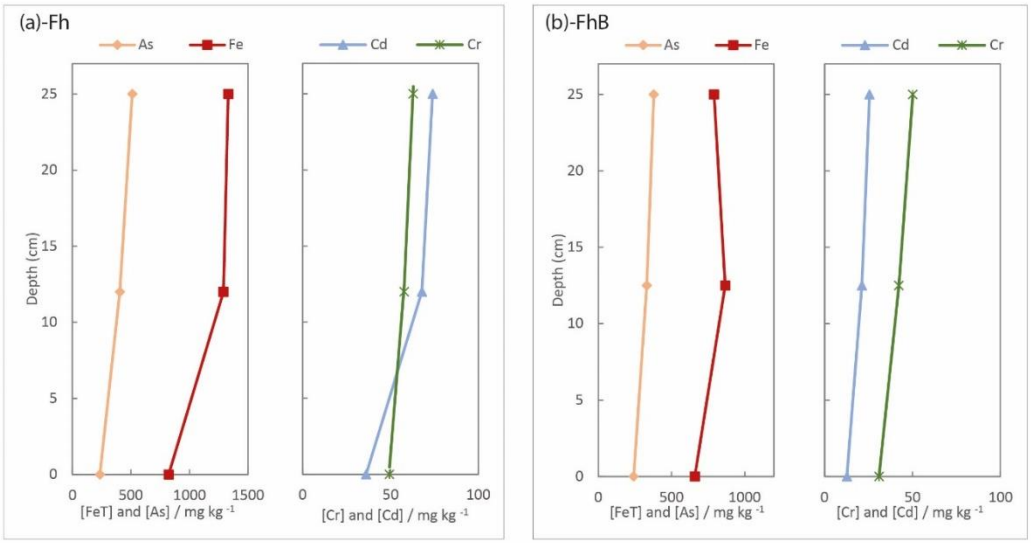


***Figure V-9.*** *Vertical distribution of remaining [FeT], [AsT], [CrT] and [CdT] in the profiles of solid phases in the ferrihydrite columns (Fh and FhB) at the end of experiment.*

*V-4.2.2.2 Goethite columns*

*Step 1: stabilization*

As for ferrihydrite columns, the goethite columns were first flushed with sterile synthetic water for 14 days in order to finalize the removal of un-adsorbed metals. During this period, prior to bacterial inoculation, released elements were detected at the column outlet as shown in Figure V-9 (lower panel). Concerning chromium, 0.4 and 0.38 mg $L^{-1}$ $[CrT]_D$ were detected at the columns (inoculated and un-inoculated respectively) outlets on the first day and then there was no Cr detected in the outlets until the inoculation period. Concerning Cd, leaching resulted in the release of 2.8 and 4.1 mg $L^{-1}$ $[CdT]_D$ on the first day, then concentrations decreased steadily to an undetected value of < 0.1 mg $L^{-1}$ on day 7. The released As concentration ($[TAs]_D$) was more than 100 mg $L^{-1}$ on the first day and then decreased rapidly and stabilized to 3 mg $L^{-1}$ on day 7. The leaching resulted in a total quantity of 9.0 and 9.6 mg (being ~ 18% and ~ 21% of the total As content of the inoculated and Blank un-inoculated columns, abbreviated as Gt and GtB respectively) during the first 14 days of rinsing followed by a stabilization of the outflow concentration at 1.0 ± 0.5 mg $L^{-1}$. Moreover, the leached Cr and Cd quantities were less than 1% of the total Cr and Cd contents of the columns. During this equilibration phase, pH oscillated between 7.5 and 9.5, and Eh oscillated between -200 mV and -100 mV, in both inoculated and un-inoculated columns.

*Steps 2 (inoculation days 15-22) and 3 (monitoring days 23-99)*

During the inoculation (days 15 to 22) and monitoring periods (days 23 to 99) (Figure V-9, upper panel), $[FeT]_D$ from the inoculated column showed the same trend as for the ferrihydrite column with a sharp increase from day 18 to day 23 (the end of inoculation period), where $[FeT]_D$ reached the value of 58 mg $L^{-1}$. Globally the Fe release was much more important in the inoculated than in the un-inoculated conditions. Here $[FeT]_D$ in the un-inoculated column did not change with the addition of substrate. After the inoculation period, $[FeT]_D$ in the inoculated column outlet decreased rapidly to minimum concentrations of 8.9 mg $L^{-1}$ on day 28 and then increased rapidly to reach the maximum value of 59 mg $L^{-1}$ then gradually to reach values of 30 - 40 mg $L^{-1}$ after day 50 until the end of the experiment. Conversely, during the experiment, $[FeT]_D$ in the un-inoculated column remained in the range of 0.1-0.3 mg $L^{-1}$ throughout the experiment. To summarize, the total dissolved and reduced Fe collected at the column outlets were 96.5 mg and 0.81 mg (being ~ 1.8-3.9% and < 0.01% of the total iron contents of the columns) from inoculated and un-inoculated columns, respectively.

From days 15-99, $[AsT]_D$ in the inoculated column peaked at 34.7 mg $L^{-1}$ during the inoculation period, with an increase from days 15 to 17 and a decrease to 7.9 mg $L^{-1}$ from day 17 to 28. This sharp peak preceded that of dissolved iron by 6-7 days. It continued to decrease until the end of the experiment except for a slight increase from day 31 to 36 (the second increase was not convincing with only one analysis at day 86). $[AsT]_D$ from the un-inoculated column exhibited a trend similar to that of the inoculated column, but with lower concentrations, with an increase from 1.1 to 6.7 mg $L^{-1}$ on day 15 to 22 and then a decrease from 6.7 to 1.7 mg $L^{-1}$ on day 22 to 28. After day 28, the release of $[AsT]_D$ reached a maximum of 2.8 mg $L^{-1}$ at day 39 and then decreased again until the end of the experiment. During the post-inoculation period of the experiment, pH in the inoculated column carried on oscillating between 8 and 9, but pH in the un-inoculated column oscillated between 7 and 8.5 except between days 15 to 35 during which it oscillated between 5.5 and 7 (Figure V-10). Globally, pH was lower in the un-inoculated column after the inoculation, but then increased progressively towards similar values. Eh was always lower in the inoculated than in the un-inoculated column after inoculation, with values close to -300 mV. In the un-inoculated column, Eh was between 0 and 50 mV in the 17-30 days period, then decreased and varied between -200 and 0 mV until the end of experiment.

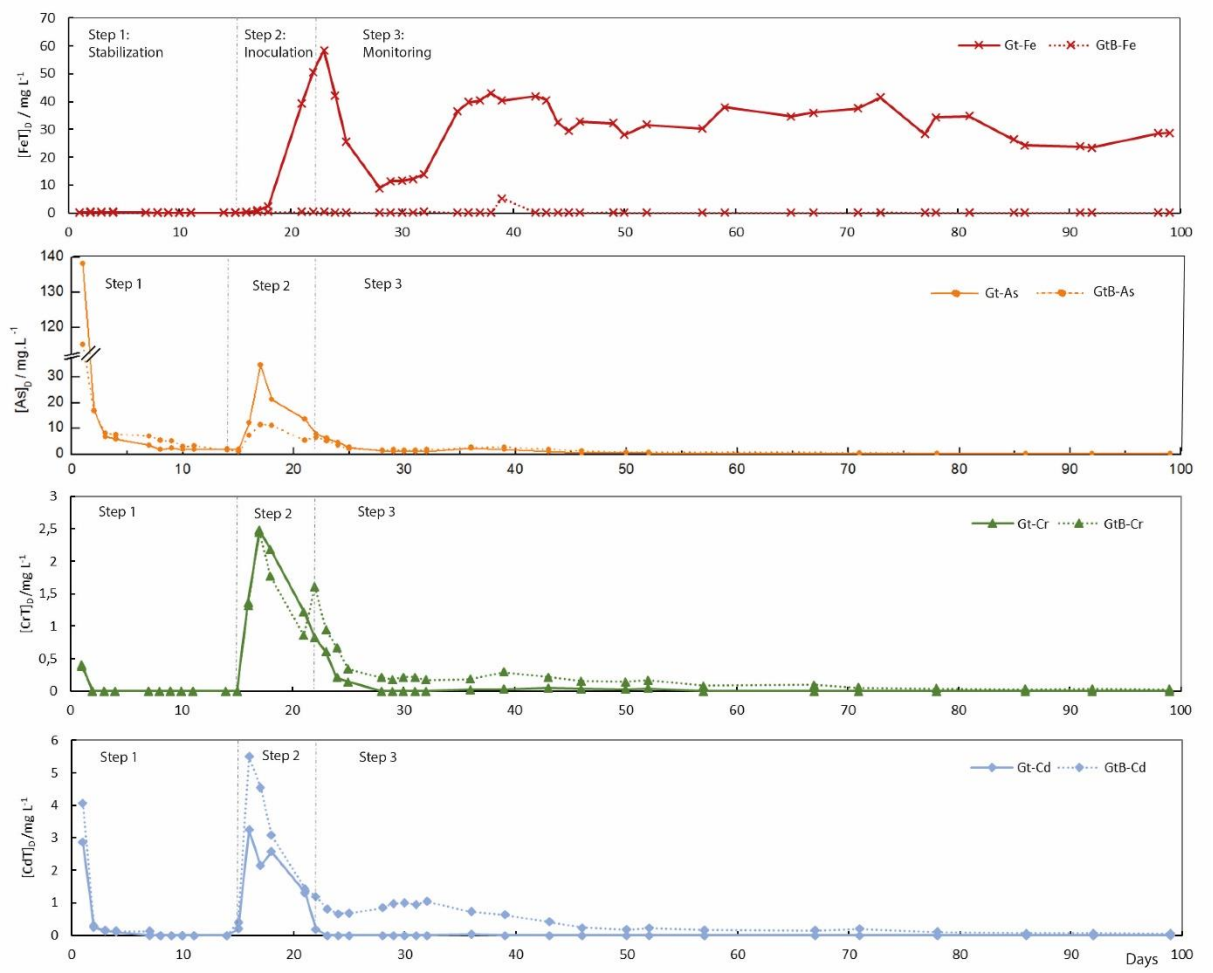


***Figure V-10.*** *Temporal evolution of dissolved $[FeT]_D$ (upper panel), $[AsT]_D$, $[CrT]_D$ and $[CdT]_D$ (lower panel) monitored at the outlet of the goethite columns: Gt (inoculated column) and GtB (un-inoculated Blank column).*

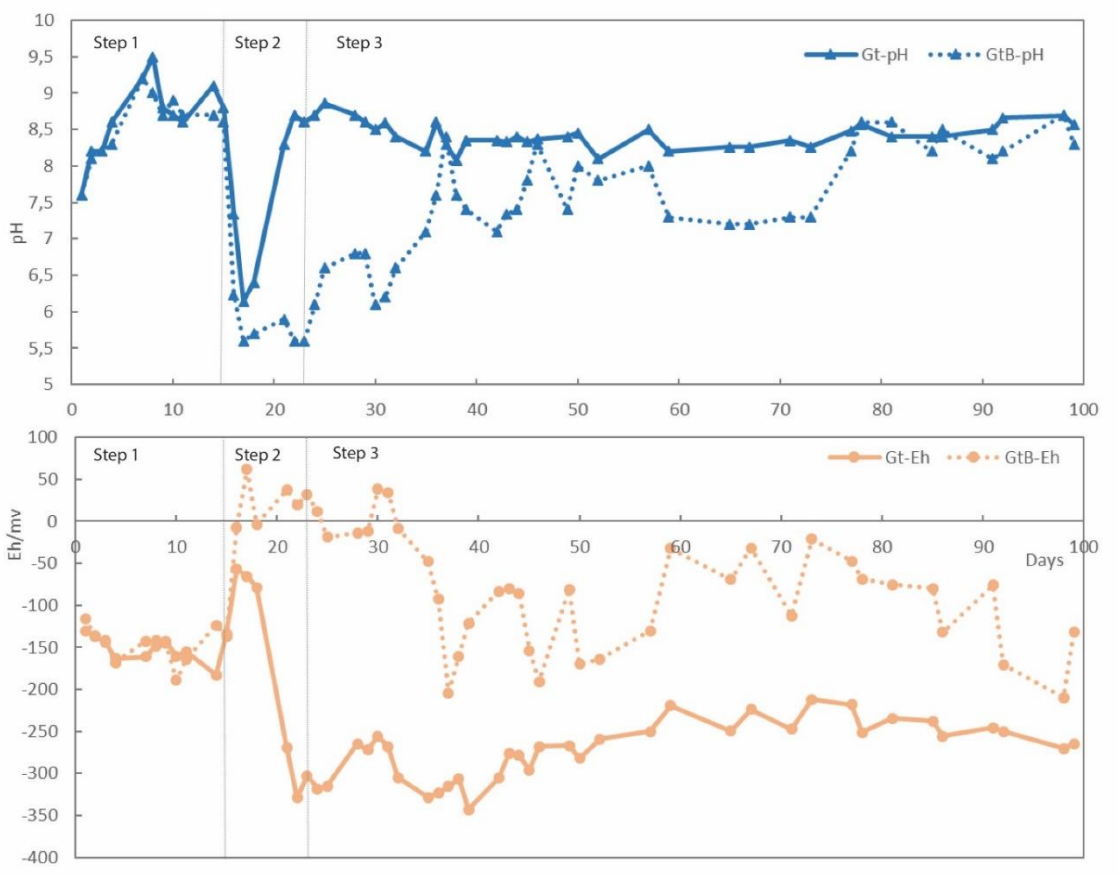


***Figure V-11.*** *Temporal pH and Eh (ref. Ag/AgCl) profiles monitored at the outlet of goethite columns.*

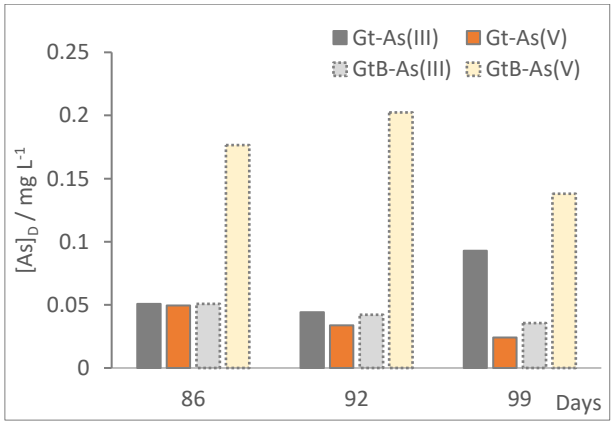


***Figure V-12.*** *Distribution of $[AsIII]_D$ and $[AsV]_D$ in goethite columns (Gt: inoculated column and GtB: un-inoculated blank column) outlets on days 86, 92 and 99.*

Overall, less As was released from the inoculated goethite column than from the inoculated ferrihydrite column. The distribution of dissolved As(III) and As(V) is shown in Figure V-11, lower panel. Between 0.05 to 0.1 mg $L^{-1}$ of As(III) and 0.03-0.05 mg $L^{-1}$ of As(V) were present

in the inoculated column outlet suggesting that here also some As(V) was reduced by bacteria to As(III). In the un-inoculated column, more As(V) than As(III) was detected in the outlets samples.

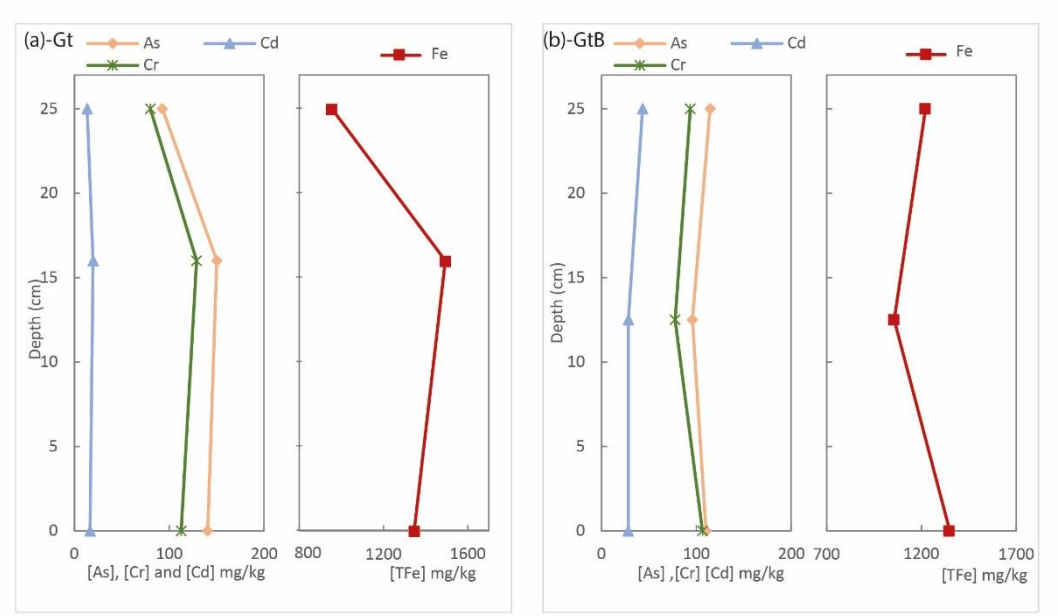


***Figure V-13.*** *Vertical distribution of remaining [FeT], [AsT], [CrT] and [CdT] profiles of solid phases in the goethite columns (Gt and GtB) at the end of experiment.*

Vertical distribution of remaining [FeT], [AsT], [CrT] and [CdT] in the profiles of solid phases in the goethite columns are shown in Figure V-12. Globally, the remaining [FeT] did not show a linear evolution from the top to the bottom of the inoculated column, rather the concentration of [FeT] was higher in the middle than in the bottom and in top of the column. The remaining [AsT] and [CrT] showed the same tendency as [FeT] but not [CdT]. In the un-inoculated column, the remaining [FeT] presented an opposite profile as [FeT] was lower in the middle than in the bottom and the top of the column. Moreover, the remaining [AsT], [CrT] and [CdT] all showed the similar trends as remaining [FeT] in the un-inoculated column.

### V-4.2.3 Relationship between remaining Fe and TEs in columns

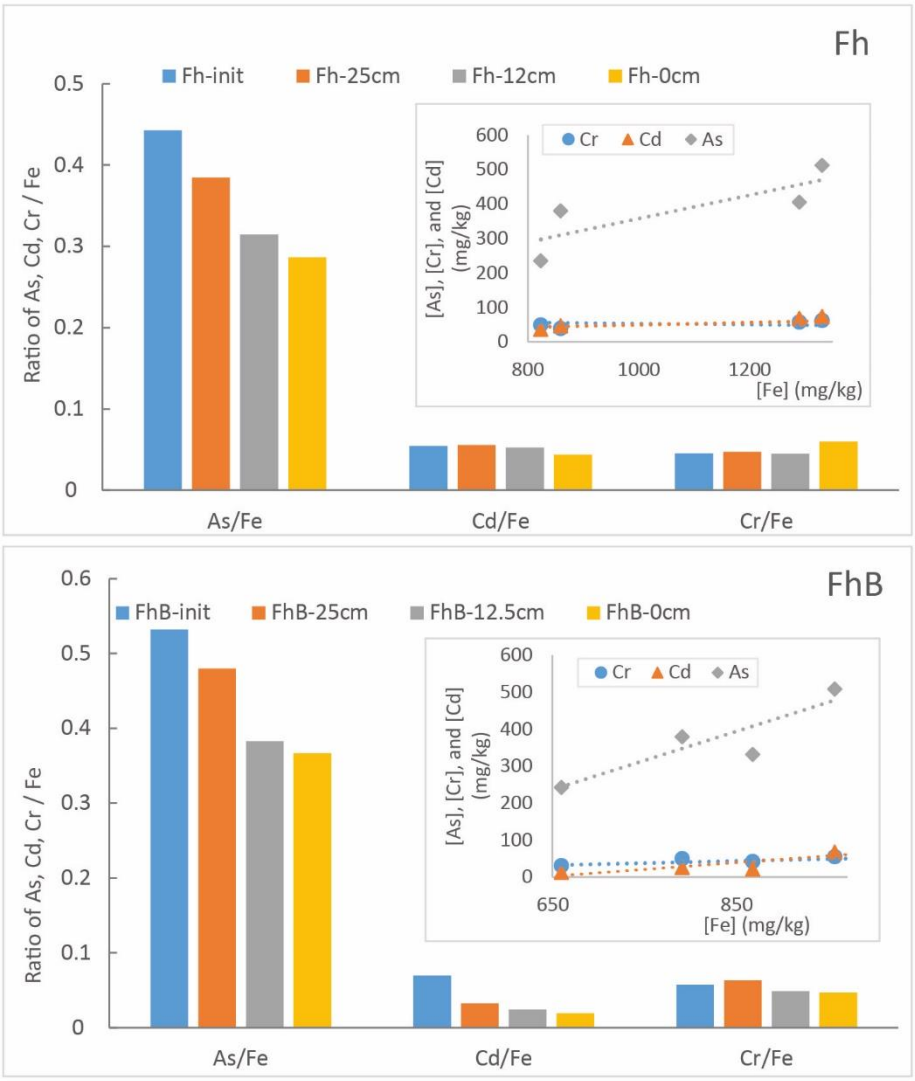


***Figure V-14.*** *Remaining [AsT], [CrT] and [CdT] / [FeT] ratios in solid samples of both ferrihydrite columns (Fh and FhB) at the end of experiment; Analysis of correlation between remaining [AsT], [CrT], [CdT] and [FeT].*

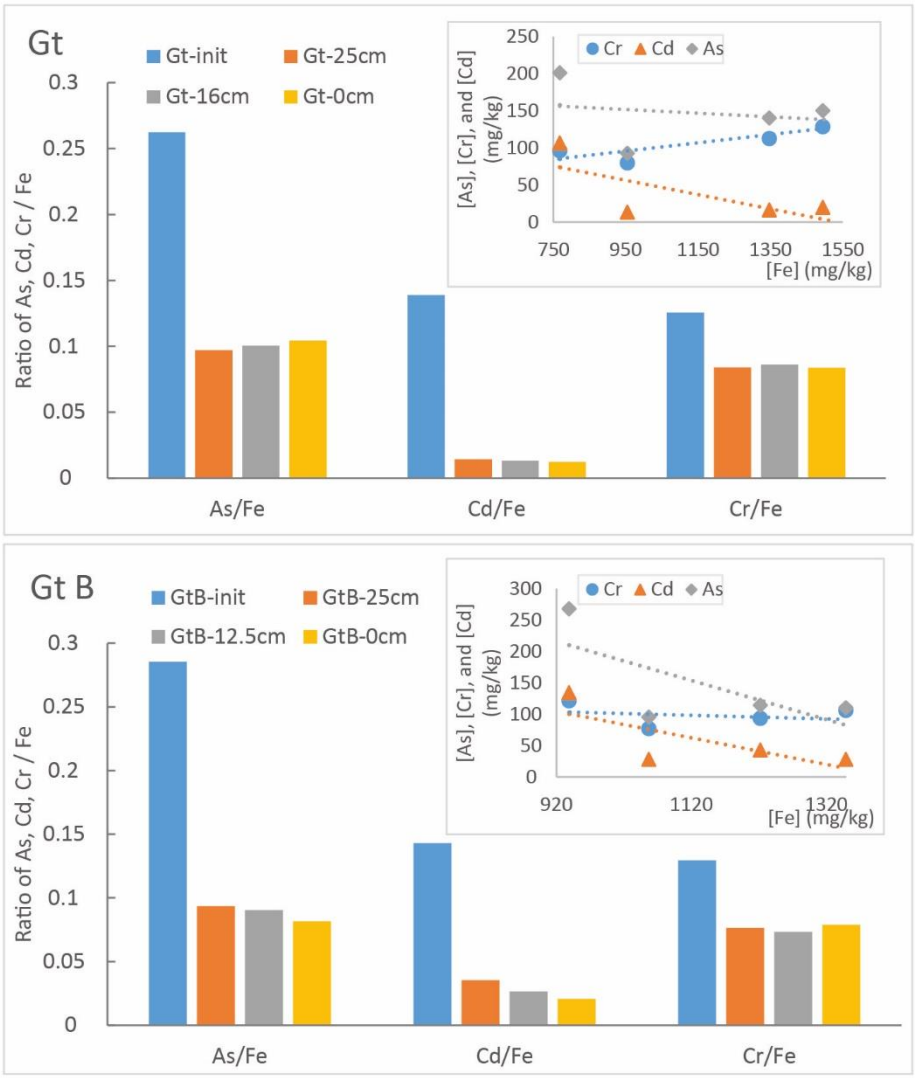


***Figure V-15.*** *Remaining [AsT], [CrT] and [CdT] / [FeT] ratios in solid samples of both goethite columns (Gt and GtB) at the end of experiment; Analysis of correlation between remaining [AsT], [CrT], [CdT] and [FeT].*

***Table V-5.*** *The correction and coefficient of determination from correlation analysis between remaining [AsT], [CrT], [CdT] and [FeT] in solid samples.*

| | | Fh | | Gt | |
|---|---|---|---|---|---|
| | | inoculated | un-inoculated | inoculated | un-inoculated |
| As/Fe | Correlation | + | + | - | - |
| | $R^2$ | 0.66 | 0.79 | 0.05 | 0.48 |
| Cd/Fe | Correlation | + | + | - | - |
| | $R^2$ | 0.78 | 0.70 | 0.49 | 0.54 |
| Cr/Fe | Correlation | + | + | + | - |
| | $R^2$ | 0.96 | 0.68 | 0.71 | 0.03 |

The ratios of As, Cd and Cr/Fe in column filling materials and their evolution between the initial and final states are given in Figure V-13, 14. In the ferrihydrite column, the As/Fe ratio decreased during the experiment, more so at the bottom than the top of the column. In the inoculated one, Cd and Cr ratios did not change during the experiment. The same phenomenon was observed for Cr in the un-inoculated column. Conversely, the Cd/Fe ratio decreased in the un-inoculated column suggesting a global leaching of this element from Fe-rich particles in un-inoculated conditions. This last result was in accordance with the evolution of Cd concentrations in the columns outlet (Figure V-5), that showed a release of Cd in un-inoculated but not in inoculated conditions. For Cr, no release was observed in the outlet, which is consistent with the results of Cr/Fe ratios in the solids.

With goethite, the decrease of the As/Fe ratio during experiment was uniform along the column. Cd and Cr/Fe ratios decreased in both un-inoculated and inoculated conditions. The decrease appeared uniformous along the column except for Cd in un-inoculated conditions, for which a small increase of Cd/Fe ratio from the bottom to the top of the column was observed. During the experiment (Figure V-8), no big differences were observed between un-inoculated and inoculated conditions in the goethite columns, except for As during the inoculation period. Thus, the very similar results observed for the As, Cd and Cr /Fe ratios in the solids is not very surprising.

### V-4.2.3 Biological Parameters

#### *V-4.2.3.1 Spatial distribution of bacterial abundance*

Molecular biomass was quantified as the total genomic DNA extracted from column solid samples and liquid (abbreviated liquid/L), recovered from both inoculated and un-inoculated columns. Globally, total DNA concentrations in solid samples of inoculated columns (DNA concentrations, Fh: 2.2E+3 - 1.7E+4 ng $g^{-1}$, Gt: 1.7E+3 - 9.9E+3 ng $g^{-1}$) were significantly higher than in solid samples of un-inoculated columns (DNA concentrations, FhB: under detection limit or < 10 ng $g^{-1}$, GtB: 0.13 - 61 ng $g^{-1}$). The DNA concentrations in liquid samples from both the un-inoculated columns were lower than the detection limit. This, along with the low DNA amounts found in the solid samples confirms that although the uninoculated columns were not complety sterile, little biomass had contaminated the columns. Bacterial abundance (qPCR of bacterial 16S rRNA encoding gene per g or mL sample), Figure. IV-15, showed similar tendencys as for molecular biomass. Results showed that 16S genes quantification in solid samples of both inoculated columns were significantly higher than in solid samples of

both un-inoculated columns (16S genes copies, FhB: under detection 3.8E+5 - 8.3E+5 $g^{-1}$, GtB: 2.3E+5 - 2.7E+6 $g^{-1}$), and there was no significant difference between ferrihydrite and goethite column globally. However, bacterial abundance in the bottom part of the goethite column (Gt0) was significantly higher than in the top of the column (GtT), and no significant difference was obtained between the middle (GtM) and bottom (Gt0) or top (GtT) samples. It seems that the bacterial biomass decreased from the bottom to the top of the goethite column. For the ferrihydrite column, both bottom (Fh0) and middle (FhM) had significantly higher bacterial 16S gene abundances than the top position (FhT), which suggested the bacterial biomass decreases from the bottom to the top of the goethite column.

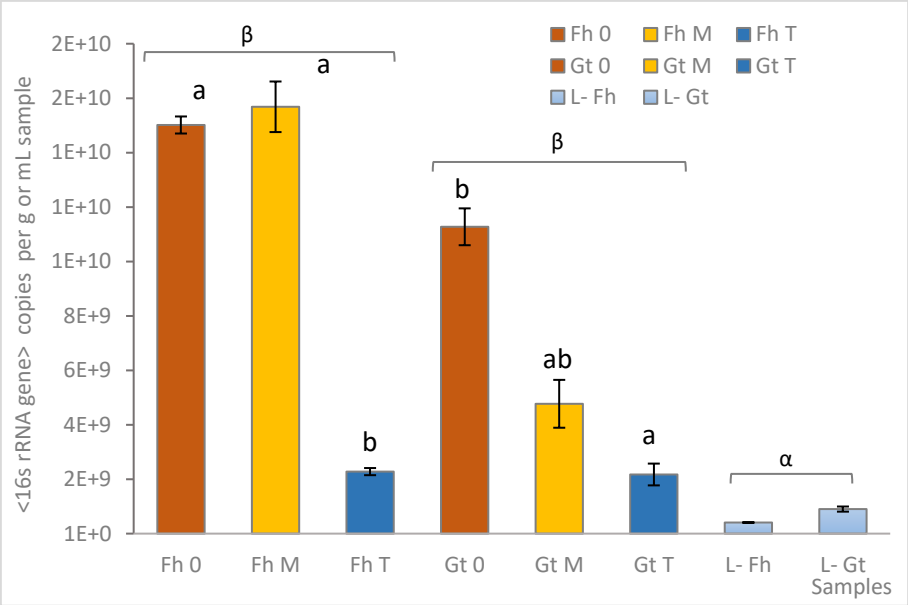


***Figure V- 16.*** *Bacterial 16S rRNA gene copies per g or mL sample. "0", "M" and "T" refer to the bottom, middle and top of the columns, ferrhydrite (Fh) column and goethite (Gt) columns. The small letters "a" and "b" differed significantly (Kruskal-Wallis test at $p<0.05$) of spatial positions of ferrihydrite and goethite column, the Greek letters were used for differing significantly by group of inoculated column of ferrihydrite (Fh) and goethite (Gt), liquid recovered from both inoculated columns (L). Data represent average values of three experimental replicates and their standard deviation (σ).*

### *V-4.2.3.2 Spatial evolution of Shewanella and Geobacter 16S rRNA gene abundances*

The abundances of micro-organisms affiliated to *Shewanella* and *Geobacter* genera were estimated in column samples using qPCR of genus-specific fragments of the 16s rRNA gene

(Figure V-16). Here only results from inoculated columns are presented because as no amplification was obtained in un-inoculated column samples.

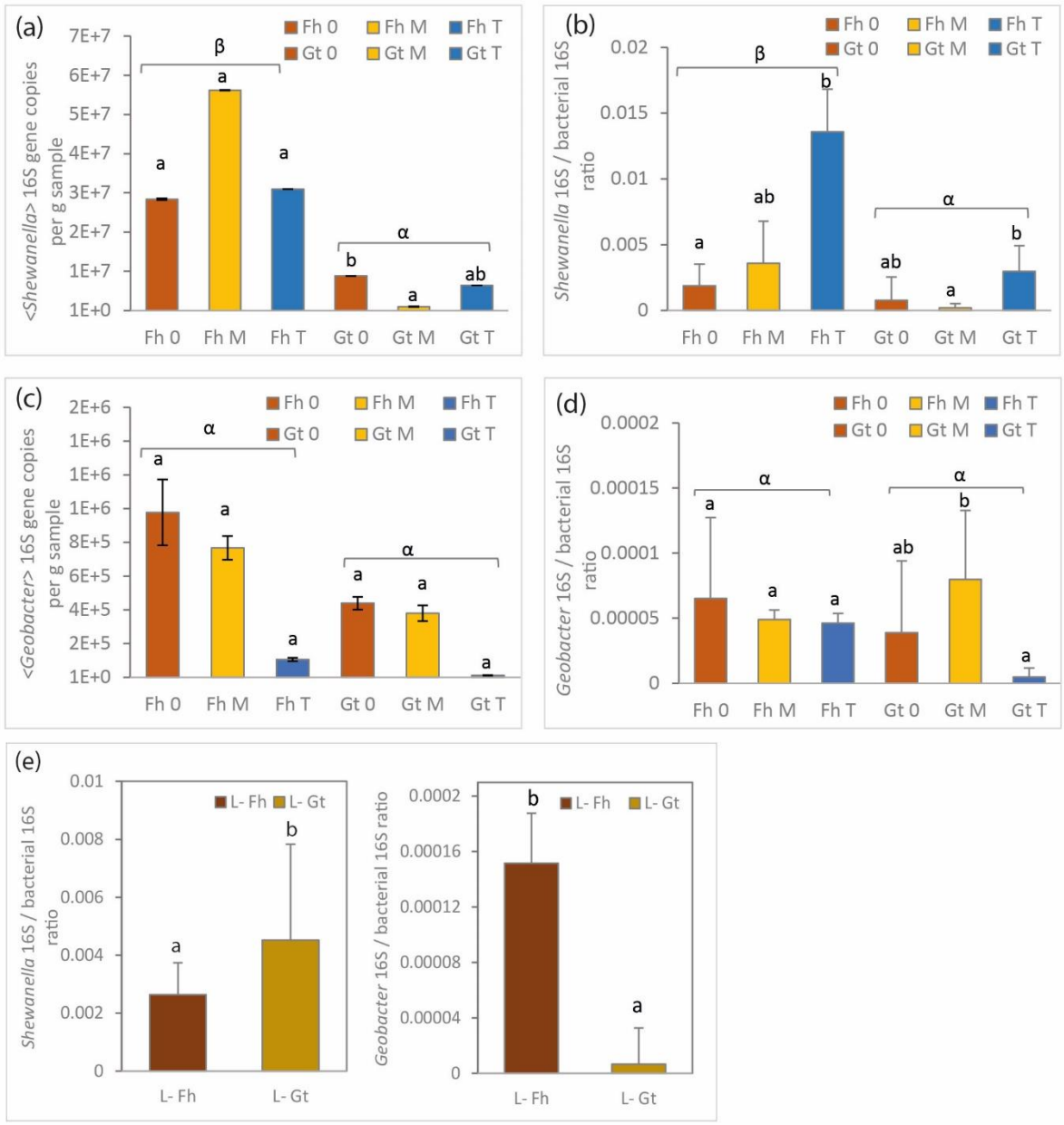


***Figure V-17.*** *Parameters linked to Shewanella and Geobacter 16S rRNA gene abundances: (**a**) Shewanella 16S gene copies per g sample, and (**b**) ratio of Shewanella 16S over bacterial 16S rRNA genes copies, (**c**) Geobacter 16S gene copies per g sample, (**d**) ratio of Geobacter 16S over bacterial 16S rRNA genes copies. (**d**) ratios of Shewanella 16S and Geobacter 16S over bacterial 16S rRNA gene copies, respectively in liquid samples recovered from both inoculated columns. The small letters "a" and "b" differed significantly (Kruskal-Wallis test at p<0.05) of spatial positions of ferrihydrite column, goethite column and liquid recovered from both*

*inoculated columns. The Greek letter were used for differing significantly by group of inoculated columns of ferrihydrite (Fh) and goethite (Gt). Data represent average values of three experimental replicates and their standard deviation (σ).*

As shown in Figure V-16 (b), a significant difference was observed between the numbers of gene copies belonging to *Shewanella* in the ferrihydrite column and the goethite column. Moreover, significant differences between vertical positions were obtained in the goethite column. Globally, the abundance of *Shewanella* 16S gene copies in the ferrihydrite column was significantly higher than in the goethite column and liquid samples. Moreover, in ferrihydrite columns, no significant differences were observed between the three sampling positions, i.e., bottom (Fh0), middle (FhM) and top (FhT) for the number of gene copies of *Shewanella*. They conversely presented significant differences in the goethite column: the bottom (Gt0) contained significantly more *Shewanella* gene copies than the middle (GtM) but there were no significant differences between the middle (GtM) and the top (GtT) (Figure V-16 (a)). The *Shewanella* 16S/ bacterial 16S ratio presented the same tendencies as the proportion of *Shewanella* was globally significantly higher in the ferrihydrite column than in the goethite column (Figure V-16 (b)). In Figure V-16 (b), results show that the ratio of *Shewanella* over bacterial 16S in the top part of the ferrihydrite column (FhT) was significantly higher than in the bottom part (Fh0). The same tendency of increase of the proportion of *Shewanella* from the bottom to the top was observed in the goethite column. However, the *Shewanella* 16S/ bacterial 16S ratio in the top part of goethite column (GtT) was significantly higher than in the middle (GtM) and no significant differences were observed either between the middle (GtM) and the bottom (Gt0), nor between the bottom (Gt0) and the top (GtT).

Concerning *Geobacter*, a significant difference was observed between the ferrihydrite and the goethite column, as shown in Figure V-16 (c). However, there were no significant differences between sampling positions although the abundance of *Geobacter* gene copies tended to decrease from the bottom to the top of the column. The *Geobacter* 16S/bacterial 16S ratio did not globally present any significant differences between column samples (Figure V-16 (d)). The proportion of *Geobacter* did not show significant differences between different sampling positions in the ferrihydrite column. Conversely, the *Geobacter* 16S/bacterial 16S ratio in the middle part of the goethite column (GtM) presented significantly higher values than in the top (GtT), but no significant differences were obtained between the middle (GtM) and the bottom (Gt0), or the bottom (Gt0) and the top (GtT) (Figure V-16 (d)).

The proportion *Shewanella* 16S/bacterial 16S in the liquid phase of the columns (Figure V-16 (e)) was of the same range as the proportion attached onto the solid phases, with the exception of the top part of the ferrihydrite column which showed a higher proportion of *Shewanella* associated with the solids. Moreover, the proportion of *Shewanella* 16S/bacterial 16S in the liquid phase was significantly higher in the goethite column than in the ferrihydrite column. On the contrary, the *Geobacter* 16S/bacterial 16S proportion was significantly higher in the ferrihydrite column than in the goethite column in the liquid phase.

*V-4.2.3.3 SEM bacteria observation*

Bacterial observations on ferrihydrite and goethite are given in Figure 17 and 18.

After incubation, bacterial cells were observed on solid samples under SEM (Figure V-17). Bacterial cells appeared intact with spherical and rod shapes (Figure V-17 (b) and (d)), separated from each other, turgid, and complete with smooth surface. Bacteria were mainly present on the surface of the sand particles (Figure V-17 (a)) but also on the surface of ferrihydrite (Figure V-17 (b) and (d)) and "secondary minerals" of iron (Figure V-17 (e)). The bacterial morphology was clear to observe under the microscope field of 5-10 µm, its size was between 1-4 µm depending on the shape.

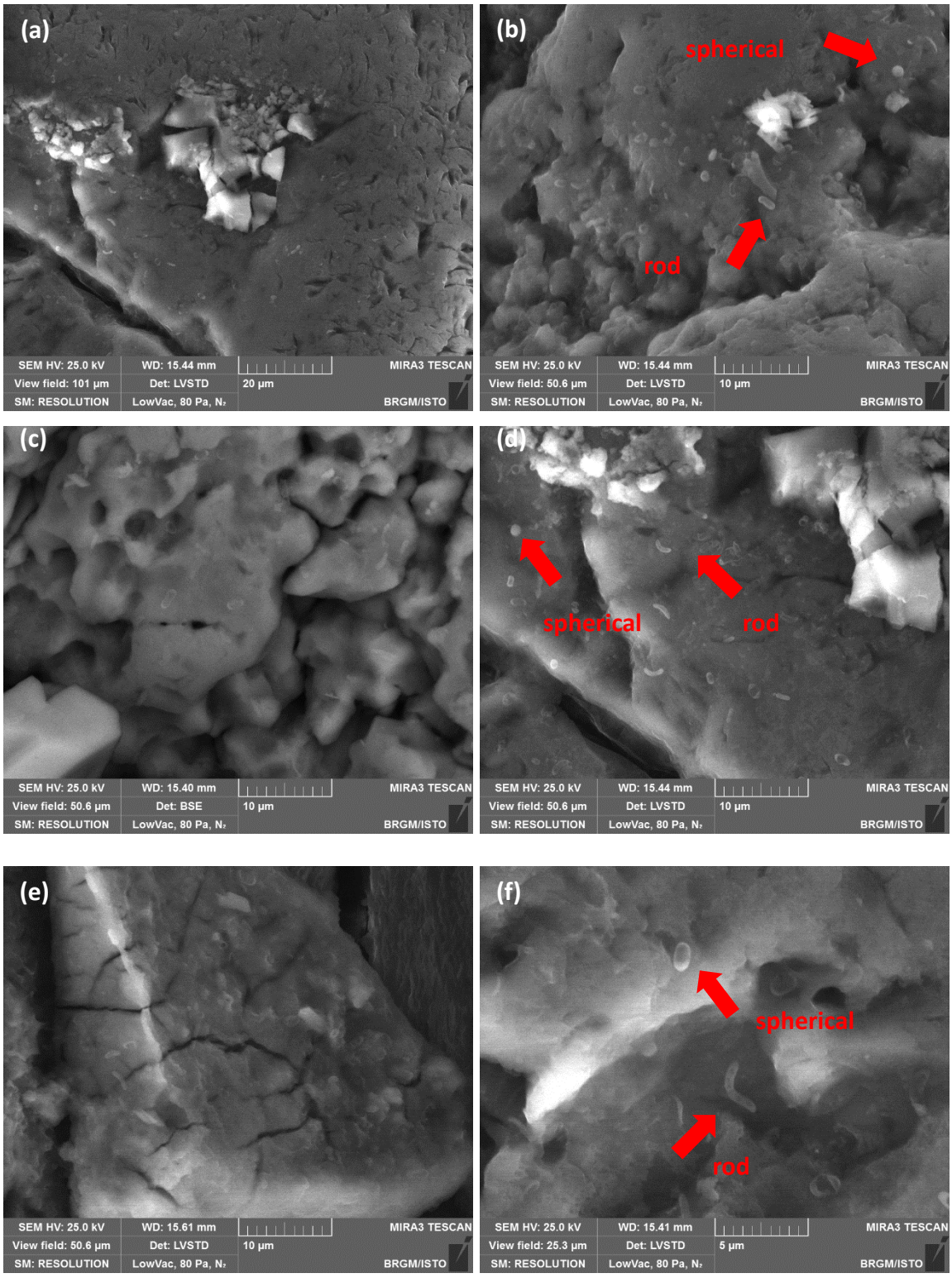


***Figure V-18.*** *Cryo-SEM micrographs of bacteria from inoculated ferrihydrite column.*

Bacterial observation on goethite

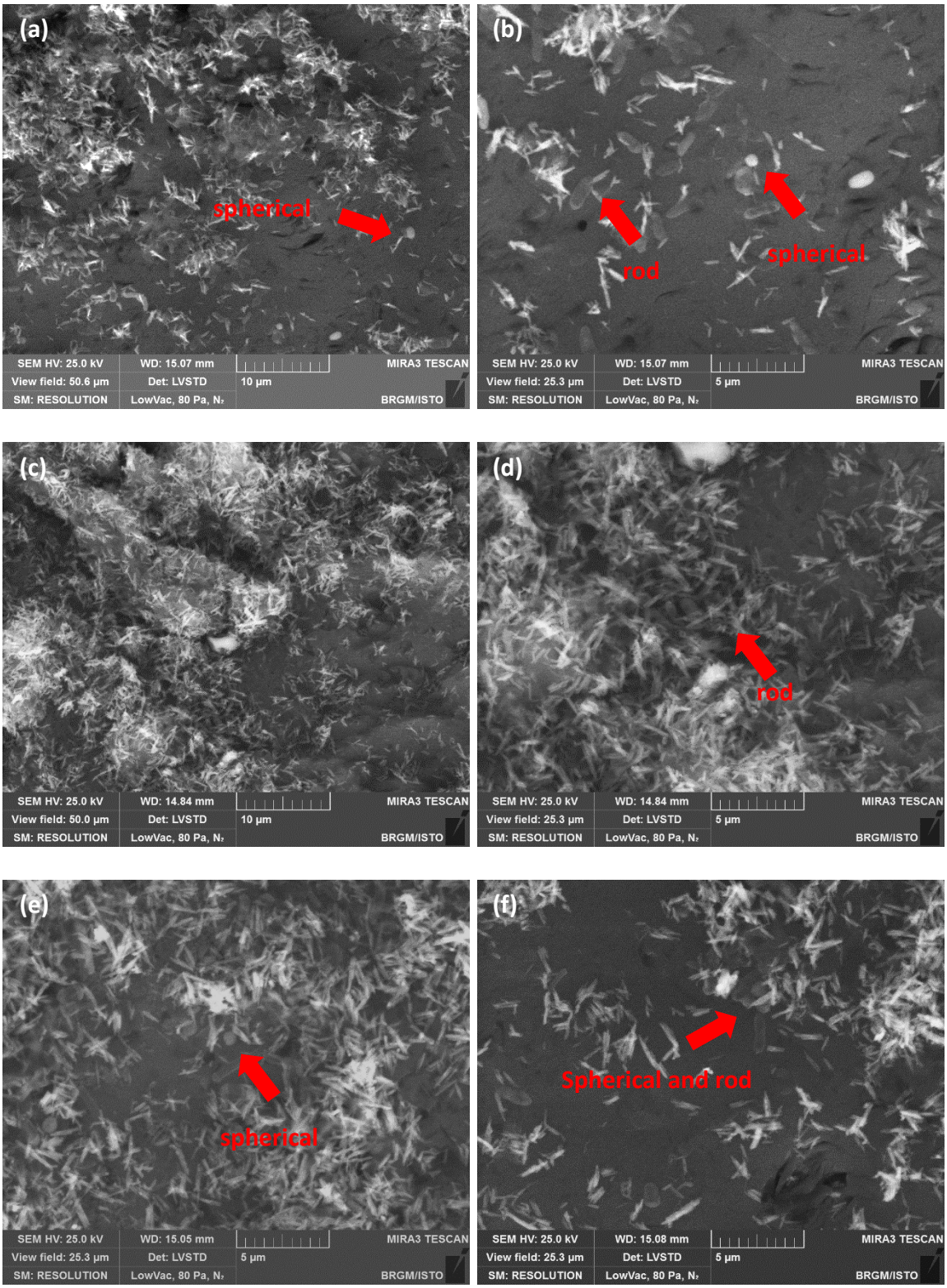


***Figure V-19.*** *Cryo-SEM micrographs of bacteria from inoculated goethite column.*

In the goethite column, the same conditions were used for bacterial observations as described for the ferrihydrite column. The same shapes of bacterial cells were observed as those in samples from the ferrihydrite column, which was intact, spherical shapes, or rod shapes, separated from each other, turgid, and complete with smooth surface (Figure V-18). Globally, bacteria cells were clear and easy to be found under the microscope field of 5-10 µm. However, it's difficult to observe bacterial cells on the surface of goethite because the bacterial cells are the same size as goethite crystals. No clear "secondary minerals" were observed in the goethite experimental system.

### V-4.2.4 Mineral SEM-EDS observation

*V-4.2.4.1 Fe speciation in the solid phases of ferrihydrite and goethite columns*

*Initial column samples*

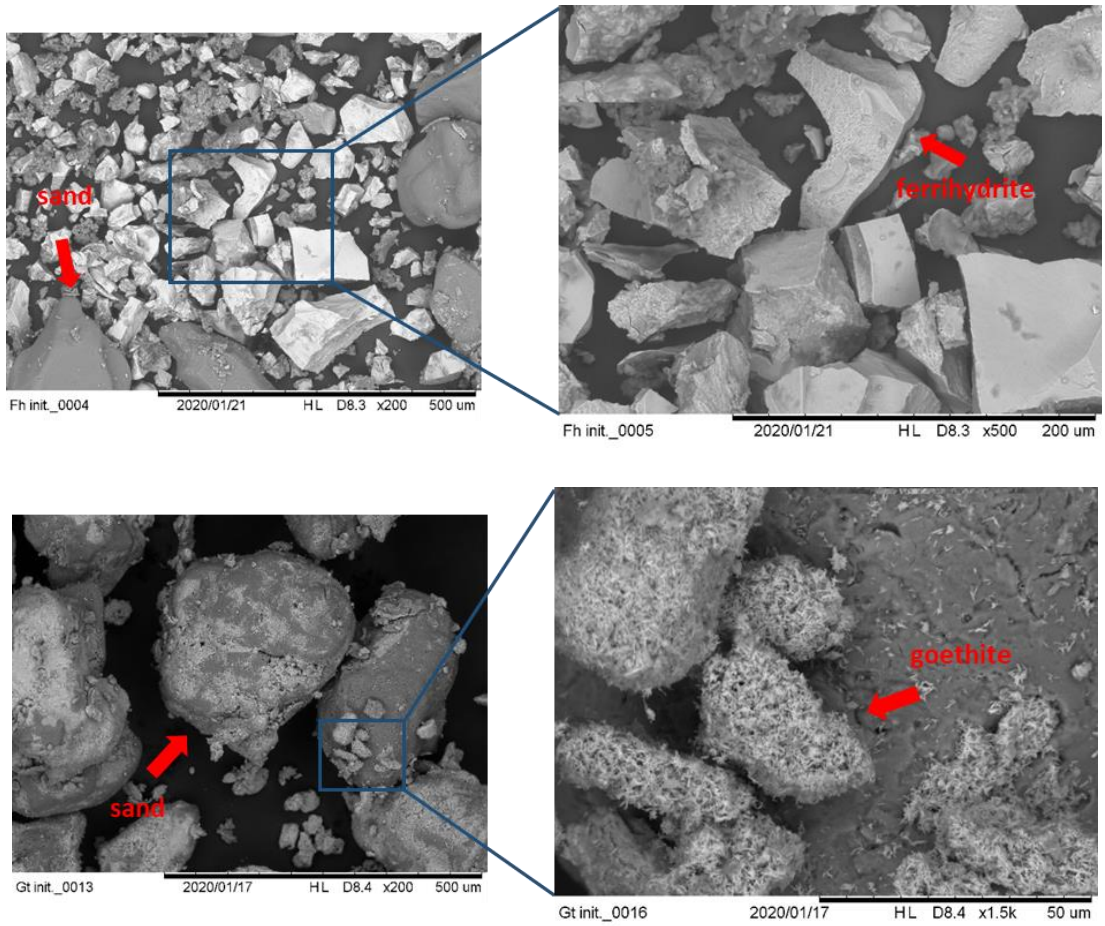


***Figure V-20.*** *SEM image of initial ferrihydrite and goethite column's sample in which it is possible to observe the shape of ferrihydrite/goethite and sands.*

SEM observations were performed to determine the structural evolution of mineral filling material (a mixture of sand, silica gel and synthetic Fe (oxyhydr)oxides with adsorbed As, Cr and Cd) between pre-incubation samples and post-incubation samples, and the differences between inoculated columns and un-inoculated columns.

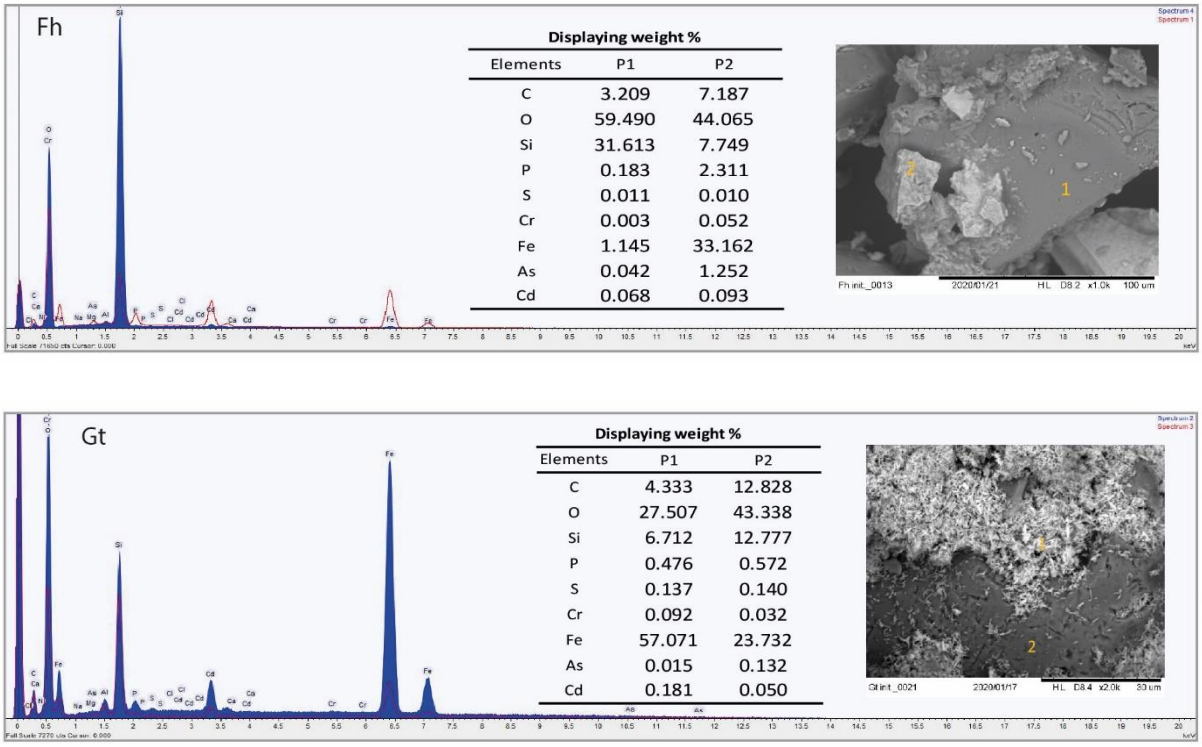


***Figure V-21.*** *SEM-EDS analysis of initial samples for ferrihydrite (Fh) and goethite (Gt) columns. The blue and red spectra correspond to the analyses of point "1" and point "2" (abbreviated P1 and P2), respectively.*

Figure V-19 shows electronic micrographs of initial samples before incubation for ferrihydrite (Fh) and goethite (Gt) columns. There were two main morphology types in the ferrihydrite column sample: (1) clear irregular block-type ferrihydrite particles with some mixtures of silica gel; (2) irregular round shaped sands. It can be seen that the initial ferrihydrite presented smooth or rough surface in different blocks with length, width and height of approximately 5-150 µm. The micrograph showed that the diameter of sand grains was around 100-150 µm. As shown in the view of goethite column sample, a single goethite crystal presented an acicular form (1-5 µm) but in this experiment goethite crystals were agglomerated into small spherical (10-50 µm) structures or distributed on the surface of sand particles.

Energy dispersive X-ray spectrometry (EDX) detector, coupled to SEM observations, was used and enabled to characterize the major elements in the sand and mineral phase. In Figure V-20, the main composition given as weight percentages shows that the major elements were Fe and O in ferrihydrite particles (P2 on the Figure V-20, Fh), and Si and O in sand particles. The same for goethite column sample which shows Fe, O and Si as major elements (Figure V-20, Gt).

*Post-incubation column samples-ferrihydrite*

The same SEM-EDS analysis were performed for post-incubation samples. Figure V-21 shows electronic micrographs of column samples (bottom, middle and top) after incubation from inoculated and un-inoculated ferrihydrite columns. For the un-inoculated column, there was no obvious difference in the types of forms in post-incubation samples in comparison to initial samples. Clear and irregular blocks of ferrihydrite could be found everywhere, whose size did not show differences either (Figure V-21 (a), (b) and (c)). However, some regular forms of minerals were present in inoculated column after incubation (Figure V-21 (A), (B) and (C)). It can be seen that regular blocks stacked or arranged together in a radial pattern with smooth surface in different blocks with length, width and height of approximately 50 -100 µm. Figure V-21 show high concentrations of Fe and O in the particles corresponding to the morphology of ferrihydrite, and higher concentration of P in the new “laminated” structures.

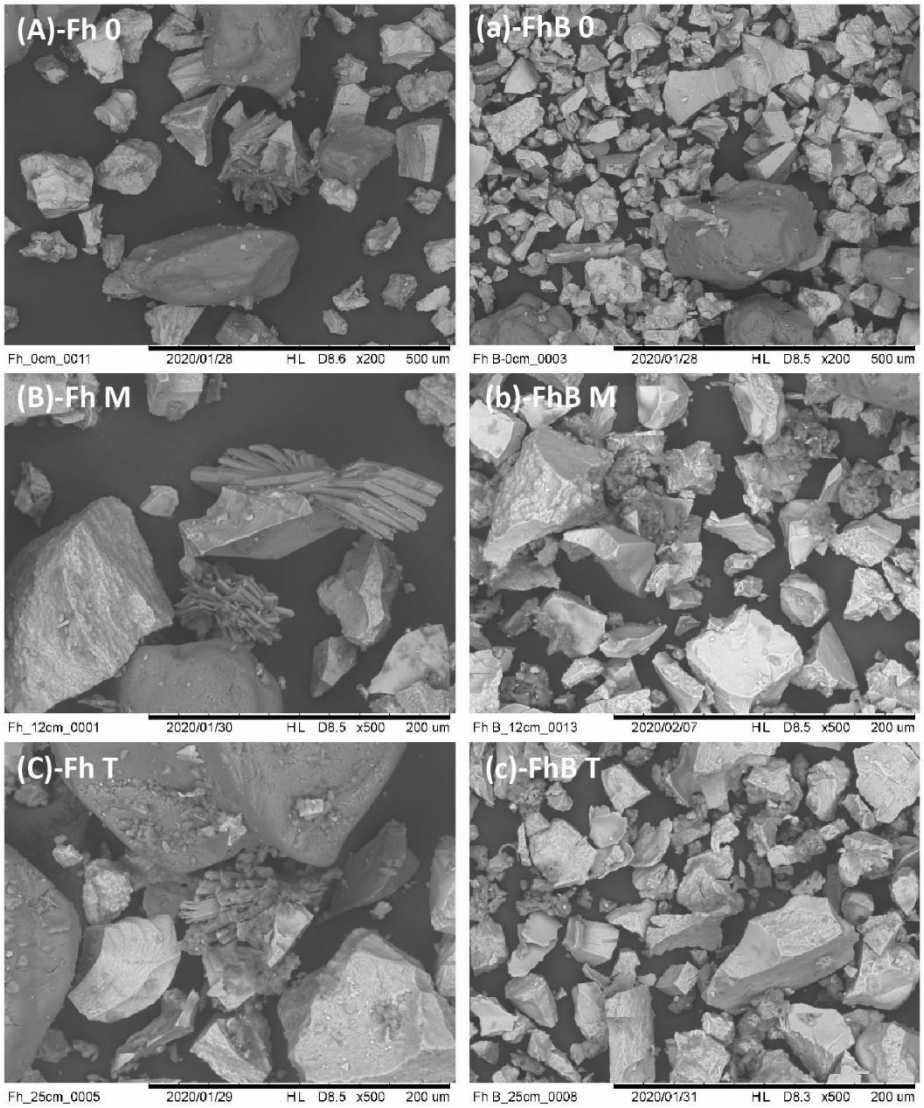


***Figure V-22.*** *SEM images of post-incubation ferrihydrite columns including samples from the bottom, middle and top of inoculated ferrihydrite column and the same in un-inoculated column.*

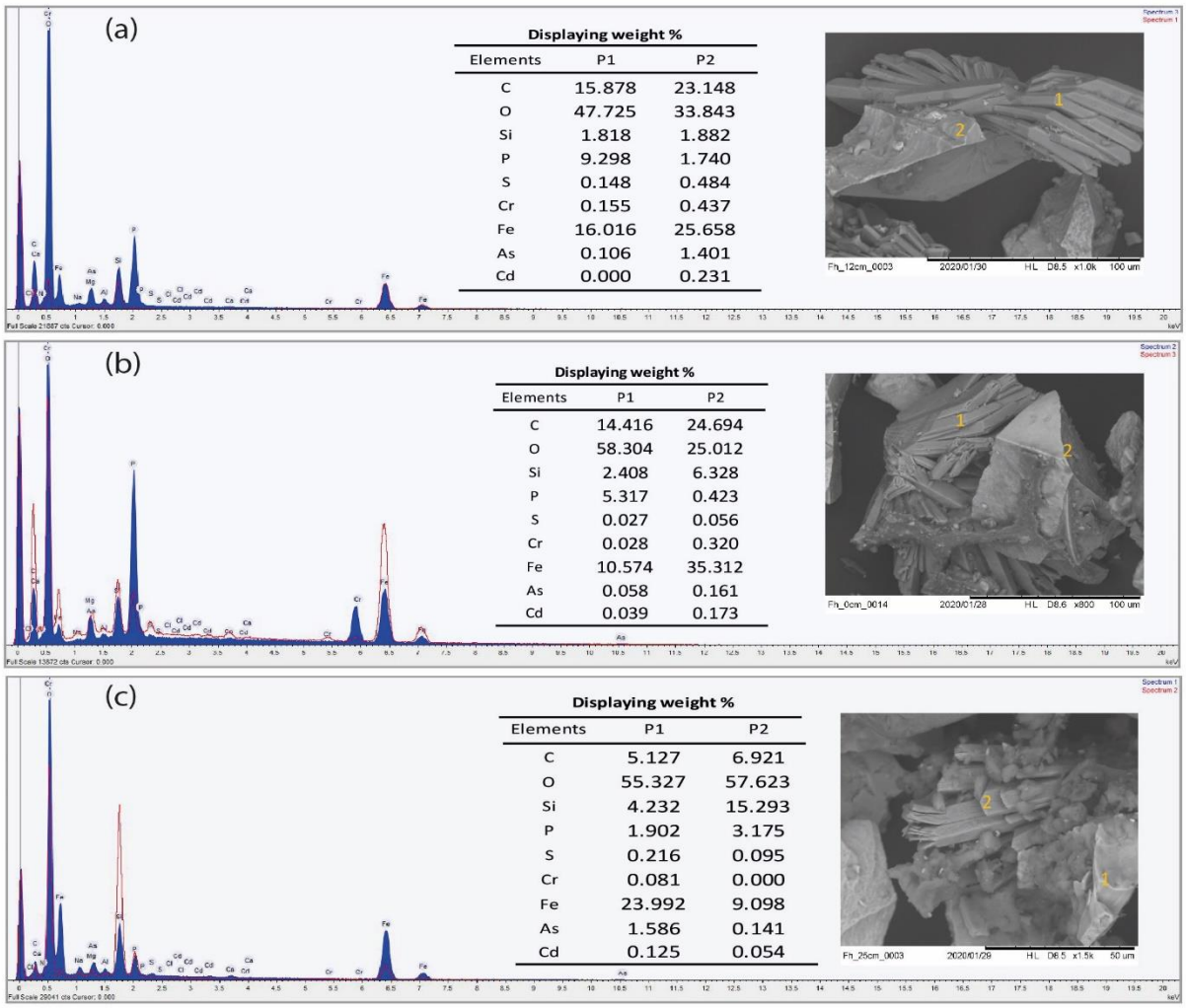


***Figure V-23.*** *SEM-EDS analysis of post-incubation inoculated ferrihydrite column, (a) Fh0: bottom of the column, (b) FhM: 12 cm of the column, (c) FhT: top of the column. The blue and red spectra correspond to the analyses of point "1" and point "2" (abbreviated P1 and P2).*

*Post-incubation column samples-goethite*

Figure V-23 shows electronic micrographs of column samples (bottom, middle and top) after incubation from both goethite columns, inoculated (Figure V-23 (A), (B) and (C)) and un-inoculated column (Figure V-23 (a), (b) and (c)). It was clear and easy to observe the morphology of goethite and the sands from all samples from goethite column, however there was no obvious morphology differences between inoculated and un-inoculated samples. As shown in Figure V-24, Fe, O and Si as major elements, as already observed in the initial material.

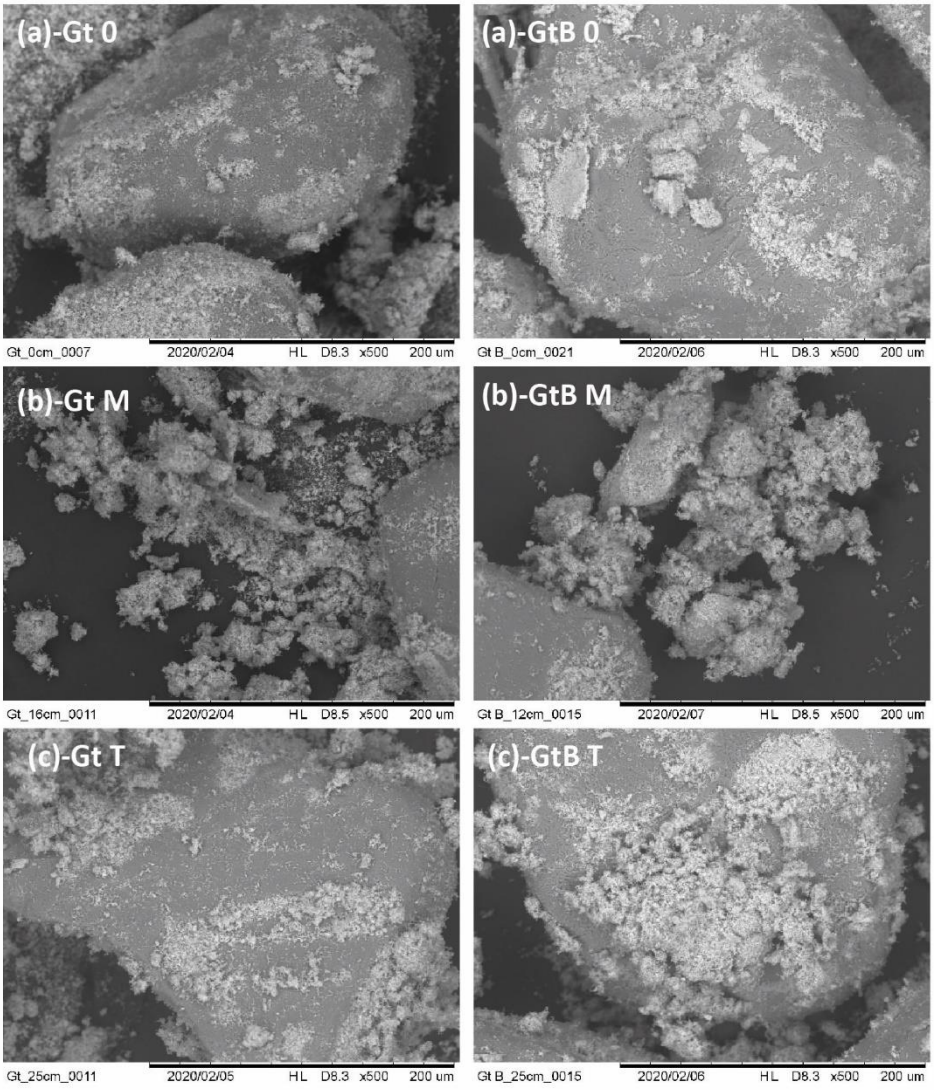


***Figure V-24.*** *SEM image of post-incubation goethite column's samples, big letters "A, B, C" presented the bottom, middle and top position in inoculated column, small letters "a, b, c" represented the same in un-inoculated column.*

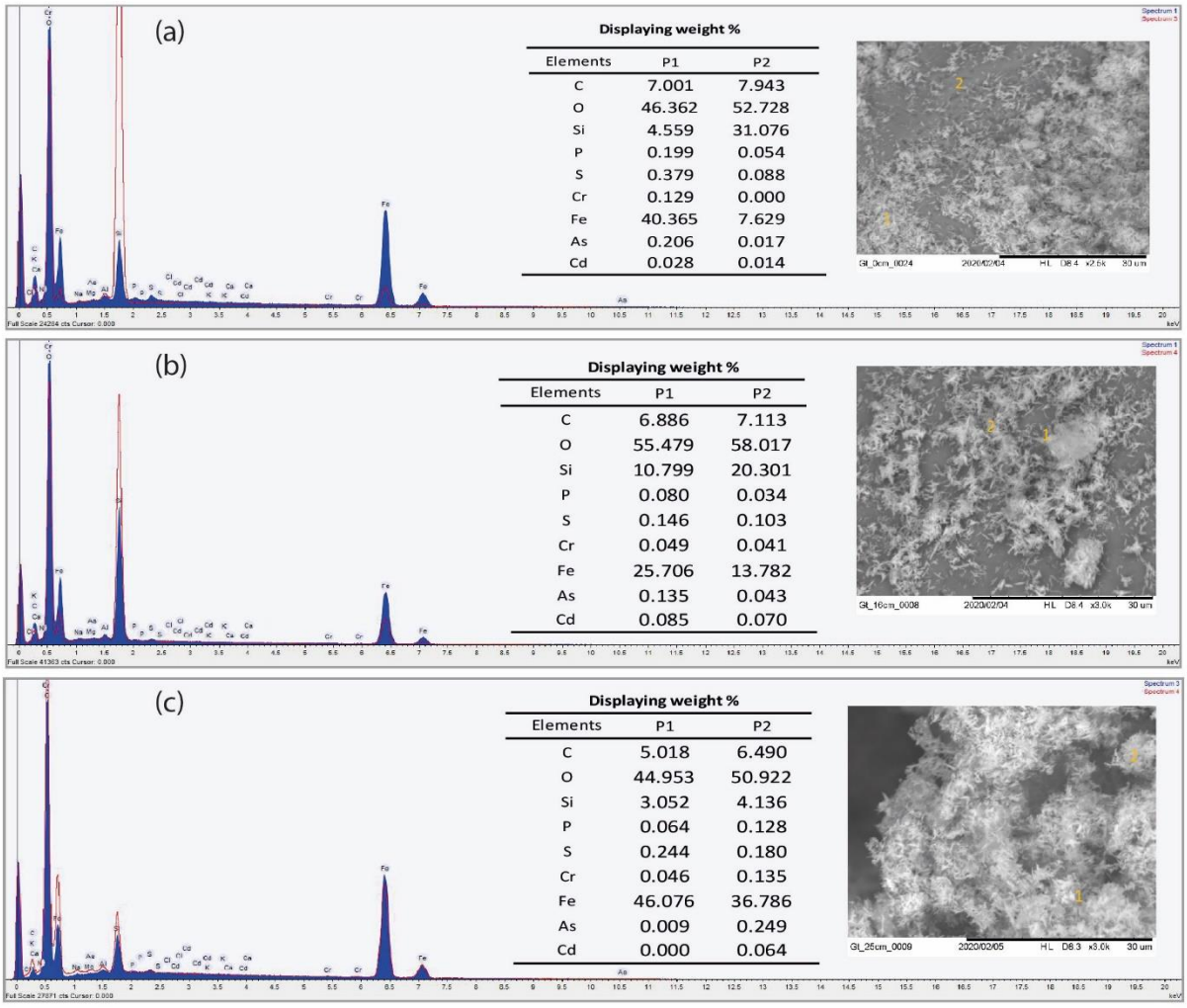


***Figure V-25.*** *SEM-EDS analysis of post-incubation inoculated goethite column, (a) Gt0: bottom of the column, (b) GtM: 12 cm of the column, (c) GtT: top of the column. The blue and red spectra correspond to the analyses of point "1" and point "2" (abbreviated P1 and P2).*

### *V-4.2.4.2 The relationship of Fe and MTEs on the surface of the samples*

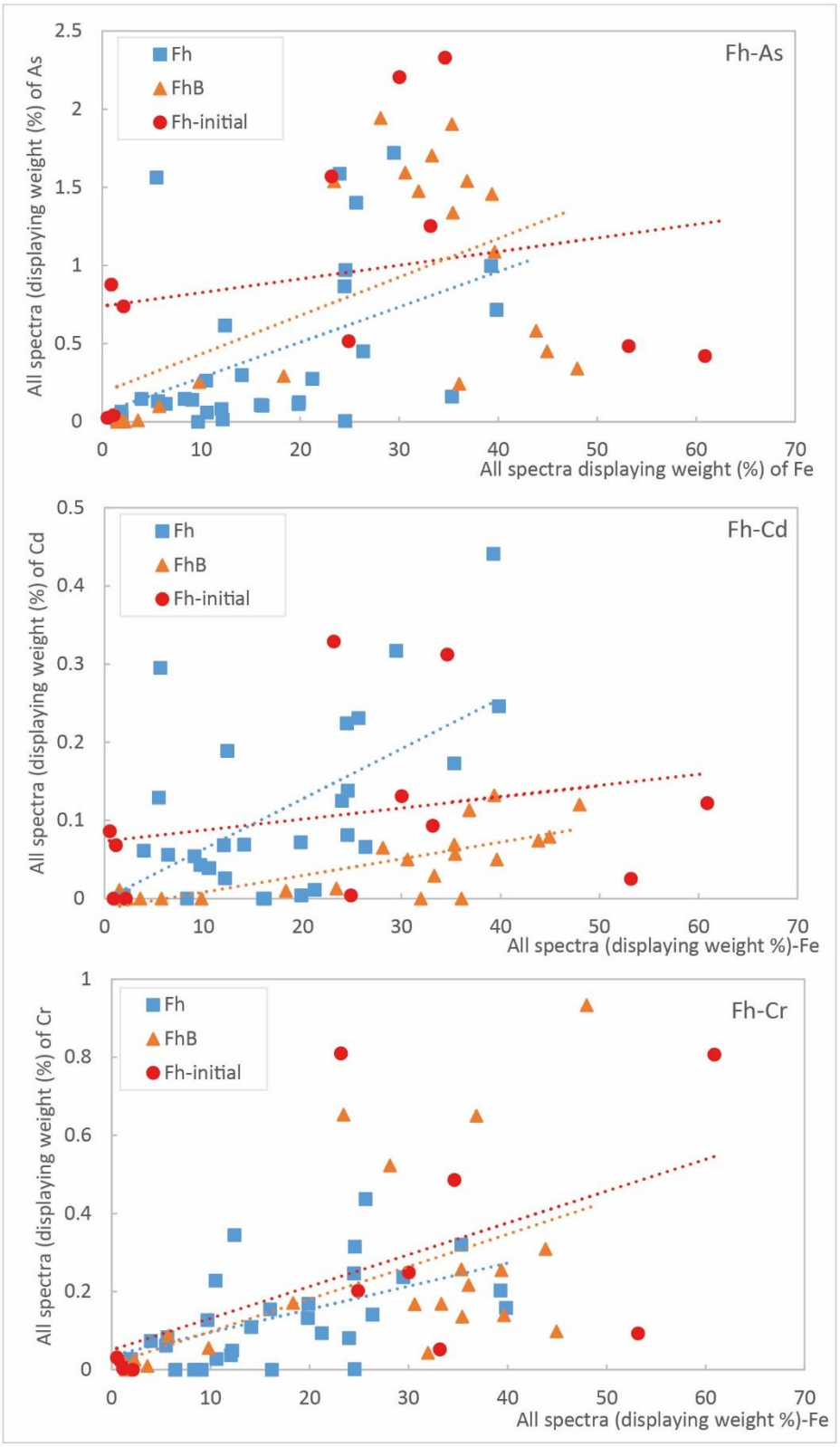


***Figure V-26.*** *Analysis of correlation between the displaying weight of As, Cr and Cd over Fe from the SEM-EDS analysis in ferrihydrite columns (initial sample and post-incubation samples: Fh and FhB: blank).*

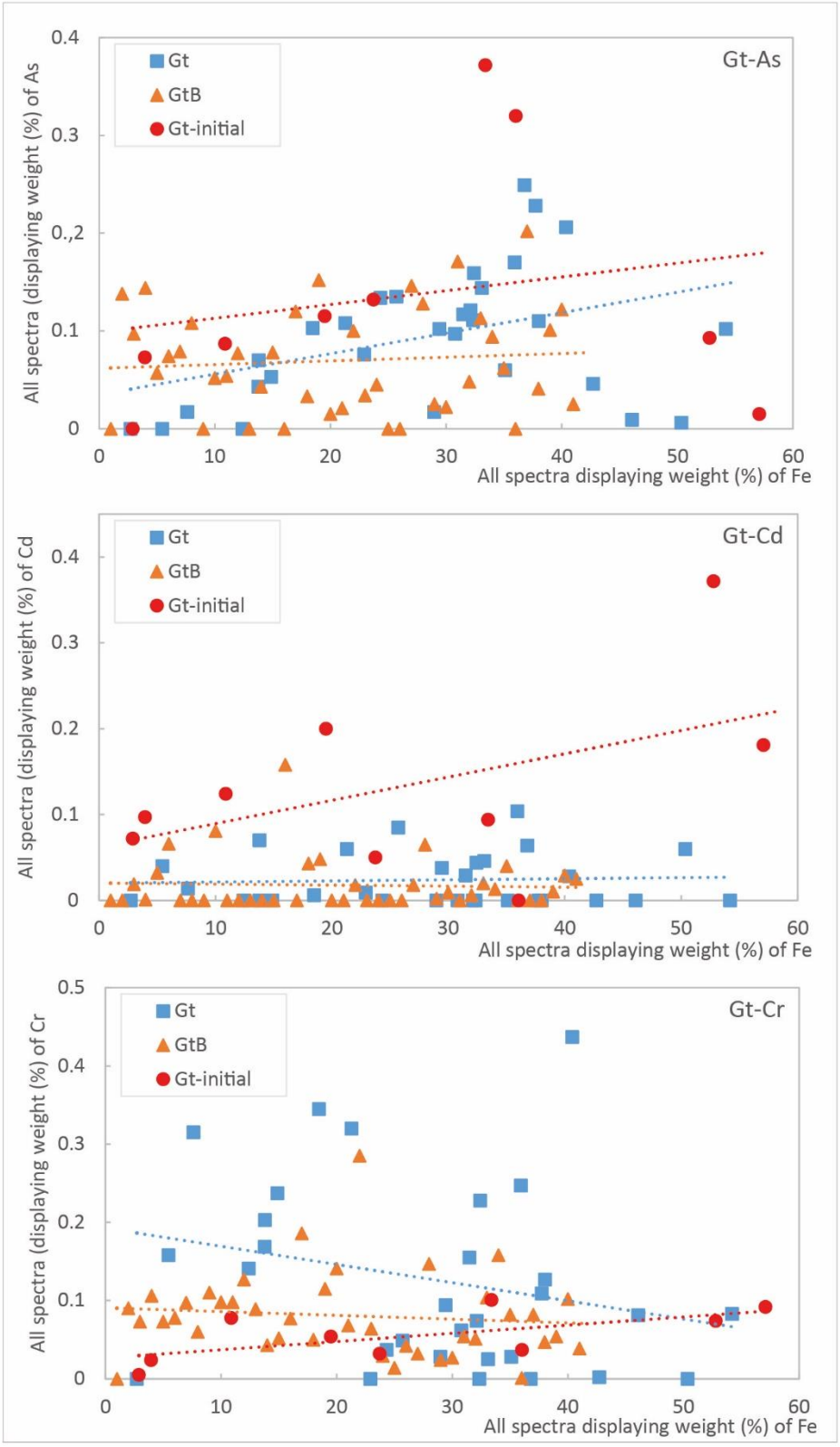


***Figure V-27.*** *Analysis of correlation between the displaying weight of As, Cr and Cd over Fe from the SEM-EDS analysis in goethite columns (initial sample and post-incubation samples: Gt and GtB: blank).*

***Table V-6.*** *The correction and coefficient of determination from correlation analysis between the displaying weight of As, Cr and Cd over Fe from the SEM-EDS analysis.*

| | | Fh | | | Gt | | |
|---|---|---|---|---|---|---|---|
| | | initial | inoculated | un-inoculated | initial | inoculated | un-inoculated |
| As/Fe | Correlation | + | + | + | + | + | + |
| | $R^2$ | 0.055 | 0.214 | 0.303 | 0.041 | 0.155 | 0.005 |
| Cd/Fe | Correlation | + | + | + | + | + | - |
| | $R^2$ | 0.065 | 0.372 | 0.553 | 0.235 | 0.002 | 0.003 |
| Cr/Fe | Correlation | + | + | + | + | - | - |
| | $R^2$ | 0.323 | 0.316 | 0.276 | 0.417 | 0.679 | 0.014 |

In the ferrihydrite columns, the amounts of As, Cd and Cr on the various grain surfaces globally increased with Fe concentration in all 3 conditions. This increase is equivalent or more pronounced after the incubation, e.g., Fe-As and Fe-Cd. The correlation between Fe and Cd is much stronger after the incubation in both inoculated and un-inoculated columns, whereas the surface concentration of Cd seemed to be globally higher and increase more rapidly in inoculated conditions when Fe concentration are high (Figure V-25, Fh-Cd). The same tendency of a positive correlation of Fe-As was found during experiment (Figure V-25, Fh-As). The association of Cr with ferrihydrite surface did not change much during the incubation according to the SEM-EDS.

The tendencies were different for goethite. The increase of surface As concentrations with Fe was less pronounced than with ferrihydrite. Surface Cd concentration seemed to decrease from the initial to the final conditions, and at the end of the experiment, Cd concentration did not increase with Fe (no correlation). Finally, surface Cr concentration tended to decrease with increasing Fe concentrations at the end of the experiment, and this tendency was more pronounced in inoculated than in un-inoculated conditions.

### V-4.2.5 Mössbauer spectroscopy

Mössbauer spectra on initial samples and post-incubation samples of ferrihydrite / goethite columns are shown in Figures V-27 and 28.

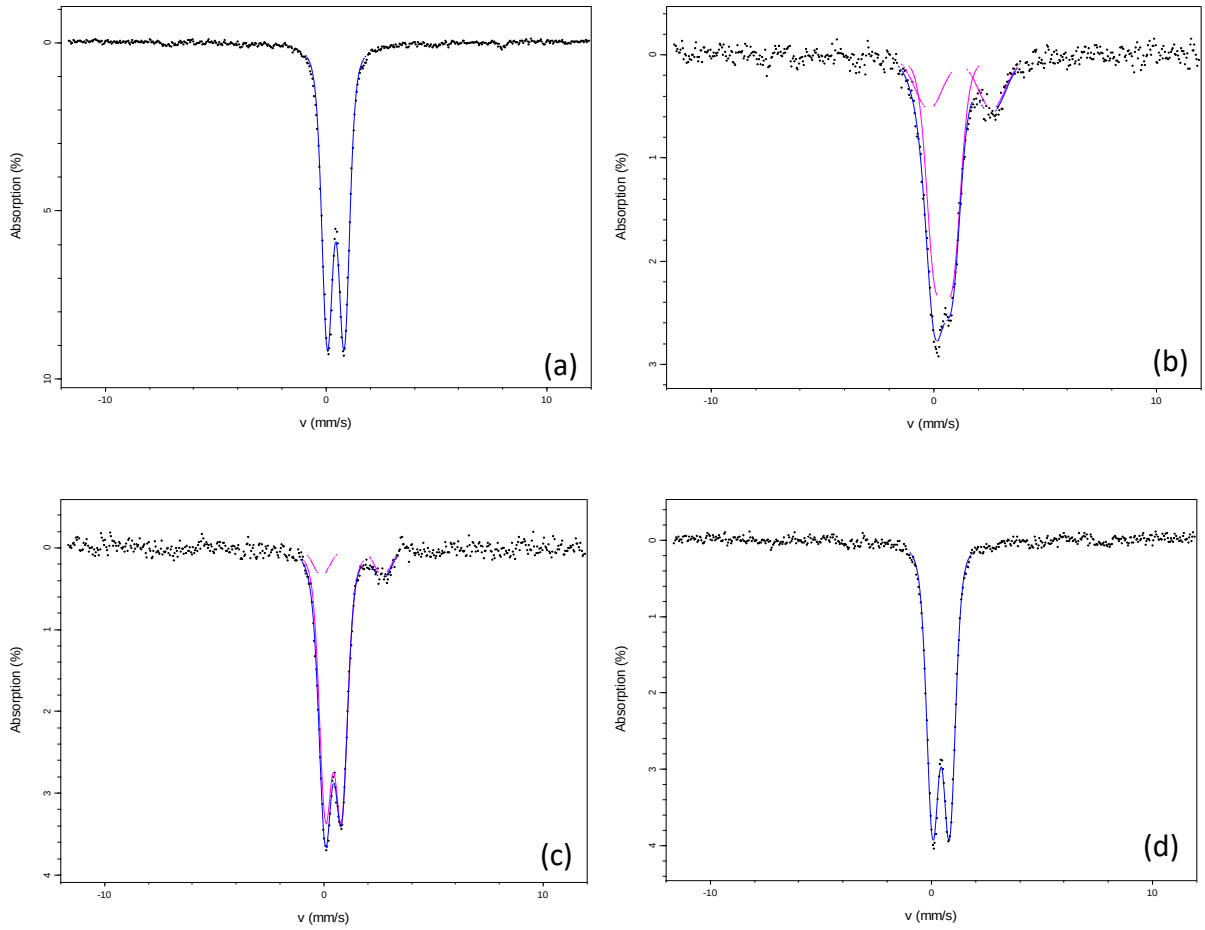


***Figure V-28.*** *Mössbauer spectra collected at 140 K for samples, (a) pre-incubation Fh initial, post-incubation (b) bottom of inoculated column Fh-bottom, (c) top of inoculated column Fh-top, and (d) un-inoculated column Fh-Blank for ferrihydrite columns.*

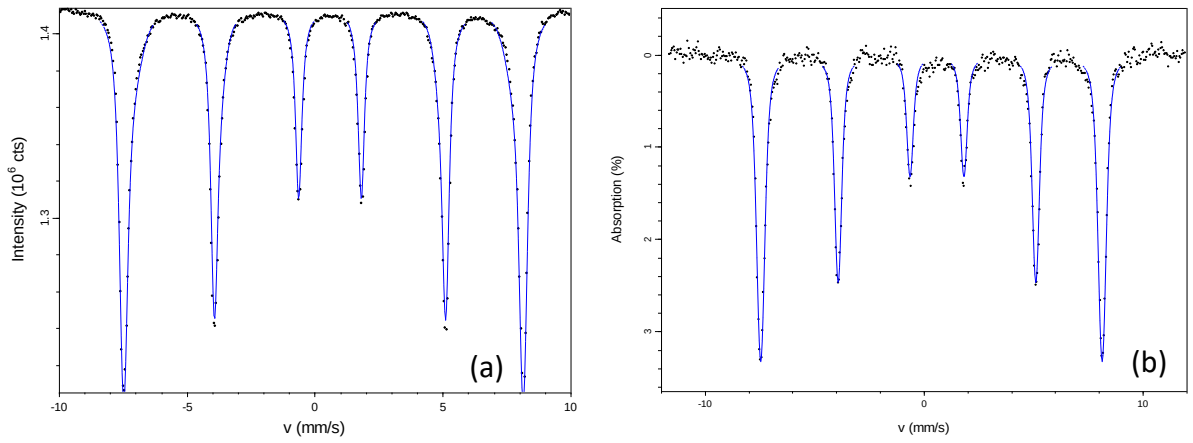

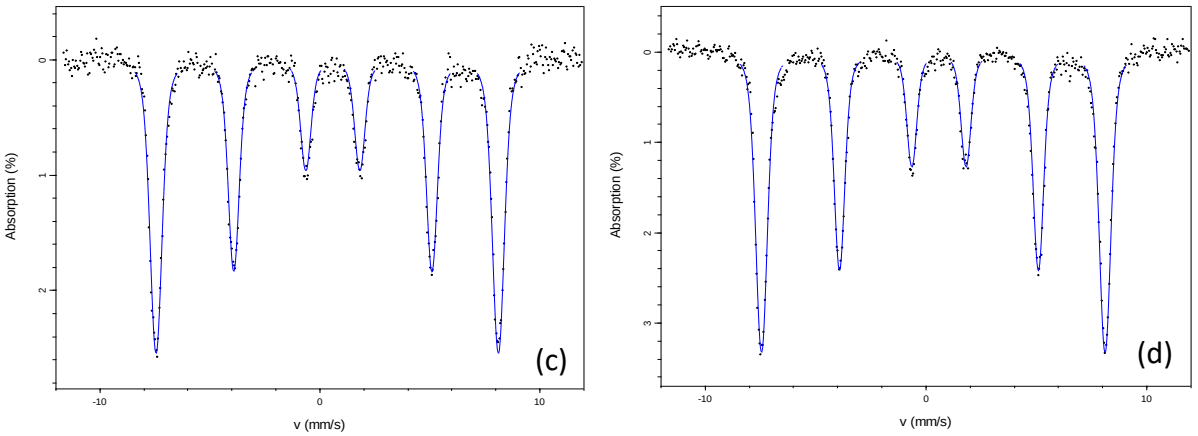


***Figure V-29.*** *Mössbauer spectra collected at 140 K for samples, (a) pre-incubation Gt init, post-incubation (b) bottom of inoculated column Gt-bottom, (c) top of inoculated column Gt-top, and (d) un-inoculated column Gt-Blank for goethite columns.*

***Table V-7.*** *Fitting results of Mössbauer spectroscopy. CS – center shift, QS – quadrupole splitting, e – quadrupole shift, H – hyperfine field, stdev(H) – standard deviation of hyperfine field, Pop. – Relative abundance, $\chi^2$ – goodness of fit.*

| Sample | Mineral phase | CS mm/s | QS mm/s | stdev(QS) mm/s | e mm/s | H T | stdev(H) T | Pop % | Error | $\chi 2$ |
|---|---|---|---|---|---|---|---|---|---|---|
| FH initial | Fe(III) | 0.43 | 0.77 | 0.35 | | | | 100 | 0 | 3.2 |
| Fh Bottom | Fe(III) | 0.40 | 0.82 | 0.44 | | | | 70.4 | 2.0 | 0.6 |
| | Fe(II) | 1.18 | 2.84 | 1.1 | | | | 29.6 | 2.0 | |
| Fh Top | Fe(III) | 0.43 | 0.73 | 0.30 | | | | 87.5 | 1.6 | 0.6 |
| | Fe(II) | 1.28 | 2.79 | 0.45 | | | | 12.5 | 1.6 | |
| Fh Blank | Fe(III) | 0.43 | 0.76 | 0.29 | | | | 100 | 0 | 0.8 |
| Gt Bottom | Fe(III) | 0.45 | | | -0.13 | 48.4 | 0.60 | 100 | 0 | 1.1 |
| Gt Top | Fe(III) | 0.46 | | | -0.13 | 48.3 | 0.76 | 100 | 0 | 0.7 |
| Gt Blank | Fe(III) | 0.45 | | | -0.13 | 48.2 | 0.77 | 100 | 0 | 1.0 |

All ferrihydrite spectra are dominated by a narrow doublet which is characteristic for a Fe(III) phase, notably ferrihydrite (CS: 0.47 mm/s; QS: 0.77 mm/s). No additional mineral phase could be detected for samples Fh initial and Fh-Blank.

The spectra for Fh-Bottom and Fh-Top were best fitted by including an additional Fe(II) phase. It is not possible to identify this Fe(II) phase because the hyperfine parameters, i.e. CS and QS, match several different minerals e.g. biotite (Cao et al., 2017), $FeCl_2$ (Laufer et al., 2017), hedenbergite (Amthauer and Rossman, 1984), etc.

The spectra collected for the goethite samples, i.e. Gt initial, Gt-Bottom, Gt-Top and Gt-Blank, are characteristic for goethite as expected. No additional mineral phases were detected. An increase in StDev(H) for Gt-Top and Gt-Blank in comparison to Gt-Bottom might reflect a minor change in the mineral structure e.g. change in particle size, however other analytical methods, e.g. TEM would be needed to confirm this.

According to the information, Fe(II) was clearly visible in samples Fh-Bottom and Fh-Top, with Fh-Bottom (29.6% Fe(II)) showing a higher degree of reduction than Fh-Top (12.5% Fe(II)) in bottom and top position of inoculated column. No evidence was found to indicate the occurrence of any Fe(III) reduction in Fh initial, and Fh-Blank samples. Moreover, no defined Fe phases (e.g. goethite, or magnetite) were detected in all Fh samples.

For goethite columns, no clear differences were observed between goethite (Gt) samples from this experiment.

## IV-5 Discussion

### IV-5.1 Spatial and temporal aspects of iron reduction of ferrihydrite and goethite

The black color that appeared in both the columns inoculated with a bacterial consortium might be linked to sulphide production. The feeding medium contained molybdate to inhibit the sulfate-reducing activity, however this was possibly not sufficient to completely inhibit sulfate reduction in the column system. As a fact, in the previous batch condition, molybdate was homogeneously available simultaneously in all the volume of culture. In column, it might have been reduced (some bacteria can reduce molybdate) and/or retained on the solid phases and inhibition of sulfate-reduction might have been weakened. Another path for sulphide formation might be the transformation proteins (AA sulphur) which are moreover abundant due to the

presence of peptone, by some bacteria such as some belonging to the *Shewanella* genus. Thus, the potential production of $H_2S$ will be considered as a possible mechanism occurring in the inoculated column, in the following discussion.

In ferrihydrite columns, Fe reduction was linked to bacterial inoculation and released iron was detected in the outlet from day 17, three days after inoculation. Dissolved and reduced Fe in this column could have been released in the outlet and/or re-precipitated onto other iron minerals. Iron reduction in this column could have resulted from chemical processes, e.g. reduction by the $H_2S$ produced by the processes mentioned above, or and/or bacterial iron reduction either through fermentation, or dissimilatory reduction. However, Fe reduction by IRB was likely a dominant reaction as sulfate reduction was at less partly inhibited by molybdate. Moreover, two IRB genera, *Shewanella* and *Geobacter*, although not the only iron reducers, were detected in the inoculated columns.

In the meantime, pH decreased suddenly on day 15 when the substrate was added to the feeding liquid. The bacterial inoculum then lead to a gradual increase of the pH and also a drop of the redox potential (Eh) in the days following inoculation. This phenomenon was already observed in presence of *Shewanella* and Fe oxides reduction in some research (Perez-Gonzalez et al., 2010; Zegeye et al., 2007). On the other hand, in this system, peptone was included in the mixture of substrates and could be fermented producing ammonium that increases the pH (Tepari et al., 2019). In addition, hydrogen ($H_2$) can be produced and consumed by the bacteria (including SRB), inducing an increase of pH (Liamleam and Annachhatre, 2007). Assumably, both the metabolic activities of the bacteria and biogenic mineral formation modified the Eh as well as the pH during the continuous feeding period through the following reactions (Ona-Nguema et al., 2002; Wolf et al, 2009):

Hydrogenotrophic sulfate reduction, or sulfidogenesis, involving

(1) $C_6H_{12}O_6 + 4H_2O \rightarrow 2CH_3COO^- + 2HCO^{3-} + 4\,H^+ + 4H_2$

(2) $4H_2 + SO_4^{2-} + H^+ \rightarrow HS^- + 4H_2O$

Also undesirable but possible reactions of hydrogenotrophic methanogenesis and homoacetogenesis reactions are the following:

(3) $4H_2 + HCO_3^- + H^+ \rightarrow CH_4 + 3H_2O$

(4) $4H_2 + 2HCO_3^- + H^+ \rightarrow CH_3COO^- + 4H_2O$.

These reactions potentially led to the increase of pH in the inoculated columns and this was in agreement with the quasi-stability of pH observed during and after the inoculation period (Fig. IV-6, upper panel).

During the post-inoculation period, while Fe reduction steadily carried on occuring, less $[FeT]_D$ was measured in the column outlet suggesting the precipitation of the produced [FeII] as carbonate, with the inorganic carbon produced by degradation of organic substrates, or sulfides FeS with $H_2S$ (Liamleam and Annachhatre, 2007; Urrutia et al., 1998; Zachara et al., 2002). The low redox potential (down to -300 mV ref Ag/AgCl) and the observation of black precipitates could be in accordance with this last hypothesis. The Mössbauer spectra did not show any presence of iron phosphate, whereas this was suggested by SEM-EDS. Indeed, $(Fe_3(PO_4)_2 \cdot 8H_2O)$ (vivianite) has a much higher center shift (1.3 mm/s) and quadrupole splitting (3 mm/s) than was observed in our samples. The new crystalline minerals observed by MEB-EDS might be iron phosphate precipitated during the inoculation period, but not the major FeII minerals formed during the biological reduction of ferrihydrite, or maybe would represent other Fe(II) phase containing the main elements quantified by MEB-EDS, e.g. Fe (20-30%), P (5-11%), 0 (40-55%), etc. (weight percentages).

In the goethite columns, black precipitates were observed, as in the ferrihydrite column, and might be caused by $H_2S$ according to the reaction described in the previous section. Globally, iron reduction occurred with a first peak corresponding to inoculation and released iron was detected in the outlet on day 18, one day later than in the ferrihydrite column. In the inoculated column, the microbial reaction was likely the dominant reaction compared with the un-inoculated column that had little $[TFe]_D$ released during the whole experiment. Moreover, this is supported by the results of the quantification of 2 IRB, *Shewanella* and *Geobacter*, which showed that these IRBs were not detected in the un-inoculated column. According to (Liu et al., 2001), microbial goethite reduction has a first-order kinetic dependence on surface site availability which was also the function of Fe(II) adsorption and secondary precipitation. Correspondingly, we observed that at the beginning of the post-inoculation period (days 15 to 46), less $[FeII]_D$ was detected from the goethite column than from the ferrihydrite column, because of the lower solubility of goethite relative to ferrihydrite resulting in lower $[FeIII]_D$ and bacterially-generated $[FeII]_D$ concentrations (Hansel et al., 2003b; Hansel et al., 2004; Zhang et al., 2020). Here, the previous batch experiments performed with the same materials (Chapter III) showed the same tendency, with higher dissolution of ferrihydrite compared to goethite. In our column systems, we observed that the total cumulated Fe released in the outlet was of the

same range for the ferrihydrite and goethite (nearly 3%). However, analyses of the final solid (SEM-EDS and Mössbauer) suggested precipitation of the dissolved Fe(II) in the ferrihydrite but not in the goethite column. This hypothesis is supported by the presence of 29.6% Fe(II) detected by Mössbauer spectrometer in the ferrihydrite column, showing a higher proportion of immobilized Fe(II) than in the goethite system. The precipitation of Fe(II) with carbonate, sulphide or phosphate in the ferrihydrite column can by hypothesized. As a fact, a higher bio-availability of electron acceptor Fe(III) in the ferrihydrite column could lead to higher mineralization of organic substrates and production of inorganic carbon available to precipitate with Fe(II) as carbonate.

### IV 5.2 Impact of iron reduction on behavior and mobilities of TEs

*Behavior and mobility of As*

During the entire experiment, $[AsT]_D$ release was measured at the column outlets and did not follow the trend of dissolved Fe concentration, appearing unrelated to bacterial iron reduction. Indeed, in Fig. IV-5 (lower panel) we saw that very little $[AsT]_D$ was detected at the outlet before day 39. In previous experiments with inoculated column systems, while ferrihydrite was dissolved and reduced, spiked As was released from ferrihydrite from the bottom and migrated towards the top, re-adsorbing itself on the remaining Fe (oxyhydr)oxides (Burton et al., 2011; Hellal et al., 2015). Thus, in the same way, As in our column was possibly mobilized and moved from the bottom to the top, progressively saturating the adsorption sites. When these adsorption sites were saturated at the top of the column, $[AsT]_D$ increased steadily until the end of the experiment. Conversely, two peaks of $[AsT]_D$ from the un-inoculated column may be attributed to the changes in pH induced by the introduction of substrate to the feeding liquid during the inoculation period (without IRB inoculation).

As mentioned in the previous section and the previous researches, ferrihydrite has a much higher adsorption capacity for As than goethite (Jain and Loeppert, 2000; Mamindy-Pajany et al., 2011). As a fact, As(III) adsorption on goethite is also less efficient than that of As(V) at pHs lower than 7 (Dixit and Hering, 2003; Burton et al., 2011) which were observed during the inoculation period. After the short period of acidification linked to the inoculation with high substrates concentration, bacterial metabolic activities resulted in an increase of pH gradually from 6.2-8.5 in days 18 to 22, whereas this was not observed in the un-inoculated column.

As was less mobile in the goethite experimental system than ferrihydrite, probably because the dissolution of adsorption sites was less pronounced than in the ferrihydrite columns. Thus, both As(III) and As(V) were more retained in the goethite than in the ferrihydite system. However our results showed that the proportion of As(V) was still higher in the outlet of the un-inoculated column than in the outlet of the inoculated column, suggesting that As(V) reduction occurred in the inoculated columns. At pH higher than 7, As(III) is more retained than As(V) on ferrihydrite and goethite (Dixit and Hering, 2003). This could explain why more As was present in the outlet of the goethite un-inoculated column than in the outlet of the corresponding inoculated column, in which As was mainly in the form of As(III).

*Behavior and mobility of Cr*

During the whole experiment, the release of Cr from the un-inoculated columns was always higher than in the inoculated columns. One peak of $[CrT]_D$ from both columns could be attributed to substrate added during the inoculation period. Then, very little $[CrT]_D$ (<0.02 mg/L) was detected after day 22 in inoculated columns until the end of the experiment. Hansel et al., (2003a) investigated the fate of Cr following a coupled inoculated–un-inoculated reduction pathway of chromate under iron-reducing conditions. They found that dissimilatory bacterial reduction of two-line ferrihydrite could indirectly stimulate Cr(VI) reduction into an insoluble mixed Fe(III)-Cr(III) hydroxide. The reduced form of Cr, Cr(III) is less mobile than Cr(VI), and bacterial reducing activities could contribute to maintain Cr in the less mobile form. Moreover, biofilm could retain the Cr(III) precipitates.

Cr(III), the form used in this experiment, presents a typical cationic sorption behavior and its adsorption by minerals, e.g. goethite, steadily increased with pH (Arnfalk et al., 1996; Richard and Bourg, 1991). This could explain why very little Cr was released during the incubation except from day 15 to 22 (inoculation step with decreased pH as mentioned in the last section). Higher values of Cr were detected from the un-inoculated column than the inoculated one suggesting that metabolic activities of the bacteria restrained pH from decreasing and consequently Cr from desorbing.

*Behavior and mobility of Cd*

During the entire experiment, very little $[CdT]_D$ from inoculated columns was measured at the columns outlet. In the post-inoculation period, the second releasing peak of Cd from the un-inoculated column might correspond to a decrease in Eh of 49.5mV to -101mV from day 32 to 37 in the pH value of 6.5-8 which suggested Cd was more unstable according to the stability in Cd system (Hermann and Neumann-Mahlkau, 1985).

According to Granados-Correa et al., (2011), the adsorption capacity of Cd(II) by goethite is gradually increased with pH from 2 to 7 and then achieves an adsorption equilibrium at pH 7 to 9. The release of Cd presented the same trend as Cr, and could be explained for the same reasons. However, Collins et al., (1999), suggested that the presence of sulfate and phosphate could enhance the adsorption of Cd on goethite by electrostatic interactions, moreover the formation of cadmium oxalate and cadmium citrate precipitates could occur in presence of citrate and oxalate. In this study, sulfate and phosphate were used in trace elements solution and substrate medium as described for the ferrifydrite column. A black precipitate was also observed in the goethite column which suggested $H_2S$ production might have happened here as discussed previously.

In our systems, if Cd was desorbed from the iron oxides, in the inoculated column, there are several hypothesis as to its fate. It would either have been re-absorbed or precipitated with the produced Fe(II) as iron organic compounds (Du et al., 2018), or precipitated as CdS if $H_2S$ production occurred (Vink et al., 2010). Finally, leached Cd could also be immobilized in biofilms (GuibaSud et al., 2006).

### IV-5.3 Distribution of global bacterial biomass and two targeted IRB (*Shewanella* and *Geobacter* 16S genes*)* in the columns

This work showed the impact(s) of bacterial iron reduction in column bioreactors on the mobility of TEs (As, Cr and Cd). A molecular approach was used to measure bacterial abundance and distribution in the columns at the end of the experiment. Molecular biomass (total genomic DNA) and abundance of the gene encoding 16S rRNA decreased from bottom to top of both inoculated columns. This result can easily be explained by the experimental design as the substrates were fed at the bottom of the column, inducing higher growth of bacterial biofilm near the substrate entrance. Furthermore, a focus was made on two well studied IRB genera, *Shewanella* and *Geobacter*, as IRB memebers of the mixed community

potentially including both IRB and fermentative bacteria that could contribute directly or indirectly to Fe(III) reduction. At the end of the experiment, the *Shewanella*/bacterial 16S ratios were 118 and 31 times higher than the *Geobacter*/bacterial 16S ratio in ferrihydrite and goethite column respectively. This result is in accordance with those of previous experiments in slurry that suggested higher association of *Geobacter* genus with goethite, and increase of *Shewanella* 16S relative abundance when Fe(III) is more bio-available. Ferrihydrite is widely considered as a more bioavailable source of Fe(III) than goethite, which might explain the abundance of *Shewanella* (Lentini et al., 2012). In the goethite column, we observed here that the *Geobacter*/bacterial 16S ratio was higher in the community associated with the solid phases than in the community suspended in liquid phase. This last result might suggest attachment of bacteria belonging to the *Geobacter* genus on goethite, as previously observed with ferrihydrite fixed on slides. However, this phenomenon was not clear in the ferrihydrite column. This might be linked to the fact that solid/liqid ratio was strongly higher in columns than in the slide experiment.

## IV-6 Conclusions and perspective

Iron (oxyhydr)oxides adsorbing MTEs obtained from adsorption tests submitted to regular variations of concentrations were able to carry 3-32 mg of As, 2-4.5 mg of Cr and 1.5-3 mg Cd by per gram of ferrihydrite, goethite, hematite or lepidocrocite. Two column experiments were performed with synthetic ferrihydrite and goethite respectively, spiked with As, Cr and Cd through a preliminary adsorption step. The experimental program included three successive phases: stabilization with synthetic water, inoculation with a complex IRB community potentially including both DIRB and fermentative IRB, feeding with mixtures of synthetic water and organic substrates (glucose, acetate, formate, lactate and peptone) under anaerobic condition. The evolution of total dissolved concentrations in Fe, As, Cd and Cr, and the values of redox potential and pH were monitored in the column's outlets.

Concerning the behavior of TEs, the results differed according to the considered pollutants. With ferrihydrite, release of As linked to biological reactions was observed only after 40 days of experiment. In contrast, the effect of inoculation of the release of As from the goethite column was only observed during the first 10 days of inoculation with organic substrates and were equivalent in the outlet of inoculated and un-inoculated columns. Cr was less mobile in inoculated than in un-inoculated conditions, for both Fe oxides, and less mobile with ferrihydrite than with goethite. Thus, Fe reducing biological activity did not induce Cr release

in our experiment. Bacterial activities did not induce a strong release of Cd from the ferrihydrite column, and with goethite, Cd was always more mobile in un-inoculated conditions than in presence of bacteria. Both total DNA and 16S genes were more abundant in the ferrihydrite than in the goethite column, and decreased from the bottom to the top of the columns, suggesting biofilm development libked to the up-flow feeding with organic substrates. As observed previously in batch and slide experiments, the proportion of *Shewanella* 16S gene copies in the bacterial communities 16S gene copies was still higher than that of *Geobacter* 16S gene copies in in the bacterial communities 16S gene copies. SEM-EDS observations suggested the formation of secondary minerals containing P and Fe in the ferrihydrite inoculated column but not in presence of goethite. Mössbauer spectroscopy analyses confirmed the presence of Fe(II)-containing minerals in the inoculated ferrihydrite column, in higher quantities in the bottom level than in the top. In contrast, Fe(II)-minerals were not detected in the goethite column.

Collectively, our results suggest that interactions between IRB and Fe (oxihydr)oxides could influence differently the motilities of different MTEs associated with Fe oxides. In particular, As is more likely to be mobilized in reducing conditions than a divalent metal such as $Cd^{2+}$, or Cr in the CrIII form. As a fact, immobilizing bio-mechanisms seems to counteract the dissolution of the primary sink of Cd and Cr, whereas for As, mobilization mechanisms are preponderant. The experiment also suggested that the type of Fe(III) used as electron acceptor could influence the final distribution and abundance of *Geobacter* and *Shewanella* 16S gene copies among a mixed IRB consortium potentially including both DIRB and fermentative bacteria. A better knowledge of the influence of biological parameters, diversity and activity, associated with iron reduction involving complex bacterial communities will help to elucidate Fe dynamics and the behaviour of different types of associated PTTE in surface environments.

## *Supplementary material*

### Supplementary table

***Table IV-S1**: Adsorption capacity of As, Cr and Cd on iron (oxyhydr)oxides*

| TEs / Fe (oxyhydr)oxides | Ferrihydrite ($(Fe^{3+})_2O_3$•$0.5H_2O$) | Goethite (α-FeO(OH)) | Hematite ($Fe_2O_3$, α-$Fe_2O_3$) | Lepidocrocite (γ-FeO(OH)) |
|---|---|---|---|---|
| As | 1) As(V): Q=130-52 mg $g^{-1}$ As(III): Q=221-208 mg $g^{-1}$ pH=7 -8 (Jain and Loeppert, 2000) 2) As(III): Q=113.64 mg $g^{-1}$ pH=5.5 (Peng et al., 2018) | 1) As(V) : Q= 9.29-7.965 mg $g^{-1}$ pH=7.0-8.5 (Antelo et al., 2005) 2) As(V) : Q=13.5-11.25 mg $g^{-1}$ As(III) : Q=18.75- 19.5 mg $g^{-1}$ pH=7.0-8.0 (Grafe et al., 2001) 3) As(V): 1.228 mg $g^{-1}$ pH= 6 (Mamindy-Pajany et al., 2011) | 1) As(V): Q=0.41 mg $g^{-1}$ pH= 6 (Mamindy-Pajany et al., 2011) | 1) As(V): Q=0.45 mg $g^{-1}$ As(III): Q=0.33 mg $g^{-1}$ pH=5.5-6.5 (Farquhar et al., 2002) |
| Cr | --- | 1) Cr(VI): 1.955 mg $g^{-1}$ pH=8 (Ajouyed et al., 2010) 2) Cr(VI) : 1.482-0.988 mg $g^{-1}$ pH=7-8 (Xie et al., 2015) | 1) Cr(VI): Q=2.299 mg $g^{-1}$ pH=8 (Ajouyed et al., 2010) | --- |
| Cd | 1) Cd(T): Q=0.0921-10.4 mg $g^{-1}$ pH = 7.58-7.68 (Swedlund et al., 2003) | 1) Cd(II) Q=3.234-4.321 mg $g^{-1}$ pH=7-8 (Boily et al., 2005; Swedlund et al., 2009) 2) Q=1.14-2.28 mg $g^{-1}$ pH=7.7-7.6 (Parkman et al., 1999) | 1) Cd(II) Q= 195.69 µg $g^{-1}$ pH= 6 (Li et al., 2006) 2) Q=0.27 mg $g^{-1}$ pH=7-9 (Granados-Correa et al., 2011) | 1) Q=0.134-0.538 mg $g^{-1}$ pH=7.8-7.42 (Parkman et al., 1999) |

# Chapter VI: Conclusions and perspectives

Mobility of contaminants in the environment, and particularly that of potentially toxic trace elements (PTTE), such as As, Cr and Cd induce risks of contamination of hydrosystems, terrestrial ecosystems and food chain. To understand and predict PTTE's reactivity and mobility in the environment will help to develop and apply appropriate strategies for remediation of polluted sites. In general, the fate and mobility of PTTEs like As, Cr, Cd in soil or aquifers are closely related to physico-chemical control factors, such as Eh and pH, but also to microbial activities by either direct or indirect biogeochemical pathways. In the meantime, PTTEs are often associated with various Fe minerals in soils and sediments. Fe reducing bacteria (IRB) are strongly involved in Fe cycling in surface environments that is increasingly attracting the attention of scientific and industrial communities.

The objectives of the present study were:

(1) to determine the influence of the type of Fe(III)-oxides on the efficiency of Fe release and formation of secondary minerals in presence of mixed Fe-reducing bacterial (IRB) communities, enriched in conditions favoring a large diversity of potential Fe(III) reducing bacteria including DIRB and fermentative bacteria, potentially contributing directly or indirectly to Fe(III) reduction;

(2) to observe how the type of Fe oxide influences the structure of these mixed communities, with a focus on the proportion in these communities of two well- known specific IRB genera: *Shewanella* and *Geobacter*, used as indicator parameters,

(3) to develop experimental strategies to investigate Fe cycling together with IRB activity and to evaluate the effect of these transformations on the speciation and mobility of three potentially toxic trace metal elements (PTTE) frequently associated with iron: As, Cr, Cd.

Scientific questions were defined based on these global objectives and the work performed during the thesis contributed to give answers to these questions.

The first scientific question associated with these objectives was related to the **influence of the type of Fe(III) mineral on the efficiency of Fe release in presence of mixed bacterial communities.**

The research performed during the present PhD included slurry incubations performed with fresh Fe (oxyhydr)oxides (synthetic ferrihydrite and lepidocrocite), goethite and hematite and tests of continuous percolation in columns performed with ferrihydrite and goethite. These experiments, involving mixed IRB consortia, confirmed that the type of Fe mineral could influence Fe solubilisation rates. When bacteria were grown on Fe (oxyhydr)oxides, Fe solubilisation rates decreased as follows: fresh Fe (oxyhydr)oxides > goethite > hematite. These results were in accordance with those of previous studies implemented with pure IRB strains only. Poorly crystallized lepidocrocite and amorphous ferrihydrite have higher specific surface areas that could favor higher rates of Fe solubilisation. Newly formed secondary Fe minerals were observed from synthetic ferrihydrite after the incubation in slurry and also in column experiment thanks to SEM-EDS and Mössbauer characterizations that indicated the presence of Fe(II) phases. The existence of these Fe(II) phases linked to interactions of microbes and Fe (oxyhydr)oxides suggested that Fe(III) reduction did not only result into production of Fe(II) in liquid phase but also generated secondary minerals.

In order to complete these results, further experiments should be performed in conditions of liquid medium composition that would change the composition of the microbial community. As a fact, diverse IRB genera use different organic substrates. During this PhD work, we used only concentrated substrates in mixture. Testing the effect of specific electron donor in less concentrated conditions on Fe (oxyhydr)oxides incubation would provide more knowledge on Fe release in conditions closer to those of in-situ biogeocycles.

A second scientific question was related to **how the type of Fe mineral influences the structure of the mixed communities and the proportion in these communities of two well-known specific Fe reducing bacterial genera, i.e. *Shewanella* and *Geobacter***.

Microbial enrichments containing IRB, prepared with a mixture of complex electron donors, were able to grow and reduce Fe(III) in a short time. They were obtained in conditions designed to maximize the growth of a large diversity of IRB, including DIRB and fermentative bacteria contributing directly or indirectly to Fe(III)-reduction.

Thus, all our results in terms of biogeochemistry resulted from the activity of a compex set of micro-organisms, possibly contributing directly and/or indirectly to iron reduction, and if we acquired interesting information about two IRB genera present in our mixed communit, i.e., *Shewanella* and *Geobacter*, the amplitude of their contribution to the overall biogeochemical reactions was not determined.

The slurry experiment showed that: (1) the sub-culturing of IRB enrichments from Fe(III)-NTA to pure Fe oxides significantly modified the bacterial communities; (2) in our experimental conditions, bacterial diversity was not significantly different from one type of pure (oxyhydr)oxide to another; (3) the type of Fe oxide could influence the proportion of *Geobacter* and *Shewanella*. Meanwhile, the nature of Fe (oxyhydr)oxides seems to have exerted a selection on the ratio of *Geobacter* 16S gene copies/ total 16S gene copies and *Shewanella* / total 16S gene copies, whereas it did not impact the bacterial community fingerprints. The concentration of bio-available Fe(III) and the mixture of electron donors in the enrichment medium might have favored the development of *Shewanella* compared with *Geobacter* genus. In presence of Fe oxides, the highest proportions of *Shewanella* 16 S gene copies / total 16S gene copies in bacterial communities were obtained with Fe oxides produced with the protocol of lepidocrocite synthesis and corresponded to the highest levels of Fe solubilisation. This result is consistent with the hypothesis that *Shewanella* development might be favored by a high bioavailability of Fe(III). In contrast, *Geobacter* 16S gene copies / total 16S gene copies was higher with goethite that is less easily dissolved. *Geobacter* seemed to be more present with Fe mineral presenting lower solubility, possibly because this genus presents a higher affinity for Fe(III). Even if *Shewanella* and Geobacter genera were far to the the only members of our complex mixed community, this result confirmed that the type of Fe(III) mineral can influence the proportion of individual IRBs in complex communites.

Globally, all results also suggested that the composition of the culture medium, in terms of organic substrates, including fermentable ones (glucose and peptone) strongly favored *Shewanella* compared with *Geobacter*. This could be linked to the fact that *Shewanella* species were reported to be able to grow by fermentation.

As mentioned before, the culture medium included a large amount of electron donors that is not representative of most natural systems. Therefore, complementary studies, performed with lower concentrations of electron donors provided in continuous feeding conditions could help to make the link with real environments, while observing both the evolution of some targeted IRB such as *Shewanella* and *Geobacter*, and that of the whole bacterial communities by DNA sequencing. As a fact, better knowledge of biological parameters, such as the research and identification of other IRB in bacterial community by sequencing would help to access the contribution of microbial Fe reduction in our experimental conditions.

A third scientific question was related to **the influence of the growth mode, i.e. planktonic or biofilm, on the proportion *Shewanella* and *Geobacter***.

The experiment performed using ferrihydrite fixed with resin onto glass slides enabled biofilm development on Fe oxides and formation of secondary minerals. In particular, we found different 16S gene copies relative abundances of two well characterized IRB genera, i.e., *Shewanella* and *Geobacter,* in the biofilm and surrounding liquid medium. Indeed, *Geobacter*, a genus that requires direct contact with solids to use Fe(III) as an electron acceptor was significantly more abundant in the biofilm than in the liquid medium, whereas *Shewanella*, a genus that can either use Fe(III) respiration or fermentation to thrive was found equally distributed between the two phases. However, in order to be closer to natural systems, less concentrated electron donors should be tested.

In future projects, the method to prepare glass slides could be applied in order to study the influence of the type of Fe(III) mineral on the composition of natural biofilms, with the possibility to immobilize a larger range of different oxides. Beyond laboratory studies, slides could be placed on site, inserted in soils or aquatic sediments, in order to acquire a better knowledge of the contribution and distribution of IRB communities attached to Fe oxides surfaces. This approach could help to further elucidate Fe redox dynamics in surface environments.

As biofilms in natural soils and sediments contain a large part of the bacterial biomass, it would be interesting to apply complementary microscopic techniques adapted to biofilms characterisation, such as Fluorescent Microscopy, Scanning Transmission Electron Microscopy (STEM)-in-Scanning Electron Microscopy (SEM) and fluorescence in situ hybridization (FISH) to detect and locate specific groups of bacteria at the surface of fixed Fe minerals.

The last scientific question was related **to the influence of the development of complex iron-reducing bacterial communities on the behavior of the targeted trace elements, As, Cr and Cd, associated to Fe (oxyhydr)oxides.**

Fe (oxyhydr)oxides spiked PTTEs, i.e., As, Cr, Cd were obtained from adsorption experiment. Biotic and abiotic column experiments were performed with synthetic ferrihydrite and goethite respectively, spiked with As, Cr and Cd through a preliminary adsorption step. Concerning the behavior of PTTEs, the results differed according to the considered pollutants.

With ferrihydrite, release of As linked to biological reactions was observed only at the last period of the experiment (after 40 days of inoculation). In contrast, the effect of inoculation on the release of As from the goethite column was only observed during the first 10 days of feeding with organic substrates. Cr was less mobile in biotic than in abiotic conditions, for both Fe oxides, and less mobile with ferrihydrite than with goethite. Thus, Fe reducing biological activity did not induce Cr release in our experiment. Bacterial activities did not induce a strong release of Cd from the ferrihydrite column, and with goethite, Cd was always more mobile in non-inoculated conditions than in presence of bacteria. Simple correlations between trace elements "As", "Cr" and "Cd" and "Fe" based on analysis of final solids and SEM-EDS analysis indicated a positive correlation, equivalent or more pronounced after incubation for the systems Fe-As and Fe-Cd, but not for the system Fe-Cd. Mössbauer spectra suggested more abundant Fe(II) minerals generated in the bottom than in the top of the ferrihydrite column. In contrast Fe(II)-minerals were not detected in the goethite column. SEM-EDS observations showed the morphology of new formed secondary minerals and indicated a higher proportion of P and O in the secondary minerals than initial in Fe (oxyhrdr)oxides in the ferrihydrite column.

Collectively, our results suggested that interactions between IRB and Fe (oxihydr)oxides could influence differently the mobility of different PTTEs associated with Fe oxides. In particular, As is more likely to be mobilized in reducing conditions than a divalent metal such as Cd, or a metal presenting trivalent form surch as Cr(III), and this phenomenon could be linked to biological processes, such as Fe(III) reduction-related phenomena, biosorption or indirect effect of pH. As a fact, immobilizing bio-mechanisms seems to counteract the dissolution of the primary sink of Cd and Cr, whereas for As, mobilization mechanisms are preponderant. The experiment also suggested that the type of Fe(III) used as electron acceptor influenced the final spatial distribution and abundance of micro-organisms affiliated to *Geobacter* and *Shewanella* genera among other iron-reducing members of the mixed IRB community.

To understand the speciation and mobility of PTTEs in relation to Fe redox cycling, complementary studies should focus on a key question: how PTTEs are associated with remaining Fe oxides and secondary minerals during the microbial Fe reduction. Thus, in the point view of mineralogy, mineral characterization technologies should be used for acquiring knowledge on the evolution of mineral features（morphology, crystal structure, chemical components et al.）, such as Transmission Electron Microscope (TEM) for inside structure of

minerals, and Extended X-ray Absorption Fine Structure (EXAFS) to access the speciation and type of adsorption of PTTEs on Fe minerals.

Sequencing all 16S genes would be required for obtaining larger information on the global microbial community, which would complete the present study of the evolution of proportions of two IRB genera, i.e., *Shewanella* and *Geobacter* in mixed consortia. Once again, as low electron donors concentrations are generally present in natural ecosystems, it would be helpful to evaluate the role of the type and concentration of electron donors on the kinetics of PTTE release during Fe(III) transformations in reducing conditions, in presence of mixed IRB consortia.

**General perspectives:**

The original observations and results presented in this manuscript are related with general physico-chemical transformations of Fe (oxyhydr)oxides and global mobility of three PTTEs during microbial Fe(III) reduction in laboratory conditions, with complex mixed microbial IRB enrichments. However, complementary studies could provide more specific answers on the role of microbial Fe(III) reduction in natural systems, investigate new on-site technologies for sediment monitoring and pollutants remediation, and molecular technologies for targeting IRB communities.

For instance, numerous data acquired during the present PhD laboratory work could be used to model the processes associated with Fe(III)-reduction. Therefore, these results will be potentially useful to acquire further knowledge about interactions between PTTEs cycles and Fe cycle based on bacterial activity, through simulation of reactive solute/precipitation transport by modelling using PhreeqC, among other methods. Moreover, it has long been shown that some microbial communities, such as IRB and SRB, play an essential role in the mobility and speciation of PTTEs contaminants linked to Fe minerals in soils and sediments. A better knowledge of microbial activity on polluted sites would also make it possible to assess the evolution of environmental quality at medium and long term, based on the data acquired from laboratory work and modelling simulation. This could help to understand the biogeochemical cycles of PTTEs associated with the microbial Fe reduction in polluted sites, through identified mechanisms, in complement to methodological development of slides covered with immobilized Fe(III) oxides which could be transported on site and inserted in soils and/or sediments.

The molecular work using specific primers to target two genus of IRB was shown suitable and efficient for studying and monitoring the abundance of *Shewanella* and *Geobacter* 16S gene copies in Fe(III)-reducing systems. Other molecular technologies could be applied according to the DNA fragment targeted by these primers, such as detection of IRB genus from rRNA, which means differentiate the active component (rRNA derived) from the total bacterial diversity (ribosomal derived rDNA). Thus, better understanding of active microbial community structure and functionality could help to evaluate and monitor biogeochemical processes in the environment.

This thesis provided some results related with the interactions between microbial activities and synthetic Fe (oxyhydr)oxides, pure or mixed with sands, instead of real site samples, and represents a basis for further researches on real PTTEs polluted environments that will help to understand natural systems and develop efficient monitoring or remediation strategies.

## References

**A**

Adhikari D, Zhao Q, Das K, Mejia J, Huang R, Wang X, et al. Dynamics of ferrihydrite-bound organic carbon during microbial Fe reduction. Geochimica et Cosmochimica Acta 2017; 212: 221-233.

Afonso MDS, Morando PJ, Blesa MA, Banwart S, Stumm W. The reductive dissolution of iron oxides by ascorbate: The role of carboxylate anions in accelerating reductive dissolution. Journal of Colloid and Interface Science 1990; 138: 74-82.

Ahmed E, Holmström SJ. Microbe–mineral interactions: the impact of surface attachment on mineral weathering and element selectivity by microorganisms. Chemical Geology 2015; 403: 13-23.

Aino K, Hirota K, Okamoto T, Tu Z, Matsuyama H, Yumoto I. Microbial communities associated with indigo fermentation that thrive in anaerobic alkaline environments. Frontiers in microbiology 2018; 9: 2196.

Ajouyed O, Hurel C, Ammari M, Allal LB, Marmier N. Sorption of Cr (VI) onto natural iron and aluminum (oxy) hydroxides: effects of pH, ionic strength and initial concentration. Journal of Hazardous Materials 2010; 174: 616-622.

Amos BK, Sung Y, Fletcher KE, Gentry TJ, Wu W-M, Criddle CS, et al. Detection and quantification of *Geobacter lovleyi* strain SZ: implications for bioremediation at tetrachloroethene-and uranium-impacted sites. Applied and environmental microbiology 2007; 73: 6898-6904.

Amthauer G, Rossman GR. Mixed valence of iron in minerals with cation clusters. Physics and Chemistry of Minerals 1984; 11: 37-51.

Antelo J, Avena M, Fiol S, López R, Arce F. Effects of pH and ionic strength on the adsorption of phosphate and arsenate at the goethite–water interface. Journal of colloid and interface science 2005; 285: 476-486.

Archer D, Johnson K. A model of the iron cycle in the ocean. Global Biogeochemical Cycles 2000; 14: 269-279.

Arnfalk P, Wasay S, Tokunaga S. A comparative study of Cd, Cr (III), Cr (VI), Hg, and Pb uptake by minerals and soil materials. Water, Air, and Soil Pollution 1996; 87: 131-148.

**B**

Bachate SP, Khapare RM, Kodam KM. Oxidation of arsenite by two β-proteobacteria isolated from soil. Applied Microbiology and Biotechnology 2012; 93: 2135-2145.

Bard A. Standard potentials in aqueous solution: Routledge, 2017.

Battaglia-Brunet F, Itard Y, Garrido F, Delorme F, Crouzet C, Greffié C, et al. A simple biogeochemical process removing arsenic from a mine drainage water. Geomicrobiology Journal 2006; 23: 201-211.

Becking LB, Kaplan IR, Moore D. Limits of the natural environment in terms of pH and oxidation-reduction potentials. The Journal of Geology 1960; 68: 243-284.

Beesley L, Moreno-Jimenez E, Clemente R, Lepp N, Dickinson N. Mobility of arsenic, cadmium and zinc in a multi-element contaminated soil profile assessed by in-situ soil pore water sampling, column leaching and sequential extraction. Environmental Pollution 2010; 158: 155-160.

Behrends T, Van Cappellen P. Transformation of hematite into magnetite during dissimilatory iron reduction—conditions and mechanisms. Geomicrobiology Journal 2007; 24: 403-416.

Bekker A, Slack JF, Planavsky N, Krapez B, Hofmann A, Konhauser KO, et al. Iron formation: the sedimentary product of a complex interplay among mantle, tectonic, oceanic, and biospheric processes. Economic Geology 2010; 105: 467-508.

Biffinger JC, Pietron J, Ray R, Little B, Ringeisen BR. A biofilm enhanced miniature microbial fuel cell using *Shewanella oneidensis* DSP10 and oxygen reduction cathodes. Biosensors and Bioelectronics 2007; 22: 1672-1679.

Boily J-F, Sjöberg S, Persson P. Structures and stabilities of Cd (II) and Cd (II)-phthalate complexes at the goethite/water interface. Geochimica et cosmochimica acta 2005; 69: 3219-3235.

Bond DR, Strycharz-Glaven SM, Tender LM, Torres CI. On electron transport through Geobacter biofilms. ChemSusChem 2012; 5: 1099-1105.

Bonneville S. Kinetics of microbial Fe (III) oxyhydroxidereduction: The role of mineral properties. Utrecht University, 2005.

Bonneville S, Van Cappellen P, Behrends T. Microbial reduction of iron (III) oxyhydroxides: effects of mineral solubility and availability. Chemical Geology 2004; 212: 255-268.

Bosch J, Heister K, Hofmann T, Meckenstock RU. Nanosized iron oxide colloids strongly enhance microbial iron reduction. Appl. Environ. Microbiol. 2010; 76: 184-189.

Bosch J, Lee K-Y, Hong S-F, Harnisch F, Schröder U, Meckenstock RU. Metabolic efficiency of *Geobacter sulfurreducens* growing on anodes with different redox potentials. Current microbiology 2014; 68: 763-768.

Bose S, Hochella Jr MF, Gorby YA, Kennedy DW, McCready DE, Madden AS, et al. Bioreduction of hematite nanoparticles by the dissimilatory iron reducing bacterium *Shewanella oneidensis* MR-1. Geochimica et Cosmochimica Acta 2009; 73: 962-976.

Bousserrhine N., Gasser UG, Jeanroy E, Berthelin J. Bacterial and Chemical Reductive Dissolution of Mn-, Co-, Cr-, and Al-Substituted Goethites, Geomicrobiology Journal 1999, 16:3, 245-258,

Bowell R. Sorption of arsenic by iron oxides and oxyhydroxides in soils. Applied geochemistry 1994; 9: 279-286.

Bowman JP, McCammon SA, Nichols DS, Skerratt JH, Rea SM, Nichols PD, McMeekin TA. *Shewanella gelidimarina* sp. nov. and *Shewanella frigidimarina* sp. nov., novel Antarctic species with the ability to produce eicosapentaenoic acid (20:5w3) and grow anaerobically by dissimilatory Fe(III) reduction. Int J Syst Bacteriol. 1997;47:1040–7

Brock TD, Brock KM, Belly RT, Weiss RL. Sulfolobus: a new genus of sulfur-oxidizing bacteria living at low pH and high temperature. Archiv für Mikrobiologie 1972; 84: 54-68.

Brunauer S, Emmett PH, Teller E. Adsorption of gases in multimolecular layers. Journal of the American chemical society 1938; 60: 309-319.

Burgess S, Statham P, Holland J, Chou Y. Standardless quantitative analysis using a drift detector, what accuracy is possible from live and reconstructed data? Microscopy and Microanalysis 2007; 13: 1432.

Burns JL, DiChristina TJ. Anaerobic respiration of elemental sulfur and thiosulfate by Shewanella oneidensis MR-1 requires psrA, a homolog of the phsA gene of *Salmonella enterica* serovar typhimurium LT2. Applied and environmental microbiology 2009; 75: 5209-5217.

Burton ED, Johnston SG, Bush RT. Microbial sulfidogenesis in ferrihydrite-rich environments: Effects on iron mineralogy and arsenic mobility. Geochimica et Cosmochimica Acta 2011; 75: 3072-3087.

Burton ED, Johnston SG, Planer-Friedrich B. Coupling of arsenic mobility to sulfur transformations during microbial sulfate reduction in the presence and absence of humic acid. Chemical Geology 2013; 343: 12-24.

Byrne JM, Klueglein N, Pearce C, Rosso KM, Appel E, Kappler A. Redox cycling of Fe (II) and Fe (III) in magnetite by Fe-metabolizing bacteria. Science 2015; 347: 1473-1476.

**C**

Caccavo F, Lonergan DJ, Lovley DR, Davis M, Stolz JF, McInerney MJ. *Geobacter sulfurreducens* sp. nov., a hydrogen-and acetate-oxidizing dissimilatory metal-reducing microorganism. Applied and environmental microbiology 1994; 60: 3752-3759.

Cai Y, Hu K, Zheng Z, Zhang Y, Guo S, Zhao X, et al. Effects of adding EDTA and $Fe^{2+}$ on the performance of reactor and microbial community structure in two simulated phases of anaerobic digestion. Bioresource technology 2019; 275: 183-191.

Calmano W, Hong J, Förstner U. Binding and mobilization of heavy metals in contaminated sediments affected by pH and redox potential. Water science and technology 1993; 28: 223-235.

Cao M, Qin K, Li G, Evans NJ, Hollings P, Maisch M, et al. Mineralogical evidence for crystallization conditions and petrogenesis of ilmenite-series I-type granitoids at the Baogutu reduced porphyry Cu deposit (Western Junggar, NW China): Mössbauer spectroscopy, EPM and LA-(MC)-ICPMS analyses. Ore Geology Reviews 2017; 86: 382-403.

Cavelan A, Boussafir M, Le Milbeau C, Rozenbaum O, Laggoun-Défarge F. Effect of organic matter composition on source rock porosity during confined anhydrous thermal maturation: Example of Kimmeridge-clay mudstones. International Journal of Coal Geology 2019; 212: 103236.

Chester R, Hughes M. A chemical technique for the separation of ferro-manganese minerals, carbonate minerals and adsorbed trace elements from pelagic sediments. Chemical geology 1967; 2: 249-262.

Childers SE, Ciufo S, Lovley DR. *Geobacter metallireducens* accesses insoluble Fe (III) oxide by chemotaxis. Nature 2002; 416: 767-769.

Cristiani P, Franzetti A, Bestetti G. Monitoring of electro-active biofilm in soil. Electrochimica Acta 2008; 54: 41-46.

Chuan M, Shu G, Liu J. Solubility of heavy metals in a contaminated soil: effects of redox potential and pH. Water, Air, and Soil Pollution 1996; 90: 543-556.

Coates JD, Ellis DJ, Gaw CV, Lovley DR. *Geothrix fermentans* gen. nov., sp. nov., a novel Fe (III)-reducing bacterium from a hydrocarbon-contaminated aquifer. International journal of systematic and evolutionary microbiology 1999; 49: 1615-1622.

Coates JD, Phillips E, Lonergan DJ, Jenter H, Lovley DR. Isolation of *Geobacter* species from diverse sedimentary environments. Applied and Environmental Microbiology 1996; 62: 1531-1536.

Collins CR, Ragnarsdottir KV, Sherman DM. Effect of inorganic and organic ligands on the mechanism of cadmium sorption to goethite. Geochimica et Cosmochimica Acta 1999; 63: 2989-3002.

Cologgi DL, Lampa-Pastirk S, Speers AM, Kelly SD, Reguera G. Extracellular reduction of uranium via *Geobacter* conductive pili as a protective cellular mechanism. Proceedings of the National Academy of Sciences 2011; 108: 15248-15252.

Colombo C, Palumbo G, He J-Z, Pinton R, Cesco S. Review on iron availability in soil: interaction of Fe minerals, plants, and microbes. Journal of soils and sediments 2014; 14: 538-548.

Cooper DC, Picardal FF, Coby AJ. Interactions between microbial iron reduction and metal geochemistry: effect of redox cycling on transition metal speciation in iron bearing sediments. Environmental science & technology 2006; 40: 1884-1891.

Cooper RE, Eusterhues K, Wegner C-E, Totsche KU, Kuesel K. Ferrihydrite-associated organic matter (OM) stimulates reduction by *Shewanella oneidensis* MR-1 and a complex microbial consortia. Biogeosciences 2017a; 14.

Cooper RE, Eusterhues K, Wegner C-E, Totsche KU, Küsel K. Ferrihydrite-associated organic matter (OM) stimulates reduction by *Shewanella oneidensis* MR-1 and a complex microbial consortia. Biogeosciences 2017b; 14: 5171.

Coppi MV, O'Neil RA, Leang C, Kaufmann F, Methe BA, Nevin KP, Woodard TL, Liu A, Lovley DR. Involvement of *Geobacter sulfurreducens* SfrAB in acetate metabolism rather than intracellular, respiration-linked Fe (III) citrate reduction. Microbiology. 2007 Oct 1;153(10):3572-85.

Cornell RM, Schwertmann U. The Iron Oxides Structure, Properties, Reactions, Occurences and Uses. Weinheim, Germany: Wiley-VCH, 2003a.

Cornell RM, Schwertmann U. The iron oxides: structure, properties, reactions, occurrences and uses: John Wiley & Sons, 2003b.

Coupland K, Johnson DB. Evidence that the potential for dissimilatory ferric iron reduction is widespread among acidophilic heterotrophic bacteria. FEMS microbiology letters 2008; 279: 30-35.

Couture R-M, Charlet L, Markelova E, Madé Bt, Parsons CT. On–off mobilization of contaminants in soils during redox oscillations. Environmental science & technology 2015; 49: 3015-3023.

Crampon M, Hellal J, Mouvet C, Wille G, Michel C, Wiener A, et al. Do natural biofilm impact nZVI mobility and interactions with porous media? A column study. Science of the Total Environment 2018; 610: 709-719.

Crosby HA, Johnson CM, Roden EE, Beard BL. Coupled Fe (II)− Fe (III) electron and atom exchange as a mechanism for Fe isotope fractionation during dissimilatory iron oxide reduction. Environmental science & technology 2005; 39: 6698-6704.

Crosby HA, Roden EE, Johnson CM, Beard BL. The mechanisms of iron isotope fractionation produced during dissimilatory Fe (III) reduction by *Shewanella putrefaciens* and Geobacter sulfurreducens. Geobiology 2007; 5: 169-189.

Cummings, D. E., Caccavo Jr, F., Spring, S., & Rosenzweig, R. F. (1999*). Ferribacterium limneticum*, gen. nov., sp. nov., an Fe (III)-reducing microorganism isolated from mining-impacted freshwater lake sediments. Archives of Microbiology, 171(3), 183-188.

Cummings DE, Caccavo F, Fendorf S, Rosenzweig RF. Arsenic mobilization by the dissimilatory Fe (III)-reducing bacterium *Shewanella alga* BrY. Environmental Science & Technology 1999; 33: 723-729.

Cummings DE, Snoeyenbos-West OL, Newby DT, Niggemyer AM, Lovley DR, Achenbach LA, et al. Diversity of Geobacteraceae species inhabiting metal-polluted freshwater lake sediments ascertained by 16S rDNA analyses. Microbial ecology 2003; 46: 257-269.

Cutting R, Coker V, Fellowes J, Lloyd J, Vaughan D. Mineralogical and morphological constraints on the reduction of Fe (III) minerals by *Geobacter sulfurreducens*. Geochimica et Cosmochimica Acta 2009; 73: 4004-4022.

Czaban J, Wróblewska B. Microbial Transformation of Cadmium in Two Soils Differing in Organic Matter Content and Texture. Polish Journal of Environmental Studies 2005; 14.

**D**

Das S, Hendry MJ, Essilfie-Dughan J. Adsorption of selenate onto ferrihydrite, goethite, and lepidocrocite under neutral pH conditions. Applied Geochemistry 2013; 28: 185-193.

Davranche M, Dia A, Fakih M, Nowack B, Gruau G, Ona-nguema G, Petitjean P, Martin S, Hochreutener R. Organic matter control on the reactivity of Fe (III)-oxyhydroxides and associated As in wetland soils: A kinetic modeling study. Chemical Geology. 2013 Jan 6;335:24-35

De Matos A, Fontes M, Da Costa L, Martinez M. Mobility of heavy metals as related to soil chemical and mineralogical characteristics of Brazilian soils. Environmental pollution 2001; 111: 429-435.

De Vet W, Dinkla I, Rietveld L, Van Loosdrecht M. Biological iron oxidation by *Gallionella* spp. in drinking water production under fully aerated conditions. Water research 2011; 45: 5389-5398.

DeAngelis KM, Silver WL, Thompson AW, Firestone MK. Microbial communities acclimate to recurring changes in soil redox potential status. Environmental Microbiology 2010; 12: 3137-3149.

Delavernhe, L., Steudel, A., Darbha, G. K., Schäfer, T., Schuhmann, R., Wöll, C., ... & Emmerich, K. (2015). Influence of mineralogical and morphological properties on the cation exchange behavior of dioctahedral smectites. Colloids and Surfaces A: Physicochemical and Engineering Aspects, 481, 591-599.

Derby H, Hammer B. Bacteriology of butter IV. bacteriological studies on surface taint butter. Research Bulletin (Iowa Agriculture and Home Economics Experiment Station) 1931; 11: 1.

Derrendinger, L., & Sposito, G. (2000). Flocculation kinetics and cluster morphology in illite/NaCl suspensions. Journal of colloid and interface science, 222(1), 1-11.

Devey, A. J., Grau-Crespo, R., & De Leeuw, N. H. (2008). Combined density functional theory and interatomic potential study of the bulk and surface structures and properties of the iron sulfide mackinawite (FeS). The Journal of Physical Chemistry C, 112(29), 10960-10967.

Dhivert E, Grosbois C, Coynel A, Lefèvre I, Desmet M. Influences of major flood sediment inputs on sedimentary and geochemical signals archived in a reservoir core (Upper Loire Basin, France). Catena 2015; 126: 75-85.

Dikow, R.B. Genome-level homology and phylogeny of Shewanella (Gammaproteobacteria: lteromonadales: Shewanellaceae). BMC Genomics 2011; 12: 237.

Dimkpa C. Microbial siderophores: Production, detection and application in agriculture and environment. Endocytobiosis & Cell Research 2016; 27.

Ding M, Shiu H-Y, Li S-L, Lee CK, Wang G, Wu H, et al. Nanoelectronic investigation reveals the electrochemical basis of electrical conductivity in *Shewanella* and *Geobacter*. ACS nano 2016; 10: 9919-9926.

Dixit S, Hering JG. Comparison of arsenic (V) and arsenic (III) sorption onto iron oxide minerals: implications for arsenic mobility. Environmental science & technology 2003; 37: 4182-4189.

Dominguez-Benetton X, Varia JC, Pozo G, Modin O, Ter Heijne A, Fransaer J, et al. Metal recovery by microbial electro-metallurgy. Progress in Materials Science 2018; 94: 435-461.

Dominik P, Pohl HN, Bousserrhine N, Berthelin J, Kaupenjohann M. Limitations to the reductive dissolution of Al-substituted goethites by Clostridium butyricum. Soil Biology and Biochemistry 2002; 34: 1147-1155.

Dong H. Mineral-microbe interactions: a review. Frontiers of Earth Science in China 2010; 4: 127-147.

Dong H, Kukkadapu RK, Fredrickson JK, Zachara JM, Kennedy DW, Kostandarithes HM. Microbial reduction of structural Fe (III) in illite and goethite. Environmental Science & Technology 2003; 37: 1268-1276.

Dos Santos Afonso M, Stumm W. Reductive dissolution of iron (III)(hydr) oxides by hydrogen sulfide. Langmuir 1992; 8: 1671-1675.

Du H, Peacock CL, Chen W, Huang Q. Binding of Cd by ferrihydrite organo-mineral composites: implications for Cd mobility and fate in natural and contaminated environments. Chemosphere 2018; 207: 404-412.

**E**

El Gheriany IA, Bocioaga D, Hay AG, Ghiorse WC, Shuler ML, Lion LW. Iron requirement for Mn (II) oxidation by *Leptothrix discophora* SS-1. Applied and Environmental Microbiology 2009; 75: 1229-1235.

Elzinga EJ, Huang J-H, Chorover J, Kretzschmar R. ATR-FTIR spectroscopy study of the influence of pH and contact time on the adhesion of *Shewanella putrefaciens* bacterial cells to the surface of hematite. Environmental science & technology 2012; 46: 12848-12855.

Emerson D, Moyer C. Isolation and characterization of novel iron-oxidizing bacteria that grow at circumneutral pH. Applied and environmental microbiology 1997; 63: 4784-4792.

Engel CEA, Schattenberg F, Dohnt K, Schröder U, Müller S, Krull R. Long-term behavior of defined mixed cultures of *Geobacter sulfurreducens* and *Shewanella oneidensis* in bioelectrochemical systems. Frontiers in Bioengineering and Biotechnology 2019; 7: 60.

Esteve-Núñez A, Rothermich M, Sharma M, Lovley D. Growth of *Geobacter sulfurreducens* under nutrient-limiting conditions in continuous culture. Environmental microbiology 2005; 7: 641-648.

Esther J, Sukla LB, Pradhan N, Panda S. Fe (III) reduction strategies of dissimilatory iron reducing bacteria. Korean Journal of Chemical Engineering 2015; 32: 1-14.

Etique M, Jorand FP, Ruby C. Magnetite as a precursor for green rust through the hydrogenotrophic activity of the iron‐reducing bacteria Shewanella putrefaciens. Geobiology. 2016 May;14(3):237-54.

**F**

Fabisch M, Beulig F, Akob DM, Küsel K. Surprising abundance of *Gallionella*-related iron oxidizers in creek sediments at pH 4.4 or at high heavy metal concentrations. Frontiers in microbiology 2013; 4: 390.

Fan L, Zhao F, Liu J, Frost RL. The As behavior of natural arsenical-containing colloidal ferric oxyhydroxide reacted with sulfate reducing bacteria. Chemical Engineering Journal 2018a; 332: 183-191.

Fan Y-Y, Li B-B, Yang Z-C, Cheng Y-Y, Liu D-F, Yu H-Q. Abundance and diversity of iron reducing only es in the sediments of a heavily polluted freshwater lake. Applied microbiology and biotechnology 2018b; 102: 10791-10801.

Farquhar ML, Charnock JM, Livens FR, Vaughan DJ. Mechanisms of arsenic uptake from aqueous solution by interaction with goethite, lepidocrocite, mackinawite, and pyrite: An X-ray absorption spectroscopy study. Environmental science & technology 2002; 36: 1757-1762.

Fein JB, Martin AM, Wightman PG. Metal adsorption onto bacterial surfaces: development of a predictive approach. Geochimica et Cosmochimica Acta 2001; 65: 4267-4273.

Fein JB, Scott S, Rivera N. The effect of Fe on Si adsorption by *Bacillus subtilis* cell walls: insights into non-metabolic bacterial precipitation of silicate minerals. Chemical Geology 2002; 182: 265-273.

Feitknecht W, Giovanoli R, Michaelis W, Müller M. Über die Hydrolyse von Eisen (III) Salzlösungen. I. Die Hydrolyse der Lösungen von Eisen (III) Chlorid. Helvetica Chimica Acta 1973; 56: 2847-2856.

Fernández-Remolar DC. Iron oxides, hydroxides and oxy-hydroxides. enas 2015: 1268-1270.

Flues M, Sato I, Scapin M, Cotrim M, Camargo I. Toxic elements mobility in coal and ashes of Figueira coal power plant, Brazil. Fuel 2013; 103: 430-436.

Fowle DA, Fein JB. Competitive adsorption of metal cations onto two gram positive bacteria: testing the chemical equilibrium model. Geochimica et Cosmochimica Acta 1999; 63: 3059-3067.

Fredrickson JK, Kota S, Kukkadapu RK, Liu C, Zachara JM. Influence of electron donor/acceptor concentrations on hydrous ferric oxide (HFO) bioreduction. Biodegradation 2003; 14: 91-103.

Fredrickson JK, Romine MF, Beliaev AS, Auchtung JM, Driscoll ME, Gardner TS, et al. Towards environmental systems biology of *Shewanella.* Nature Reviews Microbiology 2008; 6: 592-603.

Fredrickson JK, Zachara JM, Kennedy DW, Dong H, Onstott TC, Hinman NW, et al. Biogenic iron mineralization accompanying the dissimilatory reduction of hydrous ferric oxide by a groundwater bacterium. Geochimica et Cosmochimica Acta 1998; 62: 3239-3257.

Frenzel P, Bosse U, Janssen PH. Rice roots and methanogenesis in a paddy soil: ferric iron as an alternative electron acceptor in the rooted soil. Soil Biology and Biochemistry 1999; 31: 421-430.

Fuller SJ, McMillan DG, Renz MB, Schmidt M, Burke IT, Stewart DI. Extracellular electron transport-mediated Fe (III) reduction by a community of alkaliphilic bacteria that use flavins as electron shuttles. Applied and environmental microbiology 2014; 80: 128-137.

**G**

Gagen EJ, Zaugg J, Tyson GW, Southam G. Goethite Reduction by a Neutrophilic Member of the Alphaproteobacterial Genus *Telmatospirillum*. Frontiers in microbiology 2019; 10: 2938.

Gandhi S, Oh B-T, Schnoor JL, Alvarez PJ. Degradation of TCE, Cr (VI), sulfate, and nitrate mixtures by granular iron in flow-through columns under different microbial conditions. Water Research 2002; 36: 1973-1982.

Gault AG, Ibrahim A, Langley S, Renaud R, Takahashi Y, Boothman C, et al. Microbial and geochemical features suggest iron redox cycling within bacteriogenic iron oxide-rich sediments. Chemical Geology 2011; 281: 41-51.

Génin J-M, Refait P, Simon L, Drissi S. Preparation and E h--pH diagrams of Fe (II)--Fe (III) green rust compounds; hyperfine interaction characteristics and stoichiometry of hydroxy-chloride,-sulphate and-carbonate. Hyperfine interactions 1998; 111: 313-318.

Ghiorse W. Biology of iron-and manganese-depositing bacteria. Annual review of microbiology 1984; 38: 515-550.

Ghorbanzadeh N, Lakzian A, Halajnia A, Choi UK, Kim KH, Kim JO, et al. Impact of bioreduction on remobilization of adsorbed cadmium on iron minerals in anoxic condition. Water Environment Research 2017; 89: 519-526.

Ginn B, Meile C, Wilmoth J, Tang Y, Thompson A. Rapid iron reduction rates are stimulated by high-amplitude redox fluctuations in a tropical forest soil. Environmental science & technology 2017; 51: 3250-3259.

Gorby YA, Yanina S, McLean JS, Rosso KM, Moyles D, Dohnalkova A, et al. Electrically conductive bacterial nanowires produced by *Shewanella oneidensis* strain MR-1 and other microorganisms. Proceedings of the National Academy of Sciences 2006; 103: 11358-11363.

Gotoh S, Patrick Jr W. Transformation of iron in a waterlogged soil as influenced by redox potential and pH. Soil Science Society of America Journal 1974; 38: 66-71.

Gould, W. D., Stichbury, M., Francis, M., Lortie, L., & Blowes, D. W. (2003, May). An MPN method for the enumeration of iron-reducing bacteria. In Mining and the environment conference.

Gounou C, Bousserrhine N, Varrault G, Mouchel J-M. Influence of the iron-reducing bacteria on the release of heavy metals in anaerobic river sediment. Water, Air, & Soil Pollution 2010; 212: 123-139.

Grafe M, Eick M, Grossl P. Adsorption of arsenate (V) and arsenite (III) on goethite in the presence and absence of dissolved organic carbon. Soil Science Society of America Journal 2001; 65: 1680-1687.

Granados-Correa F, Corral-Capulin N, Olguín M, Acosta-León C. Comparison of the Cd (II) adsorption processes between boehmite (γ-AlOOH) and goethite (α-FeOOH). Chemical Engineering Journal 2011; 171: 1027-1034.

Greene AC, Patel BKC, Sheehy AJ. *Deferribacter thermophilus* gen. nov., sp. nov., a novel thermophilic manganese-and iron-reducing bacterium isolated from a petroleum reservoir. International Journal of Systematic and Evolutionary Microbiology 1997; 47: 505-509.

Greene AC, Patel BKC, Yacob S. *Geoalkalibacter subterraneus* sp. nov., an anaerobic Fe (III)-and Mn (IV)-reducing bacterium from a petroleum reservoir, and emended descriptions

of the family *Desulfuromonadaceae* and the genus *Geoalkalibacter*. International journal of systematic and evolutionary microbiology 2009; 59: 781-785.

Griebler C, Mindl B, Slezak D, Geiger-Kaiser M. Distribution patterns of attached and suspended bacteria in pristine and contaminated shallow aquifers studied with an in situ sediment exposure microcosm. Aquat Microb Ecol 2002; 28:117–129.

Grybos M, Davranche M, Gruau G, Petitjean P, Pédrot M. Increasing pH drives organic matter solubilization from wetland soils under reducing conditions. Geoderma. 2009 Dec 15;154(1-2):13-9.

Guibaud G, van Hullebusch E, Bordas F. Lead and cadmium biosorption by extracellular polymeric substances (EPS) extracted from activated sludges: pH-sorption edge tests and mathematical equilibrium modelling. Chemosphere 2006; 64: 1955-1962.

**H**

Halama M, Swanner ED, Konhauser KO, Kappler A. Evaluation of siderite and magnetite formation in BIFs by pressure–temperature experiments of Fe (III) minerals and microbial biomass. Earth and Planetary Science Letters. 2016 Sep 15;450:243-53.

Hamer, M., Graham, R. C., Amrhein, C., & Bozhilov, K. N. (2003). Dissolution of Ripidolite (Mg, Fe-Chlorite) in Organic and Inorganic Acid Solutions. Soil Science Society of America Journal, 67(2), 654-661.

Han R, Liu T, Li F, Li X, Chen D, Wu Y. Dependence of secondary mineral formation on Fe (II) production from ferrihydrite reduction by *Shewanella oneidensis* MR-1. ACS Earth and Space Chemistry 2018; 2: 399-409.

Hansel C, Wielinga B, Fendorf S. Structural and compositional evolution of Cr/Fe solids after indirect chromate reduction by dissimilatory iron-reducing bacteria. Geochimica et Cosmochimica Acta 2003a; 67: 401-412.

Hansel CM, Benner SG, Neiss J, Dohnalkova A, Kukkadapu RK, Fendorf S. Secondary mineralization pathways induced by dissimilatory iron reduction of ferrihydrite under advective flow. Geochimica et Cosmochimica Acta 2003b; 67: 2977-2992.

Hansel CM, Benner SG, Nico P, Fendorf S. Structural constraints of ferric (hydr)oxides on dissimilatory iron reduction and the fate of Fe(II)3 3Associate editor: J. B. Fein. Geochimica et Cosmochimica Acta 2004; 68: 3217-3229.

Harneit K, Göksel A, Kock D, Klock J-H, Gehrke T, Sand W. Adhesion to metal sulfide surfaces by cells of *Acidithiobacillus ferrooxidans*, *Acidithiobacillus thiooxidans* and *Leptospirillum ferrooxidans*. Hydrometallurgy 2006; 83: 245-254.

Harris-Hellal J, Grimaldi M, Garnier-Zarli E, Bousserrhine N. Mercury mobilization by chemical and microbial iron oxide reduction in soils of French Guyana. Biogeochemistry 2011; 103: 223-234.

Hartley W, Edwards R, Lepp NW. Arsenic and heavy metal mobility in iron oxide-amended contaminated soils as evaluated by short-and long-term leaching tests. Environmental pollution 2004; 131: 495-504.

Hartshorne RS, Reardon CL, Ross D, Nuester J, Clarke TA, Gates AJ, et al. Characterization of an electron conduit between bacteria and the extracellular environment. Proceedings of the National Academy of Sciences 2009; 106: 22169-22174.

Heiberg L, Koch CB, Kjaergaard C, Jensen HS, Hansen HCB. Vivianite precipitation and phosphate sorption following iron reduction in anoxic soils. Journal of Environmental Quality 2012; 41: 938-949.

Hellal J, Burnol A, Locatelli A, Battaglia-Brunet F. Experimental column setup for studying anaerobic biogeochemical interactions between iron (Oxy) hydroxides, trace elements, and bacteria. JoVE (Journal of Visualized Experiments) 2017: e56240.

Hellal J, Guédron S, Huguet L, Schäfer J, Laperche V, Joulian C, et al. Mercury mobilization and speciation linked to bacterial iron oxide and sulfate reduction: A column study to mimic reactive transfer in an anoxic aquifer. Journal of contaminant hydrology 2015; 180: 56-68.

Hermann R, Neumann-Mahlkau P. The mobility of zinc, cadmium, copper, lead, iron and arsenic in ground water as a function of redox potential and pH. Science of the total environment 1985; 43: 1-12.

Heron G, Crouzet C, Bourg AC, Christensen TH. Speciation of Fe (II) and Fe (III) in contaminated aquifer sediments using chemical extraction techniques. Environmental science & technology 1994; 28: 1698-1705.

Hiemstra T. Surface and mineral structure of ferrihydrite. Geochimica et Cosmochimica Acta 2013; 105: 316-325.

Himmelheber DW, Thomas SH, Löffler FE, Taillefert M, Hughes JB. Microbial colonization of an in situ sediment cap and correlation to stratified redox zones. Environmental science & technology 2009; 43: 66-74.

Hindersmann I, Mansfeldt T. Trace element solubility in a multimetal-contaminated soil as affected by redox conditions. Water, Air, & Soil Pollution 2014; 225: 2158.

Holmén BA, Casey WH. Hydroxamate ligands, surface chemistry, and the mechanism of ligand-promoted dissolution of goethite [α-FeOOH (s)]. Geochimica et Cosmochimica Acta 1996; 60: 4403-4416.

Holmes DE, Nevin KP, Lovley, DR. Comparison of 16S rRNA, nifD, recA, gyrB, rpoB and fusA genes within the family *Geobacteraceae* fam. nov.. International Journal of Systematic and Evolutionary Microbiology 2004; 54: 1591-1599.

Hong C, Si Y, Xing Y, Li Y. Illumina MiSeq sequencing investigation on the contrasting soil bacterial community structures in different iron mining areas. Environmental Science and Pollution Research 2015; 22: 10788-10799.

Hori T, Aoyagi T, Itoh H, Narihiro T, Oikawa A, Suzuki K, et al. Isolation of microorganisms involved in reduction of crystalline iron (III) oxides in natural environments. Frontiers in Microbiology 2015; 6: 386.

Holt HM, Gahrn-Hansen B, Bruun B. *Shewanella algae* and *Shewanella putrefaciens*: clinical and microbiological characteristics. Clinical microbiology and infection. 2005 May 1;11(5):347-52.

Hu X, Ding Z, Zimmerman AR, Wang S, Gao B. Batch and column sorption of arsenic onto iron-impregnated biochar synthesized through hydrolysis. Water Research 2015; 68: 206-216.

Huang J-H. Impact of microorganisms on arsenic biogeochemistry: a review. Water, Air, & Soil Pollution 2014; 225: 1848.

Huang J-H, Hu K-N, Decker B. Organic arsenic in the soil environment: speciation, occurrence, transformation, and adsorption behavior. Water, Air, & Soil Pollution 2011; 219: 401-415.

Huguet L. Caractérisation biogéochimique et potentiel de méthylation du mercure de biofilms en milieu tropical (retenue de Petit Saut et estuaire du Sinnamary, Guyane Française). Nancy 1, 2009.

Hunger, S., & Benning, L. G. (2007). Greigite: a true intermediate on the polysulfide pathway to pyrite. Geochemical transactions, 8(1), 1.

Husson O. Redox potential (Eh) and pH as drivers of soil/plant/microorganism systems: a transdisciplinary overview pointing to integrative opportunities for agronomy. Plant and Soil 2013; 362: 389-417.

Huston DL, Logan GA. Barite, BIFs and bugs: evidence for the evolution of the Earth's early hydrosphere. Earth and Planetary Science Letters 2004; 220: 41-55.

Hyun MS, Kim BH, Chang IS, Park HS, Kim HJ, Kim GT, et al. Isolation and identification of an anaerobic dissimilatory Fe (III)-reducing bacterium, *Shewanella putrefaciens* IR-1. Journal of Microbiology 1999; 37: 206-212.

Inskeep WP, Macur RE, Hamamura N, Warelow TP, Ward SA, Santini JM. Detection, diversity and expression of aerobic bacterial arsenite oxidase genes. Environmental microbiology 2007; 9: 934-943.

**I**

Ivanova EP, Gorshkova NM, Bowman JP, Lysenko AM, Zhukova NV, Sergeev AF, et al. *Shewanella pacifica* sp. nov., a polyunsaturated fatty acid-producing bacterium isolated from sea water. International journal of systematic and evolutionary microbiology 2004; 54: 1083-1087.

Ivanova EP, Sawabe T, Gorshkova NM, Svetashev VI, Mikhailov VV, Nicolau DV, Christen R. *Shewanella japonica* sp. nov. Int J Syst Evol Microbiol. 2001;51:1027–33.

**J**

Jain A, Loeppert RH. Effect of competing anions on the adsorption of arsenate and arsenite by ferrihydrite. Journal of environmental quality 2000; 29: 1422-1430.

Jiang Z, Shi M, Shi L. Degradation of organic contaminants and steel corrosion by the dissimilatory metal-reducing microorganisms *Shewanella* and *Geobacter* spp. International Biodeterioration & Biodegradation 2020; 147: 104842.

Jickells T, An Z, Andersen KK, Baker A, Bergametti G, Brooks N, et al. Global iron connections between desert dust, ocean biogeochemistry, and climate. science 2005; 308: 67-71.

Johnson D, Bridge T. Reduction of ferric iron by acidophilic heterotrophic bacteria: evidence for constitutive and inducible enzyme systems in *Acidiphilium* spp. Journal of applied Microbiology 2002; 92: 315-321.

Jørgensen BB. Bacteria and marine biogeochemistry. Marine geochemistry. Springer, 2000, pp. 173-207.

Jr FC, Das A. Adhesion of dissimilatory Fe (III)-reducing bacteria to Fe (III) minerals. Geomicrobiology Journal 2002; 19: 161-177.

**K**

Kameda, J., Yamagishi, A., & Kogure, T. (2005). Morphological characteristics of ordered kaolinite: Investigation using electron back-scattered diffraction. American Mineralogist, 90(8-9), 1462-1465.

Kanso S, Greene AC, Patel BKC. *Bacillus subterraneus* sp. nov., an iron-and manganese-reducing bacterium from a deep subsurface Australian thermal aquifer. International journal of systematic and evolutionary microbiology 2002; 52: 869-874.

Kappler A, Straub KL. Geomicrobiological cycling of iron. Reviews in Mineralogy and Geochemistry 2005; 59: 85-108.

Kashefi K, Shelobolina ES, Elliott WC, Lovley DR. Growth of thermophilic and hyperthermophilic Fe (III)-reducing microorganisms on a ferruginous smectite as the sole electron acceptor. Applied and environmental microbiology 2008; 74: 251-258.

Kato S, Hashimoto K, Watanabe K. Microbial interspecies electron transfer via electric currents through conductive minerals. Proceedings of the National Academy of Sciences 2012; 109: 10042-10046.

Kelly DP, Wood AP. Reclassification of some species of *Thiobacillus* to the newly designated genera *Acidithiobacillus* gen. nov., *Halothiobacillus* gen. nov. and *Thermithiobacillus* gen. nov. International journal of systematic and evolutionary microbiology 2000; 50: 511-516.

Keon N, Swartz C, Brabander D, Harvey C, Hemond H. Validation of an arsenic sequential extraction method for evaluating mobility in sediments. Environmental Science & Technology 2001; 35: 2778-2784.

Kim BH, Ikeda T, Park HS, Kim HJ, Hyun MS, Kano K, et al. Electrochemical activity of an Fe (III)-reducing bacterium, *Shewanella putrefaciens* IR-1, in the presence of alternative electron acceptors. Biotechnology Techniques 1999a; 13: 475-478.

Kim BH, Kim HJ, Hyun MS, Park DH. Direct electrode reaction of Fe (III)-reducing bacterium, *Shewanella putrefaciens*. Journal of Microbiology and Biotechnology 1999b; 9: 127-131.

Kim H-S, Kang W-H, Kim M, Park J-Y, Hwang I. Comparison of hematite/Fe (II) systems with cement/Fe (II) systems in reductively dechlorinating trichloroethylene. Chemosphere 2008; 73: 813-819.

Kim S-J, Koh D-C, Park S-J, Cha I-T, Park J-W, Na J-H, et al. Molecular analysis of spatial variation of iron-reducing bacteria in riverine alluvial aquifers of the Mankyeong River. The journal of microbiology 2012; 50: 207-217.

Kishimoto N, Kosako Y, Tano T. *Acidobacterium capsulatum* gen. nov., sp. nov.: an acidophilic chemoorganotrophic bacterium containing menaquinone from acidic mineral environment. Current Microbiology 1991; 22: 1-7.

Konhauser KO, Kappler A, Roden EE. Iron in microbial metabolisms. Elements 2011; 7: 89-93.

Koretsky CM, Moore CM, Lowe KL, Meile C, DiChristina TJ, Van Cappellen P. Seasonal oscillation of microbial iron and sulfate reduction in saltmarsh sediments (Sapelo Island, GA, USA). Biogeochemistry 2003; 64: 179-203.

Kotloski NJ, Gralnick JA. Flavin electron shuttles dominate extracellular electron transfer by *Shewanella oneidensis*. MBio 2013; 4.

Kraemer SM. Iron oxide dissolution and solubility in the presence of siderophores. Aquatic sciences 2004; 66: 3-18.

Kukkadapu RK, Zachara JM, Fredrickson JK, Kennedy DW. Biotransformation of two-line silica-ferrihydrite by a dissimilatory Fe (III)-reducing bacterium: formation of carbonate green rust in the presence of phosphate. Geochimica et Cosmochimica Acta 2004; 68: 2799-2814.

Kulkarni HV, Mladenov N, McKnight DM, Zheng Y, Kirk MF, Nemergut DR. Dissolved fulvic acids from a high arsenic aquifer shuttle electrons to enhance microbial iron reduction. Science of The Total Environment 2018; 615: 1390-1395.

Kumpiene J, Lagerkvist A, Maurice C. Stabilization of As, Cr, Cu, Pb and Zn in soil using amendments–a review. Waste management 2008; 28: 215-225.

Kurek E. 5 Microbial Mobilization of Metals from Soil Minerals under Aerobic. Interactions between Soil Particles and Microorganisms: Impact on the Terrestrial Ecosystem 2002; 7: 189.

Kurek E, Bollag J-M. Microbial immobilization of cadmium released from CdO in the soil. Biogeochemistry 2004; 69: 227-239.

Küsel K, Dorsch T, Acker G, Stackebrandt E. Microbial reduction of Fe (III) in acidic sediments: isolation of *Acidiphilium cryptum* JF-5 capable of coupling the reduction of Fe (III) to the oxidation of glucose. Applied and Environmental Microbiology 1999; 65: 3633-3640.

Kwon, M. J., O'Loughlin, E. J., Boyanov, M. I., Brulc, J. M., Johnston, E. R., Kemner, K. M., & Antonopoulos, D. A. (2016). Impact of organic carbon electron donors on microbial

community development under iron-and sulfate-reducing conditions. PloS one, 11(1), e0146689.

**L**

Lagroix, F., Banerjee, S. K., & Jackson, M. J. (2016). Geological occurrences and relevance of iron oxides. Iron Oxides: From Nature to Applications, 7-30.

Larsen O, Postma D. Kinetics of reductive bulk dissolution of lepidocrocite, ferrihydrite, and goethite. Geochimica et Cosmochimica Acta 2001; 65: 1367-1379.

Laufer K, Niemeyer A, Nikeleit V, Halama M, Byrne JM, Kappler A. Physiological characterization of a halotolerant anoxygenic phototrophic Fe (II)-oxidizing green-sulfur bacterium isolated from a marine sediment. FEMS microbiology ecology 2017; 93.

Laverman AM, Blum JS, Schaefer JK, Phillips E, Lovley DR, Oremland RS. Growth of strain SES-3 with arsenate and other diverse electron acceptors. Applied and Environmental Microbiology 1995; 61: 3556-3561.

Leang C, Adams LA, Chin KJ, Nevin KP, Methe BA, Webster J, et al. Adaptation to disruption of the electron transfer pathway for Fe (III) reduction in Geobacter sulfurreducens. Journal of bacteriology 2005; 187: 5918-5926.

Leang C, Qian X, Mester T, Lovley DR. Alignment of the c-type cytochrome OmcS along pili of *Geobacter sulfurreducens*. Appl. Environ. Microbiol. 2010; 76: 4080-4084.

Lee J-H, Roh Y, Kim K-W, Hur H-G. Organic acid-dependent iron mineral formation by a newly isolated iron-reducing bacterium, *Shewanella* sp. HN-41. Geomicrobiology Journal 2007; 24: 31-41.

Lee JY, Iglesias B, Chu CE, Lawrence DJ, Crane III EJ. *Pyrobaculum igneiluti* sp. nov., a novel anaerobic hyperthermophilic archaeon that reduces thiosulfate and ferric iron. International Journal of Systematic and Evolutionary Microbiology 2017; 67: 1714-1719.

Lemaire ON, Méjean V, Iobbi-Nivol C. The *Shewanella* genus: ubiquitous organisms sustaining and preserving aquatic ecosystems. FEMS Microbiology Reviews. 2020 Mar;44(2):155-70.

Lentini CJ, Wankel SD, Hansel CM. Enriched iron (III)-reducing bacterial communities are shaped by carbon substrate and iron oxide mineralogy. Frontiers in microbiology 2012; 3: 404.

Levar CE, Hoffman CL, Dunshee AJ, Toner BM, Bond DR. Redox potential as a master variable controlling pathways of metal reduction by *Geobacter sulfurreducens*. The ISME journal 2017; 11: 741-752.

Li B-B, Cheng Y-Y, Fan Y-Y, Liu D-F, Fang C-Y, Wu C, et al. Estimates of abundance and diversity of *Shewanella* genus in natural and engineered aqueous environments with newly designed primers. Science of The Total Environment 2018; 637: 926-933.

Li C, Yi X, Dang Z, Yu H, Zeng T, Wei C, et al. Fate of Fe and Cd upon microbial reduction of Cd-loaded polyferric flocs by *Shewanella oneidensis* MR-1. Chemosphere 2016; 144: 2065-2072.

Li GL, Zhou CH, Fiore S, Yu WH. Interactions between microorganisms and clay minerals: New insights and broader applications. Applied Clay Science 2019; 177: 91-113.

Li W, Beard BL, Johnson CM. Biologically recycled continental iron is a major component in banded iron formations. Proceedings of the National Academy of Sciences 2015; 112: 8193-8198.

Li W, Zhang S, Jiang W, Shan X-q. Effect of phosphate on the adsorption of Cu and Cd on natural hematite. Chemosphere 2006; 63: 1235-1241.

Li X, Liu T, Li F, Zhang W, Zhou S, Li Y. Reduction of structural Fe (III) in oxyhydroxides by *Shewanella decolorationis* S12 and characterization of the surface properties of iron minerals. Journal of soils and sediments 2012; 12: 217-227.

Liamleam W, Annachhatre AP. Electron donors for biological sulfate reduction. Biotechnology advances 2007; 25: 452-463.

Lin TJ, El Sebae G, Jung J-H, Jung D-H, Park C-S, Holden JF. *Pyrodictium delaneyi* sp. nov., a hyperthermophilic autotrophic archaeon that reduces Fe (III) oxide and nitrate. International journal of systematic and evolutionary microbiology 2016; 66: 3372.

Liu C, Gorby YA, Zachara JM, Fredrickson JK, Brown CF. Reduction kinetics of Fe (III), Co (III), U (VI), Cr (VI), and Tc (VII) in cultures of dissimilatory metal-reducing bacteria. Biotechnology and bioengineering 2002; 80: 637-649.

Liu C, Kota S, Zachara JM, Fredrickson JK, Brinkman CK. Kinetic analysis of the bacterial reduction of goethite. Environmental Science & Technology 2001; 35: 2482-2490.

Liu G, Zhou J, Wang J, Wang X, Jin R, Lv H. Decolorization of azo dyes by *Shewanella oneidensis* MR-1 in the presence of humic acids. Applied microbiology and biotechnology 2011a; 91: 417-424.

Liu H, Li P, Zhu M, Wei Y, Sun Y. Fe (II)-induced transformation from ferrihydrite to lepidocrocite and goethite. Journal of Solid State Chemistry 2007; 180: 2121-2128.

Liu L, Yuan Y, Li F-b, Feng C-h. In-situ Cr (VI) reduction with electrogenerated hydrogen peroxide driven by iron-reducing bacteria. Bioresource technology 2011b; 102: 2468-2473.

Liu T, Yu YY, Deng XP, Ng CK, Cao B, Wang JY, et al. Enhanced *Shewanella* biofilm promotes bioelectricity generation. Biotechnology and bioengineering 2015; 112: 2051-2059.

Liu X, Ye Y, Xiao K, Rensing C, Zhou S. Molecular evidence for the adaptive evolution of *Geobacter sulfurreducens* to perform dissimilatory iron reduction in natural environments. Molecular Microbiology 2019a.

Liu X, Zhuo S, Jing X, Yuan Y, Rensing C, Zhou S. Flagella act as *Geobacter* biofilm scaffolds to stabilize biofilm and facilitate extracellular electron transfer. Biosensors and Bioelectronics 2019b; 146: 111748.

Lloyd JR. Microbial reduction of metals and radionuclides. FEMS microbiology reviews 2003; 27: 411-425.

Lovley DR.Organic matter mineralization with the reduction of ferric iron: A review, Geomicrobiology Journal 1987, 5:3-4, 375-399,

Lovley D. Dissimilatory Fe (III)-and Mn (IV)-reducing prokaryotes. Prokaryotes 2006; 2: 635-658.

Lovley DR. Organic matter mineralization with the reduction of ferric iron: a review. Geomicrobiology Journal 1987; 5: 375-399.

Lovley DR. Dissimilatory Fe (III) and Mn (IV) reduction. Microbiology and Molecular Biology Reviews 1991; 55: 259-287.

Lovley DR. Dissimilatory metal reduction. Annual review of microbiology 1993; 47: 263-290.

Lovley DR. Microbial Fe (III) reduction in subsurface environments. FEMS Microbiology Reviews 1997; 20: 305-313.

Lovley DR. Fe (III) and Mn (IV) reduction. Environmental microbe-metal interactions. American Society of Microbiology, 2000, pp. 3-30.

Lovley DR. Extracellular electron transfer: wires, capacitors, iron lungs, and more. Geobiology 2008; 6: 225-231.

Lovley, DR, Giovannoni, S.J., White, D.C. et al. *Geobacter metallireducens* gen. nov. sp. nov., a microorganism capable of coupling the complete oxidation of organic compounds to the reduction of iron and other metals. Arch. Microbiol., 2000, 159: 336–344.

Lovley DR, Coates JD, Blunt-Harris EL, Phillips EJ, Woodward JC. Humic substances as electron acceptors for microbial respiration. Nature 1996; 382: 445-448.

Lovley DR, Giovannoni SJ, White DC, Champine JE, Phillips E, Gorby YA, et al. *Geobacter metallireducens* gen. nov. sp. nov., a microorganism capable of coupling the complete oxidation of organic compounds to the reduction of iron and other metals. Archives of microbiology 1993a; 159: 336-344.

Lovley DR, Holmes DE, Nevin KP. Dissimilatory fe (iii) and mn (iv) reduction. Advances in microbial physiology 2004; 49: 219-286.

Lovley, D. R., Phillips, E. J., & Lonergan, D. J. (1989). Hydrogen and formate oxidation coupled to dissimilatory reduction of iron or manganese by *Alteromonas putrefaciens*. Applied and Environmental Microbiology, 55(3), 700-706.

Lovley DR, Phillips E, Lonergan DJ, Widman PK. Fe (III) and S0 reduction by *Pelobacter carbinolicus*. Applied and environmental microbiology 1995; 61: 2132-2138.

Lovley DR, Phillips EJ. Novel mode of microbial energy metabolism: organic carbon oxidation coupled to dissimilatory reduction of iron or manganese. Applied and environmental microbiology 1988; 54: 1472-1480.

Lovley DR, Phillips EJ, Gorby YA, Landa ER. Microbial reduction of uranium. Nature 1991; 350: 413-416.

Lovley DR, Stolz JF, Nord GL, Phillips EJ. Anaerobic production of magnetite by a dissimilatory iron-reducing microorganism. Nature 1987; 330: 252-254.

Lovley DR, Widman PK, Woodward JC, Phillips E. Reduction of uranium by cytochrome c3 of *Desulfovibrio vulgaris*. Applied and environmental microbiology 1993b; 59: 3572-3576.

Lovley DR, Ueki T, Zhang T, Malvankar NS, Shrestha PM, Flanagan KA, Aklujkar M, Butler JE, Giloteaux L, Rotaru AE, Holmes DE. *Geobacter*: the microbe electric's physiology, ecology, and practical applications. InAdvances in microbial physiology 2011 Jan 1 (Vol. 59, pp. 1-100). Academic Press.

**M**

Ma C, Zhuang L, Zhou SG, Yang GQ, Yuan Y, Xu RX. Alkaline extracellular reduction: isolation and characterization of an alkaliphilic and halotolerant bacterium, *Bacillus pseudofirmus* MC02. Journal of applied microbiology 2012; 112: 883-891.

MacDonell M, Colwell R. Phylogeny of the Vibrionaceae, and recommendation for two new genera, *Listonella* and *Shewanella*. Systematic and applied microbiology 1985; 6: 171-182.

MacRae JD, Lavine IN, McCaffery KA, Ricupero K. Isolation and characterization of NP4, arsenate-reducing *Sulfurospirillum*, from Maine groundwater. Journal of Environmental Engineering 2007; 133: 81-88.

Macur RE, Jackson CR, Botero LM, Mcdermott TR, Inskeep WP. Bacterial populations associated with the oxidation and reduction of arsenic in an unsaturated soil. Environmental science & technology 2004; 38: 104-111.

Mahadevan R, Palsson BØ, Lovley DR. In situ to in silico and back: elucidating the physiology and ecology of *Geobacter* spp. using genome-scale modelling. Nature Reviews Microbiology 2011; 9: 39-50.

Maitte B, Jorand FP, Grgic D, Abdelmoula M, Carteret C. Remineralization of ferrous carbonate from bioreduction of natural goethite in the Lorraine iron ore (Minette) by *Shewanella putrefaciens*. Chemical Geology 2015; 412: 48-58.

Mamindy-Pajany Y, Bataillard P, Séby F, Crouzet C, Moulin A, Guezennec A-G, et al. Arsenic in marina sediments from the Mediterranean coast: speciation in the solid phase and occurrence of thioarsenates. Soil and Sediment Contamination: An International Journal 2013; 22: 984-1002.

Mamindy-Pajany Y, Hurel C, Marmier N, Roméo M. Arsenic (V) adsorption from aqueous solution onto goethite, hematite, magnetite and zero-valent iron: effects of pH, concentration and reversibility. Desalination 2011; 281: 93-99.

Marsili E, Baron DB, Shikhare ID, Coursolle D, Gralnick JA, Bond DR. *Shewanella* secretes flavins that mediate extracellular electron transfer. Proceedings of the National Academy of Sciences 2008; 105: 3968-3973.

Mathews FS. The structure, function and evolution of cytochromes. Progress in biophysics and molecular biology 1985; 45: 1-56.

Matsui H, Mahowald NM, Moteki N, Hamilton DS, Ohata S, Yoshida A, et al. Anthropogenic combustion iron as a complex climate forcer. Nature communications 2018; 9: 1-10.

McKeague J, Day J. Dithionite-and oxalate-extractable Fe and Al as aids in differentiating various classes of soils. Canadian journal of soil science 1966; 46: 13-22.

Meshulam-Simon G, Behrens S, Choo AD, Spormann AM. Hydrogen metabolism in *Shewanella oneidensis* MR-1. Appl Environ Microbiol. 2007;73(4):1153-1165.

Meile C, Scheibe TD. Reactive transport modeling of microbial dynamics. Elements: An International Magazine of Mineralogy, Geochemistry, and Petrology 2019; 15: 111-116.

Melton ED, Swanner ED, Behrens S, Schmidt C, Kappler A. The interplay of microbially mediated and abiotic reactions in the biogeochemical Fe cycle. Nature Reviews Microbiology 2014; 12: 797-808.

Mercier A, Joulian C, Michel C, Auger P, Coulon S, Amalric L, et al. Evaluation of three activated carbons for combined adsorption and biodegradation of PCBs in aquatic sediment. Water research 2014; 59: 304-315.

Michel FM, Ehm L, Antao SM, Lee PL, Chupas PJ, Liu G, Strongin DR, Schoonen MA, Phillips BL, Parise JB. The structure of ferrihydrite, a nanocrystalline material. Science. 2007 Jun 22;316(5832):1726-9.

Mikac N, Foucher D, Niessen S, Fischer J-C. Extractability of HgS (cinnabar and metacinnabar) by hydrochloric acid. Analytical and bioanalytical chemistry 2002; 374: 1028-1033.

Mortimer RJ, Galsworthy AM, Bottrell SH, Wilmot LE, Newton RJ. Experimental evidence for rapid biotic and abiotic reduction of Fe (III) at low temperatures in salt marsh sediments: a possible mechanism for formation of modern sedimentary siderite concretions. Sedimentology. 2011 Oct;58(6):1514-29.

Motomura S, Yokoi H. Characteristics of ferrous iron forms in paddy soil with reference to development of the soil profile. Soil Science and Plant Nutrition 1969; 15: 38-46.

Muehe EM, Obst M, Hitchcock A, Tyliszczak T, Behrens S, Schröder C, et al. Fate of Cd during microbial Fe (III) mineral reduction by a novel and Cd-tolerant *Geobacter* species. Environmental science & technology 2013; 47: 14099-14109.

Mueller RF. Bacterial transport and colonization in low nutrient environments. Water Research 1996; 30: 2681-2690.

Murti GK, Volk V, Jackson M. Colorimetric determination of iron of mixed valency by orthophenanthroline. Soil Science Society of America Journal 1966; 30: 663-664.

**N**

Neal AL, Techkarnjanaruk S, Dohnalkova A, McCready D, Peyton BM, Geesey GG. Iron sulfides and sulfur species produced at hematite surfaces in the presence of sulfate-reducing bacteria. Geochimica et Cosmochimica Acta 2001; 65: 223-235.

Nealson KH. Bioelectricity (electromicrobiology) and sustainability. Microbial biotechnology 2017; 10: 1114-1119.

Nevin KP, Holmes DE, Woodard TL, Hinlein ES, Ostendorf DW, Lovley DR. *Geobacter bemidjiensis* sp. nov. and *Geobacter psychrophilus* sp. nov., two novel Fe (III)-reducing subsurface isolates. International Journal of Systematic and Evolutionary Microbiology 2005; 55: 1667-1674.

Nevin KP, Lovley DR. Mechanisms for Fe (III) oxide reduction in sedimentary environments. Geomicrobiology Journal 2002; 19: 141-159.

Newman DK, Kolter R. A role for excreted quinones in extracellular electron transfer. Nature 2000; 405: 94-97.

Nickelsen L, Keller D, Oschlies A. A dynamic marine iron cycle module coupled to the University of Victoria Earth System Model: the Kiel Marine Biogeochemical Model 2 for UVic 2.9. Geoscientific Model Development 2015; 8: 1357-1381.

Nogi Y, Kato C, Horikoshi K. Taxonomic studies of deep-sea barophilic *Shewanella* strains and description of *Shewanella* violacea sp. nov. Archives of microbiology 1998; 170: 331-338.

**O**

O'Loughlin EJ, Gorski CA, Scherer MM, Boyanov MI, Kemner KM. Effects of oxyanions, natural organic matter, and bacterial cell numbers on the bioreduction of lepidocrocite (γ-FeOOH) and the formation of secondary mineralization products. Environmental Science & Technology 2010; 44: 4570-4576.

Ojumu TV, Petersen J. The kinetics of ferrous ion oxidation by *Leptospirillum ferriphilum* in continuous culture: The effect of pH. Hydrometallurgy 2011; 106: 5-11.

Okamoto A, Nakamura R, Nealson KH, Hashimoto K. Bound flavin model suggests similar electron-transfer mechanisms in *Shewanella* and *Geobacter*. ChemElectroChem 2014; 1: 1808-1812.

Ona-Nguema G, Abdelmoula M, Jorand F, Benali O, Géhin A, Block JC, Génin JM. Iron (II, III) hydroxycarbonate green rust formation and stabilization from lepidocrocite bioreduction. Environmental Science & Technology. 2002 Jan 1;36(1):16-20.

Ona-Nguema G, Morin G, Wang Y, Menguy N, Juillot F, Olivi L, Aquilanti G, Abdelmoula M, Ruby C, Bargar JR, Guyot F. Arsenite sequestration at the surface of nano-Fe $(OH)_2$, ferrous-carbonate hydroxide, and green-rust after bioreduction of arsenic-sorbed lepidocrocite by *Shewanella putrefaciens*. Geochimica et Cosmochimica Acta. 2009 Mar 1;73(5):1359-81.

Ortiz-Bernad I, Anderson RT, Vrionis HA, Lovley DR. Vanadium respiration by *Geobacter metallireducens*: novel strategy for in situ removal of vanadium from groundwater. Applied and Environmental Microbiology 2004; 70: 3091-3095.

Ottow J, Glathe H. Isolation and identification of iron-reducing bacteria from gley soils. Soil Biology and Biochemistry 1971; 3: 43-55.

**P**

Park, D. H., & Kim, B. H. (2001). Growth properties of the iron-reducing bacteria, *Shewanella putrefaciens* IR-1 and MR-1 coupling to reduction of Fe (III) to Fe (II). Journal of Microbiology, 39(4), 273-278.

Park HS, Kim BH, Kim HS, Kim HJ, Kim GT, Kim M, et al. A novel electrochemically active and Fe (III)-reducing bacterium phylogenetically related to *Clostridium butyricum* isolated from a microbial fuel cell. Anaerobe 2001; 7: 297-306.

Parkman R, Charnock J, Bryan N, Livens F, Vaughan D. Reactions of copper and cadmium ions in aqueous solution with goethite, lepidocrocite, mackinawite, and pyrite. American Mineralogist 1999; 84: 407-419.

Pedersen HD, Postma D, Jakobsen R, Larsen O. Fast transformation of iron oxyhydroxides by the catalytic action of aqueous Fe (II). Geochimica et Cosmochimica Acta 2005; 69: 3967-3977.

Pédrot M, Dia A, Davranche M, Bouhnik-Le Coz M, Henin O, Gruau G. Insights into colloid-mediated trace element release at the soil/water interface. Journal of Colloid and Interface Science 2008; 325: 187-197.

Pédrot M, Le Boudec A, Davranche M, Dia A, Henin O. How does organic matter constrain the nature, size and availability of Fe nanoparticles for biological reduction?. Journal of colloid and interface science. 2011 Jul 1;359(1):75-85.

Peiffer S, Walton-Day K, Macalady DL. The interaction of natural organic matter with iron in a wetland (Tennessee Park, Colorado) receiving acid mine drainage. Aquatic Geochemistry 1999; 5: 207-223.

Pekov, I. V., Perchiazzi, N., Merlino, S., Kalachev, V. N., Merlini, M., & Zadov, A. E. (2007). Chukanovite, $Fe_2(CO_3)(OH)_2$, a new mineral from the weathered iron meteorite Dronino. European Journal of Mineralogy, 19(6), 891-898.

Peng L, Liu Y, Gao S-H, Dai X, Ni B-J. Assessing chromate reduction by dissimilatory iron reducing bacteria using mathematical modeling. Chemosphere 2015; 139: 334-339.

Peng Q, Zhang F, Zhou Y, Zhang J, Wei J, Mao Q, et al. Formation of composite sorbent by *P. chrysogenum* strain F1 and ferrihydrite in water for arsenic removal. International Biodeterioration & Biodegradation 2018; 132: 208-215.

Perez-Gonzalez T, Jimenez-Lopez C, Neal AL, Rull-Perez F, Rodriguez-Navarro A, Fernandez-Vivas A, et al. Magnetite biomineralization induced by *Shewanella oneidensis.* Geochimica et Cosmochimica Acta 2010; 74: 967-979.

Pérez PL, López RA, González MN. Cadmium removal at high concentration in aqueous medium: mediated by *Desulfovibrio alaskensis*. International Journal of Environmental Science and Technology 2015; 12: 1975-1986.

Petrilli FL, De Flora S. Toxicity and mutagenicity of hexavalent chromium on *Salmonella typhimurium.* Applied and Environmental Microbiology 1977; 33: 805-809.

Pett-Ridge J, Silver WL, Firestone MK. Redox fluctuations frame microbial community impacts on N-cycling rates in a humid tropical forest soil. Biogeochemistry 2006; 81: 95-110.

Phillips EJ, Lovley DR. Determination of Fe (III) and Fe (II) in oxalate extracts of sediment. Soil Science Society of America Journal 1987; 51: 938-941.

Pinchuk GE, Geydebrekht OV, Hill EA, Reed JL, Konopka AE, Beliaev AS, et al. Pyruvate and lactate metabolism by *Shewanella oneidensis* MR-1 under fermentation, oxygen limitation, and fumarate respiration conditions. Applied and environmental microbiology 2011; 77: 8234-8240.

Poggenburg C, Mikutta R, Sander M, Schippers A, Marchanka A, Dohrmann R, et al. Microbial reduction of ferrihydrite-organic matter coprecipitates by *Shewanella putrefaciens* and *Geobacter metallireducens* in comparison to mediated electrochemical reduction. Chemical Geology 2016; 447: 133-147.

Poulton SW, Canfield DE. Development of a sequential extraction procedure for iron: implications for iron partitioning in continentally derived particulates. Chemical geology 2005; 214: 209-221.

Prakash OM, Gihring TM, Dalton DD, Chin K-J, Green SJ, Akob DM, et al. *Geobacter daltonii* sp. nov., an Fe (III)-and uranium (VI)-reducing bacterium isolated from a shallow subsurface exposed to mixed heavy metal and hydrocarbon contamination. International journal of systematic and evolutionary microbiology 2010; 60: 546-553.

Prokop Z, Vangheluwe M, Van Sprang P, Janssen C, Holoubek I. Mobility and toxicity of metals in sandy sediments deposited on land. Ecotoxicology and Environmental Safety 2003; 54: 65-73.

Pullin MJ, Cabaniss SE. The effects of pH, ionic strength, and iron–fulvic acid interactions on the kinetics of non-photochemical iron transformations. I. Iron (II) oxidation and iron (III) colloid formation. Geochimica et Cosmochimica Acta 2003; 67: 4067-4077.

**R**

Raiswell R, Canfield DE. The iron biogeochemical cycle past and present. Geochemical perspectives 2012; 1: 1-2.

Rancourt DG, Ping JY. Voigt-based methods for arbitrary-shape static hyperfine parameter distributions in Mössbauer spectroscopy. Nuclear Instruments and Methods in Physics Research Section B: Beam Interactions with Materials and Atoms 1991; 58: 85-97.

Reguera G, McCarthy KD, Mehta T, Nicoll JS, Tuominen MT, Lovley DR. Extracellular electron transfer via microbial nanowires. Nature 2005; 435: 1098-1101.

Reguera G, Pollina RB, Nicoll JS, Lovley DR. Possible nonconductive role of *Geobacter sulfurreducens* pilus nanowires in biofilm formation. Journal of bacteriology 2007; 189: 2125-2127.

Remy PP, Etique M, Hazotte AA, Sergent AS, Estrade N, Cloquet C, Hanna K, Jorand FP. Pseudo-first-order reaction of chemically and biologically formed green rusts with HgII and $C_{15}H_{15}N_3O_2$: Effects of pH and stabilizing agents (phosphate, silicate, polyacrylic acid, and bacterial cells). water research. 2015 Mar 1;70:266-78.

Richard FC, Bourg AC. Aqueous geochemistry of chromium: a review. Water research 1991; 25: 807-816.

Richter H, McCarthy K, Nevin KP, Johnson JP, Rotello VM, Lovley DR. Electricity generation by *Geobacter sulfurreducens* attached to gold electrodes. Langmuir 2008; 24: 4376-4379.

Ritz, C., Essene, E. J., & Peacor, D. R. (1974). Metavivianite, Fe3 (PO4) 2· 8H2O, a new mineral. American Mineralogist: Journal of Earth and Planetary Materials, 59(9-10), 896-899.

Roberts JA, Fowle DA, Hughes BT, Kulczycki E. Attachment behavior of *Shewanella putrefaciens* onto magnetite under aerobic and anaerobic conditions. Geomicrobiology Journal 2006; 23: 631-640.

Roden EE. Geochemical and microbiological controls on dissimilatory iron reduction. Comptes Rendus Geoscience 2006a; 338: 456-467.

Roden EE. Geochemical and microbiological controls on dissimilatory iron reduction. Comptes Rendus Geoscience 2006b; 338: 456-467.

Roden EE, Sobolev D, Glazer B, Luther GW. Potential for microscale bacterial Fe redox cycling at the aerobic-anaerobic interface. Geomicrobiology Journal 2004; 21: 379-391.

Roden EE, Wetzel RG. Kinetics of microbial Fe (III) oxide reduction in freshwater wetland sediments. Limnology and Oceanography 2002; 47: 198-211.

Rodríguez Y, Ballester A, Blázquez ML, González F, Muñoz JA. Study of bacterial attachment during the bioleaching of pyrite, chalcopyrite, and sphalerite. Geomicrobiology Journal 2003; 20: 131-141.

Roh Y, Gao H, Vali H, Kennedy DW, Yang ZK, Gao W, et al. Metal reduction and iron biomineralization by a psychrotolerant Fe (III)-reducing bacterium, *Shewanella s*p. strain PV-4. Applied and Environmental Microbiology 2006; 72: 3236-3244.

Roh Y, Zhang C-L, Vali H, Lauf R, Zhou J, Phelps T. Biogeochemical and environmental factors in Fe biomineralization: magnetite and siderite formation. Clays and Clay Minerals 2003; 51: 83-95.

Roldán R, Barrón V, Torrent J. Experimental alteration of vivianite to lepidocrocite in a calcareous medium. Clay minerals 2002; 37: 709-718.

Rollefson JB, Stephen CS, Tien M, Bond DR. Identification of an extracellular polysaccharide network essential for cytochrome anchoring and biofilm formation in *Geobacter sulfurreducens*. Journal of bacteriology 2011; 193: 1023-1033.

Rosselló-Mora RA, Ludwig W, Kämpfer P, Amann R, Schleifer K-H. *Ferrimonas balearica* gen. nov., spec. nov., a new marine facultative Fe (III)-reducing bacterium. Systematic and applied microbiology 1995; 18: 196-202.

Runov EV. Die reduktion der eisen oxyde auf microbiologichen wege. Vestn Bakta-Agronomich Stontsii 1926; 24: 75-82.

Ryan JN, Gschwend PM. Extraction of iron oxides from sediments using reductive dissolution by titanium (III). Clays and Clay Minerals 1991; 39: 509-518.

**S**

Sakamoto Y, Noda Y, Ohno K, Koike K, Fujii K, Suzuki TM, et al. First principles calculations of surface dependent electronic structures: a study on β-FeOOH and γ-FeOOH. Physical Chemistry Chemical Physics 2019; 21: 18486-18494.

Sampson M, Phillips C, Ball A. Investigation of the attachment of *Thiobacillus ferrooxidans* to mineral sulfides using scanning electron microscopy analysis. Minerals Engineering 2000; 13: 643-656.

Satomi M. Shewanella. 2014.

Sawayama M, Suzuki T, Hashimoto H, Kasai T, Furutani M, Miyata N, et al. Isolation of a *Leptothrix* strain, OUMS1, from ocherous deposits in groundwater. Current microbiology 2011; 63: 173-180.

Schilling K, Borch T, Rhoades CC, Pallud CE. Temperature sensitivity of microbial Fe (III) reduction kinetics in subalpine wetland soils. Biogeochemistry 2019; 142: 19-35.

Schroeder HA. The role of chromium in mammalian nutrition. The American Journal of Clinical Nutrition 1968; 21: 230-244.

Schwertmann U. Use of oxalate for Fe extraction from soils. Canadian Journal of Soil Science 1973; 53: 244-246.

Schwertmann U. Solubility and dissolution of iron oxides. Plant and soil. 1991 Jan 1;130(1-2):1-25.

Schwertmann U. Relations between iron oxides, soil color, and soil formation. Soil color 1993; 31: 51-69.

Schwertmann U, Cornell RM. Iron oxides in the laboratory: preparation and characterization: John Wiley & Sons, 2008.

Schwertmann U, Taylor R. Natural and synthetic poorly crystallized lepidocrocite. Clay Minerals 1979; 14: 285-293.

Semple K, Westlake D. Characterization of iron-reducing *Alteromonas putrefaciens* strains from oil field fluids. Canadian journal of microbiology 1987; 33: 366-371.

Senn AC, Kaegi R, Hug SJ, Hering JG, Mangold S, Voegelin A. Effect of aging on the structure and phosphate retention of Fe (III)-precipitates formed by Fe (II) oxidation in water. Geochimica et Cosmochimica Acta. 2017 Apr 1;202:341-60.

Serres MH, Riley M. Genomic analysis of carbon source metabolism of *Shewanella oneidensis* MR-1: predictions versus experiments. Journal of bacteriology 2006; 188: 4601-4609.

Shelobolina ES, Nevin KP, Blakeney-Hayward JD, Johnsen CV, Plaia TW, Krader P, et al. *Geobacter pickeringii* sp. nov., *Geobacter argillaceus* sp. nov. and *Pelosinus*

*fermentans* gen. nov., sp. nov., isolated from subsurface kaolin lenses. International Journal of Systematic and Evolutionary Microbiology 2007; 57: 126-135.

Shelobolina ES, Vrionis HA, Findlay RH, Lovley DR. *Geobacter uraniireducens* sp. nov., isolated from subsurface sediment undergoing uranium bioremediation. International Journal of Systematic and Evolutionary Microbiology 2008; 58: 1075-1078.

Shi L, Dong H, Reguera G, Beyenal H, Lu A, Liu J, et al. Extracellular electron transfer mechanisms between microorganisms and minerals. Nature Reviews Microbiology 2016; 14: 651.

Shi L, Squier TC, Zachara JM, Fredrickson JK. Respiration of metal (hydr) oxides by *Shewanella* and *Geobacter*: a key role for multihaem c-type cytochromes. Molecular microbiology 2007; 65: 12-20.

Shi M, Jiang Y, Shi L. Electromicrobiology and biotechnological applications of the exoelectrogens *Geobacter* and *Shewanella* spp. Science China Technological Sciences 2019: 1-9.

Siffert C, Sulzberger B. Light-induced dissolution of hematite in the presence of oxalate. A case study. Langmuir 1991; 7: 1627-1634.

Slobodkina GB, Kolganova TV, Querellou J, Bonch-Osmolovskaya EA, Slobodkin AI. *Geoglobus acetivorans* sp. nov., an iron (III)-reducing archaeon from a deep-sea hydrothermal vent. International journal of systematic and evolutionary microbiology 2009; 59: 2880-2883.

Snoeyenbos-West O, Nevin K, Anderson R, Lovley D. Enrichment of *Geobacter* species in response to stimulation of Fe (III) reduction in sandy aquifer sediments. Microbial Ecology 2000; 39: 153-167.

Somenahally AC, Hollister EB, Yan W, Gentry TJ, Loeppert RH. Water management impacts on arsenic speciation and iron-reducing bacteria in contrasting rice-rhizosphere compartments. Environmental science & technology 2011; 45: 8328-8335.

Stams AJ, De Bok FA, Plugge CM, Van Eekert MH, Dolfing J, Schraa G. Exocellular electron transfer in anaerobic microbial communities. Environmental microbiology 2006; 8: 371-382.

Stapleton Jr RD, Sabree ZL, Palumbo AV, Moyer CL, Devol AH, Roh Y, et al. Metal reduction at cold temperatures by *Shewanella* isolates from various marine environments. Aquatic Microbial Ecology 2005; 38: 81.

Starkey R, Halvorson H. Studies on the transformations of iron in nature. II. Concerning the importance of microörganisms in the solution and precipitation of iron. Soil Science 1927; 24: 381-402.

Stern N, Mejia J, He S, Yang Y, Ginder-Vogel M, Roden EE. Dual role of humic substances as electron donor and shuttle for dissimilatory iron reduction. Environmental science & technology 2018; 52: 5691-5699.

Straub, K. L., Hanzlik, M., & Buchholz-Cleven, B. E. (1998). The use of biologically produced ferrihydrite for the isolation of novel iron-reducing bacteria. Systematic and Applied Microbiology, 21(3), 442-449.

Straub KL. Geobacter. In: Reitner J, Thiel V, editors. Encyclopedia of Geobiology. Springer Netherlands, Dordrecht, 2011, pp. 412-413.

Straub KL, Buchholz-Cleven BE. *Geobacter bremensis* sp. nov. and *Geobacter pelophilus* sp. nov., two dissimilatory ferric-iron-reducing bacteria. International journal of systematic and evolutionary microbiology 2001; 51: 1805-1808.

Stumm W, Sulzberger B. The cycling of iron in natural environments: considerations based on laboratory studies of heterogeneous redox processes. Geochimica et Cosmochimica Acta 1992; 56: 3233-3257.

Su C, Zhang M, Lin L, Yu G, Zhong H, Chong Y. Reduction of iron oxides and microbial community composition in iron-rich soils with different organic carbon as electron donors. International Biodeterioration & Biodegradation 2020; 148: 104881.

Su JF, Zhang H, Huang TL, Wei L, Li M, Wang Z. A new process for simultaneous nitrogen and cadmium (Cd (II)) removal using iron-reducing bacterial immobilization system. Chemical Engineering and Processing-Process Intensification 2019; 144: 107623.

Sulzberger B, Suter D, Siffert C, Banwart S, Stumm W. Dissolution of Fe (III)(hydr) oxides in natural waters; laboratory assessment on the kinetics controlled by surface coordination. Marine Chemistry 1989; 28: 127-144.

Sun M, Xiao T, Ning Z, Xiao E, Sun W. Microbial community analysis in rice paddy soils irrigated by acid mine drainage contaminated water. Applied microbiology and biotechnology 2015; 99: 2911-2922.

Sung Y, Fletcher KE, Ritalahti KM, Apkarian RP, Ramos-Hernández N, Sanford RA, et al. *Geobacter lovleyi* sp. nov. strain SZ, a novel metal-reducing and tetrachloroethene-dechlorinating bacterium. Applied and Environmental Microbiology 2006; 72: 2775-2782.

Swedlund PJ, Webster JG, Miskelly GM. The effect of SO4 on the ferrihydrite adsorption of Co, Pb and Cd: ternary complexes and site heterogeneity. Applied Geochemistry 2003; 18: 1671-1689.

Swedlund PJ, Webster JG, Miskelly GM. Goethite adsorption of Cu (II), Pb (II), Cd (II), and Zn (II) in the presence of sulfate: properties of the ternary complex. Geochimica et Cosmochimica Acta 2009; 73: 1548-1562.

**T**

Tadic M, Citakovic N, Panjan M, Stanojevic B, Markovic D, Jovanovic Đ, et al. Synthesis, morphology and microstructure of pomegranate-like hematite (α-Fe2O3) superstructure with high coercivity. Journal of alloys and compounds 2012; 543: 118-124.

Tardy Y, Nahon D. Geochemistry of laterites, stability of Al-goethite, Al-hematite, and Fe3+-kaolinite in bauxites and ferricretes: an approach to the mechanism of concretion formation. American Journal of Science 1985; 285: 865-903.

Taylor R. Formation and properties of Fe (II) Fe (III) hydroxy-carbonate and its possible significance in soil formation. Clay minerals 1980; 15: 369-382.

Teal TK, Lies DP, Wold BJ, Newman DK. Spatiometabolic stratification of *Shewanella oneidensis* biofilms. Applied and Environmental Microbiology 2006; 72: 7324-7330.

Tebo BM, Obraztsova AY. Sulfate-reducing bacterium grows with Cr (VI), U (VI), Mn (IV), and Fe (III) as electron acceptors. FEMS Microbiology Letters 1998; 162: 193-199.

Tepari EA, Nakhla G, Haroun BM, Hafez H. Co-fermentation of carbohydrates and proteins for biohydrogen production: Statistical optimization using Response Surface Methodology. International Journal of Hydrogen Energy 2019.

Tessier A, Campbell PG, Bisson M. Sequential extraction procedure for the speciation of particulate trace metals. Analytical chemistry 1979; 51: 844-851.

Thompson A, Chadwick OA, Boman S, Chorover J. Colloid mobilization during soil iron redox oscillations. Environmental science & technology 2006a; 40: 5743-5749.

Thompson A, Chadwick OA, Rancourt DG, Chorover J. Iron-oxide crystallinity increases during soil redox oscillations. Geochimica et Cosmochimica Acta 2006b; 70: 1710-1727.

Thormann KM, Saville RM, Shukla S, Pelletier DA, Spormann AM. Initial phases of biofilm formation in *Shewanella oneidensis* MR-1. Journal of bacteriology 2004; 186: 8096-8104.

Thouin H, Le Forestier L, Gautret P, Hube D, Laperche V, Dupraz S, et al. Characterization and mobility of arsenic and heavy metals in soils polluted by the destruction of arsenic-containing shells from the Great War. Science of the Total Environment 2016; 550: 658-669.

Tiedje JM. Shewanella—the environmentally versatile genome. Nature biotechnology 2002; 20: 1093-1094.

Toffin L, Bidault A, Pignet P, Tindall B, Slobodkin A, Kato C, Prieur D. *Shewanella profunda* sp. nov., isolated from deep marine sediment of the Nankai Trough. International Journal of Systematic and Evolutionnary Microbiology 2004, 54 : 1943-1949.

Todorova SG, Costello AM. Design of Shewanella-specific 16S rRNA primers and application to analysis of *Shewanella* in a minerotrophic wetland. Environmental microbiology 2006; 8: 426-432.

Tomaszewski EJ, Lee S, Rudolph J, Xu H, Ginder-Vogel M. The reactivity of Fe (II) associated with goethite formed during short redox cycles toward Cr (VI) reduction under oxic conditions. Chemical Geology 2017.

Tor JM, Lovley DR. Anaerobic degradation of aromatic compounds coupled to Fe (III) reduction by *Ferroglobus placidus*. Environmental microbiology 2001; 3: 281-287.

Torrentó C, Urmeneta J, Edwards KJ, Cama J. Characterization of attachment and growth of Thiobacillus denitrificans on pyrite surfaces. Geomicrobiology Journal 2012; 29: 379-388.

Trolard, F., Bourrié, G., Abdelmoula, M., Refait, P., & Feder, F. (2007). Fougerite, a new mineral of the pyroaurite-iowaite group: description and crystal structure. Clays and Clay minerals, 55(3), 323-334.

Tufano KJ, Fendorf S. Confounding impacts of iron reduction on arsenic retention. Environmental Science & Technology 2008; 42: 4777-4783.

Turick C, Apel W. A bioprocessing strategy that allows for the selection of Cr (VI)-reducing bacteria from soils. Journal of Industrial Microbiology and Biotechnology 1997; 18: 247-250.

**U**

Urrutia M, Roden E, Fredrickson J, Zachara J. Microbial and surface chemistry controls on reduction of synthetic Fe (III) oxide minerals by the dissimilatory iron-reducing bacterium *Shewanella alga*. Geomicrobiology Journal 1998; 15: 269-291.

Usman M, Hanna K, Abdelmoula M, Zegeye A, Faure P, Ruby C. Formation of green rust via mineralogical transformation of ferric oxides (ferrihydrite, goethite and hematite). Applied Clay Science 2012; 64: 38-43.

**V**

Valencia-Cantero, E., Hernández-Calderón, E., Velázquez-Becerra, C., López-Meza, J. E., Alfaro-Cuevas, R., & López-Bucio, J. (2007). Role of dissimilatory fermentative iron-reducing bacteria in Fe uptake by common bean (*Phaseolus vulgaris* L.) plants grown in alkaline soil. Plant and soil, 291(1-2), 263-273.

Vandieken V, Marshall, I, Niemann, H, Engelen, B, Cypionka, H. *Labilibaculum manganireducens* gen. nov., sp. nov. and *Labilibaculum filiforme* sp. nov., Novel Bacteroidetes Isolated from Subsurface Sediments of the Baltic Sea. Frontiers in Microbiology 2018; 10.3389.

Van Scherpenzeel D, Boon M, Ras C, Hansford G, Heijnen JJ. Kinetics of ferrous iron oxidation by *Leptospirillum* bacteria in continuous cultures. Biotechnology progress 1998; 14: 425-433.

van Schie PM, Fletcher M. Adhesion of biodegradative anaerobic bacteria to solid surfaces. Applied and Environmental Microbiology 1999; 65: 5082-5088.

Venkateswaran K, Dollhopf ME, Aller R, Stackebrandt E, Nealson KH. *Shewanella amazonensis* sp. nov., a novel metal-reducing facultative anaerobe from Amazonian shelf muds. International Journal of Systematic and Evolutionary Microbiology 1998; 48: 965-972.

Vignier N, Barreau M, Olive C, Baubion E, Théodose R, Hochedez P, et al. Human infection with *Shewanella putrefaciens* and *S. algae*: report of 16 cases in Martinique and review of the literature. The American journal of tropical medicine and hygiene 2013; 89: 151-156.

Vink JP, Harmsen J, Rijnaarts H. Delayed immobilization of heavy metals in soils and sediments under reducing and anaerobic conditions; consequences for flooding and storage. Journal of soils and sediments 2010; 10: 1633-1645.

Von Canstein H, Ogawa J, Shimizu S, Lloyd JR. Secretion of flavins by *Shewanella* species and their role in extracellular electron transfer. Applied and environmental microbiology 2008; 74: 615-623.

**W**

Wang JW, Bejan D, Bunce NJ. Removal of arsenic from synthetic acid mine drainage by electrochemical pH adjustment and coprecipitation with iron hydroxide. Environmental science & technology 2003; 37: 4500-4506.

Wang, Q., & Morse, J. W. (1996). Pyrite formation under conditions approximating those in anoxic sediments I. Pathway and morphology. Marine Chemistry, 52(2), 99-121.

Wang T, Müller DB, Graedel T. Forging the anthropogenic iron cycle. Environmental science & technology 2007; 41: 5120-5129.

Wang Y-T, Chirwa E. Bioremediation of chromium by packed-bed bioreactors. Hazardous and Industrial Wastes- Proceedings of the Mid-Atlantic Industrial Waste Conference, 1996, pp. 381-388.

Wang Y, Morin G, Ona-Nguema G, Brown Jr GE. Arsenic (III) and arsenic (V) speciation during transformation of lepidocrocite to magnetite. Environmental science & technology. 2014 Dec 16;48(24):14282-90.

Wang Y, Morin G, Ona-Nguema G, Juillot F, Guyot F, Calas G, Brown Jr GE. Evidence for different surface speciation of arsenite and arsenate on green rust: an EXAFS and XANES study. Environmental science & technology. 2010 Jan 1;44(1):109-15.

Weber KA, Achenbach LA, Coates JD. Microorganisms pumping iron: anaerobic microbial iron oxidation and reduction. Nature Reviews Microbiology 2006; 4: 752-764.

Wichlacz PL, Unz RF, Langworthy TA. *Acidiphilium angustum* sp. nov., *Acidiphilium facilis* sp. nov., and *Acidiphilium rubrum* sp. nov.: acidophilic heterotrophic bacteria isolated from acidic coal mine drainage. International Journal of Systematic and Evolutionary Microbiology 1986; 36: 197-201.

Wielinga B, Mizuba MM, Hansel CM, Fendorf S. Iron promoted reduction of chromate by dissimilatory iron-reducing bacteria. Environmental science & technology 2001; 35: 522-527.

Wiesli RA, Beard BL, Johnson CM. Experimental determination of Fe isotope fractionation between aqueous Fe (II), siderite and "green rust" in abiotic systems. Chemical Geology 2004; 211: 343-362.

Wilkin R. Iron sulfide-arsenite interactions: adsorption behavior onto iron monosulfides and controls on arsenic accumulation in pyrite. 2001.

Wilkins MJ, Livens FR, Vaughan DJ, Lloyd JR. The impact of Fe (III)-reducing bacteria on uranium mobility. Biogeochemistry 2006; 78: 125-150.

Wolf M, Kappler A, Jiang J, Meckenstock RU. Effects of humic substances and quinones at low concentrations on ferrihydrite reduction by *Geobacter metallireducens*. Environmental science & technology 2009; 43: 5679-5685.

Wu W, Li B, Hu J, Li J, Wang F, Pan Y. Iron reduction and magnetite biomineralization mediated by a deep-sea iron-reducing bacterium *Shewanella piezotolerans* WP3. Journal of Geophysical Research: Biogeosciences 2011; 116.

Wu Y, Luo X, Qin B, Li F, Haggblom MM, Liu T. Enhanced Current Production by Exogenous Electron Mediators via Synergy of Promoting Biofilm Formation and the Electron Shuttling Process. Environmental Science & Technology 2020.

Muehe EM, Morin G, Scheer L, Pape PL, Esteve I, Daus B, Kappler A. Arsenic (V) incorporation in vivianite during microbial reduction of arsenic (V)-bearing biogenic Fe (III)(oxyhydr) oxides. Environmental Science & Technology. 2016 Mar 1;50(5):2281-91.

**X**

Xiao X, Wang P, Zeng X, Bartlett DH, Wang F. *Shewanella psychrophila* sp. nov. and *Shewanella piezotolerans* sp. nov., isolated from west Pacific deep-sea sediment. International journal of systematic and evolutionary microbiology 2007; 57: 60-65.

Xie J, Gu X, Tong F, Zhao Y, Tan Y. Surface complexation modeling of Cr (VI) adsorption at the goethite–water interface. Journal of colloid and interface science 2015; 455: 55-62.

Xinjun W, Xueping C, Jing Y, Zhaosu W, Guoxin S. Effect of microbial mediated iron plaque reduction on arsenic mobility in paddy soil. Journal of Environmental Sciences 2009; 21: 1562-1568.

**Y**

Yan B, Wrenn BA, Basak S, Biswas P, Giammar DE. Microbial reduction of Fe (III) in hematite nanoparticles by *Geobacter sulfurreducens*. Environmental science & technology 2008; 42: 6526-6531.

Yan W, Wang H, Jing C. Adhesion of *Shewanella oneidensis* MR-1 to goethite: a two-dimensional correlation spectroscopic study. Environmental Science & Technology 2016; 50: 4343-4349.

Yang G, Lin J, Zeng EY, Zhuang L. Extraction and characterization of stratified extracellular polymeric substances in *Geobacter* biofilms. Bioresource technology 2019; 276: 119-126.

**Z**

Zachara JM, Fredrickson JK, Li S-M, Kennedy DW, Smith SC, Gassman PL. Bacterial reduction of crystalline Fe (super 3+) oxides in single phase suspensions and subsurface materials. American mineralogist 1998; 83: 1426-1443.

Zachara JM, Fredrickson JK, Smith SC, Gassman PL. Solubilization of Fe (III) oxide-bound trace metals by a dissimilatory Fe (III) reducing bacterium. Geochimica et Cosmochimica Acta 2001; 65: 75-93.

Zachara JM, Kukkadapu RK, Fredrickson JK, Gorby YA, Smith SC. Biomineralization of poorly crystalline Fe (III) oxides by dissimilatory metal reducing bacteria (DMRB). Geomicrobiology Journal 2002; 19: 179-207.

Zegeye A, Ona-Nguema G, Carteret C, Huguet L, Abdelmoula M, Jorand F. Formation of hydroxysulphate green rust 2 as a single iron (II-III) mineral in microbial culture. Geomicrobiology Journal. 2005 Oct 1;22(7-8):389-99.

Zegeye A, Ruby C, Jorand F. Kinetic and thermodynamic analysis during dissimilatory γ-FeOOH reduction: formation of green rust 1 and magnetite. Geomicrobiology Journal 2007; 24: 51-64.

Zeng X, Zhang Z, Li X, Jebbar M, Alain K, Shao Z. *Caloranaerobacter ferrireducens* sp. nov., an anaerobic, thermophilic, iron (III)-reducing bacterium isolated from deep-sea hydrothermal sulfide deposits. International journal of systematic and evolutionary microbiology 2015; 65: 1714-1718.

Zhang C, Ge Y, Yao H, Chen X, Hu M. Iron oxidation-reduction and its impacts on cadmium bioavailability in paddy soils: a review. Frontiers of Environmental Science & Engineering 2012; 6: 509-517.

Zhang C, Yu Z, Zeng G, Huang B, Dong H, Huang J, et al. Phase transformation of crystalline iron oxides and their adsorption abilities for Pb and Cd. Chemical Engineering Journal 2016; 284: 247-259.

Zhang Q, Zhang L, Liu T, Liu B, Huang D, Zhu Q, et al. The influence of liming on cadmium accumulation in rice grains via iron-reducing bacteria. Science of The Total Environment 2018; 645: 109-118.

Zhou J. The development of molecular tools for the evaluation of the bioremediation of chlorinated solvents: Utah State University, 2008.

Zhou Z, Muehe EM, Tomaszewski EJ, Lezama-Pacheco J, Kappler A, Byrne JM. Effect of Natural Organic Matter on the Fate of Cadmium During Microbial Ferrihydrite Reduction. Environmental Science & Technology 2020; 54: 9445-9453.

Zhu Y, Wang H, Li X, Hu C, Yang M, Qu J. Characterization of biofilm and corrosion of cast iron pipes in drinking water distribution system with UV/Cl2 disinfection. Water research 2014; 60: 174-181.

Zhuang K, Izallalen M, Mouser P, Richter H, Risso C, Mahadevan R, et al. Genome-scale dynamic modeling of the competition between *Rhodoferax* and *Geobacter* in anoxic subsurface environments. The ISME journal 2011; 5: 305-316.

Ziemke F, Höfle MG, Lalucat J, Rossellö-Mora R. Reclassification of *Shewanella putrefaciens* Owen's genomic group II as *Shewanella baltica* sp. nov. International Journal of Systematic and Evolutionary Microbiology 1998; 48: 179-186.

Zinder B, Furrer G, Stumm W. The coordination chemistry of weathering: II. Dissolution of Fe (III) oxides. Geochimica et Cosmochimica Acta 1986; 50: 1861-1869.

# List of Figures

## Chapter I



## Chapter II

## Chapter III



## Chapter IV

**Chapter V**

# List of Tables

## Chapter I



## Chapter II



## Chapter III



## Chapter IV



## Chapter V

# Annex 1

**Accepted:**

# Impact of Fe(III) (oxyhydr)oxides Mineralogy on Iron Solubilisation and Associated Microbial Communities

**F. Zhang[1,2], F. Battaglia-Brunet[1,2,] J. Hellal[2], C. Joulian[2], P. Gautret[1], M. Motelica-Heino[1]**

[1]Univ. Orléans, CNRS, BRGM, ISTO, UMR 7327, F-45071, Orléans, France

[2]BRGM, 3 avenue Claude Guillemin, 45060 Orléans cedex 02, France

*** Correspondence:**
Fabienne Battaglia-Brunet
f.battaglia@brgm.fr

**Keywords: iron-reducing bacteria[1], *Shewanella*[2], *Geobacter*[3], iron (oxyhydr)oxides[4], solubilisation[5]**

## Abstract

Iron-reducing bacteria (IRB) are strongly involved in Fe cycling in surface environments. Transformation of Fe and associated trace elements is strongly linked to the reactivity of various iron minerals. Mechanisms of Fe (oxyhydr)oxides bio-reduction have been mostly elucidated with pure bacterial strains belonging to *Geobacter* or *Shewanella* genera, whereas studies involving mixed IRB populations remain scarce. The present study aimed to evaluate the iron reducing rates of IRB enriched consortia originating from complex environmental samples, when grown in presence of Fe (oxyhydr)oxides of different mineralogy. The abundances of *Geobacter* and *Shewanella* were assessed in order to acquire knowledge about the abundance of these two genera in relation to the effects of mixed IRB populations on kinetic control of mineralogical Fe (oxyhydr)oxides reductive dissolution. Laboratory experiments were carried out with two freshly synthetized Fe (oxyhydr)oxides presenting contrasting specific surfaces, and two defined Fe-oxides, i.e., goethite and hematite. Three IRB consortia were enriched from environmental samples from a riverbank subjected to cyclic redox oscillations related to flooding periods (Decize, France): an unsaturated surface soil, a flooded surface soil and an aquatic sediment, with a mixture of organic compounds provided as electron donors. The consortia could all reduce iron-nitrilotriacetate acid (Fe(III)-NTA) in 1-2 days. When grown on Fe (oxyhydr)oxides, Fe solubilisation rates decreased as follows: fresh Fe (oxyhydr)oxides > goethite > hematite. Based on a bacterial *rrs* gene fingerprinting approach (CE-SSCP), bacterial community structure in presence of Fe(III)-minerals was similar to those of the site sample communities from which they originated but differed from that of the Fe(III)-NTA enrichments. *Shewanella* was more abundant than *Geobacter* in all cultures. It's abundance was higher in presence of the most efficiently reduced Fe (oxyhydr)oxide than with other Fe(III)-minerals. *Geobacter* as a proportion of the total community was highest in the presence of the least easily solubilized Fe (oxyhydr)oxides. This study highlights the influence of Fe mineralogy on the abundance of *Geobacter* and *Shewanella* in relation to Fe bio-reduction kinetics in presence of a complex mixture of electron donors.

## Introduction

Fe (oxyhydr)oxides are ubiquitous components in several compartments of the critical zone (e.g., soils, sediments and aquifers) and are present in many different mineralogical forms. Understanding biogeochemical behavior and Fe cycling is fundamental for many scientific communities (Bonneville et al., 2004; Roden et al., 2004). Indeed, the mobility of associated trace elements (TE) is partly controlled by Fe speciation, mineralogy and reactivity (Cornell and Schwertmann, 2003). The natural solubility of crystalline Fe (oxyhydr)oxides is low. However, the interaction with microbes and organic substances can enhance the formation of soluble Fe(III) and increase the availability of Fe and associated TE (Colombo et al., 2014). Many biogeochemical aspects of Fe cycling, including the major microbially mediated and abiotic reactions, have been extensively covered (Melton et al., 2014), together with Fe redox transformations and availability of TE (Zhang et al., 2012), as well as Fe redox cycling in bacteriogenic Fe oxide-rich sediments (Gault et al., 2011). In aerobic environments at circumneutral pH conditions, Fe is generally relatively stable and highly insoluble in the form of (oxyhydr)oxides (e.g., $Fe(OH)_3$, FeOOH, $Fe_2O_3$). However, in anaerobic conditions these minerals can be reductively dissolved (Roden and Wetzel, 2002; Roden et al., 2004) by microbial and abiotic pathways (Bonneville et al., 2004; Hansel et al., 2004; Thompson et al., 2006; Shi et al., 2016). In particular, reductive dissolution of Fe (oxyhydr)oxides can be driven by dissimilatory iron-reducing bacteria (DIRB), significantly contributing to biogeochemical cycling of Fe and subsequent TE mobilisation (Cooper et al., 2006; Ghorbanzadeh et al., 2017; Levar et al., 2017). Microbial dissimilatory iron reduction (DIR) is a ubiquitous biogeochemical process in suboxic environments (Lovley, 2000; Crosby et al., 2005; Wilkins et al., 2006; Schilling et al., 2019). DIRB use Fe (oxyhydr)oxides as electron acceptors instead of oxygen for oxidizing organic matter. Moreover, the rate of Fe(III) reduction will also influence mobility of TE initially immobilized on or in Fe (oxyhydr)oxides through adsorption or co-precipitation. Crystallinity, specific surface area and size among other factors may influence reactivity of Fe (oxyhydr)oxides in relation to the metabolic activity and diversity of DIRB (Cutting et al., 2009; Aino et al., 2018).

The role of iron-reducing bacteria (IRB) in Fe redox transformations has been evidenced for more than three decades (Lovley et al., 1987; Lovley, 1991; Stern et al., 2018; Meile and Scheibe, 2019; Su et al., 2020), during which more than 100 distinct IRB species have been found. However, *Geobacter* and *Shewanella* are the two most studied IRB genera up to now (Li et al., 2012; Han et al., 2018; Engel et al., 2019; Jiang et al., 2020). Some studies have focused on the observation of secondary mineral formation in presence of *Geobacter* or *Shewanella* strains during the bio-transformation of amorphous, poorly crystalline and highly crystalline iron (oxyhydr)oxides i.e., ferric (ferrihydrite, goethite, hematite, lepidocrocite), ferrous (siderite, vivianite), and mixed valence (magnetite, green rust) (Fredrickson et al., 1998; Zachara et al., 2002; Han et al., 2018). Moreover, molecular mechanisms that occur during Fe reduction have been characterized by electro microbiology for *Geobacter* and *Shewanella* (Nealson, 2017; Shi et al., 2019). Additionally, IRB communities may be influenced by initial Fe mineralogy and the nature of available electron donors. Lentini et al., (2012) compared IRB cultures obtained with different organic substrates, i.e., glucose, lactate and acetate, and different Fe(III)-minerals, i.e., ferrihydrite, goethite and hematite. Type of electron donor was the most important factor influencing community structure, that also varied with the nature of the Fe(III)-mineral. The availability of carbon sources, other than acetate, induced the

development of sulfate-reducing bacteria, that could indirectly dissolve Fe(III)-minerals through the production of $H_2S$, whereas acetate alone induced the dissolution of ferrihydrite and the development of *Geobacter*. Hori et al., (2015) obtained IRB enrichments from diverse environments with only acetate that favored the selection and isolation of organisms belonging to the *Geobacter* genus. Acetate is a common small organic acid that cannot support fermentation, thus its consumption is generally linked to respiratory mechanisms. However, mixtures of organic substrates can be found in soils and sediments. In order to obtain complementary information on complex IRB communities that could be helpful to make the link with previous experiments involving pure strains only, the present study was performed with a mixture of simple (acetate, formate, lactate, glucose) and complex (peptone) electron donors and focused on the abundance of the two model genera, *Geobacter* and *Shewanella*, in bacterial communities originating from natural environments. Bio-reduction of four different Fe (oxyhydr)oxides presenting contrasting specific surfaces, crystallinity and solubility features, i.e., two freshly synthetized Fe (oxyhydr)oxides, and the two defined Fe-oxides goethite and hematite, was investigated with the obtained IRB enrichments. The objective of this experiment was to assess (1) the dissolution rate of these minerals in presence of mixed IRB communities while inhibiting sulfate reduction, and (2) the influence of the type of Fe(III)-mineral on the relative abundances of *Shewanella* and *Geobacter*, when a complex mixture of organic substrates is provided.

## Materials and Methods

### 1.1 Soil and sediment sampling and enrichment of iron-reducing bacteria (IRB)

Soils and riverbanks periodically subjected to flooding and thus to cyclic redox oscillations represent one of the surface environments where IRB should actively contribute to Fe bio-reduction. This study was based on IRB enrichments from soil and sediment samples from a riverbank, in a site already studied in terms of Fe and TE total concentration profiles in sediment cores (Dhivert et al., 2015). The sampling site is located in a Loire river channel, in Decize, France (Dhivert et al., 2015). Three samples were collected using an auger and stored under a $N_2$ atmosphere: soil from the riverbank (10-15 cm depth), soil from flooded ground (0-7 cm depth) and under-water sediment (7-17 cm depth), which were named D1, D2 and D3, respectively. In order to obtain cultures enriched in Fe(III)-reducing bacteria, enrichment medium containing Fe(III) as electron acceptor and Na-molybdate to inhibit the development of sulfate-reducing bacteria was used. 10 g of each soil sample were inoculated into 200 mL basic medium (composition detailed in the **Supplementary Figure S2**, Huguet, 2009; Lovley, 2006) autoclaved (121°C, 20 min) then flushed with sterile $N_2$ just after autoclaving. The headspace of vials (small volume because 200 mL bottles were used) was $N_2$. The following components were added to this medium: 10 mM of Fe(III) Nitrilotriacetic Acid as electron acceptor, 1.5 $g \cdot L^{-1}$ peptone, 10 mM of acetate, lactate, and formate, 2 mM glucose as electron donors (Coates et al., 1996; Lovely et al., 1989; Kwon et al., 2016; Shelobolina et al., 2007) in anaerobic conditions, and 0.4 mM of sodium molybdate. Fe(III)-NTA (100 mM stock solution) was prepared by dissolving 1.64 g of $NaHCO_3$ in 80 ml water, adding 2.56 g $C_6H_6NO_6Na_3$ and 2.7 g $FeCl_3 \cdot 6H_2O$, bringing the solution up to 100 ml, flushing with $N_2$ and filter sterilizing (0.2 µm, Millex -GP Syringe Filter, 33 mm diameter) into a sterile, anaerobic serum bottle. Sterilization of the electron donors was performed by autoclaving for acetate, lactate and

formate, and filtration at 0.2 µm for peptone and glucose. Sodium molybdate was autoclaved. All stock solutions were kept anaerobic under $N_2$ after sterilization. Cultures were incubated at 20°C under agitation (100 rpm) for 10 days. Samples (1.5-2 mL) were collected in an anaerobic glove box, filtered at 0.45 µm (Millex -GP Syringe Filter, 33 mm diameter) and analyzed for Fe(II) content in order to evaluate Fe(III) reduction. After 3-5 steps of sub-culturing (inoculation at 10% in fresh medium, every two weeks), the three Fe-reducing cultures were able to reduce 10 mM Fe(III) into 1-2 days, and were used as inocula for the following IRB incubation experiments (see 2.3).

## 1.2 Fe(III) (oxyhydr)oxides

Two fresh Fe (oxyhydr)oxides were synthesized in the laboratory under the modified protocol of (Schwertmann and Cornell, 2008). The Fe (oxyhydr)oxide named FoF was prepared according to the protocol for ferrihydrite, by dissolving 40 g $Fe(NO_3)_3 \cdot 9H_2O$ in 500 mL distilled water and adding 330 mL of 1 M KOH to adjust the pH to 7-8. The mixture was centrifuged at 5,000 rpm for 10 min and the supernatant was subsequently removed. The solid fraction was then washed 5 times with ultrapure water according to MilliQ quality. The Fe (oxyhydr)oxide named FoL was prepared according to the protocol for lepidocrocite with 11.93 g of unoxidized $FeCl_2 \cdot 4H_2O$ salts dissolved into 300 mL distilled water by stirring. The solution was adjusted to pH 6.7-6.9 with NaOH using a pH-stat under aeration (100 mL/min air). Washing was performed as described for FoF. Both synthesized minerals were freeze-dried. Goethite from Sigma-Aldrich (CAS No. 20344-49-4) and hematite from VWR Chemicals (CAS No. 1309-37-1) were also used. Mineralogical morphologies of all Fe (oxyhydr)oxides were characterized using a scanning electron microscope (SEM) and Brunauer, Emmett and Teller (BET) surface area measurement (determined by multipoint BET $N_2$ adsorption) (Brunauer et al., 1938). Specific surface areas were determined from $N_2$ adsorption isotherms in the best linear range (with a minimum of 15 points) between the relative pressure P/Po 0.03 and 0.33 (Cavelan et al., 2019).

Specific surface areas of Fe (oxyhydr)oxides varied from 11.7 to 337 $m^2.g^{-1}$ (Table 1), and compared well to some other synthetic (oxyhydr)oxides (Larsen and Postma, 2001; Bonneville et al., 2004; Pedersen et al., 2005; Das et al., 2013). SEM was performed on a TM 3000 coupled to a SwiftED3000 X-Stream module (Hitachi), and operated at 15 kV accelerating voltage (Thouin et al., 2016). The corresponding observed morphologies (Supplementary Figure S1) are given in Table 1.

**“Insert Table 1”**

## 1.3 IRB incubation experiments

Incubation experiments were performed in 50 mL glass bottles containing 50 mL medium, equipped with chlorobutyl rubber stoppers, using 10 % (v/v) of inocula from D1, D2 and D3 (see 2.1) enriched from the site samples of Decize and the four Fe (oxyhydr)oxides presenting contrasting specific surfaces (FoF, FoL, goethite and hematite), under anaerobic conditions. The compositions of the different solutions used to prepare the culture medium were the same as for the enrichment cultures and are also listed in **Supplementary Figure S2**. The total Fe(III)

concentration added as Fe (oxyhydr)oxides was adjusted to be close to 20 mM, as Fe(III)-NTA or solid iron oxides, based on the theoretical formula of each (**Supplementary Table S1**). The inoculation of Fe-reducing cultures was performed in an anaerobic glove box. The gas phase of the bottles was $N_2$ and the bottles were flushed with $N_2$ before and after sampling. The flasks were incubated at 20°C, under agitation (100 rpm). Not inoculated controls were prepared in the same conditions. Samples (1.5-2 mL) were collected as described in 2.1 and analyzed for $[FeT]_D$. The Fe solubilisation rates were calculated using the data of $[FeT]_D$ collected during the first phase of the incubation, when this parameter increased linearly. After 27 days incubation, the remaining cultures were centrifuged at 5,000 rpm for 10 min. Supernatants were removed and solids freeze-dried for observation under SEM-XEDS.

## 1.4 Fe analyses and pH/Eh

For Fe analyses, 1.5 mL aliquot was sampled with a syringe and filtered through a 0.2 µm filter into 5 mL tubes and immediately acidified with concentrated HCl in the glove box. $[FeII]_D$ (dissolved Fe(II) concentration) was determined using the ortho-phenanthroline colorimetry method (Murti et al., 1966; Mamindy-Pajany et al., 2013). $[FeT]_D$ (total dissolved iron concentration) was determined using the same method but with the addition of hydroquinone to reduce dissolved $[FeIII]_D$ into $[FeII]_D$. pH and redox potential (Eh, ref. Ag/AgCl) were measured in samples taken from the incubation flasks using standard hand-held portable meters (WTW Multi340i set) in glove box before and after the incubation.

## 1.5 DNA extraction and qPCR of 16S rRNA genes

DNA extractions were performed on all samples at the end of the experiments. Biomass was harvested by centrifugation at 10,000 rpm for 10 min of 2 mL of culture. Microbial DNA was extracted using the Fast DNA™ SPIN Kit for Soil (MP Biomedicals, USA) according to the manufacturer's instructions. The integrity of the DNA products was checked with agarose gel electrophoresis. The DNA concentrations were determined with a Quantus™ Fluorometer (Promega, USA).

Quantification of *Shewanella* and *Geobacter* were performed by quantitative PCR (qPCR) of a fragment of the gene encoding 16S rRNA (*rrs* gene) (abbreviated *Shewanella* 16S and *Geobacter* 16S), using a CFX96 Touch™ Real-Time PCR Detection System (Bio Rad, USA). Primers Sw 640-F (5'-RAC TAG AGT CTT GTA GAG G-3') and Sw 815-R (5'-AAG DYA CCA AAY TCC GAG TA-3') specific to *Shewanella rrs* gene (Snoeyenbos-West et al., 2000; Li et al., 2018), and primers Geo 564-F (5'-AAG CGT TGT TCG GAW TTA T-3') and Geo 840-R (5'-GGC ACT GCA GGG GTC AAT A-3') specific to *Geobacter rrs* gene (Kim et al., 2012) were used. qPCR reactions were performed in a total volume of 20 µL containing: 7.68 µL of sterile nuclease- and nucleic acids-free water, 10 µL of SSO Advanced Universal SYBR Green Supermix (Bio-Rad), 0.16 µL of each primer at 50 µM, and 2 µL of DNA (1-5 ng·µL$^{-1}$). qPCR reaction programs were as follows: for *Shewanella*, 1 min at 95°C, followed by 40 cycles: 5s at 95°C/30s at 55°C/30s at 72°C/30s at 80°C; for *Geobacter*, 2 min at 95°C, followed by 45 cycles: 10s at 95°C/20s at 60°C/20s at 72°C/30 s at 80°C. Plasmid DNA containing the target genes were constructed from *Shewanella putrefaciens* and *Geobacter metallireducens rrs* gene, PCR amplified with primers 640F/815R and 564F/840R, respectively, and cloned using the TOPO™ TA Cloning™ Kit for Sequencing (Invitrogen, USA) according to the instructions. A calibration curve was obtained from serial dilutions of a known quantity of linearized plasmids

containing known copy numbers of *Shewanella putrefaciens* or *Geobacter metallireducens rrs* genes. All samples, controls and standards were analyzed in duplicates. Results were reported as gene copies per gram or microliter of culture. Generation of a specific PCR product was confirmed by DNA melting curve analysis and agarose gel electrophoresis.

Quantification of the bacterial *rrs* gene coding 16S rRNA (abbreviated bacterial 16S), was performed with primers 341-F (5'-CCT ACG GGA GGC AGC AG-3') and 515-R (5'-TGC CAG CAG CCG CGG TAA T-3'), as described for *Shewanella* and *Geobacter* except 0.2 µL T4GP32 at 500 ng·µL$^{-1}$ was added into the reaction mixture. qPCR reaction program was as follows: 3 min at 95°C, followed by 35 cycles: 30s at 95°C/30s at 60°C/30s at 72°C/30s at 80°C. Plasmid DNA containing the bacterial *rrs* gene of *Pseudomonas putida* KT 2440 was 10-fold serially diluted to obtain a calibration curve of known copy numbers of *Pseudomonas putida* KT 2440 *rrs* gene.

## 1.6 CE-SSCP fingerprints

CE-SSCP (Capillary Electrophoresis-Single Strand Conformational Polymorphism, Delbes et al., 2000) profiles were performed in order to characterize the bacterial community structure in cultures. About 200 bp of the V3 region of the bacterial *rrs* gene was amplified from DNA extracts with the forward primer w49 (5′-ACGGTCCAGACTCCTACGGG-3′; *E. coli* position, 331) and the reverse primer w34 (5′-TTACCGCGGCTGCTGGCAC-3′; *E. coli* position, 533), 5′end labelled with the fluorescent dye FAM, using 25 cycles, hybridization at 61°C, and 30 s elongation at 72°C. One µL of diluted (20 or 50 fold in nuclease-free water) PCR product was added to a mixture of 18.6 µL of deionized formamide and 0.4 µL of Genescan-600 LIZ internal standard (Applied Biosystems). To obtain single-strand DNA, samples were heat-denaturized for 5 min at 95°C, and immediately cooled on ice. CE-SSCP analyses were performed on an ABI Prism 310 genetic analyzer using a 47-cm length capillary, a non-denaturating 5.6 % CAP polymer (Applied Biosystems) and the following electrophoresis conditions: run temperature 32°C, sample injection for 5 s at 15 kV, data collection for 35 min at 12 kV. CE-SSCP data analyzes and lining CE-SSCP profiles up to the internal standard and to a common baseline were performed using BioNumerics V7.5 (Applied Maths).

## 1.7 Determination of iron oxides solubilisation parameters

The total dissolved Fe (Fe solubilisation) was calculated from the $[FeT]_D$ curves during all the incubation period for the batch experiments. The initial Fe reduction rate (mg L$^{-1}$·h$^{-1}$) was calculated for the period of rapid increase of $[FeT]_D$ during the first stage (3-8 days) of the batch experiments. The total dissolved Fe and initial Fe (oxyhydr)oxide dissolution rates are indicated as “Fe solubilisation” and “solubilisation rate” in the following statistics.

## 1.8 Statistics

DNA quantification and qPCR data were analyzed using a Kruskal-Wallis test with XLSTAT software (version 2019 21.1.3) to determine the significant differences between each culture or between iron oxides. Variations in bacterial community structure were further analyzed by Non-Metric multiDimensional Scaling –nMDS) and ANOSIM analysis applied to a Bray-Curtis dissimilarity matrix of CE-SSCP data (generated in BioNumerics V7.5), using R-Studio software (Vegan Package) (Team R, 2015).

Principal component analysis (PCA) was used to summarize the relationships between chemical (Fe-reducing speed for the first few days and Fe reduction proportion) and microbial (molecular biomass, i.e., DNA concentration, and *Geobacter* and *Shewanella* gene abundances) data with XLSTAT software (version 2019 21.1.3).

# 2 Results

## 2.1 Dissolution of Fe (oxyhydr)oxides

**"Insert Figure 1"**

Fe (oxyhydr)oxide solubilisation in the incubations was mainly influenced by the type of Fe (oxyhydr)oxide. For all cultures, D1 (Fig.1 a), D2 (Fig.1 b) and D3 (Fig.1 c), the highest iron solubilisation rates were observed in presence of FoL. The iron solubilisation rates during the first week of the experiment, regardless of mineral structure, roughly matched the order of specific surface area except for goethite/hematite with D1 and D2 (**Supplementary Table S2**). In abiotic control flasks, iron dissolution remained lower than 0.4 %.

Initial pH of the medium was close to 7.5. This parameter did not significantly change during the incubation in presence of FoL and goethite. The final pH increased slightly to 7.6 in presence of FoF and decreased to 7.4 in presence of hematite. The initial Eh was -30 mV (ref. Ag/AgCl). This parameter decreased to -230 ±10 mV after incubation in presence of bacteria. In abiotic control flasks, the Eh value decreased down to -130 mV.

**"Insert Figure 2"**

According to the $[FeT]_D$ during the incubation period, total dissolved Fe from Fe (oxyhydr)oxides was calculated (Fig.2). Considering that total Fe provided as Fe minerals was close to 20 mM, the percentage of Fe solubilisation was in the range from 1 to 15 %. The highest quantities of dissolved Fe were obtained for FoL, with 0.074 mg iron per mL with D3 inoculum. The extent of FoL solubilisation was more than 3 times higher than that of hematite with the same inoculum. For goethite, low solubilisation, around 0.022 mg iron per mL, were obtained, with no significant differences between the three inocula. Moreover, when Fe (oxyhydr)oxides are grouped without distinguishing the origin of the inocula, the solubilisation of FoL was significantly different to that of goethite and hematite (Fig.2), and that of FoF was significantly different to that of hematite. For the same data set, the significant differences shown between the different inocula (**Supplementary Figure S4**) shows that for both D1 and D2, FoL solubilisation was significantly different to that of hematite. However, there was no significant difference in iron solubilisation between iron oxides with D3. This suggests that D3 could be less influenced by Fe mineralogy than the other two inocula.

## 2.2 Biological parameters

### 2.2.1 Soil samples

The ratio of gene copies of *Shewanella* and *Geobacter* (Fig.4 b) over total bacterial abundance increased from D1 to D2 and D3. Globally, *Geobacter* was clearly present in higher proportions

than *Shewanella* in the bacterial communities present in the environmental samples used to enrich D1, D2 and D3.

### 2.2.2 Effect of Fe (oxyhydr)oxides on bacterial community structure

The bacterial community structure profiles of the initial soil and sediment samples, the Fe-NTA enrichments and the cultures in presence of the four different (oxyhydr)oxides were compared using an nMDS ordination approach (Fig.3). Full CE-SSCP profiles are available in **Supplementary Figure S5**. These profiles show a high diversity with many peaks.

**"Insert Figure 3"**

The structures of the initial communities were modified after inoculation on solid Fe (oxyhydr)oxides (Fig.3): enrichments on Fe(III)-NTA are grouped on the right side of the representation, whereas communities obtained by cultures with iron oxides are gathered on the left side. The three initial communities from environmental samples are located between these two poles. No clear separation is observed between the communities obtained with the four pure iron oxides. Although, according to ANOSIM analysis, no significant difference in community composition was found between initial inoculums (significance >0.05), a significant dissimilarity was found between community origins (i.e. initial soils and form of Fe(III) provided to the consortia) (R = 0.345 and significance = 0.0249).

### *2.2.3* Bacterial abundance and abundances of *Shewanella* and *Geobacter*

**"Insert Figure 4"**

The *rrs* gene abundances and *Shewanella* 16S/bacterial 16S ratio did not highlight any significant differences between the three initial enrichments D1, D2 and D3 (Fig.4). As shown in Fig.4 (a), globally, the *rrs* gene abundance in goethite samples was significantly different to FOF samples. It decreased in iron oxide cultures compared with Fe(III)-NTA cultures (**Supplementary Figure S6**). Conversely, the abundance of the two quantified IRB, i.e., *Geobacter* and *Shewanella*, differ between the types of Fe oxides provided as Fe(III) source (Fig.4 c and e). Globally, compared with *Geobacter*, *Shewanella* was present in a larger proportion in all bacterial communities with the four iron oxides. Moreover, the number of gene copies of *Shewanella* for FoL is significantly different in presence of other iron oxides but there are no significant differences between the cultures for FoF, goethite and hematite samples. When the type of inocula is not taken into account, the proportion of *Shewanella* 16S genes for FoL samples is significantly different for goethite samples.

Considering specifically each quantified genus, the cultures in presence of goethite inoculated with D3 bacteria contained a significantly different proportion of *Geobacter* 16S genes than the same culture (D3) with FoL (Fig.4 f). In the other conditions (D1, D2 with all oxides), no significant differences between the proportion of *Geobacter* 16S genes in the global bacterial population was observed.

# 3 Discussion

## 3.1 Influence of the type of iron oxide on bacterial iron solubilisation

FoL and FoF were synthetized in the laboratory and were more amorphous, thus more reactive, than goethite and hematite (Usman et al., 2012). According to the literature, abiotic rates of reductive iron dissolution are correlated with the solubility of Fe (oxyhydr)oxides (Larsen and Postma, 2001). The rates of this abiotic reductive bulk dissolution decrease according to ferrihydrite >lepidocrocite> goethite> hematite, emphasizing the importance of the crystal structure on the dissolution rate (Larsen and Postma, 2001). However, Roden (2006) found that in presence of IRB, oxides' mineralogical and thermodynamical properties exert a minor influence on reduction rates compared with the abundance of available oxide surface sites controlled by oxide surface areas and the accumulation of surface-bound biogenic Fe(II). This last process, of the precipitation of new Fe(II) minerals (Urrutia et al., 1998; Zachara et al., 2002), could explain the late decrease of soluble Fe (Figure 1). Present results are partially in accordance with this last hypothesis, as Fe solubilisation effectiveness increased with the specific surface, in particular for the two freshly synthesized oxides. Here, the fresh mineral prepared with the protocol of lepidocrocite (FoL) synthesis presented a higher specific surface than the mineral produced using the protocol for ferrihydrite (FoF). Synthetic lepidocrocites can present a very large range of specific surface areas, depending on their level of crystallinity (Schwertmann, 1973). In the present case, the specific area of synthetic FoL (337 $m^2.g^{-1}$) is much higher than for other Fe (oxyhydr)oxides, possibly due to a rapid oxidation of Fe(II) during synthesis that produced poor crystallization and formation of lepidocrocite impurities (Schwertmann and Taylor, 1979). Schwertmann (1973) showed that the specific surface of lepidocrocite increases with its solubility in presence of oxalate, and this specific surface area is anti-correlated with the crystallinity. In the present experiment, at the end of the incubation, we detected 8 $mg.L^{-1}$ total Fe in the FoL abiotic control, but almost no Fe in FoF abiotic control. This supports the idea that FoL was more soluble than FoF. The high specific surface area and probable poor crystallinity of FoL could have favored solubilisation by IRB.

Fe solubilisation rates were limited after a few days, probably due to evolution of the composition of the liquid medium, or the accumulation of surface-bound biogenic Fe(II) (Roden, 2006), as Fe(III) was not the limiting factor. Parameters such as humic substances, quinones and organic carbon can strongly influence microbial Fe(III) reduction rates for *Shewanella* (Adhikari et al., 2017) or *Geobacter* (Wolf et al., 2009) in natural environments. Generally, in these studies, the highest reducing rates were observed during the first few days of microbial Fe(III) reduction. In our study, the influence of the type of Fe (oxyhydr)oxides on initial iron oxide-reducing rates were consistent with those of previous studies performed with pure strains.

## 3.2 Bacterial communities

The structures of the initial bacterial communities present in the environmental samples were modified by the enrichment in Fe(III)-NTA medium, and again showed an evolution when the enrichments were grown in presence of solid Fe (oxyhydr)oxides (Fig.4). This last result could be due to the difference of bio-availability of Fe with minerals compared to Fe(III)-NTA. Cai et al., (2019) also showed an influence of bio-available Fe(III) on microbial community structure. Here, the accessibility of Fe(III) in the Fe(III)-NTA incubations favored the iron reducing community that may have rapidly consumed available organic substrates and probably lowered the development of other bacteria. With minerals, however, Fe(III) is less accessible

and competition for Fe(III) may induce changes in community structure. For example, Zhuang et al., (2011) indicated that *Rhodoferax* and *Geobacter* species were acetate-oxidizing Fe(III)-reducers that compete in anoxic subsurface environments and this competition could influence the *in situ* bioremediation of uranium-contaminated groundwater by changing diversity structure. On the other hand, no clear effect of the type of Fe mineral on the global community profile was observed. This may be linked to the culture medium composition. Indeed, the addition of diverse C sources could enable fermentative bacteria to develop without using Fe(III) for their growth. In contrast, Lentini et al., (2012) observed an effect of the type of Fe (oxyhydr)oxide, i.e., FoF, goethite or hematite, on the structure of bacterial communities in enrichment cultures using T-RFLP fingerprints. However, these authors did not use an initial Fe(III)-NTA enrichment step and did not use a sulfate-reduction inhibitor, as in our study.

## 3.3 *Geobacter* and *Shewanella* 16S genes abundances

The relative abundance of *Geobacter* and *Shewanella* in the initial soils and sediment used as sources of IRB in our experiment could be linked to the redox conditions of the environment. Indeed, *Geobacter* and *Shewanella* were present in higher proportions in the river sediment D3, than in the flooded soil D2, itself richer than the non-saturated soil D1. This suggests that the reducing conditions in the aquatic sediment was more favorable for anaerobic bacteria, such as IRB.

*Shewanella* and *Geobacter* represented in our incubation experiments a small proportion of the total community, however we made a focus on these two genera because they are the most studied iron reducing bacteria. However, the other members of the community could contribute either directly or indirectly to the iron solubilisation process. Considering the evolution of the two targeted IRB genera, namely *Geobacter* and *Shewanella*, after the enrichment with Fe(III)-NTA, the *Shewanella* / *Geobacter* abundance ratio increased significantly compared to the site samples (Figure 3 compared with Figure 5), suggesting that the presence of a large amount of bio-available Fe(III) in the enrichment culture medium was in favor of *Shewanella*. Another explanation for the sharp increase of *Shewanella* compared to *Geobacter* could be the composition of the culture medium in terms of organic substrates. *Geobacter* can use acetate as electron donors while performing the dissimilatory Fe reduction (Caccavo et al., 1994; Coates et al., 1996), but does not use lactate nor glucose. Conversely, some *Shewanella* species were shown to be able to use glucose and can present either respiratory or fermentative types of metabolisms (Nogi and Horikoshi, 1998; Ziemke et al., 1998, Ivanova et al., 2004). Lentini et al., (2012) showed that the presence of *Geobacter* was favored by acetate whereas the growth of *Shewanella* was rather stimulated by lactate. Moreover, these authors suggested that production of acetate through incomplete degradation of lactate by *Shewanella* could benefit *Geobacter* (Hori et al., 2015). Our medium contained both acetate, formate, lactate and glucose, thus it should potentially support growth of both *Shewanella* and *Geobacter*. However, a fermentative metabolism could explain the selection of *Shewanella* over *Geobacter* in our enrichments and in all incubation conditions, because this genus can grow either using fermentation or Fe(III) reduction (Bowman, 1997). Moreover, there is a multitude of other bacteria that can also explain the contribution of fermentative products, maybe some of them are in favor of *Shewanella* sp. (or spp.) but not *Geobacter* spp. As our medium contained 1.5 $g.L^{-1}$ peptone, this substrate could also favor the growth of bacteria belonging to the *Shewanella* genus.

When these communities were grown in presence of solid iron oxides, the abundance of *Shewanella* (average of D1, D2 and D3) was 112, 30, 52 and 3058 times higher than the abundance of *Geobacter*, for FoF, goethite, hematite and FoL, respectively. Moreover, we found that the cultures in presence of goethite inoculated with D3 bacteria contained higher proportions of *Geobacter* than the same culture (D3) with FoL. These results might suggest that *Geobacter* could be more favored, in the competition with other IRB such as *Shewanella*, for growth in presence of goethite and hematite than for growth in presence of the more easily dissolved oxides, i.e., FoF and FoL. The type of Fe mineral can exert a selection pressure on the communities of IRB, as previously shown by Lentini et al., (2012). This result could be linked to a higher affinity of *Geobacter* for Fe(III), that would favor this organism at low Fe(III) availability levels. Reported Ks values for Fe(III) are 1.0 mM with *G. sulfurreducens* (Esteve-Nunez et al., 2005) compared to 29 mM with *S. putrefaciens* (Liu et al., 2001).

Yet, the solubility of ferrihydrite and lepidocrocite are higher than that of goethite and hematite (Cornell and Schwertmann, 2003; Liu et al., 2007), thus the availability of Fe(III) could be higher with the first two oxides. *Shewanella* might be favored by high bio-available Fe(III), but could be less efficient for growth in presence of less soluble Fe-oxides such as goethite and hematite. The anaerobic respiration of *Shewanella* was highly dependent on electron shuttles. Nevin and Lovley (2002) suggested that *Shewanella alga* strain BrY released compounds that could solubilize Fe(III) from Fe(III) oxides, however, *Geobacter metallireducens* did not produce electron shuttles or Fe(III) chelators to solubilize Fe(III) oxides (Nevin and Lovley, 2002). Kotloski and Gralnick (2013) determined the contribution of flavin electron shuttles in extracellular electron transfer by *Shewanella oneidensis* and Wu et al., (2020) showed that exogenous electron mediators (EMs) favored high density current production and increased the synthesis of extracellular polymeric substances which promoted biofilm formation during electron shuttling process (Wu et al., 2020). The conduction of electrons along pili or other filamentous structures is one of the mechanisms proposed for electron transfer to solid iron oxides. Leang et al., (2010) showed that OmcS, a cytochrome that is required for Fe(III) reduction by *Geobacter sulfurreducens*, was localized along the pili (Leang et al., 2010). The electrically conductive pili play a major role in the adaptation of *Geobacter* to perform dissimilatory iron reduction in natural environments (Liu et al., 2019). These differences in the Fe(III)-reducing mechanisms between the two species might explain their difference of affinity for Fe(III) (Liu et al., 2001; Esteve-Nunez et al., 2005) and the relative increase of *Geobacter* abundance, observed here in presence of goethite and hematite, with the enrichment culture that was the most efficient for Fe-oxide solubilisation, i.e., culture D3.

## 3.4 Relation between iron solubilisation effectiveness and *Geobacter* and *Shewanella* abundances

In batch experiments, the three inocula D1, D2 and D3, enriched from soil from the river bank, flooded soil and an aquatic sediment of the Decize site gave similar results in terms of Fe solubilisation effectiveness of iron (oxyhydr)oxides. However, there were differences between different Fe (oxyhydr)oxides: the type of Fe (oxyhydr)oxides had more influence on Fe solubilisation effectiveness than the origin of the inocula. Fe solubilisation rates were slower with goethite and hematite compared to FoF and FoL. The same tendency was observed by Bonneville et al., (2004), who found that, with the pure strain *S. putrefaciens* in presence of 20 mM Fe(III), reduction of 6-line ferrihydrite was faster than that obtained with lepidocrocite, and faster than that obtained with low surface area hematite. Li et al., (2012) reported similar

results for the microbial reduction of Fe(III) oxides by *S. decolorationis* strain S12, the reducing speed decreasing according to the following order: lepidocrocite > goethite > hematite.

Principal Component Analysis (PCA) integrating chemical (**Supplementary Table S2**) and molecular data was performed to identify the relationships and contributions between iron solubilisation effectiveness and *Geobacter* / *Shewanella* abundances in batch experiment samples (Mercier et al., 2014; Zhu et al., 2014; Hong et al., 2015). In this study, a biplot (**Supplementary Figure S7**) summarizes PCA results. The first principal component is strongly influenced by the iron solubilisation effectiveness (higher on the right than on the left side of the representation), with higher values associated with FoL, and the lowest associated with goethite and hematite (not separated), FoF being in an intermediary position. Meanwhile proportion of *Shewanella* in the bacterial community, but not to the proportion of *Geobacter*, seems to be correlated to FoL. The second principal component reflects high values of the proportion of *Geobacter* in the bacterial communities. Thus, the proportion of *Shewanella* seems to be more correlated to iron solubilisation parameters than *Geobacter*. PCA allows clear discrimination with different groups of iron oxides, however not for the different types of inoculum (D1, D2 and D3).

According to Bonneville et al., (2004), the dissolution and solubility of goethite and hematite are lower than that of ferrihydrite and lepidocrocite in the presence of *Shewanella.* Cutting et al., (2009) indicated that hematite and goethite are susceptible to limited Fe(III) reduction in presence of *G. sulfurreducens.* Moreover, Poggenburg et al., (2016) mentioned that Fe(III)-organic compounds (coprecipitates from solutions of $FeCl_3$ and natural organic matter) reduction by *Shewanella putrefaciens* was influenced by the amount of available electron shuttling molecules induced by sorbed natural organic matter. Fe(III)-organic compounds' reduction by *Geobacter metallireducens* was more influenced by particle size, physicochemical properties and iron (oxyhydr)oxides (composition of sorbed natural organic matter and aggregation state) (Poggenburg et al., 2016). In our study, FoL samples with a higher proportion of *Shewanella* in their bacterial communities were correlated with high initial iron solubilisation rates and electron shuttling molecules might have a role in this phenomenon. In contrast, *Geobacter* was not specifically associated to FoL but was found in higher proportions with goethite in one condition. This tendency is in accordance with findings of previous research performed with the less soluble iron oxides (Crosby et al., 2007), showing that *Geobacter sulfurreducens* reduced 0.7 % hematite and 4.0 % goethite while *Shewanella putrefaciens* reduced only 0.5 % of hematite 3.1 % goethite after 280 days of incubation. Thus, our results suggest that *Geobacter* might suffer less from the competition with *Shewanella* in low bio-available Fe(III) conditions, whereas the contribution of this genus, present in lower quantities than *Shewanella*, to the iron solubilisation effectiveness is not demonstrated. Moreover, other members in the community of IRB might have potential contribution to Fe solubilisation. Our culture medium contained substrates such as glucose and peptone that could support the growth of fermentative organisms. Lentini (2012) and Gagen (2019) indicated that fermentation likely plays a key role in reduction of crystalline iron oxides by diverse species, such as *Telmatospirillum,* both through direct reduction and by the production of $H_2$, potentially used by dissimilatory iron reducers, during fermentation.

## Conclusion

Microbial enrichments containing IRB, obtained with a mixture of simple and complex electron donors, were able to grow and reduce Fe(III) in a short time. Experiments performed with fresh Fe (oxyhydr)oxides, goethite and hematite confirmed that the type of Fe mineral could influence Fe solubilisation rates and the abundances of two IRB commonly involved as pure strains in Fe-reducing experiments, i.e., *Geobacter* and *Shewanella*.

The present study's results showed that: (1) the sub-culturing of IRB enrichments from Fe(III)-NTA to pure iron oxides significantly modified the bacterial communities; (2) in our experimental conditions, bacterial diversity was not significantly different from one type of pure (oxyhydr)oxide to another; (3) the type of Fe oxide can influence the proportion of *Geobacter* and *Shewanella*. Meanwhile, the nature of Fe (oxyhydr)oxides seems to have exerted a selection on the ratio of *Geobacter* and *Shewanella*, whereas it did not impact the bacterial community fingerprints. The concentration of bio-available Fe(III) and the mixture of electron donors in the enrichment medium favored the development of *Shewanella* compared with *Geobacter* genus. However, the culture medium included a large amount of electron donors that is not representative of most natural systems. Therefore, complementary studies, performed with lower concentrations of electron donors provided in continuous feeding conditions would help to make the link with real environments. In presence of iron oxides, the highest proportions of *Shewanella* in bacterial communities were obtained with FoL and corresponded to the highest levels of iron solubilisation, possibly linked to the fact that FoL was the most soluble (oxyhydr)oxide in our experiments. This result is consistent with the hypothesis that *Shewanella* development could be favored by a high bioavailability of Fe(III). In contrast, *Geobacter* was detected in higher proportions with goethite that is less easily dissolved, when D3 culture was used.

Globally, all results suggested that both initial community composition of the sample used to prepare the enrichments, as well as the type of Fe(III) oxide used as electron acceptor influenced the final proportions and abundances of *Geobacter* and *Shewanella*. A better knowledge of complementary biological parameters associated with these two organisms, such as their activity during Fe(III) solubilisation and reduction in complex communities and distribution between planktonic and Fe(III)-mineral-attached cells, could help to elucidate their role in natural environments. As biofilms in soils and sediments contain a large part of the bacterial biomass, future research could be focused on the distribution and activity of *Geobacter* and *Shewanella* attached on iron oxides surfaces.

## Conflict of Interest

*The authors declare that the research was conducted in the absence of any commercial or financial relationships that could be construed as a potential conflict of interest*.

## Author Contributions

F. Battaglia-Brunet, J. Hellal and M. Motelica-Heino conceived and designed the experiments and arranged funds. F. Zhang performed major experiments. F. Zhang and F. Battaglia-Brunet were responsible for manuscript preparation. M. Motelica-Heino, F. Battaglia-Brunet, J. Hellal and F. Zhang arranged sampling from Decize, France. P. Gautret and F. Zhang performed SEM. C. Joulian, J. Hellal and F. Zhang performed the qPCR of *Shewanella* / *Geobacter* and bacterial 16S rRNA (*rrs* gene) quantification.

## Acknowledgments

This research work was performed in the frame of a PhD project, a scholarship co-funded by the BRGM – Région Centre Val de Loire 2017-2020, contract N° SIRET 582 056 149 00120. Additionally, the INSU-EC2CO project "Dycyfer" also contributed to this work. This work was supported by a grant overseen by the French National Research Agency (ANR) as part of the "Investments d'Avenir" Programme LabEx VOLTAIRE, 10-LABX-0100.

## References

Adhikari, D., Zhao, Q., Das, K., Mejia, J., Huang, R., Wang, X., Poulson, S.R., Tang, Y., Roden, E.E., and Yang, Y. (2017). Dynamics of ferrihydrite-bound organic carbon during microbial Fe reduction. *Geochimica et Cosmochimica Acta* 212**,** 221-233.

Aino, K., Hirota, K., Okamoto, T., Tu, Z., Matsuyama, H., and Yumoto, I. (2018). Microbial communities associated with indigo fermentation that thrive in anaerobic alkaline environments. Frontiers in microbiology 9, 2196.

Bonneville, S., Van Cappellen, P., and Behrends, T. (2004). Microbial reduction of iron (III) oxyhydroxides: effects of mineral solubility and availability. *Chemical Geology* 212**,** 255-268.

Bowman, J. P. (2015). Shewanella. Bergey's Manual of Systematics of Archaea and Bacteria, 1-22.

Brunauer, S., Emmett, P.H., and Teller, E. (1938). Adsorption of gases in multimolecular layers. *Journal of the American chemical society* 60**,** 309-319.

Caccavo, F., Lonergan, D. J., Lovley, D. R., Davis, M., Stolz, J. F., & McInerney, M. J. (1994). Geobacter sulfurreducens sp. nov., a hydrogen-and acetate-oxidizing dissimilatory metal-reducing microorganism. Applied and environmental microbiology, 60(10), 3752-3759.

Cai, Y., Hu, K., Zheng, Z., Zhang, Y., Guo, S., Zhao, X., Cui, Z., and Wang, X. (2019). Effects of adding EDTA and Fe2+ on the performance of reactor and microbial community structure in two simulated phases of anaerobic digestion. *Bioresource technology* 275**,** 183-191.

Cavelan, A., Boussafir, M., Le Milbeau, C., Rozenbaum, O., and Laggoun-Défarge, F. (2019). Effect of organic matter composition on source rock porosity during confined anhydrous thermal maturation: Example of Kimmeridge-clay mudstones. *International Journal of Coal Geology* 212**,** 103236.

Coates, J. D., Phillips, E. J., Lonergan, D. J., Jenter, H., & Lovley, D. R. (1996). Isolation of Geobacter species from diverse sedimentary environments. Applied and Environmental Microbiology, 62(5), 1531-1536.

Colombo, C., Palumbo, G., He, J.-Z., Pinton, R., and Cesco, S. (2014). Review on iron availability in soil: interaction of Fe minerals, plants, and microbes. *Journal of soils and sediments* 14**,** 538-548.

Cooper, D.C., Picardal, F.F., and Coby, A.J. (2006). Interactions between microbial iron reduction and metal geochemistry: effect of redox cycling on transition metal speciation in iron bearing sediments. *Environmental science & technology* 40**,** 1884-1891.

Cornell, R.M., and Schwertmann, U. (2003). *The iron oxides: structure, properties, reactions, occurrences and uses.* John Wiley & Sons.

Crosby, H.A., Johnson, C.M., Roden, E.E., and Beard, B.L. (2005). Coupled Fe (II)− Fe (III) electron and atom exchange as a mechanism for Fe isotope fractionation during dissimilatory iron oxide reduction. *Environmental science & technology* 39**,** 6698-6704.

Crosby, H.A., Roden, E.E., Johnson, C.M., and Beard, B.L. (2007). The mechanisms of iron isotope fractionation produced during dissimilatory Fe (III) reduction by Shewanella putrefaciens and Geobacter sulfurreducens. *Geobiology* 5**,** 169-189.

Cutting, R., Coker, V., Fellowes, J., Lloyd, J., and Vaughan, D. (2009). Mineralogical and morphological constraints on the reduction of Fe (III) minerals by Geobacter sulfurreducens. *Geochimica et Cosmochimica Acta* 73**,** 4004-4022.

Delbès, C., Moletta, R., & Godon, J. J. (2000). Monitoring of activity dynamics of an anaerobic digester bacterial community using 16S rRNA polymerase chain reaction–single-strand conformation polymorphism analysis. Environmental Microbiology, 2(5), 506-515.

Das, S., Hendry, M.J., and Essilfie-Dughan, J. (2013). Adsorption of selenate onto ferrihydrite, goethite, and lepidocrocite under neutral pH conditions. *Applied geochemistry* 28**,** 185-193.

Dhivert, E., Grosbois, C., Rodrigues, S., and Desmet, M. (2015). Influence of fluvial environments on sediment archiving processes and temporal pollutant dynamics (Upper Loire River, France). *Science of the total Environment* 505**,** 121-136.

Engel, C.E.A., Schattenberg, F., Dohnt, K., Schröder, U., Müller, S., and Krull, R. (2019). Long-term behavior of defined mixed cultures of Geobacter sulfurreducens and Shewanella oneidensis in bioelectrochemical systems. *Frontiers in Bioengineering and Biotechnology* 7**,** 60.

Esteve-Núñez, A., Rothermich, M., Sharma, M., & Lovley, D. (2005). Growth of Geobacter sulfurreducens under nutrient-limiting conditions in continuous culture. Environmental microbiology, 7(5), 641-648.

Fredrickson, J.K., Zachara, J.M., Kennedy, D.W., Dong, H., Onstott, T.C., Hinman, N.W., and Li, S.-M. (1998). Biogenic iron mineralization accompanying the dissimilatory reduction of hydrous ferric oxide by a groundwater bacterium. *Geochimica et Cosmochimica Acta* 62**,** 3239-3257.

Gagen, E. J., Zaugg, J., Tyson, G. W., & Southam, G. (2019). Goethite Reduction by a Neutrophilic Member of the Alphaproteobacterial Genus Telmatospirillum. Frontiers in microbiology, 10, 2938.

Gault, A.G., Ibrahim, A., Langley, S., Renaud, R., Takahashi, Y., Boothman, C., Lloyd, J.R., Clark, I.D., Ferris, F.G., and Fortin, D. (2011). Microbial and geochemical features suggest iron redox cycling within bacteriogenic iron oxide-rich sediments. *Chemical Geology* 281**,** 41-51.

Ghorbanzadeh, N., Lakzian, A., Halajnia, A., Choi, U.K., Kim, K.H., Kim, J.O., Kurade, M., and Jeon, B.H. (2017). Impact of bioreduction on remobilization of adsorbed cadmium on iron minerals in anoxic condition. *Water Environment Research* 89**,** 519-526.

Han, R., Liu, T., Li, F., Li, X., Chen, D., and Wu, Y. (2018). Dependence of secondary mineral formation on Fe (II) production from ferrihydrite reduction by Shewanella oneidensis MR-1. *ACS Earth and Space Chemistry* 2**,** 399-409.

Hansel, C.M., Benner, S.G., Nico, P., and Fendorf, S. (2004). Structural constraints of ferric (hydr) oxides on dissimilatory iron reduction and the fate of Fe (II). *Geochimica et Cosmochimica Acta* 68**,** 3217-3229.

Hong, C., Si, Y., Xing, Y., and Li, Y. (2015). Illumina MiSeq sequencing investigation on the contrasting soil bacterial community structures in different iron mining areas. *Environmental Science and Pollution Research* 22**,** 10788-10799.

Hori, T., Aoyagi, T., Itoh, H., Narihiro, T., Oikawa, A., Suzuki, K., ... & Kamagata, Y. (2015). Isolation of microorganisms involved in reduction of crystalline iron (III) oxides in natural environments. Frontiers in Microbiology, 6, 386.

Huguet, L. (2009). Caractérisation biogéochimique et potentiel de méthylation du mercure de biofilms en milieu tropical (retenue de Petit Saut et estuaire du Sinnamary, Guyane Française) (Doctoral dissertation, Nancy 1). Jiang, Z., Shi, M., and Shi, L. (2020). Degradation of organic contaminants and steel corrosion by the dissimilatory metal-reducing microorganisms Shewanella and Geobacter spp. *International Biodeterioration & Biodegradation* 147**,** 104842.

Kim, S.-J., Koh, D.-C., Park, S.-J., Cha, I.-T., Park, J.-W., Na, J.-H., Roh, Y., Ko, K.-S., Kim, K., and Rhee, S.-K. (2012). Molecular analysis of spatial variation of iron-reducing bacteria in riverine alluvial aquifers of the Mankyeong River. *The journal of microbiology* 50**,** 207-217.

Kotloski, N. J., & Gralnick, J. A. (2013). Flavin electron shuttles dominate extracellular electron transfer by Shewanella oneidensis. MBio, 4(1).

Kwon, M. J., O'Loughlin, E. J., Boyanov, M. I., Brulc, J. M., Johnston, E. R., Kemner, K. M., & Antonopoulos, D. A. (2016). Impact of organic carbon electron donors on microbial community development under iron-and sulfate-reducing conditions. PloS one, 11(1), e0146689.

Larsen, O., and Postma, D. (2001). Kinetics of reductive bulk dissolution of lepidocrocite, ferrihydrite, and goethite. *Geochimica et Cosmochimica Acta* 65**,** 1367-1379.

Leang, C., Qian, X., Mester, T., and Lovley, D.R. (2010). Alignment of the c-type cytochrome OmcS along pili of Geobacter sulfurreducens. *Appl. Environ. Microbiol.* 76**,** 4080-4084.

Lentini, C.J., Wankel, S.D., and Hansel, C.M. (2012). Enriched iron (III)-reducing bacterial communities are shaped by carbon substrate and iron oxide mineralogy. *Frontiers in microbiology* 3**,** 404.

Levar, C.E., Hoffman, C.L., Dunshee, A.J., Toner, B.M., and Bond, D.R. (2017). Redox potential as a master variable controlling pathways of metal reduction by Geobacter sulfurreducens. *The ISME journal* 11**,** 741-752.

Li, B.-B., Cheng, Y.-Y., Fan, Y.-Y., Liu, D.-F., Fang, C.-Y., Wu, C., Li, W.-W., Yang, Z.-C., and Yu, H.-Q. (2018). Estimates of abundance and diversity of Shewanella genus in natural and engineered aqueous environments with newly designed primers. *Science of The Total Environment* 637**,** 926-933.

Li, X., Liu, T., Li, F., Zhang, W., Zhou, S., and Li, Y. (2012). Reduction of structural Fe (III) in oxyhydroxides by Shewanella decolorationis S12 and characterization of the surface properties of iron minerals. *Journal of soils and sediments* 12**,** 217-227.

Liu, C., Kota, S., Zachara, J. M., Fredrickson, J. K., & Brinkman, C. K. (2001). Kinetic analysis of the bacterial reduction of goethite. Environmental Science & Technology, 35(12), 2482-2490.

Liu, H., Li, P., Zhu, M., Wei, Y., and Sun, Y. (2007). Fe (II)-induced transformation from ferrihydrite to lepidocrocite and goethite. *Journal of Solid State Chemistry* 180**,** 2121-2128.

Liu, X., Ye, Y., Xiao, K., Rensing, C., and Zhou, S. (2019). Molecular evidence for the adaptive evolution of Geobacter sulfurreducens to perform dissimilatory iron reduction in natural environments. *Molecular Microbiology*.

Lovley, D.R. (1991). Dissimilatory Fe (III) and Mn (IV) reduction. *Microbiology and Molecular Biology Reviews* 55**,** 259-287.

Lovley, D.R. (2000). "Fe (III) and Mn (IV) reduction," in *Environmental microbe-metal interactions*. American Society of Microbiology), 3-30.

Lovley, D. (2006). Dissimilatory Fe (III)-and Mn (IV)-reducing prokaryotes. Prokaryotes, 2, 635-658.

Lovley, D. R., Phillips, E. J., & Lonergan, D. J. (1989). Hydrogen and formate oxidation coupled to dissimilatory reduction of iron or manganese by Alteromonas putrefaciens. Applied and Environmental Microbiology, 55(3), 700-706.

Lovley, D.R., Stolz, J.F., Nord, G.L., and Phillips, E.J. (1987). Anaerobic production of magnetite by a dissimilatory iron-reducing microorganism. *Nature* 330**,** 252-254.

Ivanova, E. P., Gorshkova, N. M., Bowman, J. P., Lysenko, A. M., Zhukova, N. V., Sergeev, A. F., ... & Nicolau, D. V. (2004). Shewanella pacifica sp. nov., a polyunsaturated fatty acid-producing bacterium isolated from sea water. International journal of systematic and evolutionary microbiology, 54(4), 1083-1087.

Mamindy-Pajany, Y., Bataillard, P., Séby, F., Crouzet, C., Moulin, A., Guezennec, A.-G., Hurel, C., Marmier, N., and Battaglia-Brunet, F. (2013). Arsenic in marina sediments from the Mediterranean coast: speciation in the solid phase and occurrence of thioarsenates. *Soil and Sediment Contamination: An International Journal* 22**,** 984-1002.

Meile, C., and Scheibe, T.D. (2019). Reactive transport modeling of microbial dynamics. *Elements: An International Magazine of Mineralogy, Geochemistry, and Petrology* 15**,** 111-116.

Melton, E.D., Swanner, E.D., Behrens, S., Schmidt, C., and Kappler, A. (2014). The interplay of microbially mediated and abiotic reactions in the biogeochemical Fe cycle. *Nature Reviews Microbiology* 12**,** 797-808.

Mercier, A., Joulian, C., Michel, C., Auger, P., Coulon, S., Amalric, L., Morlay, C., and Battaglia-Brunet, F. (2014). Evaluation of three activated carbons for combined adsorption and biodegradation of PCBs in aquatic sediment. *Water research* 59**,** 304-315.

Murti, G.K., Volk, V., and Jackson, M. (1966). Colorimetric determination of iron of mixed valency by orthophenanthroline. *Soil Science Society of America Journal* 30**,** 663-664.

Nealson, K.H. (2017). Bioelectricity (electromicrobiology) and sustainability. *Microbial biotechnology* 10**,** 1114-1119.

Nevin, K.P., and Lovley, D.R. (2002). Mechanisms for Fe (III) oxide reduction in sedimentary environments. *Geomicrobiology Journal* 19**,** 141-159.

Nogi, Y., Kato, C., & Horikoshi, K. (1998). Taxonomic studies of deep-sea barophilic Shewanella strains and description of Shewanella violacea sp. nov. Archives of microbiology, 170(5), 331-338.

Pedersen, H.D., Postma, D., Jakobsen, R., and Larsen, O. (2005). Fast transformation of iron oxyhydroxides by the catalytic action of aqueous Fe (II). *Geochimica et Cosmochimica Acta* 69**,** 3967-3977.

Poggenburg, C., Mikutta, R., Sander, M., Schippers, A., Marchanka, A., Dohrmann, R., and Guggenberger, G. (2016). Microbial reduction of ferrihydrite-organic matter coprecipitates by Shewanella putrefaciens and Geobacter metallireducens in comparison to mediated electrochemical reduction. *Chemical Geology* 447**,** 133-147.

Roden, E. E. (2006). Geochemical and microbiological controls on dissimilatory iron reduction. Comptes Rendus Geoscience, 338(6-7), 456-467.

Roden, E.E., Sobolev, D., Glazer, B., and Luther, G.W. (2004). Potential for microscale bacterial Fe redox cycling at the aerobic-anaerobic interface. *Geomicrobiology Journal* 21**,** 379-391.

Roden, E.E., and Wetzel, R.G. (2002). Kinetics of microbial Fe (III) oxide reduction in freshwater wetland sediments. *Limnology and Oceanography* 47**,** 198-211.

Schilling, K., Borch, T., Rhoades, C.C., and Pallud, C.E. (2019). Temperature sensitivity of microbial Fe (III) reduction kinetics in subalpine wetland soils. *Biogeochemistry* 142**,** 19-35.

Schwertmann, U. (1973). Use of oxalate for Fe extraction from soils. Canadian Journal of Soil Science, 53(2), 244-246.

Schwertmann, U., & Taylor, R. M. (1979). Natural and synthetic poorly crystallized lepidocrocite. Clay Minerals, 14(4), 285-293.

Schwertmann, U., and Cornell, R.M. (2008). *Iron oxides in the laboratory: preparation and characterization.* John Wiley & Sons.

Shelobolina, E. S., Nevin, K. P., Blakeney-Hayward, J. D., Johnsen, C. V., Plaia, T. W., Krader, P., ... & Lovley, D. R. (2007). Geobacter pickeringii sp. nov., Geobacter argillaceus sp. nov. and Pelosinus fermentans gen. nov., sp. nov., isolated from subsurface kaolin lenses. International Journal of Systematic and Evolutionary Microbiology, 57(1), 126-135.

Shi, L., Dong, H., Reguera, G., Beyenal, H., Lu, A., Liu, J., Yu, H.-Q., and Fredrickson, J.K. (2016). Extracellular electron transfer mechanisms between microorganisms and minerals. *Nature Reviews Microbiology* 14**,** 651.

Shi, M., Jiang, Y., and Shi, L. (2019). Electromicrobiology and biotechnological applications of the exoelectrogens Geobacter and Shewanella spp. *Science China Technological Sciences***,** 1-9.

Snoeyenbos-West, O., Nevin, K., Anderson, R., and Lovley, D. (2000). Enrichment of Geobacter species in response to stimulation of Fe (III) reduction in sandy aquifer sediments. *Microbial Ecology* 39**,** 153-167.

Stern, N., Mejia, J., He, S., Yang, Y., Ginder-Vogel, M., and Roden, E.E. (2018). Dual role of humic substances as electron donor and shuttle for dissimilatory iron reduction. *Environmental science & technology* 52**,** 5691-5699.

Su, C., Zhang, M., Lin, L., Yu, G., Zhong, H., and Chong, Y. (2020). Reduction of iron oxides and microbial community composition in iron-rich soils with different organic carbon as electron donors. *International Biodeterioration & Biodegradation* 148**,** 104881.

Team, R. (2015). RStudio: integrated development for R. RStudio. Inc., Boston, MA, 700.

Thompson, A., Chadwick, O.A., Rancourt, D.G., and Chorover, J. (2006). Iron-oxide crystallinity increases during soil redox oscillations. *Geochimica et Cosmochimica Acta* 70**,** 1710-1727.

Thouin, H., Le Forestier, L., Gautret, P., Hube, D., Laperche, V., Dupraz, S., and Battaglia-Brunet, F. (2016). Characterization and mobility of arsenic and heavy metals in soils polluted by the destruction of arsenic-containing shells from the Great War. *Science of the Total Environment* 550**,** 658-669.

Urrutia M, Roden E, Fredrickson J, Zachara J. Microbial and surface chemistry controls on reduction of synthetic Fe (III) oxide minerals by the dissimilatory iron‐reducing bacterium Shewanella alga. Geomicrobiology Journal 1998; 15: 269-291.

Usman, M., Hanna, K., Abdelmoula, M., Zegeye, A., Faure, P., and Ruby, C. (2012). Formation of green rust via mineralogical transformation of ferric oxides (ferrihydrite, goethite and hematite). *Applied Clay Science* 64**,** 38-43.

Wilkins, M.J., Livens, F.R., Vaughan, D.J., and Lloyd, J.R. (2006). The impact of Fe (III)-reducing bacteria on uranium mobility. *Biogeochemistry* 78**,** 125-150.

Wolf, M., Kappler, A., Jiang, J., and Meckenstock, R.U. (2009). Effects of humic substances and quinones at low concentrations on ferrihydrite reduction by Geobacter metallireducens. *Environmental science & technology* 43**,** 5679-5685.

Wu, Y., Luo, X., Qin, B., Li, F., Haggblom, M. M., & Liu, T. (2020). Enhanced Current Production by Exogenous Electron Mediators via Synergy of Promoting Biofilm Formation and the Electron Shuttling Process. Environmental Science & Technology.

Zachara, J.M., Kukkadapu, R.K., Fredrickson, J.K., Gorby, Y.A., and Smith, S.C. (2002). Biomineralization of poorly crystalline Fe (III) oxides by dissimilatory metal reducing bacteria (DMRB). *Geomicrobiology Journal* 19**,** 179-207.

Zhang, C., Ge, Y., Yao, H., Chen, X., and Hu, M. (2012). Iron oxidation-reduction and its impacts on cadmium bioavailability in paddy soils: a review. *Frontiers of Environmental Science & Engineering* 6**,** 509-517.

Zhu, Y., Wang, H., Li, X., Hu, C., Yang, M., and Qu, J. (2014). Characterization of biofilm and corrosion of cast iron pipes in drinking water distribution system with UV/Cl2 disinfection. *Water research* 60**,** 174-181.

Zhuang, K., Izallalen, M., Mouser, P., Richter, H., Risso, C., Mahadevan, R., and Lovley, D.R. (2011). Genome-scale dynamic modeling of the competition between Rhodoferax and Geobacter in anoxic subsurface environments. *The ISME journal* 5**,** 305-316.

Ziemke, F., Höfle, M. G., Lalucat, J., & Rossellö-Mora, R. (1998). Reclassification of Shewanella putrefaciens Owen's genomic group II as Shewanella baltica sp. nov. International Journal of Systematic and Evolutionary Microbiology, 48(1), 179-186.

## Figures

**Figure 1.** Evolution of the concentration of total Fe during incubation experiments with four Fe(III) (oxyhydr)oxides in presence of D1(a), D2(b) and D3(c) iron-reducing cultures, *Fe(III)-NTA is given in* ***Supplementary Figure S3***. Error bars represent the standard deviation of triplicate measurements.

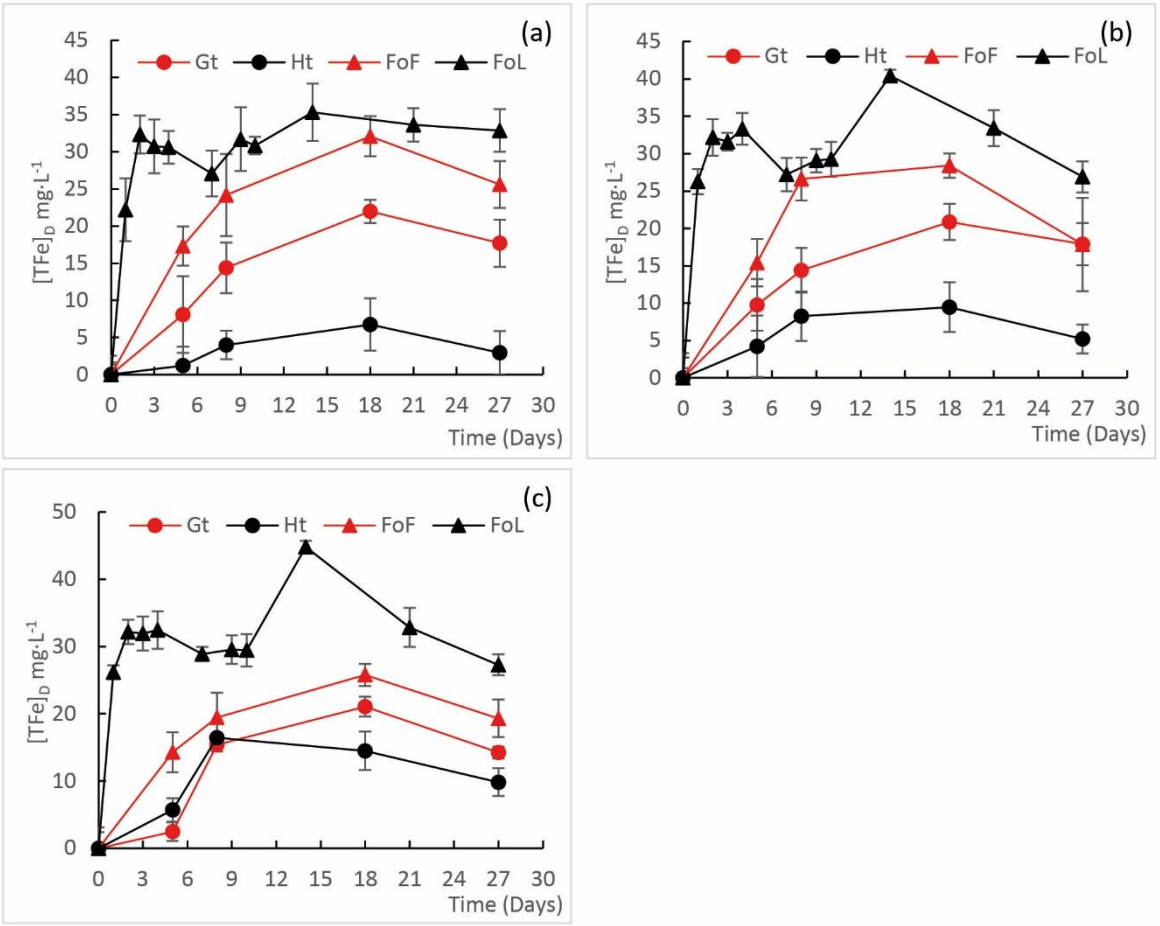

**Figure 2.** Final total amount of solubilized Fe from Fe (oxyhydr)oxides: goethite, hematite, FoF and FoL in presence of D1, D2 and D3 inocula with a mixture of C sources. The letters "a" and "b" represent the significance of differences (Kruskal-Wallis test at $p<0.05$) between cultures. Values in the same Fe (oxyhydr)oxides group are not significantly different from one another. Error bars represent the standard deviation of triplicate measurements.

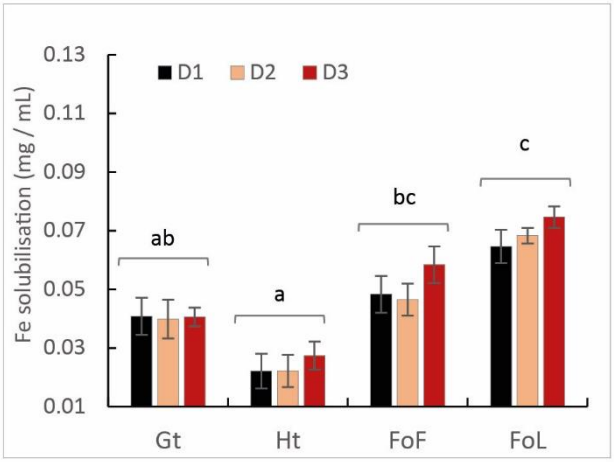


**Figure 3.** nMDS ordination of D1, D2 and D3 community fingerprints applied to a Bray-Curtis dissimilarity matrix. Plot stress = 0.15. Ht: hematite; Fh: FoF; Lp: FoL; Gt: goethite.

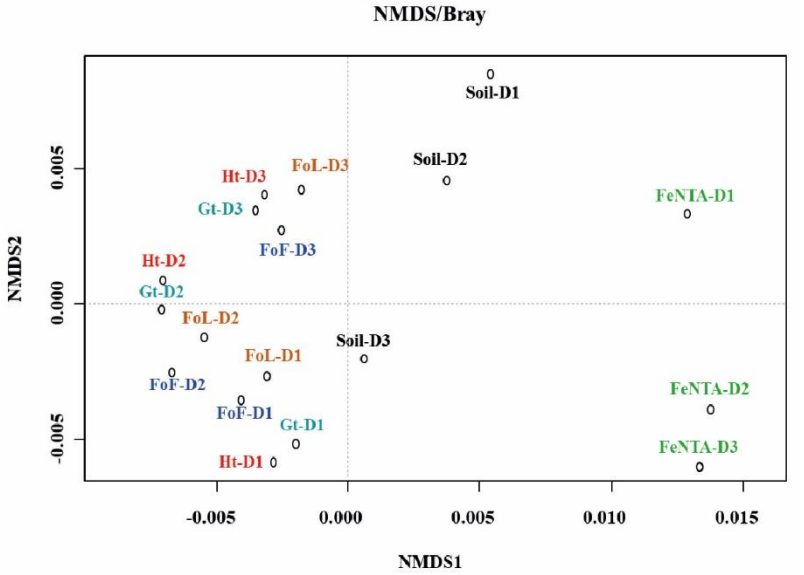

**Figure 4.** Parameters linked to bacterial abundance: (**a**) Log10 of bacterial 16S rRNA (*rrs* gene) copies, (**b**) Ratio of *Shewanella* and *Geobacter* over bacterial 16S rRNA (*rrs* gene) copies for all three site samples D1, D2 and D3, (**c**) Log 10 of *Geobacter* 16S gene copies, (**d**) Ratio *Geobacter* 16S over bacterial 16S rRNA (*rrs* gene) copies, (**e**) Log 10 of *Shewanella* 16S gene copies, and (**f**) Ratio *Shewanella* 16S over bacterial 16S rRNA (*rrs* gene) copies. Details of bacterial, *Shewanella* and *Geobacter* 16S rRNA (*rrs* gene) copies for all three site samples D1, D2 and D3 are given in **Supplementary Figure S6**. The letters "a" and "b" differed significantly (Kruskal-Wallis test at $p<0.05$) between group of iron oxide for graph "(**a**), (**b**), (**c**), and (**e**)"; the small letter, capital letter and Greek letter were used for differing significantly by group of inocula D1, D2 and D3 for graphs "(**d)** and **(f**)". Data represent average values of three experimental replicates and their standard deviation (σ) for graph "(**b**), (**d)** and (**f**)", 3 inocula * 3 replicates for graphs "(**a**), (**c**), and (**e**)". Ht: hematite; Fh: FoF; Lp: FoL; Gt: goethite. Error bars represent the standard deviation of triplicate measurements.

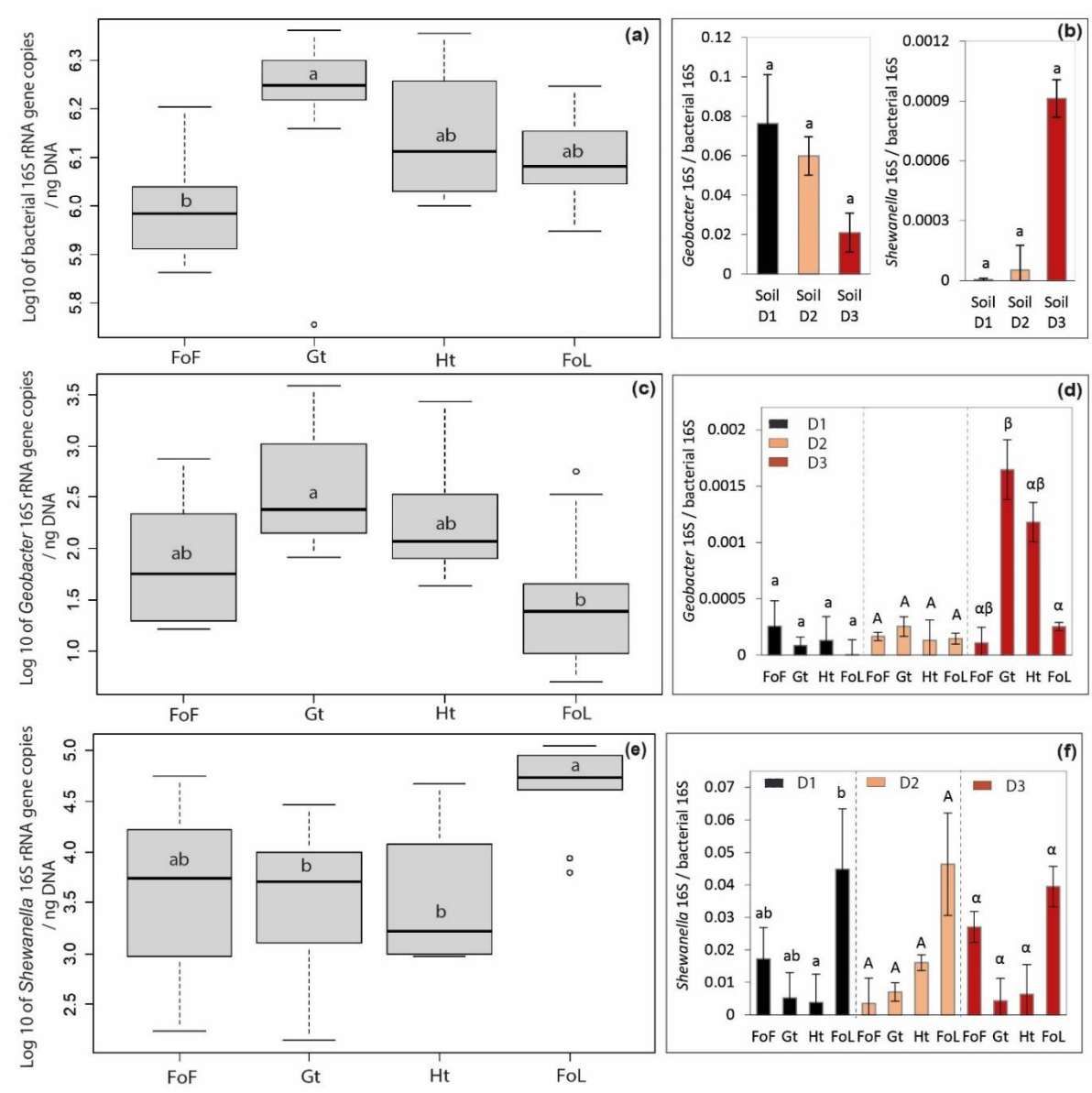

# Tables

**Table 1**. Characteristics of Fe(III) oxides submitted to Fe-reducing bacteria.

| Iron oxide | Assumed morphology[a] | Surface area[b] ($m^2g^{-1}$) |
|---|---|---|
| goethite | acicular | 11.7 |
| hematite | cylinder/rod | 31.4 |
| FoF | blocky | 232 |
| FoL | blocky | 337 |

[a]For use in estimating mean particle size from morphology by SEM-EDS (TM3000 accompanied by a SwiftED3000 X-Stream module (Hitachi)); [b]Determined by multipoint BET $N_2$ adsorption.

# *Supplementary Material*

## Supplementary Figures

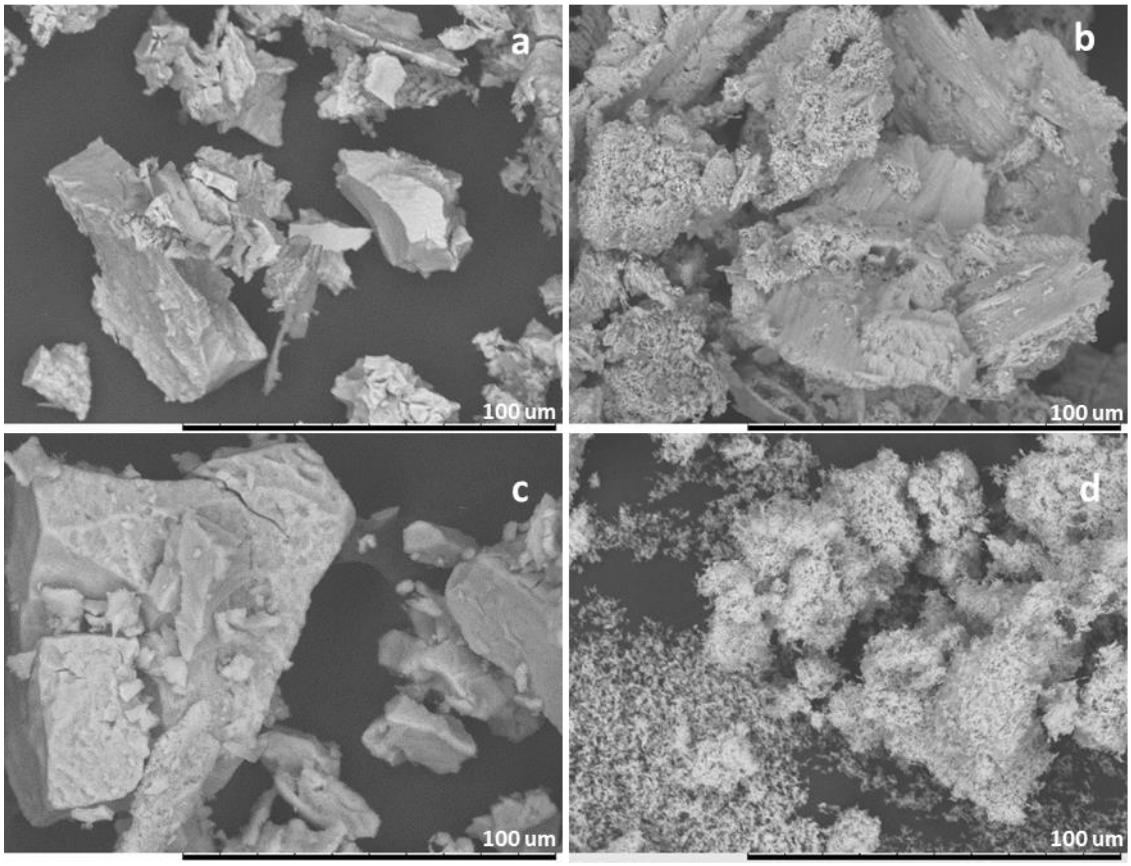


**Supplementary Figure S13.** SEM observation on initial Fe (oxyhydr)oxides: Morphology of FoF (a), hematite (b), FoL (c) and goethite (d)

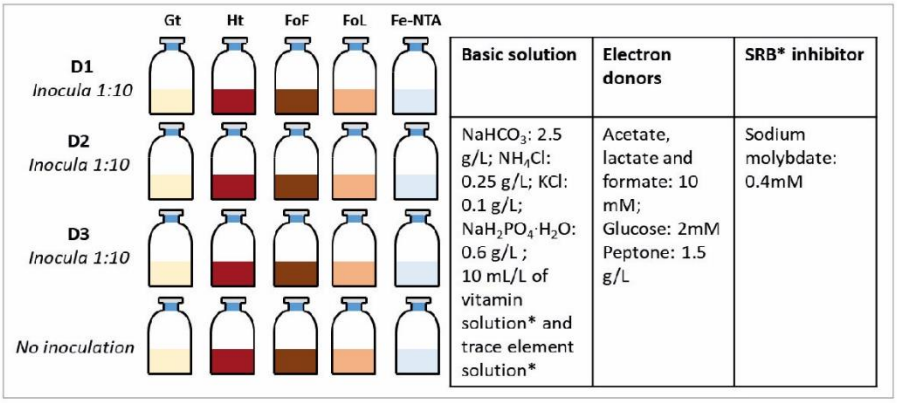


**Supplementary Figure S2**: Design and initial compositions of the batch experiments.

**SRB**[1] : sulfate-reducing bacteria ; 2. **Vitamin solution** (1L): 2 mg biotin, 2 mg folic acid, 10 mg pyridoxine HCL, 5 mg Riboflavin,5 mg Thiamine, 5 mg Nicotinic acid, 5 mg Pantothenic acid, 0.1g B12 vitamin, 5 mg p-aminobenzoic acid, 5 mg thioctic acid ; 3. **Trace element solution** (1L): 1.5 g Trisodium nitrilotriacetic, 0.5 g $MgSO_4$, 0.5 g $MgSO_4 \cdot H_2O$, 1 g NaCl, 0.1 g $FeSO_4 \cdot 7\ H_2O$, 0.1 g $CaCl_2 \cdot 2H_2O$, 0.1 g $CoCl_2 \cdot 6H_2O$, 0.13 g ZnCl, 0.1 g $CuSO_4\ 5H_2O$, 0.1 g $AlK(SO_4) \cdot 12H_2O$, 0.1 g $H_3BO_3$, 0.25 g $NaMoO_4$, 0.24 g $NiCl \cdot 6H_2O$, 0.25 g $Na_2WO_4 \cdot 2H_2O$

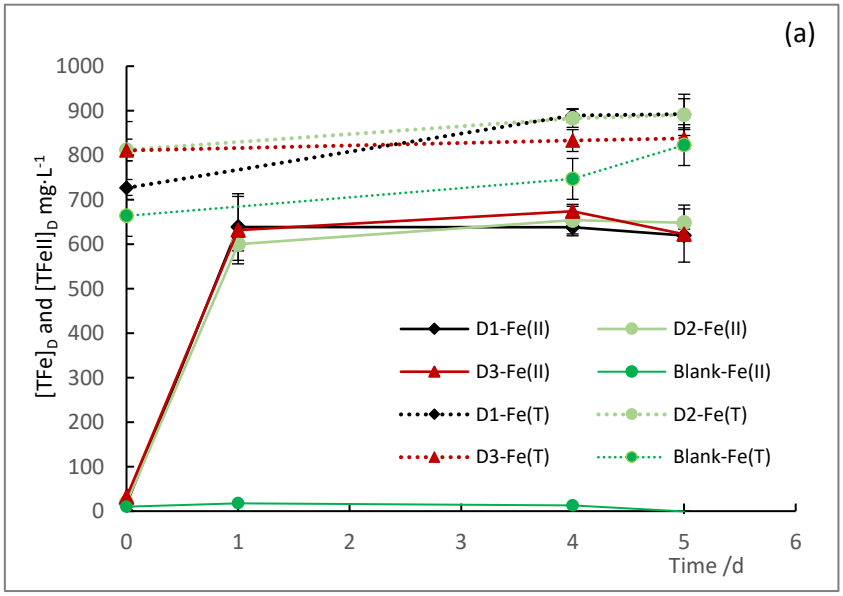

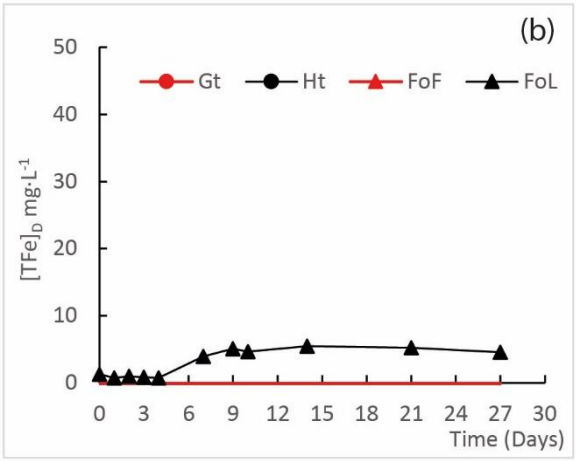


**Supplementary Figure S3.** Concentration of Fe(II) and total Fe (FeT) of D1, D2 and D3 incubated on Fe(III)-NTA medium (a), and evolution of the concentration of total Fe during incubation experiments with four abiotic Fe(III) (oxyhydr)oxides (b). Error bars represent the standard deviation of triplicate measurements.

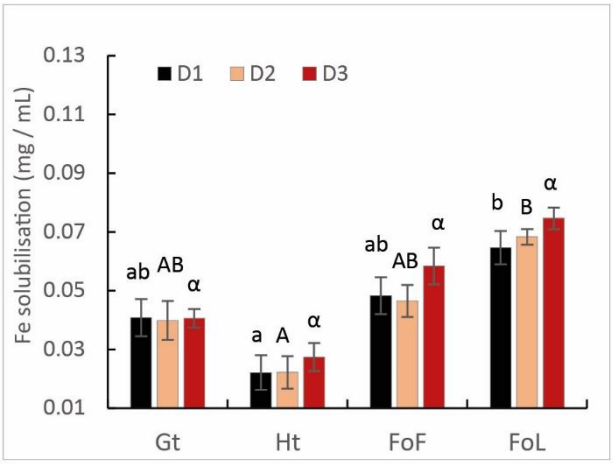


**Supplementary Figure S4.** Fe(III) dissolution of Fe oxides: goethite, hematite, FoF and FoL in presence of D1, D2 and D3 inocula. The small letter, capital letter and Greek letter were used for differing significantly (Kruskal-Wallis test at $p<0.05$) by group of inocula D1, D2 and D3 for different iron oxides. Error bars represent the standard deviation of triplicate measurements.

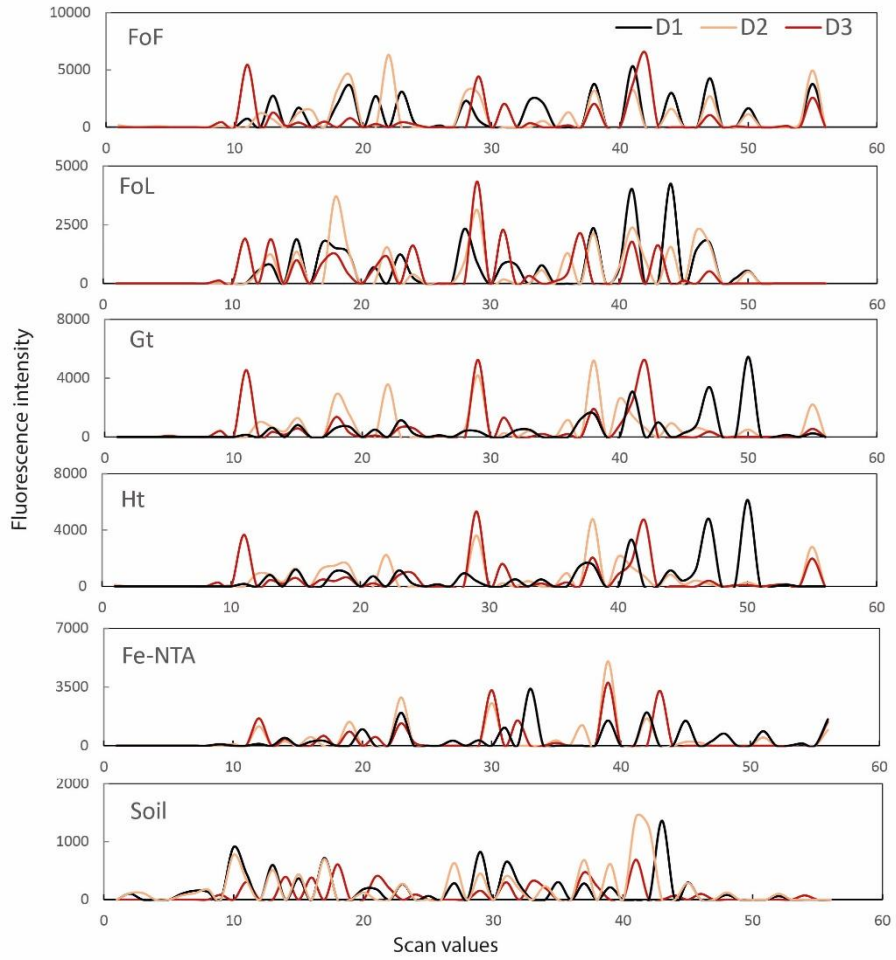


**Supplementary Figure S5.** CE-SSCP diversity profiles of the site samples (Soil), the Fe(III)-NTA enrichments (Fe-NTA) and cultures in presence of the four Fe oxides: FoF, FoL, goethite (Gt) and hematite (Ht). D1: soil from river bank; D2: sediment interface, flooded soil; D3: sediment under water. SSCP is a fingerprinting approach, fluorescently labeled blunt-ended PCR products are obtained from the highly variable V3 region of the 16S rRNA (*rrs* gene), denatured at high temperature, and then rapidly cooled to form unique single-strand conformations, which are separated based on their electrophoretic mobility in a polymer-filled capillary (Delbes et al., 2000). The scales are relative to standards. These profiles present high diversity with many peaks, with thus the presence of different bacterial strains.

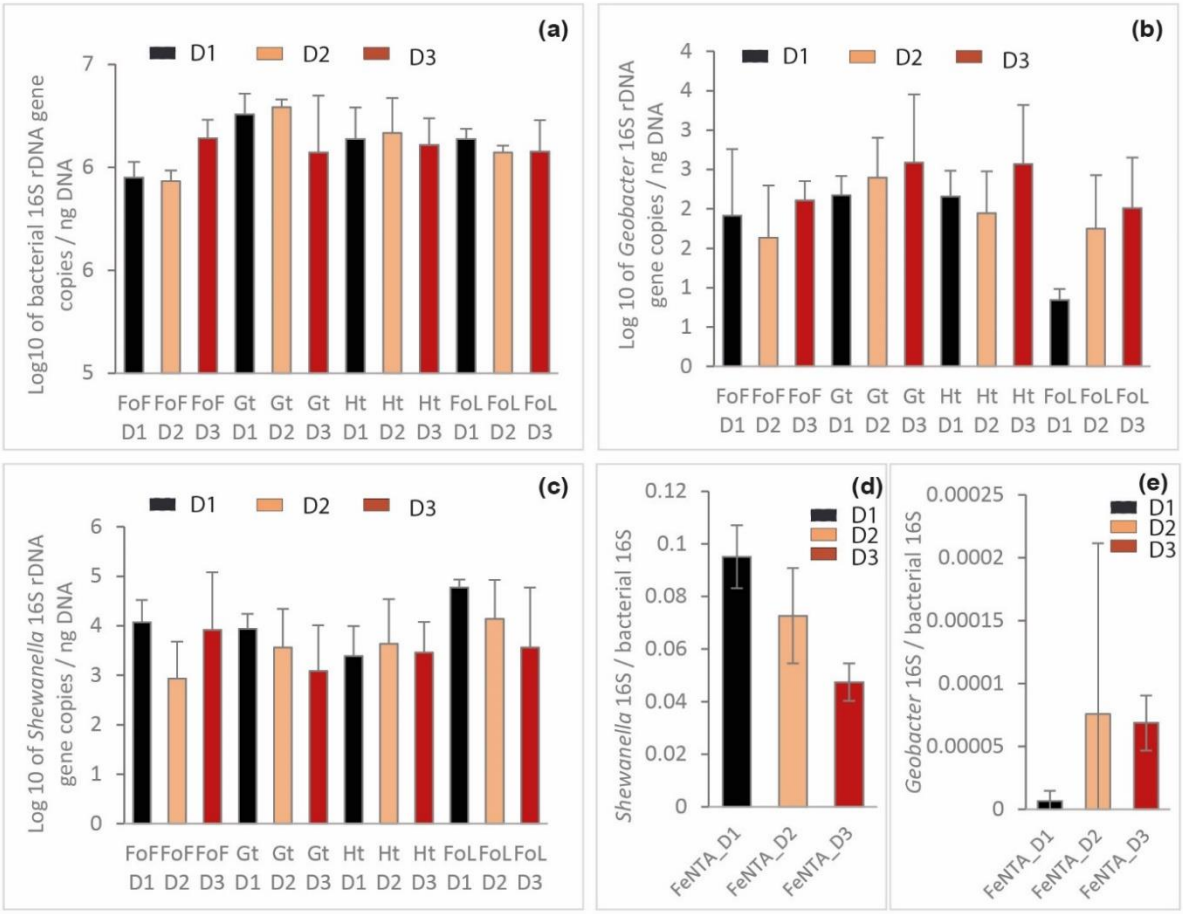


**Supplementary Figure S6.** Parameters linked to bacterial abundance: (**a**) Log10 of bacterial 16S rRNA (*rrs* gene) copies, (**b**) Log 10 of *Geobacter* 16S gene copies, (**c**) Log 10 of *Shewanella* 16S gene copies, for the three site samples D1, D2 and D3; Ratios of *Shewanella* 16S (**d**) and *Geobacter* 16S (**e**) over bacterial 16S rRNA genes copies in Fe(III)-NTA enrichments. Error bars represent the standard deviation of triplicate measurements.

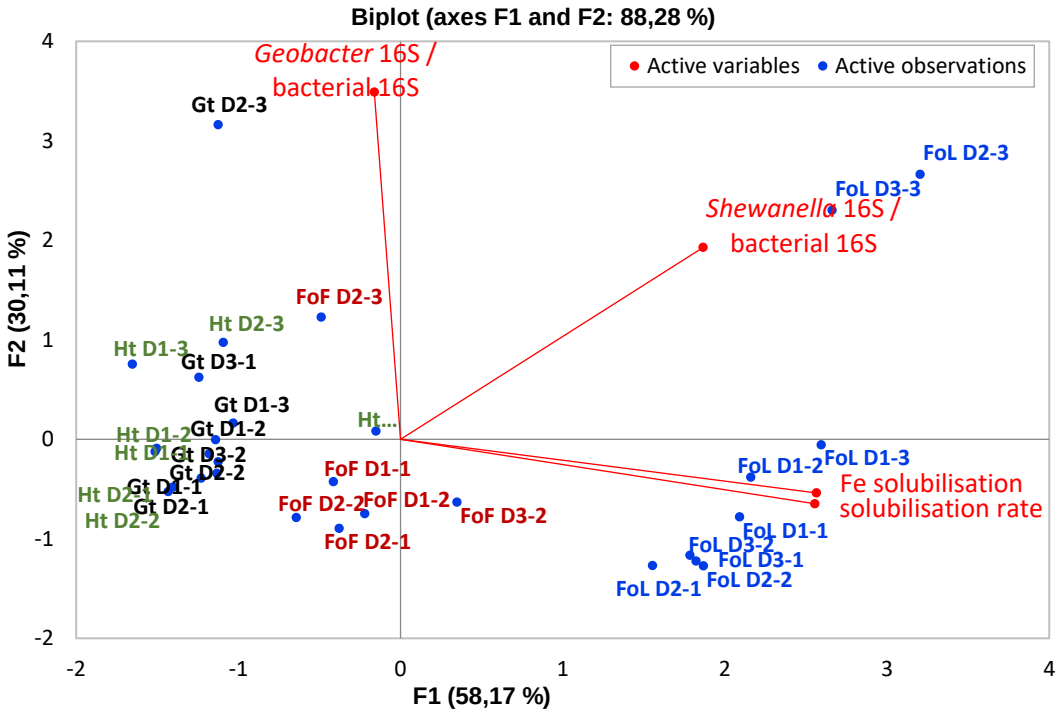


**Supplementary Figure S7.** Principal component analysis (F1 × F2) biplot map generated from iron solubilisation (percentage and rate of iron solubilisation) and ratios of *Shewanella* (*Shewanella* 16S / bacterial 16S) and *Geobacter* (*Geobacter* 16S / bacterial 16S) in the bacterial community, obtained for the FoF, goethite hematite and FoL incubations with D1, D2 and D3

## Supplementary Tables

**Supplementary Table S1.** Calculation of the iron oxides concentrations to obtain 20 mM Fe in the incubation experiments

| Minerals | Formula | Fe | Products of Fe(III) oxide |
|---|---|---|---|
| "Ferrihydrite" FoF | $Fe_2O_3 \cdot 0.5H_2O$ | 20 mM | 1.68 g/L |
| Goethite | FeOOH (30-63%: 46%) | | 3.86 g/L |
| Hematite | $Fe_2O_3$ (97%) | | 1.65 g/L |
| "Lepidocrocite" FoL | FeOOH | | 1.78 g/L |

**Supplementary Table S2.** Initial iron reduction*/solubilisation** rates (mg $L^{-1} \cdot h^{-1}$) on incubation experiment with dissolved Fe(III) and solid minerals.

| Inocula/ Minerals | Fe-NTA* | Goethite** | Hematite** | FoF** | FoL** |
|---|---|---|---|---|---|
| D1-1 | 26.17 | 0.07 | 0.03 | 0.09 | 0.47 |
| D1-2 | 29.42 | 0.09 | 0.03 | 0.16 | 0.42 |
| D1-3 | 22.26 | 0.07 | 0.00 | 0.13 | 0.38 |
| D2-1 | 23.51 | 0.07 | 0.04 | 0.16 | 0.42 |
| D2-2 | 24.29 | 0.09 | 0.05 | 0.11 | 0.48 |
| D2-3 | 24.87 | 0.06 | 0.04 | 0.14 | 0.42 |
| D3-1 | 29.21 | 0.08 | NA | NA | 0.46 |
| D3-2 | 23.82 | 0.09 | 0.27 | 0.33 | 0.45 |
| D3-3 | 21.98 | 0.08 | MA | NA | 0.42 |

**Fengfeng ZHANG**

# Transformation des oxydes de fer par des populations bactériennes mixtes ferri-réductrices et dynamique des éléments traces associés As, Cr, et Cd

La mobilité des contaminants dans l'environnement, et en particulier celle des éléments traces potentiellement toxiques (ETPT), tels que l'arsenic, le chrome et le cadmium induisent des risques de contamination des hydrosystèmes et de la chaîne alimentaire. Comprendre et prévoir la mobilité et la biogéochimie de ces ETPT dans l'environnement permettra de développer et d'appliquer des stratégies de remédiation appropriées pour les sites pollués. Afin d'évaluer l'impact de l'activité microbiologique et des transformations géochimiques / minéralogiques des oxydes de fer et d'observer leur effet sur la spéciation et la mobilité de trois ETPT associés au fer, trois expériences de laboratoire ont été menées : en batch avec des suspensions d'oxydes de fer et des oxydes fixés sur lames de verre, puis en continu dans des colonnes de percolation. Les résultats ont montré que la minéralogie de l'oxyde de fer influençait la vitesse de solubilisation bactérienne du fer. Les deux espèces bactériennes ferri-réductrices les plus étudiées au laboratoire, *Shewanella* et *Geobacter*, ont été quantifiées par qPCR. *Shewanella* a toujours été prépondérante par rapport à *Geobacter* dans les communautés bactériennes, et ces deux espèces étaient différentiellement réparties entre les populations attachées et planctoniques : *Geobacter* pourrait être moins dépendant du Fe(III) soluble et plus présent dans la communauté attachée à la surface des oxydes qu'en suspension dans le milieu liquide. De plus, la distribution spatiale des deux espèces suivies différait dans le système de colonnes alimentées en continu. Dans cette expérience, la bioréduction des oxydes de fer s'est accompagnée d'une mobilisation de l'As, surtout avec la ferrihydrite. Le Cd n'a été mobilisé que transitoirement, ce qui suggère des mécanismes d'immobilisation biologiques de cet élément. Aucune mobilisation biologique du Cr n'a été observée. La production de minéraux secondaires de Fer a été mise en évidence par MEB-EDS et spectroscopie Mössbauer au cours de la réduction microbienne de la ferrihydrite. Ces résultats permettent de mieux comprendre la dynamique bactérienne du fer et des ETPT associés dans l'environnement, à travers des conditions expérimentales originales avec des systèmes multi-polluants et des communautés bactériennes mixtes réductrices de fer.

Mots clés : Oxy-hydroxydes de Fe, réduction microbienne du fer, bactéries ferri-réductrices, *Shewanella*, *Geobacter*, MEB-EDS, Mössbauer, spéciation et mobilité des ETPT, As, Cr, Cd

# Transformation of iron oxides in presence of mixed iron-reducing bacterial communities and dynamics of the associated trace elements As, Cr, and Cd

Contaminants' mobility in the environment, and in particular mobility of potentially toxic trace elements (PTTE), such as arsenic, chromium and cadmium induces risks of contamination of hydrosystems and of the food chain. Understanding and predicting PTTEs' mobility and biogeochemistry in the environment will help to develop and apply appropriate remediation strategies for polluted sites. In order to assess the impact of microbiological activity and geochemical/mineralogical transformations of iron oxides and to observe their effects on the speciation and mobility of three PTTEs associated with iron, three laboratory experiments were conducted: batch experiments with oxides in slurry, batch with oxides immobilized on slides, then continuous percolation in columns containing oxides with adsorbed PTTEs. Results showed that the mineralogy of iron oxides influenced the bacterial iron solubilization rate. The two most studied iron-reducing bacteria (IRB), i.e. *Shewanella* and *Geobacter*, were quantified by qPCR. Considering the two IRB species monitored during this thesis, *Shewanella* was always preponderant compared with *Geobacter* in bacterial communities, and these two species were differentially distributed between attached and planktonic populations. *Geobacter* might be less dependent from soluble Fe(III) and more present in the bacterial community attached to iron oxides than free suspended in the liquid medium. Moreover, the spatial distribution of the two monitored species differed in column systems. In this experiment, iron oxides bioreduction induced As mobilization, particularly in presence of ferrihydrite. Cadmium was only transiently mobilized, suggesting mechanisms of biological immobilization of this element. Chromium was not biologically mobilized. The production of secondary iron minerals was evidenced my SEM-EDS and Mössbauer spectroscopy during the microbial reduction of ferrihydrite. These results enlighten the bacterial dynamics of iron and associated PTTE in environment, through original experimental conditions including several pollutants and mixed iron-reducing bacterial communities.

Key words: Fe (oxyhydr)oxides, microbial iron reduction, IRB, *Shewanella*, *Geobacter*, SEM-EDS, Mössbauer, speciation and mobility of PTTEs, As, Cr, Cd

**BRGM - Service géologique national**
**Institut des Science de la Terre d'Orléans**

**CNRS/INSU, ISTO, UMR 7327, 45071 Orléans, France**